Université de Montréal

Mécanismes de capture et de détachement de gouttelettes d'huile par les organismes filtreurs aquatiques et les implications liées à l'utilisation de surfactants.

par

Francis Letendre

Département de sciences biologiques
Faculté des arts et des sciences

Thèse présentée en vue de l'obtention du grade de
Philosophiæ Doctor (Ph.D.)
en sciences biologiques

26 janvier 2022

Université de Montréal

Faculté des arts et des sciences

Cette thèse intitulée

Mécanismes de capture et de détachement de gouttelettes d'huile par les organismes filtreurs aquatiques et les implications liées à l'utilisation de surfactants.

présentée par

Francis Letendre

a été évaluée par un jury composé des personnes suivantes :

Colin Favret
(président-rapporteur)

Christopher Cameron
(directeur de recherche)

Jean-François Lapierre
(membre du jury)

Frédérick Gosselin
(examinateur externe)

Kevin James Wilkinson
(représentant du doyen de la FESP)

Résumé

L'alimentation par filtration est omniprésente chez les invertébrés aquatiques. On retrouve des organismes se nourrissant de cette manière dans la plupart des embranchements du règne animal. Les organismes filtreurs capturent les particules présentes dans la colonne d'eau à l'aide d'appendices ramifiés. Ces particules peuvent alors être manipulées, goûtées et potentiellement ingérées. Les particules filtrées sont généralement des algues unicellulaires, des débris variés ou encore des protistes. Cependant, ces organismes filtreurs peuvent aussi filtrer, capturer et consommer des particules liquides de lipides. Ces particules liquides peuvent provenir de la décomposition naturelle d'un organisme vivant ou par le biais d'un déversement d'hydrocarbures dans les milieux aquatiques. L'objectif principal de ma thèse était de déterminer les mécanismes principaux de capture des gouttelettes d'huile et de décrire les paramètres contrôlant leur capture et leur détachement.

Tout d'abord, les principes de mécanique des fluides permettant de décrire la capture de particules solides et le courant passant près d'une fibre cylindrique ont été adaptés aux particules liquides. Une revue exhaustive de la littérature existante a été synthétisée sous un article de synthèse. Une étude du volume critique de détachement en fonction de la tension d'interface y est présentée. De plus, les modes de filtration de la balane et de la daphnie sont décrits.

Par la suite, le détachement de gouttelettes d'un appendice filtreur a été observé à l'aide de la vidéographie haute vitesse. Nous avons déterminé les facteurs régissant le détachement et établi une courbe permettant de prédire le comportement des gouttelettes, à savoir si celles-ci vont demeurer sur l'appendice filtreur ou si elles vont retourner dans la colonne d'eau. En effet, pour qu'une gouttelette se détache du collecteur, le ratio des forces inertielles et des forces capillaires doit atteindre un seuil critique. Plus le ratio de taille entre la gouttelette et le collecteur sera petit, plus le seuil critique sera élevé. Cet outil a ensuite été validé en

utilisant la taille maximale des gouttelettes retrouvées sur les appendices filtreurs de trois espèces de copépodes marins. Ce résultat permet de facilement déterminer quelle distribution de gouttelettes est à risque de demeurer sur les appendices des organismes filtreurs, advenant un rapide survol des espèces présentes au lieu du déversement.

Je me suis ensuite intéressé aux mécanismes de capture des gouttelettes. Pour ce faire, l'alimentation de *Daphnia magna*, *Balanus crenatus* et *Balanus glandula* a été observé sous le microscope et dans une chambre de courant à l'aide d'une caméra haute vitesse afin de décrire précisément les méthodes de capture. *Daphnia magna* capturent les gouttelettes à l'aide des couches limites très épaisses des paires de pattes thoraciques 3 et 4. Ainsi, les gouttelettes capturées ne touchent pas les setae et les sétules. À faible nombre de Reynolds, les balanes vont capturer les gouttelettes par un processus similaire. Par contre, à haut nombre de Reynolds, les gouttelettes seront majoritairement capturées par interception directe. À l'aide de la microscopie électronique à balayage et de la microscopie à fluorescence, nous avons observé que les surfaces filtrantes sont très lisses et hautement lipophobes, Ainsi les angles de contact des gouttelettes capturées sont supérieurs à 90°.

Finalement, puisque la dispersion de surfactants est un des moyens principaux de nettoyage après un déversement, son rôle sur la capture et le détachement des gouttelettes se devait d'être étudié. Donc, l'impact d'un surfactant sur la taille des gouttelettes dans la colonne d'eau et dans le tube digestif de *Daphnia magna* a été étudié. De plus, nous avons comparé les conditions de détachement de gouttelettes avec et sans surfactant présent dans l'émulsion. Ainsi, l'ajout d'un surfactant diminue significativement la taille des gouttelettes dans la colonne d'eau. Avec ou sans surfactant présent, la taille des gouttelettes ingérées par *Daphnia magna* est similaire. L'ajout d'un surfactant facilite le détachement de gouttelettes d'une fibre en diminuant la tension d'interface. Une gouttelette dispersée avec un surfactant se détachera donc à plus faible vélocité qu'une gouttelette dispersée mécaniquement.

Ces travaux apportent de nouvelles connaissances nous permettant de comprendre comment le pétrole est capturé par le zooplancton. Ceci est d'une grande importance considérant que c'est par ce groupe que la majorité du pétrole entre dans les réseaux trophiques marins.

Cette thèse décrit les principaux mécanismes de capture, de détachement et l'impact de l'ajout d'un surfactant sur ce dernier.

Mots-clés : zooplancton, mécanique des fluides, alimentation par filtration, pétrole brut, surfactant, nombre de Reynolds, mouillabilité, daphnies, copépodes, balanes

Abstract

Filter feeding is ubiquitous in aquatic invertebrate clades. Species feeding this way are found in almost every animal phyla. Filter feeders capture food particles from the water column using ramified appendages. These particles can then be manipulated, tasted and potentially ingested. Captured particles generally include unicellular algae, various debris and protists. However, these filter feeders can also filter, capture and consume lipid particles. These lipid particles can come from decaying organisms or from the release of hydrocarbons during an oil spill. The main goal of this thesis was to identify the main capturing mechanisms of oil droplets and to describe the parameters controlling the capture and detachment from a filtering appendage.

At first, the general principles of fluid mechanics required to describe the capture of solid particles and the flow around a cylindrical fiber were adapted to liquid particles. An exhaustive review of the literature was published as a review paper. A study of the critical volume needed for vertical detachment in function of the interfacial tension was presented. Also, the feeding mechanisms of daphnids and barnacles were described.

Then, we used high speed videography to observe the detachment process of oil droplets from fibers. We described the key factors responsible for detachment and established a curve to predict whether a captured droplet will remain on the fiber or detach and re-enter the water column. Indeed, for a droplet to detach from a fiber, the ratio of inertial to capillary forces must reach a critical value. The smaller the droplet to fiber size ratio, the higher this critical value will be. This predictive tool was then validated using the size of droplets captured by three marine copepods. This result allows us to predict the size distribution of droplets that will remain captured by filtering appendages, following a quick survey of the filter feeding species in the vicinity of the spill.

Afterward, I studied the capture mechanisms of oil droplets. To do so, the feeding behavior of *Daphnia magna*, *Balanus crenatus* and *Balanus glandula* was observed under the microscope and in a flume using high speed videography to precisely describe capture events. *Daphnia magna* captures droplets using the thick boundary layers around the third and fourth pair of thoracic legs. Thus, the oil droplets are captured without direct contact with the fibers. At low Reynolds number, barnacles capture droplets using a similar process. However, at high Reynolds number, droplets are mainly captured via direct interception. Using scanning electron microscopy and fluorescence microscopy, we observed that the filtering surfaces of the organisms are smooth and extremely lipophobic. Indeed, the contact angles of captured droplets were well above 90°.

Finally, because chemical dispersion is one of the main clean-up methods used after an oil spill, the effect it can have on capture and detachment of droplets needed further research. I studied the impact of a chemical surfactant on the size distribution of oil droplets in the water column and in the gut of *Daphnia magna*. I also compared the detachment conditions of droplets with and without a surfactant present during the mixing of the emulsion. Adding a surfactant significantly reduces and narrows the size distribution of droplets in the water column. With or without a surfactant, the size of ingested droplets remains the same. The presence of a surfactant facilitates droplet detachment from a fiber by lowering the interfacial tension. For similar droplet to fiber size ratios, a chemically dispersed droplet will detach at a lower velocity than a mechanically dispersed droplet.

This research brings a better understanding on how oil droplets are handled by the zooplankton. These results are significant considering that most spilled crude oil enters the marine food webs via this group of organisms. This thesis describes the main mechanisms of capture, detachment and the impact of a surfactant on the latter.

Keywords: zooplankton, fluid mechanics, filter feeding, crude oil, surfactant, Reynolds number, wettability, daphnids, copepods, barnacles

Table des matières

Liste des tableaux

Table des figures

Liste des sigles et des abréviations

Bo	nombre de Bond/Bond number
Ca	nombre capillaire/capillary number
$^{\circ}C$	temperature (Celsius)
D	diffusibilité de particule/particle diffusivity (m^2/s)
DOR	ratio de dispersant et d'huile/dispersant to oil ratio
DOSS	sulfosuccinate de dioctyle et de sodium/dioctyl sulfoccinate sodium salt
F_d	traînée/drag force (N)
F_g	force gravitationnelle/gravitational force (N)
F_b	force de flottabilité/buoyancy forces (N)
fps	images par seconde/frames per second
g	accélération gravitationnelle/gravitational acceleration (m/s^2)
G	intensité du dépôt gravitationnel/dimensionless number for intensity of gravitational deposition
h	épaisseur maximale d'une couche d'huile sur une fibre/maximum thickness of oil coating a fiber (m)
K	constante de Bolzmann/Boltzmann's constant ($g \cdot cm^2 \cdot s^{-2} \cdot^o K^{-}1$)
l	longueur du mouillage sur un fibre/wetting length on a fiber (m)
L	distance inter-fibre/inter-fiber distance (m)
m	masse/mass (kg)
M	molarité/molarity
$MgCl_2$	chlorure de magnésium/magnesium chloride
n	ratio de l'épaisseur de la couche d'huile et de la fibre/dimensionless oil film thickness coating the fiber ($= h/R_f$)
OsO_4	Tetraoxide d'osmium/osmium tetroxide
p	ratio de viscosité huile-eau /oil-to-water viscosity ratio
p	p-value
Pe^{-1}	intensité du mouvement brownien/dimensionless number for intensity of diffusion deposition
r	ratio des rayons/dimensionless radius ratio
$\bar{R}$	intensité de l'interception directe/dimensionless number for intensity of direct interception
R	rayon/radius (m)
Re	nombre de Reynolds/Reynolds number
SEM	microscopie électronique à balayage/scanning electron microscopy
St	nombre de Stokes pour l'intensité de l'interaction inertielle/Stokes number

	for intensity of inertial interaction
T	temperature (Kelvin)
U	vitesse/velocity (m/s)
V	volume d'huile sur une fibre/volume of oil on fiber (m^3)
$\mathbf{v}_T$	vitesse terminale/terminal velocity (m/s)
We	nombre de Weber/Weber number
$\mathbf{x}_s$	distance d'arrêt/stopping distance (m)
δ	épaisseur de la couche limite/boundary layer thickness (m)
θ	angle de contact/contact angle (degrees)
μ	viscosité dynamique/dynamic viscosity $(Pa \cdot s)$
ρ	densité/density (kg/cm^3)
σ	tension de surface/interfacial tension (N/m)
%	Pourcentage

Subscripts

f	fibre/fiber
p	particule/particle
o	gouttelette d'huile/oil droplet
s	solide/solid
w	eau/water

À Catherine et Alice,

Not all those who wander are lost
J.R.R Tolkien - The Fellowship of the Ring

Remerciements

Je tiens tout d'abord à remercier mon directeur de thèse Christopher Cameron, sans qui je ne serais pas le chercheur que je suis aujourd'hui. Merci de tes conseils toujours à propos et du partage de ton expertise lors du travail de terrain. Les solutions les plus utiles sont souvent les plus improvisées ! Tu m'as transmis ta passion pour les invertébrés marins, un monde rempli de surprises et bien souvent méconnu. Combien de fois ai-je du expliquer à ma famille et à mes amis ce qu'est un copépode ! Mais c'est cela qui rend ce domaine si passionnant ; de faire découvrir ces animaux microscopiques qui sont pourtant si nombreux. Je te remercie de m'avoir fait confiance avec ce projet reliant la physique et la biologie. Si je rédige ceci aujourd'hui, c'est que tu as réussi à développer chez moi un sens de la curiosité, de la persévance et de l'autonomie, trois traits qui, selon moi, sont des plus importants chez un chercheur. Nul ne sait mieux que toi à quel point il est difficile de filmer ces petits animaux, mais nous avons réussi !

Un grand merci à Sasan Mehrabian pour ses connaissances indispensables sur la mécanique des fluides. Sans toi, il est certain que mon doctorat aurait pris quelques années supplémentaires. Merci de m'avoir pris sous ton aile lors de ma première année et de m'avoir appris les bases de cette branche de la physique dont je n'en connaissais que le nom. Merci de m'avoir initié à l'éditeur LaTeX, cela a grandement facilité la rédaction de ma thèse. Merci à Anaïs Tétrault, Diane Olivares et Arena Ramos pour leurs contributions à mon projet. Vous avez non seulement aidé à la collecte de données, mais vous avez été mes cobayes pour mes premières expériences de supervision de stage.

Je tiens à remercier Roxanne Maranger et Stéphane Etienne pour votre présence et participation à mon comité-conseil. Merci à Sandra Binning et à David Rival pour leur implication lors de mon examen de synthèse. Merci à Colin Favret, à Jean-François Lapierre et à Frédérick Gosselin pour leurs commentaires lors de la révision de ma thèse.

Comme la grande majorité des thèses, celle-ci ne s'est pas faite sans embuche et difficulté. Le plus grand merci aux deux femmes de ma vie, Catherine et Alice. Catherine, tu as su m'épauler tout au long de mon parcours académique, que ce soit lors de mes accomplissements ou lors des moments de doute et de stress. Merci d'avoir plongé avec moi dans cette aventure, car un doctorat est loin d'être une expérience que l'on vit seul. Merci de m'avoir poussé à accomplir le mieux de moi-même et de toujours avoir les bons mots. Du fond du coeur, je te remercie pour tous tes sacrifices, en tant que mère, conjointe, meilleure amie et confidante. Ce doctorat t'appartient tout autant.

Merci à ma famille et à mes amis pour le soutien et l'aide continue. Un merci tout spécial à Sophie, Stéphane, Claire, Philippe, Annick et Henriette. Sans vous, cette thèse serait loin d'être terminée. Merci à Jean-Michel Brunet pour ton temps de relecture et de révision. Merci à Patrick Groulx pour ton support moral et tes conseils en analyses statistiques. Ton tour approche !

Merci à tous les étudiants à qui j'ai eu le bonheur d'enseigner. Au plaisir de se recroiser dans les années à venir !

Merci à Alestorm, Amon Amarth, Behemoth, Black Sabbath, Children of Bodom, Death, Death Angel, Dimmu Borgir, Dissection, Dream Theater, Epica, Ghost, Haken, Immortal, Lamb of God, Mayhem, Megadeth, Metallica, Opeth, Slayer, Symphony X, Testament, Tool, Tyr, Wintersun et bien d'autres pour les nombreuses heures de correction, de rédaction et d'expérimention passées avec vous !

Je tiens à remercier le CRSNG, la FRQNT et la FESP pour le financement de notre projet et de mes études doctorales. Merci à Westwind Sealabs pour votre aide dans la collecte des spécimens. Merci au Darling Marine Center de nous avoir ouvert ses portes et son estuaire pour notre collecte de données et nos expérimentations. Votre personnel expert et vos installations ont grandement facilité et accéléré notre travail. Merci à tous les éditeurs et examinateurs impliqués dans la publications de nos articles. Vos conseils ont sans aucun doute contribué à l'amélioration de cette thèse.

Chapitre 1.

Introduction

Les organismes filtreurs sont omniprésents dans la plupart des écosystèmes aquatiques et sont une partie intégrante des réseaux trophiques. La diversité d'organismes filtreurs, qu'elle soit morphologique, taxonomique ou fonctionnelle, est immense (Jørgensen, 1983). Les rôles d'un organisme filtreur sont nombreux, tout dépendant de sa manière de filtrer la colonne d'eau, de sa taille et de la morphologie de ses appendices filtreurs. Les services écologiques apportés par ces espèces incluent mais ne se limitent certainement pas à : l'amélioration globale de la qualité des eaux côtières ainsi que le contrôle biotique des algues nocives (Wilkinson et al., 1996; Nakamura and Kerciku, 2000), la séquestration du carbone marin (Cavan et al., 2017; Jónasdóttir et al., 2015; Steinberg and Landry, 2017) et même la prévention d'éclosions virales dans les écosystèmes marins (Bidegain et al., 2016). Les organismes filtreurs utilisent leurs appendices ramifiés afin de capturer les particules en suspension dans la colonne d'eau. Ces organismes sont généralement des consommateurs primaires, car le phytoplancton en suspension est une partie importante de leur alimentation. L'alimentation par filtration est un mécanisme qui est présent dans la plupart des embranchements aquatiques (*e.g.* Porifera, Cnidaria, Annelida, Mollusca, Echinodermata, Arthropoda) (Riisgård and Larsen, 2000). Il s'agit donc d'un groupe fonctionnel important car, dans plusieurs systèmes, il est l'intermédiaire entre le phytoplancton et les plus grands consommateurs (Wallace et al., 1977). Les organismes filtreurs représentent donc souvent le niveau trophique où la majorité des nutriments provenant des producteurs primaires est assimilée.

L'alimentation par filtration est possible via plusieurs mécanismes. Par contre, ils ont tous certains éléments en commun. La filtration et la capture des particules en suspension est généralement faite par des cils, flagelles ou une patte modifiée. Ces structures sont nombreuses et regroupées sur un appendice, qui lui agira en tant que tamis ou palme (Koehl, 1993). Lorsqu'un appendice agit comme un tamis, le fluide est poussé entre les nombreuses fibres de l'appendice et les particules entrant en contact avec un collecteur seront capturées.

De plus, si une particule est plus grosse que l'écart entre deux collecteurs, celle-ci peut être capturée via tamissage. Un appendice filtreur peut aussi agir en tant que palme lorsqu'il déplace une parcelle de fluide avec son mouvement. Lorsque c'est le cas, les particules sont capturées dans la couche limite de l'appendice, puis transportées vers la bouche et ingérées. Donc, les particules capturées par ce mécanisme ne contactent pas directement le collecteur, mais sont plutôt figées dans la parcelle de fluide transportée par le mouvement de l'appendice. Le comportement de l'appendice est dicté par plusieurs facteurs, comme la viscosité du milieu, la vitesse d'écoulement, la taille et l'écart entre les collecteurs et les caractéristiques hydrophobes/hydrophiles de l'appendice (Koehl, 2001).

La majorité de l'alimentation des organismes filtreurs se compose de particules solides, *e.g.* algues unicellulaires, protistes, débris organiques divers, etc. Par contre, ces filtreurs vont aussi s'alimenter de gouttelettes de lipides (Conover, 1971; Sargent and Falk-Petersen, 1988). Ces gouttelettes vont être présentes dans la colonne d'eau sous forme de microparticules, pouvant atteindre une fraction de micron en diamètre. Ces particules liquides ont des origines et des fonctions multiples. Par exemple, pour les crustacés de la sous-classe Copepoda, les gouttelettes d'huile ingérées peuvent être utilisées lors du processus de gamétogenèse (Demott and Dörthe, 1997; Jónasdóttir, 1999), en tant que réserve d'énergie lors de la diapause et comme moyen de réguler leur flottabilité lors de la migration verticale journalière (Kattner et al., 2007; Visser and Jónasdóttir, 1999). Ces gouttelettes d'huile peuvent provenir de la dégradation naturelle d'un animal ou d'une plante. Elles peuvent aussi être relachées dans l'environnement lors d'un déversement de pétrole.

Lors d'un déversement de pétrole, le pétrole brut se répend à la surface de l'eau, car sa masse volumique est plus faible que celle de l'eau salée. Pour éviter que de grands volumes d'hydrocarbures ne se rendent aux écosystèmes côtiers, les gouvernements et les compagnies pétrolières ont recours à plusieurs méthodes, *e.g.* l'utilisation de bouées flottantes, de filets à très fines mailles et les surfactants (Jordan and Payne, 1980; Nelson-Smith, 1972). Un surfactant est une molécule amphiphile, c'est-à-dire qu'elle possède une tête hydrophile et une queue hydrophobe. Ainsi, en présence d'hydrocarbures, le surfactant englobe les particules de pétrole avec ses queues hydrophobes et empêche la coalescence des gouttelettes dans la colonne d'eau. Ce surfactant va aussi diminuer la tension de surface entre l'eau et le pétrole, ce qui va faciliter la rupture des grosses gouttelettes en microparticules et créer une

émulsion d'huile dans l'eau (Li and Garrett, 1998). Dépendamment du surfactant utilisé, des propriétés chimiques des hydrocarbures et du niveau de turbulence dans la colonne d'eau, la taille des gouttelettes d'huile peut varier entre 1 et 100 μm de diamètre (Almeda et al., 2014a; Conover, 1971). Il est donc tout à fait possible que la taille de ces gouttelettes coincide avec la taille des particules ingérées par les organismes filtreurs. *Daphnia magna*, par exemple, ingère en moyenne des particules variant entre 3 et 30 μm de diamètre (Geller and Müller, 1981). Par contre, cet intervalle varie énormément d'une espèce à l'autre, et durant le développement d'un individu, car celui-ci peut passer par plusieurs stades larvaires et car la taille des particules ingérées est fortement corrélée à la taille de l'individu.

L'écotoxicologie des hydrocarbures, ainsi que les mécanismes de capture des particules solides, sont très bien documentés et étudiés, mais nos connaissance sur la capture de particules liquides reste pour le moment limitées (Hansen et al., 2015; Rubenstein and Koehl, 1977). Le pétrole déversé dans nos environnements aquatiques est lourd en conséquences et c'est majoritairement au niveau des organismes filtreurs qu'il fait son entrée dans les réseaux trophiques (Almeda et al., 2016; Gemmell et al., 2016; Nepstad et al., 2015). En étudiant la capture, la filtration et le détachement de ces particules de pétrole, il devient alors possible de comprendre comment le pétrole brut entre dans les réseaux trophiques aquatiques.

1.1. Concepts généraux de la mécanique des fluides

Bien que plusieurs de ces mécanismes seront décrits en détails dans le **chapitre 2**, il est tout de même important d'introduire ici quelques concepts de mécanique des fluides permettant une bonne compréhension de l'alimentation par filtration.

1.1.1. Nombre de Reynolds

Le nombre de Reynolds est un nombre sans dimension illustrant le rapport entre les forces inertielles et les forces visqueuses d'un système. Le nombre de Reynolds peut être obtenu de la façon suivante :

$$Re = \frac{\rho_w U_w (2R_f)}{\mu_w} \tag{1.1}$$

Où ρ_w est la densité de l'eau, U_w est la vitesse d'écoulement, R_f est le rayon du collecteur et μ_w est la viscosité de l'eau. Donc, plus la viscosité du milieu est élevée, plus le nombre de Reynolds sera petit. On obtient la même tendance si l'on diminue l'échelle ou la vitesse

de l'écoulement du fluide. Ainsi, lorsque le nombre de Reynolds du système étudié est en-dessous de 1, les forces visqueuses dominent sur les forces inertielles et inversement lorsqu'il est au-dessus de 1. Ce nombre permet de décrire rapidement les conditions d'un système et de prédire le comportement d'un appendice filtreur, *i.e.* un regroupement de collecteurs. Le nombre de Reynolds d'un setae peut varier énormément en fonction de sa morphologie, du comportement de l'individu et des conditions environnementales. En effet, tout dépendant de l'espèce et du milieu, celui-ci varie entre 10^{-5} et 10^{1} (Cheer and Koehl, 1987a; Rubenstein and Koehl, 1977). De façon générale, le nombre permet de déterminer les conditions critiques où un système donné passe d'un écoulement laminaire à turbulent (Schlichting and Gersten, 2016). Dans le cadre de cette thèse, le nombre de Reynolds est utilisé comme valeur charnière entre les mécanismes «palme» et «tamis» d'un appendice filtreur (Koehl, 2004). Ainsi, en calculant le nombre de Reynolds d'un setae ou d'un sétule, nous pouvons prédire le comportement du fluide lorsqu'il s'approchera de l'appendice filtreur et les mécanismes par lesquels les gouttelettes seront capturés.

1.1.2. La couche limite

Lorsqu'un fluide s'écoule sur une surface, la couche de fluide en contact avec celle-ci ne va pas à la même vitesse que celle qui est libre dans la colonne d'eau. Il existe donc un gradient de vitesse d'écoulement entre le courant et la surface étudiée. Ce phénomène est la couche limite. La couche limite est en fait la distance minimale à laquelle on doit s'éloigner de la surface afin d'atteindre la vitesse d'écoulement réelle du courant. Lorsqu'il est question de l'écoulement autour d'un cylindre, comme c'est le cas dans ce projet, l'épaisseur de cette couche limite peut varier en fonction de la taille dudit cylindre et du nombre de Reynolds (Sumer et al., 2006). Plus le nombre de Reynolds est haut, moins cette couche limite sera épaisse, donc on atteindra la vitesse d'écoulement réelle plus près du collecteur. La vitesse d'écoulement du fluide à la surface du cylindre est près de zéro et augmente lorsque l'on s'en éloigne, jusqu'à ce qu'elle atteigne celle du courant. Ce concept est extrêmement important lorsque l'on veut caractériser le mode de filtration d'un appendice filtreur, car la couche limite peut parfois dicter la façon dont les particules vont être capturées, *i.e.* mécanismes «palme» et «tamis». En effet, si la couche limite est épaisse et que les collecteurs sont suffisamment rapprochés, il n'y aura pas ou très peu de fluide qui passera au travers de l'appendice filtreur.

L'épaisseur de la couche limite peut être estimée de la façon suivante (LaBarbera, 1984) :

$$\delta = D/\sqrt{Re} \tag{1.2}$$

Où D est le diamètre de la fibre collectrice et Re est le nombre de Reynolds.

1.1.3. Interactions avec une seule fibre

Bien que les appendices des organismes filtreurs opèrent généralement à un nombre de Reynolds très faible et possèdent une couche limite épaisse, il est tout de même possible qu'une particule entre en contact avec une fibre collectrice. Rubenstein and Koehl (1977) ont adapté le modèle théorique de filtration des aérosols aux systèmes biologiques et ont proposé cinq mécanismes de capture possibles. Ceux-ci sont l'interaction inertielle, le dépôt gravitationnel, l'interception directe, le dépôt par diffusion et l'attraction électrostatique. Le **chapitre 2** décrira ces mécanismes et leurs équations plus en détail. Il est par contre pertinent de les introduire succinctement ici afin de comprendre les objectifs et hypothèses des chapitres de recherche. Pour le moment, les mécanismes principaux de capture de particules liquides sont peu étudiés et observés. Connaître les principaux mécanismes de capture d'une gouttelette individuelle par une fibre nous informe sur les facteurs qui favorisent sa rétention par l'organisme ou son retour dans la colonne d'eau.

L'interaction inertielle se produit lorsque la particule est capturée par une fibre en raison de l'inertie de son mouvement (Boudina et al., 2020; Cai and Yu, 1988). Lorsque le fluide passe près de la fibre, il est dévié de chaque côté de celle-ci et cela crée une courbe dans l'écoulement du fluide. Ainsi, la particule se trouvant dans ce courant est donc contrainte à suivre cette déviation. Cependant, tout dépendant de son diamètre et de la vitesse du courant, il se peut que l'inertie de son mouvement l'empêche de suivre cette déviation et la particule se retrouvera donc en contact avec la fibre (Rubenstein and Koehl, 1977).

Le dépôt gravitationnel se produit lorsqu'il existe une différence de densité entre la particule et le fluide dans lequel elle se trouve. Ainsi, celle-ci aura tendance à couler ou à remonter. Lorsque le fluide diverge de chaque côté de la fibre collectrice, la particule peut passer au-dessus ou en-dessous de la fibre. Il est alors possible que la particule dévie de sa trajectoire en raison de la différence en densité. Si cette déviation est suffisante, la particule se retrouvera à

une distance au moins équivalente à son rayon et entrera en contact avec la fibre (Rubenstein and Koehl, 1977).

Si la particule possède la même densité que le fluide, elle est dite en flottabilité neutre. Une particule en flottabilité neutre suivra les profils du courant sans déviation. Ainsi, si le courant apporte la particule à une distance d'au moins son rayon, celle-ci sera interceptée par la fibre (Boudina et al., 2020). Ce mécanisme de capture se nomme l'interception directe. Il est semblable aux deux autres mécanismes précédents, seulement l'interception directe se fait sans aucune déviation de la particule.

Le mouvement brownien est un mouvement stochastique d'une particule causé par ses collisions avec d'autres particules en suspension (Saffman and Delbrück, 1975). Chaque collision de la particule va causer un changement de trajectoire, résultant en un parcours complètement aléatoire. Ainsi, la trajectoire de ces particules diffère des profils de courant. Le mécanisme de dépôt par diffusion se fait par ce type de mouvement. En effet, puisqu'une particule suivant une trajectoire brownienne se déplace aléatoirement, il est possible qu'elle entre en contact avec une fibre (Rubenstein and Koehl, 1977). Ce mécanisme est à considérer lorsque les particules sont extrêmement petites et/ou lorsque l'écoulement est quasi inexistant.

Le dernier mécanisme est celui de l'attraction électrostatique. La capture d'une particule par ce mécanisme se produit lorsqu'il y a une différence de charge entre la particule et la fibre. La particule se trouve alors attirée et peut être capturée par la fibre. Par contre, puisque l'eau salée contient énormément d'ions de différentes charges, il est fort probable que ce mécanisme de capture ne soit pas celui qui prédomine dans le milieu marin, mais il pourrait potentiellement jouer un rôle dans les milieux lacustres (Rubenstein and Koehl, 1977).

1.1.4. Interactions avec deux fibres ou plus

La très grande majorité des organismes filtreurs marins se nourrissent en utilisant des structures extrêmement similaires. Malgré la grande diversité de taxons où l'on retrouve cette méthode d'alimentation, les structures permettant la filtration des particules en suspension sont généralement cylindriques et parfois ramifiées, ce qui suggère que le nombre de mécanismes de capture est peu nombreux et partagés par plusieurs (LaBarbera, 1984). Ainsi, même si les animaux filtreurs n'ont pas tous la même taille (*e.g.* un cilié de quelques

microns et une baleine à fanons de plusieurs mètres) ou le même mode de vie (sessile, libre ou parasitaire), les mêmes phénomènes peuvent être observés et quantifiés sur plusieurs échelles différentes à l'aide de nombres sans dimension (*e.g.* nombre de Reynolds, nombre capillaire, nombre de Weber).

Lorsque la capture des particules dans la colonne d'eau se fait à l'aide d'un arrangement d'appendices filtreurs, ceux-ci peuvent se comporter soit à la manière d'une palme, soit à la manière d'un tamis. Dans un milieu où le nombre de Reynolds est très bas (10^{-3}), donc si l'écoulement du fluide est lent ou si l'échelle étudiée est petite, le fluide se comportera de façon très visqueuse. Ainsi, le fluide aura beaucoup de difficulté à passer entre les fibres de l'appendice filtreur et celui-ci se comportera à la manière d'une palme (Koehl, 2004). Le fluide, qui contient des particules en suspension, sera donc poussé vers la bouche de l'animal par le mouvement de l'appendice. Les particules en suspension ne pourront pas passer entre les deux appendices, et cela même si elles sont plus petites que l'espacement entre deux fibres (Koehl, 1993). En effet, tout dépendant de l'espacement entre les deux fibres adjacentes de l'appendice, leurs couches limites respectives peuvent potentiellement se chevaucher, réduisant drastiquement la vitesse d'écoulement et la quantité de fluide pouvant passer au travers de l'appendice, capturant ainsi les particules sans même y toucher. Ceci est illustré dans la Figure 1.1, où l'intensité de l'écoulement est clairement plus faible lorsque le fluide doit passer entre deux fibres que lorsqu'il n'y est pas contraint. L'efficacité de ce mécanisme dépend du nombre de Reynolds, mais aussi du rapport entre l'espacement entre deux fibres et le diamètre d'une fibre ; soit le rapport Gap/Diameter (G/D). On caractérise donc ce mécanisme de «palme», car la très grande majorité du fluide sera poussée par l'assemblage de fibres, de la même manière qu'un nageur va pousser l'eau avec une palme. Un organisme filtrant selon ce mécanisme ne touche pas directement les particules. Ainsi, la mouillabilité d'un appendice est moins importante dans un tel contexte d'alimentation. Pour la grande majorité des espèces de zooplanctons filtreurs, le mode exact de filtration demeure inconnu, en raison de la difficulté à filmer adéquatement le mouvement d'un appendice (mouvement très rapide et à petite échelle). Les travaux de cette thèse viennent augmenter nos connaissances sur la méthode de filtration des daphnies, des copépodes et des balanes.

À l'inverse, si l'écoulement du fluide est rapide ou si la structure est plus grosse, alors le nombre de Reynolds sera plus élevé. Lorsque cela est le cas, la quantité de fluide capable de

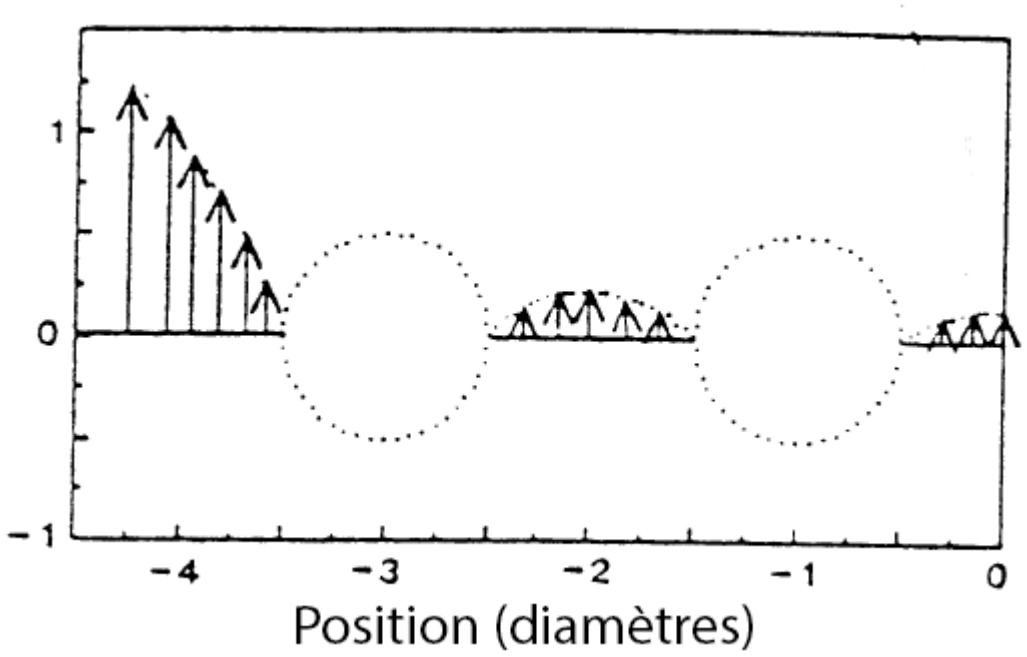

Figure 1.1. Schématisation de l'écoulement d'un fluide entre deux fibres cylindriques en coupe transversale. La longueur des flèches est corrélée à l'intensité de l'écoulement. Cette figure est tirée de Koehl (1993).

passer entre les différentes fibres de l'appendice est plus grande et celui-ci agit alors comme un tamis. En effet, les particules en suspension vont passer entre les fibres de l'appendice et seront retenues si leur taille est suffisante.

Puisque ces deux méthodes de filtration sont très différentes l'une de l'autre, il a longtemps été considéré que le comportement palme ou tamis était une caractéristique intrinsèque de l'appendice. Cependant, Koehl (2001) a démontré que c'est en fait les caractéristiques du milieu qui déterminent le comportement de l'appendice. Elle a été en mesure d'induire les deux comportements chez un même appendice filtreur en changeant seulement les paramètres du milieu environnant.

La Figure 1.2 démontre bien cette transition entre les deux comportements. L'abscisse de la figure montre le changement dans le nombre de Reynolds du milieu. Donc, plus l'axe se déplace vers la droite, moins le milieu est visqueux ou encore plus l'écoulement du fluide est rapide. En ordonnée est représenté le changement dans la proportion du fluide passant entre les deux fibres d'un appendice. Un appendice laissant une grande proportion de fluide passer se comporterait à la manière d'un tamis, comme mentionné précédemment. Chaque courbe de la figure est en fait un différent appendice possédant son propre rapport Gap/Diameter

(G/D). Il s'agit du rapport entre l'espacement de deux fibres et le diamètre d'une fibre. Dans un milieu où le nombre de Reynolds est faible (entre 10^{-5} et 10^{-3}), le changement dans la quantité de liquide passant entre les fibres est très faible, et cela peu importe le rapport G/D. Cela implique donc que dans de tels milieux, un changement morphologique apporte peu de changements dans le comportement de l'appendice. On obtient donc un appendice qui agit comme une palme. Par contre, dans des milieux moins visqueux (Re = 10^{-2}), le changement dans la proportion de liquide passant entre les fibres est important. Puisque le milieu est moins visqueux et que l'écoulement du fluide est plus rapide, il est plus facile pour le fluide de passer entre les fibres de l'appendice. Il se comportera donc plus comme un tamis. Cette transition entre ces deux mécanismes survient lorsque le nombre de Reynolds est entre 10^{-2} et 1 (Koehl, 2001). Il est aussi possible de remarquer que ce changement survient plus tôt pour des rapports G/D plus élevés. Cela s'explique par le fait que les fibres de l'appendice sont plus espacées ce qui facilite le passage du fluide. Donc, dans un milieu où le nombre de Reynolds est élevé, il est possible de voir les deux mécanismes chez un seul appendice (tout dépendant du rapport G/D), ce qui n'était pas le cas pour un nombre de Reynolds très bas. Dans de tels milieux, un changement morphologique peut avoir une grande influence sur la fonction de l'appendice.

Ce phénomène est plus facilement observable dans la Figure 1.3. Prenons la courbe correspondant à Re = 10^{-5}. Peu importe le rapport G/D, la proportion de liquide passant entre les fibres reste relativement constante. Un changement morphologique n'affecte donc pas la fonction de l'appendice. Par contre, pour la courbe $Re = 0{,}5$, un léger changement morphologique affecte énormément la quantité de fluide passant entre les fibres de l'appendice, donc son comportement. Il est alors possible pour un animal de changer la fonction de ses appendices (palme et tamis) en changeant la vitesse de mouvement de ceux-ci. Un changement dans la vitesse de mouvement augmenterait la vitesse d'écoulement du fluide, ce qui ferait augmenter le nombre de Reynolds et la proportion de fluide pouvant passer entre les fibres de l'appendice (changement strictement vertical dans la Figure 1.3). C'est en fait de cette façon qu'un copépode calanoïde nettoie ses appendices filtreurs (Koehl and Strickler, 1981).

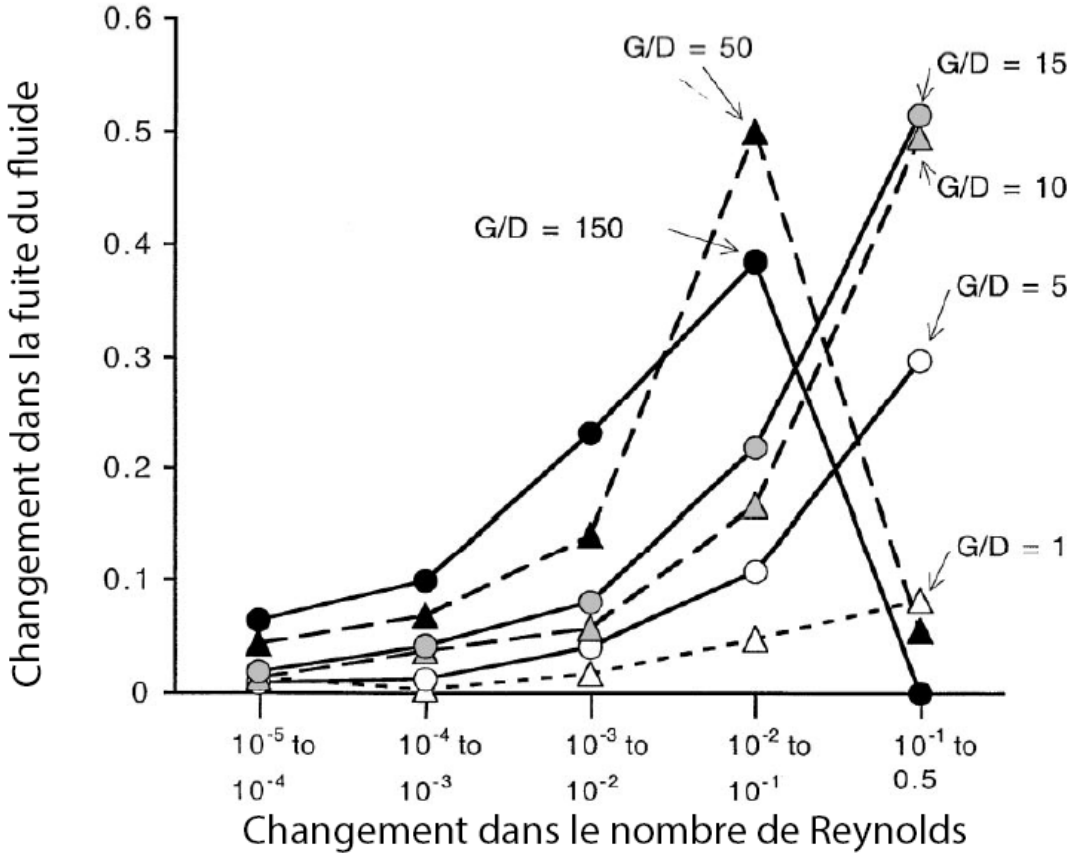

Figure 1.2. Changement dans la proportion de fluide passant entre les fibres d'un appendice en fonction du changement dans le nombre de Reynolds du milieu, selon différents ratio G/D. Cette figure est tirée de Koehl (2001).

1.2. L'alimentation par filtration chez les invertébrés marins

1.2.1. Porifera

Les éponges sont des organismes benthiques se nourrissant de la matière en suspension dans la colonne d'eau. Ce sont des organismes que l'on retrouve dans la grande majorité des écosystèmes marins et dulcicoles. Malgré la simplicité de leur plan d'organisation, les éponges apportent des bénéfices importants aux milieux aquatiques, de la bioremédiation des eaux polluées (Ledda et al., 2014; Stabili et al., 2006) à la prévention de la prolifération d'algues nocives dans les milieux côtiers (Peterson et al., 2006). Leur capacité de filtration est telle qu'elles peuvent filtrer leur volume en eau toutes les 5 secondes (Reiswig, 1974).

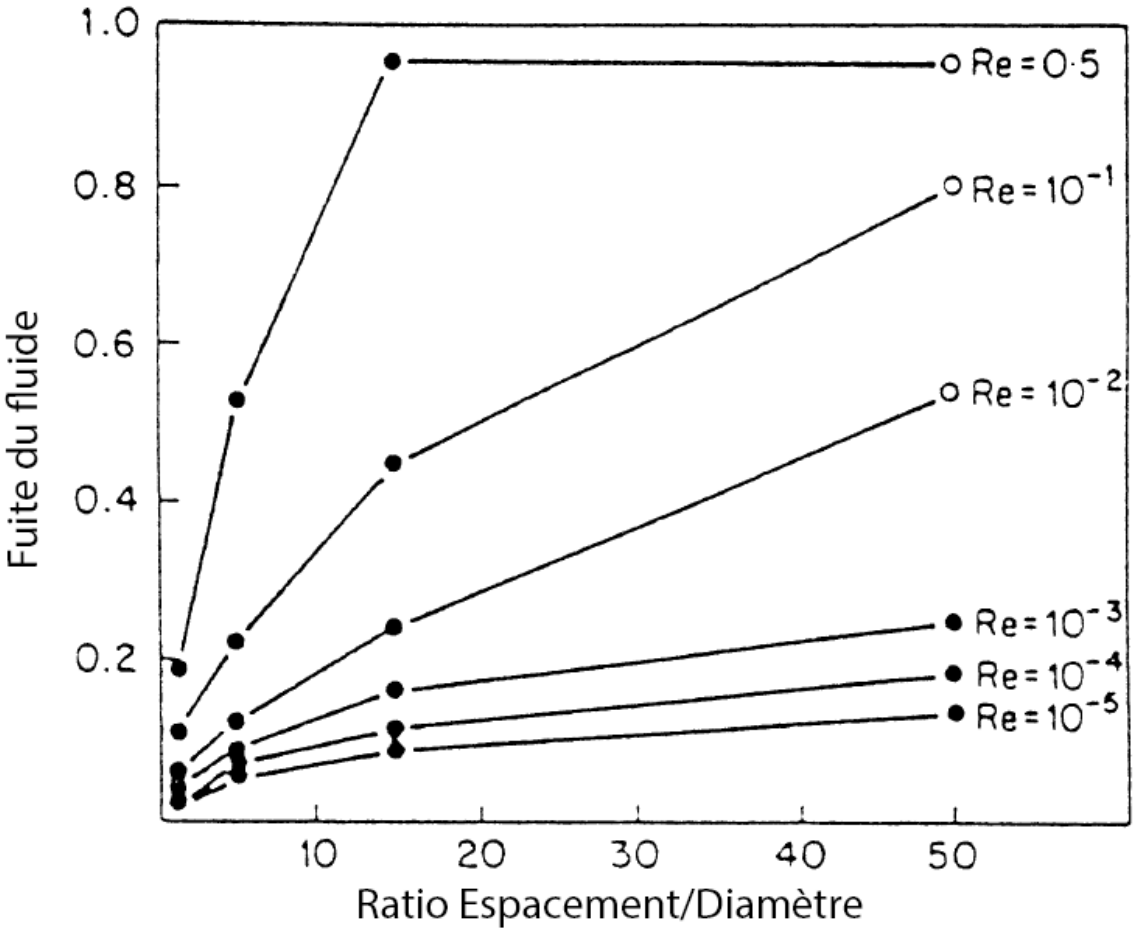

Figure 1.3. Changement dans la proportion de fluide passant entre les fibres d'un appendice en fonction du rapport G/D de celui-ci, selon différents nombres de Reynolds. Cette figure est tirée de Koehl (1993).

Les éponges se nourrissent en créant un courant qui entrera premièrement par les nombreux pores inhalants pour ensuite passer dans les chambres choanocytaires, qui sont tapissées de choanocytes. Ce sont ces cellules spécialisées fixées à la paroi intérieure de la chambre qui créent le courant de filtration par le biais de leur flagelle. Les particules en suspension entreront dans les canaux de l'éponge et seront capturées et phagocytées par les choanocytes. Seules les particules de 5 μm et moins de diamètre seront capturées par ce mécanisme (Reiswig, 1971). Les particules de plus grande taille peuvent être capturées par les archéocytes situés dans les canaux inhalants, en amont des chambres choanocytaires. L'eau filtrée est ensuite poussée dans l'atrium de l'éponge et retourne dans la colonne d'eau via l'oscule. Même si ce processus semble simple, plusieurs adaptations notables permettent à l'éponge

d'augmenter son efficacité de filtration. Ces adaptations sont possibles par le principe de la continuité. En effet, la vitesse d'écoulement de l'eau n'est pas constante au travers des différentes structures. Lorsque l'eau arrive aux chambres choanocytaires, le diamètre des canaux augmentent drastiquement et cela à pour cause de ralentir la vitesse d'écoulement. Ce changement permet alors plus de temps et de surface de contact entre les choanocytes et l'eau, maximisant le potentiel filtrant de l'éponge. Jørgensen (1955) estime à 12 $\mu m/s$ la vitesse d'écoulement de l'eau dans ces chambres de filtration. L'éponge a aussi développé une adaptation lui permettant d'éviter de filtrer le même volume d'eau plusieurs fois. En effet, la superficie totale des pores inhalants est environ 6000 fois supérieure à celle de l'oscule, *i.e.* le pore exhalant (Vogel, 1994). Par le principe de continuité, la vitesse d'écoulement à la sortie de l'éponge est donc supérieure à celle d'entrée. Cela a pour effet de propulser le fluide loin de l'éponge, prévenant ainsi une seconde filtration d'un volume d'eau dont les particules ont déjà été capturées. Ainsi, la taille et la forme des différentes structures filtrantes de l'éponge permettent un changement de vélocité et maximisent l'alimentation de l'organisme (Brusca et al., 2003).

1.2.2. Mollusca

L'alimentation par filtration est présente chez au moins deux classes de mollusques, les gastéropodes et les bivalves (Brusca et al., 2003). Ces derniers utilisent leurs cténidies hautement repliées afin d'augmenter la surface de contact avec l'eau filtrée (Jørgensen, 1996). L'eau est pompée par le siphon inhalant et ses cirri pour ensuite se rendre dans la cavité du manteau. À cet endroit, l'eau est en contact avec les nombreux replis des cténidies, qui vont agir à titre de tamis et sélectionner les particules de tailles adéquates. Pour les espèces ne vivant pas dans les sédiments, le mouvement des cirri est suffisant pour créer un flot continu, car les valves sont généralement ouvertes et l'eau passe naturellement dans l'organisme (Jørgensen et al., 1986). Les particules sélectionnées et retenues sont alors transportées à la bouche par le mouvement de cils, où elles seront goûtées et potentiellement ingérées. Advenant une obstruction des siphons, le courant généré peut être inversé pour déloger les débris (Morton, 1990). Les bivalves possèdent aussi des palpes labiaux qui aident à acheminer les particules filtrées vers la bouche en créant un courant à l'intérieur de la cavité du manteau. Une fois que les particules de tailles adéquates ont été retenues par les cténidies,

l'eau filtrée est alors expulsée par le siphon exhalant. Cette méthode de filtration est extrêmement efficace, puisqu'elle permet de retenir 100% des particules de 4 μm de diamètre, et approximativement 50% des particules de moins de 1 μm (Shumway et al., 1985). En fait, cette méthode est si efficace qu'il est estimé que la population de moule zébrée de la baie de Saginaw est capable de filtrer l'entiereté du volume de la baie en une journée (Fanslow et al., 1995). C'est en partie pourquoi cette espèce est devenue une espèce envahissante et un problème important dans le secteur des Grands Lacs.

1.2.3. Echinodermata

Les cinq classes d'échinodermes possèdent des espèces qui se nourrissent en filtrant la colonne d'eau ou en capturant la matière en suspension. Cependant, celles-ci ne créent généralement pas leur propre courant comme c'est le cas chez les mollusques ou certains arthropodes. Les crinoïdes, par exemple, ont de nombreux bras ramifiées de pinnules ressemblant à un cirre de balane. En positionnant ces bras perpendiculairement au courant, l'organisme peut capturer les particules dans la colonne d'eau. Le mouvement des podia apportera ensuite les particules capturées vers le sillon ambulacraire, puis la bouche (Meyer, 1979). Ces podias peuvent aussi sécréter un mucus aussi capable de capturer des particules.

Les podias sont une structure utilisée à des fins de locomotion et d'alimentation chez les quatre autres classes d'échinodermes, *i.e.* Asteroidea, Ophiuroidea, Echinoidea et Holothuroidea. Même s'il s'agit d'une espèce prédatrice, comme une étoile de mer par exemple, celle-ci peut utiliser ses podias pour capturer une source alimentaire supplémentaire. Pour les espèces de l'ordre Clypeasteroidea (dollar des sables), les particules en suspension sont leur unique source de nutriments (Brusca et al., 2003). En effet, ceux-ci vont s'orienter face au courant et partiellement s'enfouir dans les sédiments. Les particules en suspension vont alors frapper la surface de l'oursin et seront capturées par les podias, puis transportées vers la bouche via les cinq sillons ambulacraires. Cette stratégie n'implique pas la création d'un courant par l'individu, mais il y a tout de même une sélection active de la taille et de la composition des particules.

Toutefois, il est important de noter que ces organismes, comme bien d'autres embranchements d'invertébrés, ont un stade larvaire. En effet, ces larves sont généralement trop petites pour être des prédateurs et vont donc se nourrir de la matière en suspension. Pour ce

faire, les larves d'échinodermes possèdent une bande ciliée autour de la bouche qui s'étend sur chaques bras, contrairement aux les larves de mollusques, d'annélides et d'autres embranchements qui ont deux bandes ciliées circulaires anti-parallèles autour du corps (Strathmann, 1978). Ces cils battent en vagues métachronales afin de créer un léger courant près de la larve (Hart, 1991; Strathmann, 1982). Lorsqu'une particule approche d'un cil, celui-ci va rapidement inverser son mouvement, ce qui va capturer la particule et inverser le courant localement. Puis, les cils suivant vont à leur tour inverser leur mouvement, ce qui va créer une zone où le courant est inversé (Strathmann, 1971; Strathmann et al., 1972). Cette vague métachronale inversée et locale va permettre à la particule capturée de se diriger vers la bouche où elle sera alors potentiellement ingérée. Les particules capturées ainsi sont principalement capturées par interception directe et ce mécanisme est présent chez au moins dix autres embranchements (Strathmann, 1978).

1.2.4. Arthropoda

Le sous-embranchement Crustacea est un des groupes taxonomique les plus diversifiés, qu'il soit question du nombre d'espèces ou des adaptations. La diversité morphologique est énorme et plusieurs méthodes d'alimentation ont émergé. Par contre, plusieurs clades de crustacés se nourrissent en filtrant la colonne d'eau. Décrire tous ces clades serait impossible. Ici, nous discuterons de trois clades filtreurs que l'on retrouve dans la plupart des écosystèmes aquatiques, c'est-à-dire les daphnies, les balanes et les copépodes.

Les espèces du genre *Daphnia*, ou puces d'eau, sont des organismes filtreurs. Ces organismes utilisent leurs pattes thoraciques modifiées en peignes pour filtrer la colonne d'eau. Celles-ci sont imbriquées l'une dans l'autre, telles les barbules d'une plume d'oiseaux, formant un réseau filtreur. Ces pattes sont capables de filtrer des particules allant de 1 à 25 μm, dépendamment de l'espèce et de la taille de l'individu (Dodson, 2004). En effet, de manière générale, un individu plus grand sera capable de filtrer des particules de plus grande taille (LaBarbera, 1984; Porter et al., 1983; Riisgård and Larsen, 2010). Ces appendices filtreurs peuvent augmenter leur rythme de battement en fonction de la quantité de matière en suspension, mais ils vont rapidement atteindre un plateau, où une augmentation de la concentration en nutriments n'aura plus d'effet sur la vitesse de battement (McMahon and Rigler, 1963). Ces quatre paires de pattes thoraciques modifées sont ramifiées de setae, qui eux-mêmes sont

ramifiés de sétules. Ces fibres vont permettre un flot uniforme et guider les particules vers le sillon central situé entre les deux valves de l'organisme (Lampert and Brendelberger, 1996). Porter et al. (1983) ont observé que les particules ayant des caractéristiques hydrophobes sont capturées plus aisément que les particules hydrophiles. Ils suggèrent que les particules hydrophiles, puisqu'elles sont généralement chargées, seraient repoussées ioniquement par la structure en peignes des daphnies.

Les membres de la sous-classe Cirripedia sont, tout comme les daphnies, des organismes filtreurs. Ils ont donc plusieurs adaptations morphologiques leur permettant de s'alimenter via la colonne d'eau. Les balanes sont des organismes sessiles possédant un corps hautement réduit encapsulé dans une carapace de calcaire. Leurs pattes, elles, sont hautement modifiées et ramifiées afin de permettre une filtration efficace. Leurs appendices, les cirres, sont aussi ramifiés de setae et de sétules. Les balanes ont développé deux modes d'alimentation dépendamment du flot externe, soit la filtration active et la filtration passive (Pechenik, 2014). Dépendamment de la taille de l'individu et de son espèce, il existe une vitesse d'écoulement charnière séparant ces deux modes d'alimentation (Arsenault et al., 2001; Marchinko and Palmer, 2003; Trager and Genin, 1993). Lorsque celle-ci est sous ce seuil, les balanes vont filtrer activement en ouvrant et en étirant leurs cirri dans la colonne d'eau pour ensuite les ramener dans leur carapace. Puisque cela s'effectue généralement à basse vitesse d'écoulement, le nombre de Reynolds du système est bas et les appendices des balanes fonctionnent plutôt comme des palmes (Vo et al., 2018). Les particules qui seront capturées ainsi sont capturées par la couche limite autour des cirri et des setae, pour être ensuite acheminées près de la bouche et ingérées. Lorsque la vitesse d'écoulement est supérieure au seuil critique, les balanes vont filtrer passivement, c'est-à-dire qu'elles vont laisser leurs cirri à l'extérieur de leur carapace et les positionner perpendiculairement au courant. En raison d'une plus grande vitesse d'écoulement, les couches limites autour des collecteurs sont plus minces et plus de fluide peut passer entre les cirri et les setae. Donc, les particules peuvent être capturées directement par les fibres via tamissage, interception directe ou interaction inertielle. Les balanes sont des espèces pour lesquelles la plasticité phénotypique est extrêmement importante. Celles-ci vivent dans des milieux où les courants peuvent varier de $0.05\,m/s$ à $10\,m/s$ (Li and Denny, 2004). En effet, les individus de *Balanus glandula* vivant en milieux sujets à de forts courants auront généralement des cirres plus larges et plus courts afin de mieux

résister à la force de traînée (Marchinko and Palmer, 2003). Leurs carapaces auront aussi une morphologie plus applatie et seront plus épaisses qu'en milieux calmes afin de mieux résister à la force brute des vagues (Pentcheff, 1991). Les individus vivant dans des environnements plus calmes auront des cirres minces et allongés afin d'augmenter le potentiel de filtration.

Les copépodes représentent une importante proportion de la biomasse aquatique. Ils utilisent leurs pattes thoraciques ainsi que leurs antennes pour activement filtrer la colonne d'eau. En effet, en raison de leur petite taille, *i.e.* une fraction de millimètre à $1\,cm$, ces organismes ne peuvent pas compter sur le courant de la colonne d'eau. Leurs appendices filtreurs fonctionnent à un nombre de Reynolds entre 10^{-2} à 10^{-1}, rendant le milieu environnant très visqueux. Le consensus scientifique du modèle de filtration des copépodes a longtemps été celui d'un gyre de chaque côté de l'animal compressé sur l'axe ventro-dorsal de celui-ci. Les deux gyres se rencontreraient sous le ventre de l'animal, où les appendices sont situés. Or, ces observations étaient faites sous le microscope à l'aide de lames et de lamelles, ce qui compressait les courants filtreurs en deux dimensions. La vidéographie haute vitesse a permi d'observer les mécanismes en trois dimensions (Koehl and Strickler, 1981). Le cycle de fitration débute avec un mouvement médio-latéral de la première maxille. Ce mouvement crée un vide sous l'animal et a pour effet d'aspirer une parcelle d'eau. Par la suite, la deuxième paire de maxille va effectuer un mouvement antério-ventral extrêmement rapide, ce qui aura pour effet d'augmenter localement le nombre de Reynolds près de ces fibres. Ce changement dans le régime d'écoulement va changer le comportement de l'appendice, c'est-à-dire que le fluide ne passera plus de chaque côté de celui-ci mais bien entre les différents setae. Ce mouvement, ajouté au fait que les premières maxilles sont situées de chaque côté, force l'eau à passer au travers des deuxièmes maxilles et ainsi être tamissée. Les particules de tailles adéquates seront capturées par cette appendice et transportées vers la bouche. Les copépodes filtreurs ont aussi développé un mécanisme de rejet, si la particule capturée est trop grosse ou est jugée non comestible. Dans une telle situation, la deuxième maxille, *i.e.* l'appendice ayant capturé la particule, s'éloigne lentement du ventre de l'organisme, entraînant avec elle la particule en question dans sa couche limite. Puis, l'animal écartera ses setae et rammènera rapidement l'appendice vers son ventre, ce qui libérera les particules jugées inintéressantes. Ce mouvement permettra aux particules de passer entre les fibres de la maxille et de réintégrer la colonne d'eau. La filtration de la colonne d'eau

par les copépodes est un bon exemple d'un système où la variation du rapport G/D permet une oscillation dans les comportements de l'appendice. Ceci est important, car les travaux présentés aux **Chapitre 4** propose un mécanisme similaire lors de la filtration des balanes à nombre de Reynolds intermédiaires.

1.3. Organisation, objectifs et hypothèses de la thèse

Mon projet vise à intégrer les principes de mécanique des fluides détaillés dans ce chapitre à la capture et au détachement de gouttelettes d'huile par les animaux filtreurs aquatiques. En effet, plusieurs études ont été faites, mais en considérant seulement les particules solides. Ici, nous tentons d'étudier la capture de particules liquides. Les paramètres et les facteurs contrôllant la capture et le détachement des gouttelettes de pétrole sont pour la plupart inconnus lorsqu'il est question de systèmes biologiques. Cette thèse est composée de quatre objectifs globaux. Ces objectifs sont les suivants :

(1) Déterminer si les organismes filtreurs vont ingérer les gouttelettes d'huile en émulsion dans la colonne d'eau et établir la distribution de taille des gouttelettes capturées et ingérées.

(2) Observer la capture et le détachement de gouttelettes d'huile et déterminer les paramètres qui contrôlent ces différents mécanismes.

(3) Déterminer les caractères lipophobes/hydrophobes et la mouillabilité des appendices des organismes filtreurs.

(4) Déterminer l'effet que les surfactants ont sur le détachement des gouttelettes d'huile et sur les distributions de taille des gouttelettes ingérées.

Avec ces quatre objectifs, nous obtenons une vue globale des mécanismes de filtration de gouttelettes d'huile par les organismes filtreurs. Les mécanismes de capture et de détachement sont étudiés et les tailles des gouttelettes ingérées et capturées sont mesurées et comparées. Les surfaces collectrices des organismes filtreurs sont observées et décrites, et la lipophobicité de celles-ci est discutée. Finalement, l'effet de l'ajout d'un surfactant, la méthode de remédiation la plus utilisée, est étudié et discuté.

De manière générale, trois clades d'organismes filtreurs ont été séléctionnés pour les travaux de cette thèse. Deux espèces de balanes, *Balanus crenatus* et *Balanus glandula*, sont des filtreurs sessiles. Ces espèces ont été choisies, car elles sont facilement accessibles et ont une grande distribution. De plus, les balanes sont souvent utilisées lors des recherches

sur la capture de particules et de la filtration d'un fluide par des collecteurs biologiques. Elles sont également d'excellentes candidates, car ce sont des animaux fixés au substrat, ce qui rend l'observation beaucoup plus aisée. *Daphnia magna* est aussi une espèce étudiée extensivement en raison de sa facilité d'élevage et de son rôle écologique. Dans le cadre de cette thèse, *D. magna* est un excellent candidat, car son exosquelette est translucide. Cela permet une observation des appendices filtreurs sous le microscope et une visualisation des gouttelettes ingérées dans le tube digestif. Plusieurs espèces de copépodes calanoïdes provenant du Golfe du Maine ont aussi été filmées à l'aide d'une caméra haute-vitesse. Ces trois espèces ont été collectées au large et identifiées comme étant *Acartia tonsa, Calanus finmarchicus, et Centropages typicus*. Ce clade filtreur a été considéré pour nos études en raison de son rôle de consommateur primaire important, de sa biomasse marine énorme et de ses mécanismes de filtration bien documentés.

Le **chapitre 1** de cette thèse a pour objectif de présenter les concepts de base liés à la mécanique des fluides et les principaux mécanismes de capture de particules. Les éléments présentés dans ce chapitre servent de base essentielle sur laquelle repose mes travaux de doctorat. En effet, mes recherches m'ont permis d'utiliser ces concepts établis et de les appliquer aux particules liquides, soient les gouttelettes d'huile et de pétrole. J'y présente aussi une revue non exhaustive des principaux clades d'invertébrés filtreurs, afin d'avoir une idée générale de la diversité morphologique et des différentes stratégies d'alimentation.

Puisque cette thèse tente d'unir la biologie et la mécanique des fluides, il est nécessaire de connaître les bases de chacune de ces disciplines. Le **chapitre 2** consiste en une revue de la littérature existante sur la capture et la filtration des particules, d'un point de vue mécanique et biologique. C'est dans ce chapitre que les hypothèses principales de la thèse sont construites. J'y introduis les principaux mécanismes de capture de particules, la création et la stabilité d'une émulsion huile/eau ainsi que le concept de mouillabilité. Les objectifs de ce chapitre sont de (1) décrire les concepts importants en mécanique des fluides, (2) d'établir le cadre conceptuel et théorique du reste de la thèse et (3) de déterminer l'effet que la densité et la tension de surface d'une huile ont sur son volume critique de détachement.

Le **chapitre 3** reprend les concepts du chapitre précédent, mais ceux-ci sont maintenant appliqués sur des systèmes biologiques. On y teste et valide ici quelques hypothèses théoriques introduites au chapitre 2. Une chambre de courant a été construite afin (1) de déterminer

les paramètres régissant le détachement de gouttelettes d'huile. Nous avons aussi tenté (2) de quantifier l'ingestion de ces particules chez trois espèces de copépodes calanoïdes. Les résultats de ce chapitre ont permis de déterminer que le ratio de taille entre la gouttelette et la fibre collectrice ainsi que la vitesse d'écoulement sont deux variables importantes dans la prédiction du détachement d'une gouttelette. Ces recherches ont aussi mené à la création d'une courbe permettant de prédire si une gouttelette restera capturée ou si elle réintégrera la colonne d'eau en utilisant des nombres sans dimension. Ces expérimentations ont été reproduites en utilisant des cirres de balanes, afin de déterminer si la surface des structures biologiques a un impact sur le détachement de gouttelettes.

Le **chapitre 4** est davantage concentré sur les mécanismes de capture des gouttelettes. En effet, il est important de comprendre ce qui permet le détachement d'une particule, mais aussi ce qui favorise sa capture. La vidéographie haute vitesse a été utilisée afin de décrire les méthodes de filtration de ces organismes. Un microscope électronique à balayage a été utilisé afin d'observer et de décrire les surfaces collectrices. Ainsi, les objectifs de ce chapitre sont (1) de déterminer les principaux mécanismes de capture chez deux espèces de balanes, *Balanus crenatus* et *Balanus glandula*, et chez le cladocère *Daphnia magna*. J'ai aussi (2) étudié la mouillabilité des surfaces collectrices de ces organismes et ses potentielles implications sur la capture d'huile. Il est attendu que les balanes vont capturer les gouttelettes dans un large éventail de nombre de Reynolds et selon les mécanismes tamis et palme. L'interception directe sera le mécanisme de capture le plus probable. *Daphnia magna* capturera des particules de pétrole dans les couches limites de ses pattes thoraciques. Les espèces étudiées auront des surfaces très lipophobes et les gouttelettes capturées montreront des angles de contact au-dessus de 90°.

Le **chapitre 5** vise à déterminer l'effet qu'un surfactant, lorsque mélangé à l'émulsion de pétrole brut dans l'eau, a sur la taille des gouttettes ingérées par *Daphnia magna*, des gouttelettes dans la colonne d'eau, ainsi que sur les conditions critiques de détachement. En effet, la chambre de courant et les expérimentations du **chapitre 3** sont ici reprises en y ajoutant un surfactant. L'idée est de définir si ces molécules amphiphiles ont un effet sur le détachement d'une gouttelette d'un collecteur. Les objectifs de ce chapitre sont donc de (1) déterminer l'effet d'un surfactant sur le détachement du pétrole brut et de (2) comparer la taille des gouttelettes ingérées par *Daphnia magna* avec ou sans la présence d'un surfactant

dans l'émulsion. Il est attendu que la présence d'un surfactant facilitera le détachement, car celui-ci diminuera la tension de surface entre le pétrole et l'eau environnante. De plus, la présence d'un surfactant diminuera la taille des gouttelettes présentes dans la colonne d'eau.

Le **chapitre 6** conclut cette thèse. On y retrouve une discussion des implications des résultats principaux obtenus dans les chapitres précédents. Les contributions de cette thèse à la littérature scientifique y sont discutées et plusieurs pistes de recherches futures sont proposées.

Chapitre 2 .

The mechanisms of filter feeding on oil droplets : Theoretical considerations

par

Sasan Mehrabian[1], Francis Letendre[1] et Christopher B. Cameron[1]

([1]) Département de sciences biologiques, Complexe des sciences, Université de Montréal, 1375 Avenue Thérèse-Lavoie-Roux, Montréal, Québec, H2V 0B3, Canada

Cet article a été publié dans :

Marine Environmental Research (2018), 135 : 29-42

DOI :/10.1016/j.marenvres.2018.01.006

Cet article a été modifié pour les besoins de la thèse.

Rôle des auteurs

Sasan Mehrabian : Conceptualisation du désign expérimental, conception de la méthodologie, revue de littérature, collecte des données, analyse des données, rédaction du manuscript

Francis Letendre : Conceptualisation du désign expérimental, conception de la méthodologie, revue de littérature, maintien des cultures de zooplancton, collecte des données, analyse des données, création des figures, rédaction du manuscript, soumission et révision du manuscript

Christopher Cameron : Conceptualisation du désign expérimental, validation des résultats, rédaction du manuscript, révision du manuscript, supervision et administration du projet, acquisition du financement

Résumé.

Les organismes filtreurs capturent les particules en suspension dans la colonne d'eau en utilisant des cils ou des appendices ramifiés d'un ensemble de fibres. Cet article résume les modèles théoriques utilisés lors de l'observations de la capture de particules et lors de l'estimation de l'intensité relative des différents mécanismes. Nous discutons aussi du cadre théorique nécessaire à l'étude et à la caractérisation de la filtration de particules d'huile. Dans les environnements aquatiques et marins, les gouttelettes d'huile sont relâchées dans la colonne d'eau lors de la décomposition naturelle d'organismes ou lors d'activités anthropiques. Les paramètres clés régissant la capture d'une gouttelette d'huile sont la taille de la particule, la vitesse d'écoulement, le ratio de viscosité et de tension de surface huile-eau, la différence de densité des deux fluides et la mouillabilité de l'appendice. Suite à un événement de capture, les forces capillaires rentiennent la gouttelette au lieu de contact grâce à la tension d'interface entre l'eau et l'huile. Si la gouttelette est soumise à des forces externes comme la force gravitationelle (différence de densité) ou les forces inertielles et visqueuses, la gouttelette pourra alors être déformée et potentiellement se détacher du collecteur et retourner dans la colonne d'eau. Nous montrons ici la capture de telles gouttelettes par *Daphnia magna* et la balane *Balanus glandula* ainsi que les implications écologiques qu'une telle capture peut avoir dans nos milieux aquatiques. La connaissance de ces mécanismes de capture permettent la création d'une fondation solide sur laquelle il devient possible de bâtir des recherches sur les différents modes de filtration de ces gouttelettes d'huile.

Mots clés : alimentation par filtration, nombre de Reynolds, nombre capillaire, nombre de Bond, déversements de pétrole brut, émulsion

Abstract.

Filter feeding animals capture food particles and oil droplets from the fluid environment using cilia or appendages composed of arrays of fibers. Here we review the theoretical models that have provided a foundation for observations on the efficiency of particle capture. We then provide the mathematical theoretical framework to characterize the efficient filtration of oil droplets. In the aquatic and marine environments oil droplets are released from the decay of organisms or as hydrocarbons. Droplet size and flow velocity, oil-to-water viscosity ratio, oil-water interfacial tension, oil and water density difference, and the surface wettability, or surface texture, of the filter fiber are the key parameters for oil droplet capture. Following capture, capillary force maintains the droplet at its location due to the oil-water interfacial tension. If the oil-coated fiber is subject to any external force such as viscous or gravitational forces, it may deform and separate from the fiber and re-enter the fluid stream. We show oil droplet capture in *Daphnia* and the barnacle *Balanus glandula*, and outline some of the ecological unknowns regarding oil capture in the oceans. Awareness of these mechanisms and their interrelationships will provide a foundation for investigations into the efficiency of various modes of filter feeding on oil droplets.

Keywords: filter feeding, suspension feeding, Reynolds number, capillary number, Bond number, oil spills, emulsion

2.1. Introduction

Filter feeders use a diverse range of filamentous appendages to capture food from the water (Riisgård and Larsen, 2010). Although most appendages essentially consist of arrays of bristles or cylinders, some behave as sieves to intercept particles from suspension passing through (e.g. bands of stiff cilia, setae, or mucous nets), while others create feeding currents or act as paddles to direct pockets of fluid for further processing (e.g. flagella, cirri, or tentacles) (Riisgård and Larsen, 2010; Vogel, 1994). With respect to food capture (i.e. particles or oil droplets), the structure and motion of the fibres, and their interaction with the flow of water, form the essence of the filtering mechanism. The capture of particles has been explored from theoretical (Rubenstein and Koehl, 1977), experimental (Koehl, 2004; Labarbera, 1978; Riisgård and Larsen, 2010), and modeling perspectives (Koehl, 2003; Shimeta and Jumars, 1991; Vogel, 1994; Spielman and Goren, 1968). Experimental (Almeda et al., 2013) and modelling (Nepstad et al., 2015) perspectives of oil capture by filter feeders have been addressed. Here we provide a theoretical basis of oil droplet capture and retention by filter feeding appendages. From here onwards, we adopt the terminology of those that contributed before us, and refer to these diverse appendages as fibers, and treat them as cylindrical, solid, surfaces.

Oil droplets in the aquatic and marine environment may be derived from animals, plants, algae, microbes or fossil hydrocarbons. Oil may be nutritionally rich or a toxic component of the filter feeding diet (Conover, 1971; Jónasdóttir, 1999; Miller et al., 2000; Friedman and Strickler, 1975). It is used by zooplankton to modulate buoyancy (Miller et al., 2000; Thorisson, 2006), and as part of the diet of copepods it increases the production of eggs (Thorisson, 2006; Jónasdóttir, 1999; Demott and Dörthe, 1997). The capture and ingestion of oil, most significantly by zooplankton, provides the entry point into the aquatic food webs that can terminate with top predators including humans (Turner and Ferrante, 1979; Longhurst and Williams, 1992). Oil that is pelletized into fecal castings is a key link in the global carbon cycle (Siegel et al., 2014). Oil occurs in aquatic environments as large surface slicks, as sub-surface blobs, down to micron-sized oil droplets. Droplets form due to the natural shear created by waves, or natural and industrial surfactants (dispersant) (Rico-Martínez et al., 2013). The ingestion of micron-sized oil droplets, those within the size range consumed by filter feeders, is significant and documented (Rico-Martínez et al., 2013;

Almeda et al., 2014a, 2013), but the interaction between these organisms and the oil particles are not. The mechanics of filter feeding on micron-sized droplets, by animal appendages, is lesser known, and is the subject of this review.

Oil-water-fiber interaction is a complex concept and requires an extensive review of the fundamentals of fluid dynamics and interface science. In Sect. 2.2, we review the theoretical basis of solid particle capture from a fluid dynamic perspective, that includes a discussion of the mechanisms of particle capture introduced to the biology community by Rubenstein and Koehl (1977). In Sect. 2.3 a comprehensive review to colloid and interface science is provided. Some of the practical processes and problems that relate the science of emulsion and wettability to aquatic animals is given. In Sect. 2.4, the capture and release mechanisms of oil droplet by fibers are discussed. We introduce the role of different parameters including oil-to-water viscosity ratio, oil-water interfacial tension, oil-water density difference, and the wettability of the fiber on the success of oil droplet capture and detachment. The capturing and detachment of an oil droplet from a fiber is quantified using appropriate dimensionless numbers. Finally in Sect. 2.5, real examples of oil droplets interacting with *Daphnia* and barnacles are shown.

2.2. Mechanisms of solid particle capture by fibers : a review

2.2.1. Capture by single fiber

Rubenstein and Koehl (1977) introduced a set of simplified equations, to the biology community, that form the basis of particle capture by fibers and pores. Particles may be captured (filtered) through inertial interaction, gravitational deposition, direct interception, diffusion deposition, or sieving. They proposed non-dimensional numbers to estimate the encounter efficiency "intensities" of filtration for different mechanisms. The proposed dimensionless numbers account for filter size, particle size, fluid viscosity and velocity and other parameters, and remain the fundamental tools of most present-day animal-fluid studies.

Fluid mechanical models of filter feeding generally assume a steady, viscous, incompressible flow with free stream velocity (U_w) over a smooth, stationary cylinder with infinite length, and the particle is spherical, and flows in the direction of the free stream normal to

the axis of the cylinder (Fig. 2.1a). This model requires the knowledge of two well-known problems in the literature of fluid dynamics : 1) Viscous flow over a cylinder, and 2) viscous flow over a spherical solid particle. These problems are summarized in Fig. 2.1.

Consider the motion of a particle with radius R_p, volume V, density ρ_p and mass m_p moving at velocity U_p in a viscous fluid (e.g. water) having viscosity and density of μ_w and ρ_w, respectively, flow at velocity of U_w. The particle is under the influence of gravity in the y-direction, where g is the gravitational acceleration. At low Reynolds numbers (Stokes' low-Reynolds number solution), the force balance on the moving particle in vector form is :

$$m_p \frac{d\vec{U}}{dt} = F_d + F_g + F_b = -6\pi\mu_w R_p(\vec{U_p} - \vec{U_w}) + m_p g + V g \rho_p \tag{2.1}$$

The left side of Eq. 2.1 describes the acceleration of the moving particle ($\frac{d\mathbf{U}}{dt}$), where m_p is the mass of the particle, F_d is the drag force, F_g is the gravitational force anf F_b is the buoyancy force. The right side of Eq. 2.1 is the sum of all external forces (i.e, drag, gravitational and buoyancy forces). Drag force always exists whenever there is a velocity difference between the particle and the free stream flow, and the negative sign implies that the drag force is in the opposite direction of the flow. After simplifying Eq. 2.1 using some mathematical maneuvers (see Chen (1955); Harrop and Stenhouse (1969); Lee and Liu (1982); Yeh and Liu (1974) for details), the stopping distance and terminal velocity of a particle moving in a fluid is obtained. These two parameters, defined below, are used to determine the efficiency of particle capture by a fiber.

Stopping distance : The distance over which a particle velocity will reach zero ($U_p = 0$) if the fluid flow ceased is known as the stopping distance. The cause of the "ceasing of the flow" can be due to the particle entering the boundary layer of the fiber. The stopping distance is defined as :

$$\mathbf{x}_s = \frac{2R_p^2(\rho_p - \rho_w)U_w}{9\mu_w} \tag{2.2}$$

Terminal velocity : If fluid flow is ceased, after long enough time, the particle will only move in the y-direction and reach a steady velocity that is caused only by gravitational forces, also known as the terminal velocity :

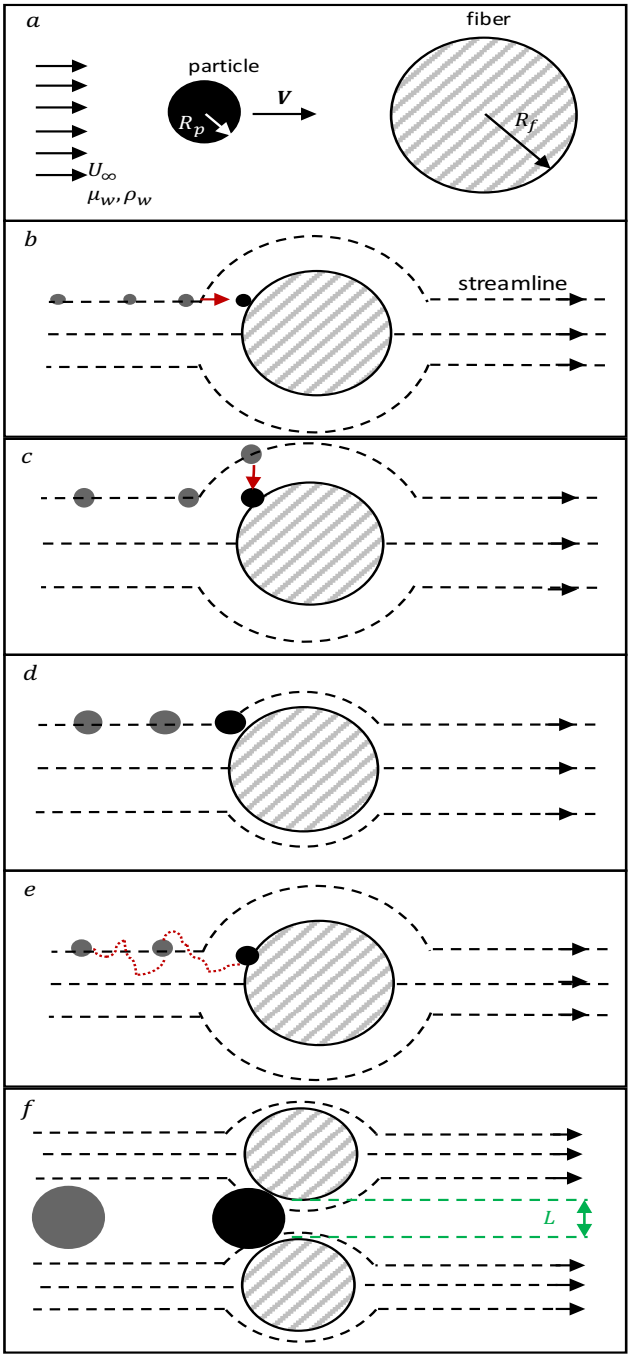

Figure 2.1. (a) Illustration of the movement of a spherical particle with radius R_p approaching a cylindrical fiber with radius R_f in a viscous fluid at velocity V_p. The viscous fluid has a viscosity and density of μ_w and ρ_w, respectively, and flows at velocity U_w. (b) Is illustrates how a particle is captured through Inertial interaction, (c) gravitational settling, (d) direct interception, (e) diffusion deposition, and (f) sieving. Shaded-gray circle represents a cylindrical fiber, black circle represents a solid particle, and dashed lines represent the streamlines of the surrounding fluid (adapted from Rubenstein and Koehl (1977)). Dashed lines indicate streamlines, black arrows show flow direction, black circles are solid particles, and shaded circles are fibers (feeding appendages).

$$\mathbf{v}_T = \frac{2R_p^2(\rho_p - \rho_w)g}{9\mu_w} \tag{2.3}$$

Equations 2.2 and 2.3 are the fundamental equations used to describe the efficiency of particle capture.

Inertial interaction. Particles will follow streamlines in the water column. Given its mass and velocity, the particle can deviate from the streamline if it has sufficient inertia. This deviation will cause the particle to be captured by the fiber (Fig. 2.1b). Inertial interaction is characterized using the Stokes number that is the ratio of the stopping distance to the fiber radius

$$St = \frac{\vec{x_s}}{R_f} = \frac{D_p^2(\rho_p - \rho_w)U_w}{18\mu_w R_f} \tag{2.4}$$

where St is a measure of the particle inertia, D_p is the diameter of the particle and R_f is the radius of the fiber. A particle with low St adopts its motion with the fluid motion and follows the fluid streamlines, while a particle with high $St1$ is dominated by its inertia and will continue its trajectory. Eq. 2.4 shows that the intensity of particle capture through inertial interaction is strongly affected by the free stream velocity U_w and particle size R_p.

Gravitational deposition. Similar to inertial interaction, in gravitational deposition particles can diverge from the streamlines in the horizontal direction due to their density difference with the continuous phase. These particles can cross streamlines and encounter a fiber (see Fig. 2.1c). Rubenstein and Koehl (1977) characterized this mechanism using a dimensionless number that expresses the ratio of the terminal velocity to the free stream velocity :

$$G = \frac{\mathbf{v}_T}{U_p} = \frac{D_p^2(\rho_p - \rho_w)g}{18\mu_w U_w} \tag{2.5}$$

Eq. 2.5 shows that the intensity of particle capture drops when the flow velocity U_w is increased, implying that gravitational deposition takes place mostly at low-velocity environments, unlike the inertial interaction mechanism.

Direct interception. In this mechanism, the particles are assumed to be neutrally buoyant ($\rho_p = \rho_w$) and therefore follow the streamlines of fluid motion (Fig. 2.1d). If a particle is following a fluid streamline and approaches the fiber within one particle radius, it will be

captured by sticking to the filter (Rubenstein and Koehl, 1977; Fenchel, 1980; LaBarbera, 1984; Labarbera, 1978; Shimeta and Jumars, 1991; Chen, 1955). The intensity of direct interception can be characterized using an arbitrary dimensionless number in the form of :

$$\bar{R} = \frac{R_p}{R_f} \tag{2.6}$$

where larger particles and smaller fiber diameters increase the chances of direct interception.

Diffusional deposition. Very small particles have Brownian motion that causes them to diffuse within the continuous phase. The diffusion constant of a spherical particle is given by the Einstein relation in the form of $D = KT/6\pi\mu_w R_p$, where K is the Boltzmann's constant ($= 1.38 \times 10^{-23} J \cdot K^{-1}$), and T is the absolute temperature in Kelvin. Rubenstein and Koehl (1977) stated that if the particle, due to Brownian motion, comes within one particle radius of the fiber it will be captured (Fig. 2.1e). The non-dimensional number that expresses diffusional deposition is the inverse of the Peclet number :

$$Pe^{-1} = \frac{KT}{3\pi\mu_w D_p D_f U_w} \tag{2.7}$$

Eqs. 2.7 suggest that diffusion deposition takes place when the particle size is very small and in low-velocity flow.

Eqs. 2.4 to 2.7 indicate which measurable characteristics of the filter, the particle, and the flow affect the intensity of particle capture. The main mechanism of particle capture can be determined by comparing the magnitude of these dimensionless numbers. Eqs. 2.4 to 2.7 indicate that the particle size R_p and flow velocity U_w are the most important parameters that determine the efficiency of particle capture. The relationship between these parameters and particle capture are summarized in Fig. 2.2. For a given particle size, as the flow velocity is increased the efficiency of inertial interaction is improved, but the efficiencies of gravitational deposition, and diffusion deposition are decreased. Direct interception dominates the flow at some intermediate velocity. Also, for a given flow velocity, as particle size is increased, particle capture through direct interception, inertial interaction, and gravitational deposition is improved, whereas, the efficiency of diffusional deposition is decreased.

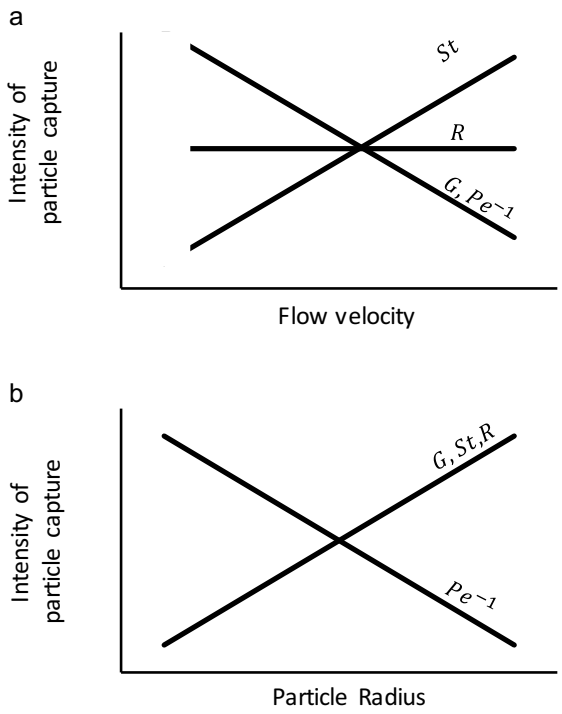

Figure 2.2. Hypothetical effect of (a) flow velocity U_w (b) and particle radius R_p on the intensity of particle capture (adapted from Rubenstein and Koehl (1977)). St is the Stokes number that refers to inertial interaction, G refers to gravitational deposition, $\bar{R}$ refers to direct interception, and Pe^{-1} is the inverse of the Peclet number that refers to diffusional deposition.

2.2.2. Capture by sieving

The capture of a particle between two cylindrical fibers is called sieving. Particle capture through sieving is the most familiar kind of biological filter, where particles greater than inter-fiber distance L can only be caught by the filter (Fig. 2.1f). Particle capture through sieving is characterized by the inter-fiber distance L and a Reynolds number Re defined as :

$$Re = \frac{\rho_w U_w (2R_f)}{\mu_w} \tag{2.8}$$

A biological example of sieving is the particle capture by the second maxillae in copepods. Second maxillae are composed of setae with side fibrous branches, or setules (Koehl and Strickler, 1981). They squeeze and push small parcels of water containing food towards the mouth. The Reynolds number of second maxillae range from 10^{-5} to 10, and behave as sieves in the upper range, and as paddles in the lower range (Koehl, 1993).

Previous authors (Cheer and Koehl, 1987b; Spielman and Goren, 1968; Ayaz and Pedley, 1999; Koo and James, 1973) have used different mathematical models to better understand how fibrous appendages perform biological activities, such as filter feeding. The mathematical models for sieving (summarized by Cheer and Koehl (1987a)) enable us to predict the effect of different parameters, such as flow velocity and size of the appendage, on the efficiency of particle capture by filter feeders. Cheer and Koehl (1987b) modeled the flow between the fibrous structure by considering the fluid motion between and around a pair of cylinders at low Re using a two-dimensional model. The direction of the flow is perpendicular to the line intersecting the centers of the two cylinders, as depicted in Fig. 2.1f. The flow velocity near the cylinders were calculated using the Stokes' low-Reynolds number solution, and the flow velocities far from the cylinders, where inertial forces are noticeable, were calculated using Oseen's low-Reynolds number approximation. The two solutions were matched together using an asymptotic scheme. They quantified their results by defining a leakiness parameter that expresses the ratio of the volume of fluid that flows through the gap between the cylinders in a unit of time to the volume that would have flowed through that gap if there were no cylinders. Leakiness can be described by the amount of fluid that can pass in between two fibers. An appendage that is fully leaky will have the same volume of fluid passing in between fibers than if the fibers were absent. Their results indicated that increasing the Reynolds number leads to higher leakiness, however changes in leakiness becomes highly significant at $Re > 10^{-2}$. Also, leakiness decreases as L becomes smaller, because less fluid can flow. A boundary layer of thickness δ is created when the fluid adjacent to each cylinder experiences the no-slip condition (White and Corfield, 2006). Therefore, the fluid experiences less velocity when travelling between two closely-spaced cylinders compared to widely-spaced cylinders. The boundary layer around a cylinder is on the order of $R_f/\sqrt{Re}$, and increases as Re decreases.

What distinguishes oil droplets from solid particles in marine environment is that they can deform and breakup into smaller droplets or they can coalesce and form bigger droplets depending on their physico-chemical properties (e.g. oil viscosity, oil-water interfacial tension, size, and density) and the flow velocity. We hypothesize that once an oil droplet is captured by a fiber, it may creep down toward the mouth, or deform and detach from the fiber and re-enter the fluid stream. Therefore, the whole capturing process of an oil droplet by filter

feeders is more complex. Very small droplets are not captured since the energy required for capture and ingestion is insufficient compared to the energy provide by that droplet. Nevertheless, if the droplet is too large it can easily deform and detach from the fiber due to external forces that are caused by the flow velocity and gravity. Therefore, for a given filter feeder, there is an intermediate droplet size below which it does not capture, and above which the captured droplet will detach from its feeding appendage. In general, larger filter feeders can filter and ingest larger food particles (Burns, 1968). A similar hypothesis can be made regarding flow velocity. At very low flow velocity, droplets cannot be captured, whereas at very large flow velocities the captured droplet will detach from the feeding appendage. We also hypothesize that filter feeders will have lipophobic surfaces to inhibit oil droplet spreading on their feeding surfaces.

2.3. Colloid and interface science in aquatic biology

The interaction of an oil droplet with a filter feeding organism in water is a three-phase problem, and requires a rigorous understanding of fluid dynamics, interfacial chemistry, surface chemistry, and surface topography. With respect to aquatic (including marine) science, fluid dynamics encompasses the flow of water around the fibrous filters of marine organisms. Interfacial chemistry describes the interaction of oil and water interfaces (e.g. emulsion formation and stability). Surface chemistry describes how liquid and solid interfaces behave when they are in contact (e.g. the degree of a liquid spreading on a surface). Surface topography encompasses the physical shape of the surface (e.g. the roughness of the fibrous feeding appendages). Solid/water/oil systems have been extensively studied in the engineering literature (Mehrabian et al., 2015, 2016; Smith and van de Ven, 1985a,b,c), but less so from a biology perspective. We are aware of no published theoretical work on the subject of fiber/water/oil systems for filter feeders, and experimental work is limited (Almeda et al., 2013). Understanding these complex interactions will help to understand the dynamics of oil droplet capture, and how it changes based on properties of the oil, the appendage(s), and the environmental (e.g. flow) parameters. Theoretically, we should be able to predict what species, based on appendage parameters, capture which oil droplets. This review is significant to understand how oil enters the aquatic food chain, and questions that the utility of

applying oil dispersant, a mixture of emulsifiers and solvents, to breakup oil spills into small droplets, where that may be captured and ingested by zooplankton.

2.3.1. Emulsion

An emulsion is a dispersion of one immiscible liquid within a second liquid, where one of the liquids is water and the other is an oil, including animal, plant, or fossil hydrocarbons. Usually one of the liquids forms the continuous phase, while the other is dispersed into small droplets. Fig. 2.3a illustrates oil-in-water emulsion schematically.

The topic of emulsion has received great attention from the point of view of oil removal from accidental oil spills in seawater (Shen and Yapa, 1988; Li and Garrett, 1998; Rasmussen, 1985). When oil is spilled on the surface of the sea, a thin film (oil slick) spreads over the surface. The spilled oil will cause environmental damage in various forms, impacting organisms that live near the surface (i.e., pleuston) and coastal ecosystems. The motion of the waves and wind cause the oil slick to breakup into smaller droplets and disperse into the sea. A water-in-oil emulsion is formed below the oil slick, and an oil-in-water emulsion is formed at greater depths, where oil is consumed by filter feeders (Rasmussen, 1985). Typically, oil droplet size distributions range from a fraction of a micrometer to millimetres, and more than 90% of filter feeders ingest petroleum oil droplets after a spill (Almeda et al., 2014a). Small droplets are stable, and persist for long periods in the water column because they move slowly, where they can be captured by filter feeders. Larger droplets, if not captured by filter feeders, will eventually rise to the surface where they may be re-emulsified, re-enter the oil slick, or be blown to shore, as has been seen with the contamination of birds and beaches (Li and Garrett, 1998). Removing oil spills is a process that typically takes months to years, and long term studies have shown the adverse effects on aquatic organisms, populations, and ecosystems. Understanding the basic principles and mechanisms in which oil interacts with aquatic organisms is imperative to mitigate the impact of oil on aquatic organisms.

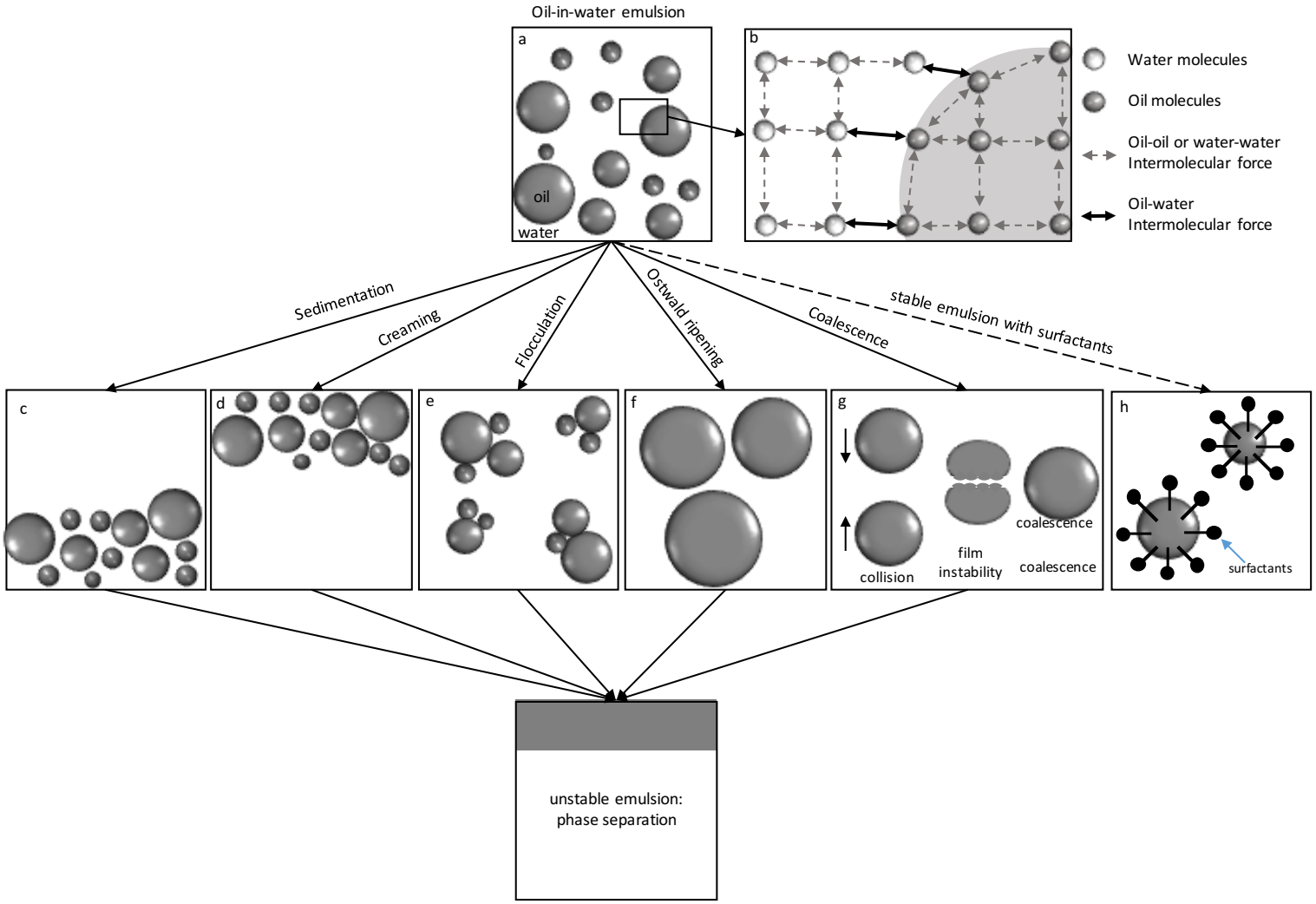

Figure 2.3. (a) Schematic of an oil-in-water emulsion. (b) Intermolecular forces to show the effect of interfacial tension. (c) to (g) Illustrate the mechanisms of unstable emulsions leading to phase separation. (h) Represents stable emulsion due to the presence of surfactants at the oil-water interface.

2.3.1.1. Emulsion Formation. An oil droplet can breakup into smaller droplets (emulsion formation) depending on the balance between the external forces caused by the motion of the surrounding fluid, which act on the oil-water interface and induce deformation and breakup, and the capillary forces, which oppose deformation. The breakup of oil droplets in well-defined flow fields has been explored theoretically and experimentally in the engineering literature (Taylor, 1932, 1934; Kolmogorov, 1949; Hinze, 1955; Walstra, 1993; Grace, 1982; Stone et al., 1986; Stone and Leal, 1990; Bentley and Leal, 1986a,b; Zhao, 2007; Milliken et al., 1993; Eggers and Villermaux, 2008), and the points that are relevant to filter feeding are briefly summarized here.

At low $Re_o = \rho_w U_w (2R_o)/\mu_w$, the external forces that breakup a droplet are viscous forces, of the order of $\mu_w \frac{U_w}{R_o}$. Where μ_w and ρ_w are the viscosity and density of the surrounding fluid (water), respectively, R_o is the radius of the oil droplet, and U_w is the free stream velocity. Viscous forces are due to the friction between the layers, or molecules, of the fluid when in motion. A fluid with higher viscosity has higher friction, and hence higher viscous force.

Capillary forces oppose deformation and strive to maintain a spherical droplet. Capillary forces result from the pressure difference between the inside and outside of the droplet and are defined by the Young-Laplace equation :

$$\Delta P = \sigma_{o/w} \left(\frac{1}{R_1} + \frac{1}{R_2} \right) \tag{2.9}$$

where R_1 and R_2 are the two principle radii of curvatures of the interface. For a spherical droplet $R_1 = R_2 = R_o$, while Eq. 2.9 reduces to $\Delta P = 2\sigma_{o/w}/R_o$. $\sigma_{o/w}$ is the oil-water interfacial tension, and is the intermolecular force (van der Waals forces) acting on the molecules at the interface of the two fluids (Fig.˙ 2.3b). To be more clear, consider the molecules of each fluid : each molecule exhibits intermolecular attractive force from neighbouring molecules from all sides and balance each other, such that the net force acting on any single molecule is zero (indicated in dashed gray arrows in Fig. 2.3b). This is not true for molecules at the interface, because of the difference in the properties and spacing of the molecules on the other side of the interface. The net force acting on the molecules at the interface are not balanced (indicated in black solid arrows in Fig. 2.3b). This imbalance of intermolecular

forces results in contraction of the interface, and the interface will tend to minimize its surface area by adopting a spherical shape. Similarly, for a liquid-solid boundary an imbalance of intermolecular forces characterize the liquid-solid boundary, and the contracting force is called surface tension. Interfacial tension and surface tension are usually represented by σ, and is the force per unit length (N/m). For details on how σ is derived from the laws of thermodynamics see Schramm (2006).

The ratio of viscous forces to capillary forces is expressed as a capillary number (neglecting constants) :

$$Ca = \frac{\textbf{viscous forces}}{\textbf{capillary forces}} = \frac{\mu_w U_w}{\sigma_{o/w}} \tag{2.10}$$

If Ca exceeds a critical capillary number Ca_{crit}, which is a function of the oil-to-water viscosity ratio $p = \mu_o/\mu_w$, the droplet will breakup Grace (1982). Values of Ca_{crit} as function of p for simple shear were presented by Grace (1982). Contrary to common belief, a very low oil viscosity does not necessarily breakup easier. In fact, Grace (1982) show that when oil and water have almost similar viscosities, $0.1 < p < 1$, minimum shear are required to breakup an oil droplet (Ca_{crit} is smallest). Water has a viscosity of 1 cP at 20^oC. Hydrocarbon diesel has a viscosity of 4.15 cP. The plant oils soy, corn, and rapeseed have viscosities of 67.12, 70.29, and 74.19 cP, respectively (Esteban et al., 2012; Knothe and Steidley, 2007). The viscosity of animal fatty acid methyl esters, listed here as systematic (and trivial) names, vary tremendously : methyl decanoate (caprate) is 2.45 cP, methyl 9(Z)-octadecenoate (oleate) is 7.33 cP, and methyl 12-hydroxy-9(Z)-octadecenoate (ricinoleate) is 37.47 cP (see Knothe and Steidley 2007 for more details). Fish oil is between 46-67 cP (Cournarie et al. 2004) and chitosans, from crustaceans, vary between 350 and 460 cP (Maghami and Roberts 1988). Bitumen from Athabasca oil sands is quite viscous and does not flow easily at 20^oC ($\approx 10^5 cP$), but it is usually diluted with solvents to lower its viscosity several orders of magnitude down to $10^2\, cP$ (Mehrabian et al., 2018a; Santos et al., 2014). In short, most naturally occurring oils are prone to breakup into to small droplet sizes in the presence of natural waves, making them available for entry into the aquatic food web.

2.3.1.2. Emulsion stability. Since oil and water are immiscible and have different densities (oil is typically, though not always, lighter), emulsion droplets will rise and reform a layer on the surface. The instability of an oil-in-water emulsion (formation of an oil layer)

can take place through four different mechanisms : creaming or sedimentation, flocculation, Ostwald ripening (disproportionation), or coalescence (Schramm, 2006) (Fig. 2.3). All four mechanisms may occur simultaneously and in any order. Creaming or sedimentation (Fig. 2.3c and d) results from the density difference between the oil and water phase. If the oil is lighter than water, then gravitational forces will move the oil to the top (creaming), and when the oil is heavier than water, the oil will move downwards (sedimentation). The smaller the emulsion size, the slower it will move. The oil droplets will form a closed-packed array at the top or bottom, whereas the remainder of the volume will be occupied by water. Neutrally buoyant droplets will have more opportunity to be captured by filter feeders because they have a longer duration in the environment.

Flocculation (Fig. 2.3e) is the process where droplets aggregate into larger units as a result of attractive van der Waals forces, though individual droplets remain as separate entities. Ostwald ripening (Fig. 2.3f) is a result of the solubility of the liquid phases. Solubility is a chemical property that defines the amount of oil that can dissolve in water through diffusion. Smaller droplets have higher solubility, which causes them to dissolve (disappear) over time. The molecules of the dissolved smaller droplets are then transferred to the larger droplets. Over time, the larger droplets enlarge while the smaller droplets diminish.

Coalescence (Fig. 2.3g) is the process where droplets initially collide and a thin film is formed between them. At a certain separation, where the hydrodynamic forces become significant, the film drains, and narrows asymptotically to zero. As a critical film thickness is reached, instabilities grow at the interface of the film and the droplets coalesce. The capillary number and the oil-to-water viscosity ratio are the two key numbers used to quantify conditions for the coalescence of two droplets (Janssen and Meijer, 1995; Yang et al., 2001).

Emulsion droplets can be stabilized through different mechanism (Aveyard et al., 2003; Binks, 2002; Pichot et al., 2010; Schramm, 2006). The most common mechanism is by the use of surfactants. Surfactants are used to disperse oil spills, or may be a natural component of sea-water (Satpute et al., 2010) and oils, specifically crude oil and bitumen (Gafonova and Yarranton, 2001; Yan et al., 1999). Surfactants tend to be located at the oil-water interface. The phenomenon according to which a surfactant molecule comes from the bulk of a solution to place itself at the interface (with some specific orientation) is called adsorption. Surfactants are amphiphilic molecules that have hydrophobic tails oriented towards the oil

phase, and hydrophilic heads that lie in the water phase (Fig. 2.3h). Once the interface is covered by a monolayer of surfactant molecules, they form a solid-like interfacial film, which retards the rate of droplet-droplet coalescence. The consequence is that surfactants hinder the formation of a single layer on the surface, and maintain oil droplets at small sizes in the water column, where they may be captured and ingested.

2.3.2. Wettability

Wettability is the degree that a liquid spreads on a surface. The topic has received tremendous interest from an applied point of view, and is critical to oil-animal dynamics, including oil droplet capture in aquatic environments. The wettability of an animals appendage is determined by its hydrophobicity, shape, and surface texture.

When oil and water come in contact with a flat surface, they compete for wetting the surface. The one with the higher surface energy wets the surface. An oil may completely wet, partially wet, or remain spherical and not wet the surface (see Fig. 2.4a). Wettability is quantified using the well-known Young equation that describes the balance of the three phase contact :

$$\cos\theta = \frac{\sigma_{s/w} - \sigma_{s/o}}{\sigma_{o/w}} \tag{2.11}$$

where σ are the interfacial tensions and the subscripts s,w,o denote the solid, water, and the oil, respectively. For a drop of oil on a surface in water, the contact angle θ is measured through the oil at the junction of the three phases. If $\theta < 90$ the surface is hydrophobic, and when $\theta > 90$ the surface is hydrophilic. In general, the more hydrophilic a surface, the less oil will spread on it (Cremaldi et al., 2015).

A similar process takes place when a droplet adheres to a cylindrical surface, including a fibrous animal appendage. Fig. 2.4b shows different configurations of a droplet on a fiber, barrel shaped (bottom left) and clam-shell shaped (bottom right). When the contact angle is small the droplet adapts a symmetrical barrel shape with respect to the fiber axis, but when the contact angle is large, the droplet forms an asymmetric shape. In the case of the clam-shell shape, the area of the fiber in contact with the droplet is lower than the case of barrel shape and therefore the strength of adhesion of the drop to the fiber is less. In other words, an oil droplet with a smaller contact area will detach easier than one with a

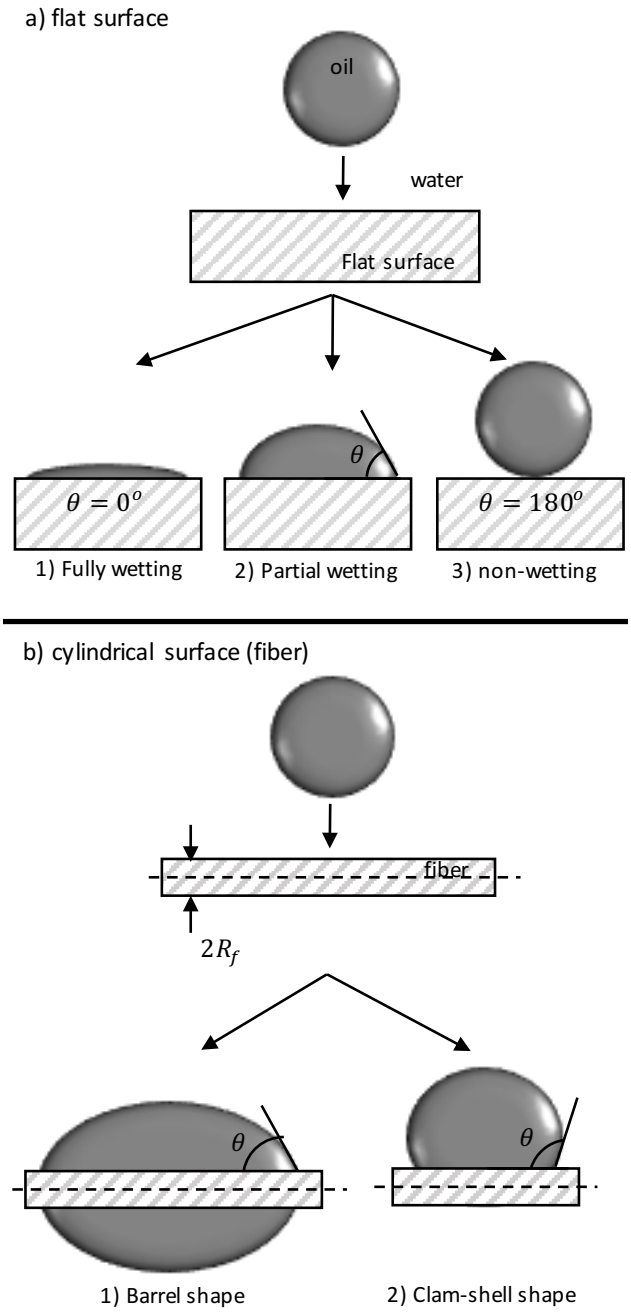

Figure 2.4. The contact angle θ is the angle measured through oil at the junction of the three phases. Different configuration of the shape of an oil droplet on (a) a flat surface, and (b) a cylindrical surface (e.g. fiber).

larger contact area when exposed to external shear (e.g. viscous or gravitational force). The threshold from barrel to clam-shell shape takes place at contact angle of $\theta = 60$ degrees (Carroll, 1976).

Carroll (1976) obtained a solution of the droplet profile of the barrel shape analytically (see Sect. 2.4). One of the features of the barrel shape configuration is that the droplet does not completely spread over the fiber even when $\theta = 0$. Carroll (1981, 1986) then extended his study to examine the evolution of the contact angle in the presence of surfactants. When an oil-coated fiber is put in water containing surfactants, the rate of solubilization depends strongly on the surfactant concentration, oil polarity and molecular weight. The contact angle gradually increases, and the volume of the oil decreases because of oil solubilization, leading to a transformation from barrel to clam-shell shape. Surfactants, then, will reduce the volume of oil adhering to fibrous appendages. This is unlikely to have substantial biological consequences to filter feeders, because the retention time between capture and ingestion is typically low.

The theoretical relation presented in Eq. 2.11 (Young equation) assumes that the surface is chemically homogeneous and topographically smooth. In reality, most solid surfaces, in particular biological ones, have texture. Surface features from the nano-scale to the micro-scale play a role in droplet hydrophobic versus hydrophilic interaction (Quéré 2008). Instead of having one equilibrium contact angle value, most surfaces exhibit a range of contact angles. The texture of the surface will effect the interaction, including oil droplet capture and retention. A complete review of wettability on textured surfaces and the limitations of Wenzel's model is given by Quéré (2008). The addition of surface structure, even on strongly hydrophobic surfaces, can reduce a surface's affinity for oil and prevent adhesion (Cremaldi et al., 2015). A biological example of this phenomenon will be given in the next section.

Carroll (1984) studied the influence of surface roughness on the contact angle, and wettability of fibers, with three different surface configurations : (1) a surface roughened randomly, (2) a surface roughened in the radial direction (axial symmetrical grooving), with cusp-shaped, V-shaped, or semicircular profiles, (3) a surface roughened parallel to the cylinder axis, also with cusp-shaped, V-shaped, or semicircular profiles. He showed that, similar to a smooth fiber, a droplet cannot spread over a fiber even when the contact angle is zero when it is randomly roughened or has axially symmetrical grooves. Alternately, when the the grooving is parallel to the cylinder axis, the droplet will spread when the contact angle is below a critical value. Similarly, the stability of a droplet on mammal hairs depends on the geometrical configuration of grooves in the fiber. An oil droplet placed on a fiber which has

a series of axially symmetrical grooves along its length is not stable with respect to lateral movement along the fiber unless one end of the the droplet is in contact with the edge of one of the grooves Carroll (1989).

A review of the surface texture and the hydrophobicity of bacteria, plants, land and aquatic animals, and marine sea shells (Bhushan 2009; Bhushan and Jung 2011) found several unique adaptations. The dermal denticles of shark skin are grooved parallel to the flow direction of the water, reducing drag, resulting in efficient locomotion (figure 6 of Bhushan and Jung (2011)). Shark skin is moreover hydrophilic, which prevents fouling by marine organisms and oil droplets. The leaves of *Nelumbo nucifera* (lotus) and *Colocasia esculenta* (taro) are water repellent due to the rough surfaces caused by papillose epidermal cells. In addition to the micro-scale roughness, the surface of the papillae are rough, with nano-scale asperities composed of three-dimensional epicuticular waxes, which are long chain hydrophobic hydrocarbons. A water droplet sits on the apex of the nanostructures because air bubbles fill the valleys of the structure under the droplet.

A diversity of surface textures exists among invertebrate suspension feeding fibres, but its role in oil droplet retention and transport is little known. The second maxillae of three species of copepod from the family Pontellidae appear smooth, the primary difference between them is the spacing of the setae and the spacing and length of the setules (Turner and Ferrante 1979). The setae of two scolecitrichid copepods have a rough nano-surface speckeled with electron dense particles (Nishida and Ohtsuka 1981). Oil droplets captured by a calanoid from the Gulf of Maine appear lipophobic (Fig. 2.5a). The fresh water shrimp *Atya innocous* have filtering setae with pores in the surface (Felgenhauer and Abele 1983). Daphnids feed with their antennae and the surface of the antennae of *Daphnia himalaya* are rough and covered with thin setules (Manca et al. 2006). Ostracods filter feed with their maxillae, which are smooth, but for abundant setules (Sandberg 1970). Cirrepedia (barnacles) use cirri to filter feed and the nano-surface texture is generally smooth (Maruzzo et al. 2009), though the micro-surface is rough due to abundant setae. The cirri of *Balanus glandula* are lipophobic because they do not exhibit oil droplet spreading (Fig. 2.5b).

Depending on the flow conditions and the surface texture of the setae, an oil droplet approaching a series of setae will 1) be captured by a single seta, 2) or be captured between two setea (i.e. sieving), or 3) it will pass through or around the setae. The capture of an oil

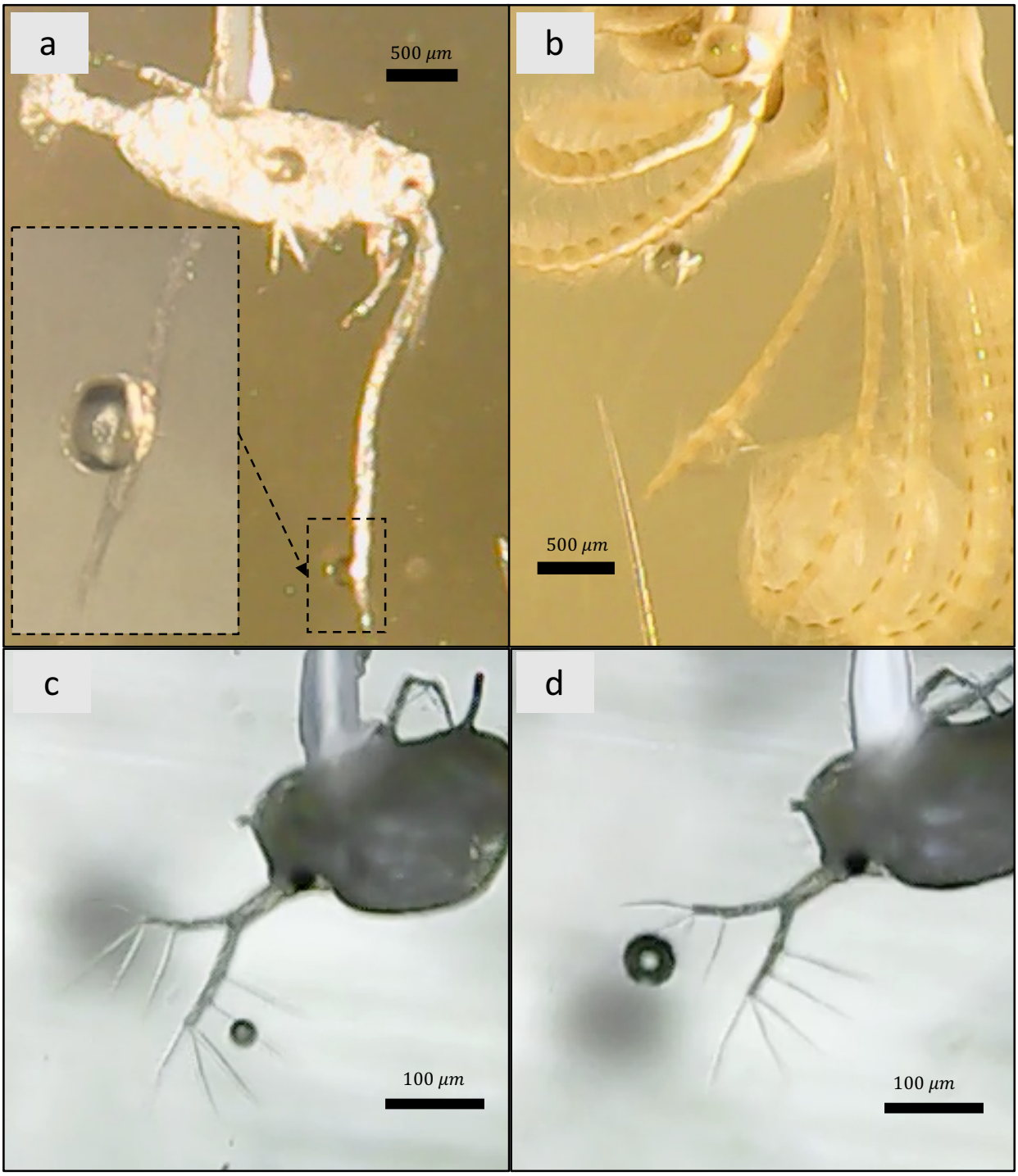

Figure 2.5. (a) An oil droplet attached to the swimming antenna of a calanoid *copepod* ($\theta = 75 \pm 7$). (b) An oil droplet not wetting the feeding appendage of the barnacle *B. glandula* ($\theta = 180$). (c) A small oil droplet being captured by a seta of the second antenna of *Daphnia*. (d) A large droplet being captured by two setae via sieving.

droplet by *Daphnia* on a single seta, and by sieving on the second antenna are demonstrated

in Fig. 2.5c and d, respectively. The conditions for capturing and detachment are fully discussed in Sect. 2.4.

2.4. Oil droplet capture and detachment by fibers

2.4.1. Oil capture by a single fiber

Based on the literature survey presented in Sects. 2.2 and 2.3, the filtration of an oil droplet can be characterized by the physico-chemical properties of the water and oil (e.g. oil-to-water viscosity ratio, and oil-water interfacial tension), the surface chemistry, and texture of the fiber (i. e. wettability). The first step to characterize the mechanisms of oil droplet capture is to describe the fluid dynamics associated with the droplet and the fiber. The force balance on a moving oil droplet in a fluid stream is written in the same format as a particle (Eq. 2.1), but unlike a solid-liquid boundary, the oil-water interface is mobile resulting in less drag force. The drag force of an oil droplet moving at velocity U_o in water flowing at velocity U_w is

$$F_d = -4\pi\mu_w R_o(U_o - U_w)\left(\frac{3p+2}{2p+2}\right) \tag{2.12}$$

where $p = \mu_o/\mu_w$ is the oil-to-water viscosity ratio. Eq. 2.12 was obtained by Hadamard (1911) and Rybczynski (1911), who analytically examined the motion of a fluid sphere (e.g. oil droplet) at low $Re_o = 2\rho_w U R_o/\mu_w$ and obtained a solution for the drag force and velocity profiles of the oil and water, a solution that reverts to the Stokes' low-Reynolds number solution for flow over a solid sphere when the viscosity of the oil is set to infinity.

Due to the mobility of the oil-water interface there is an internal flow within the oil droplet that causes the oil to recirculate. The droplet remains spherical (un-deformed) at low Reynolds numbers (Taylor 1934). The solution of Hadamard (1911) and Rybczynski (1911) is limited by its failure to include inertial effects and is only valid for $Re_o < 1$. Taylor and Acrivos (1964) applied the method of matched asymptotic expansion to account for inertial effects, which resulted in additional terms in the velocity profiles, drag force and droplet shape. Their solution was experimentally verified up to $Re_d \approx 20$ (Wellek et al. 1966; Wagner and Slattery 1971; Subramanyam 1969). Even at $Re_o > 1$, for a small droplet ($R_o \ll R_f$), due to the high capillary force $O(\frac{\sigma_{o/w}}{R_o})$, interfacial effects dominate the process and resist any kind of droplet deformation.

Substituting Eq. 2.12 into Eq. 2.1, and following the same mathematical operations as discussed in Sect. 2.2, the stopping distance and the terminal velocity of an oil droplet are :

$$\mathbf{x}_{s-o} = \frac{R_o^2 U_w(\rho_o - \rho_w)}{3\mu_w}\left(\frac{2p+2}{3p+2}\right) \tag{2.13}$$

$$\mathbf{v}_{T-o} = \frac{R_o^2 g(\rho_o - \rho_w)}{3\mu_w}\left(\frac{2p+2}{3p+2}\right) \tag{2.14}$$

The intensity for inertial interaction, gravitational deposition, direct interception, and diffusion deposition change to :

$$St_o = \frac{R_o^2 U_w(\rho_o - \rho_w)}{3R_f\mu_w}\left(\frac{2p+2}{3p+2}\right) \tag{2.15}$$

$$G_o = \frac{R_o^2 g(\rho_o - \rho_w)}{3U_w\mu_w}\left(\frac{2p+2}{3p+2}\right) \tag{2.16}$$

$$\bar{R}_o = \frac{R_o}{R_f} \tag{2.17}$$

$$Pe_o^{-1} = \frac{KT}{8U_w\pi\mu_w R_o R_f} \tag{2.18}$$

The equations to quantify the intensity of direct deposition and diffusion deposition (Eqs. 2.17 and 2.18) are similar to those for solid particles (Eqs. 2.6 and 2.7). All parameters being equal, as droplet size R_o increases, droplet capture in inertial interaction, gravitational deposition and direct interception is improved. The effect of oil-to-water viscosity ratio p becomes important only in inertial interaction and gravitational deposition (Eqs. 2.15 and 2.16). As already mentioned in Sect. 2.3.1.1. oil viscosity is generally greater than water viscosity. Therefore, all parameters being equal, a less viscous oil droplet has a higher chance of being captured by a filter feeder compared to a higher viscous oil droplet through inertial interaction and gravitation deposition.

The effect of buoyancy is similar to what was discussed in Sect. 2.2 for solid particles. Oil droplets with high density difference will have high momentum and therefore inertial interaction and gravitational deposition mechanisms become more significant. Bitumen droplets produced from accidental oil spills or any other kind of heavy oil in sea water are assumed to be captured through direct deposition, since they have densities similar to water.

Oil-water interfacial tension $\sigma_{o/w}$ and surface chemistry of the fiber do not play a direct role in the capturing mechanism. However, once an oil droplet has been captured by a fiber through one of the above mechanisms, depending on the oil-water interfacial tension and surface roughness of the fiber, the oil droplet might attach to the fiber and adjust to a barrel or clam-shell shape configuration before ingestion (Fig. 2.4b). The attached droplet might detach from the fiber due to the external forces before ingestion and re-enter the fluid stream. The attachment and detachment time of the droplet depends on the viscosity and oil-water interfacial tension, which is not part of this study. In general, a more viscous oil will have a longer detachment time.

2.4.2. Oil droplet detachment from a fiber

When an oil-coated fiber is subjected to external forces, the oil droplet may creep down toward the mouth, or deform and detach from the fiber and re-enter the fluid stream. The detachment of an oil droplet from the solid surface can take place through two different mechanisms (Miller and Raney 1993; Thompson 1994; Mehrabian et al. 2015) : roll-up, or snap-off (emulsification). Fig. 2.6 illustrates these mechanisms on a fiber. In the snap-off mechanism the fiber is oil-wetting, meaning that the oil prefers to wet the fiber, and so the external forces have to be significant to detach the oil. This mechanism usually leads to partial detachment. Snap-off requires overcoming the work of cohesion, because the separation is due to the breakup of the oil-oil interface (Fig. 2.6a-c). Roll-up occurs when the oil does not wet the fiber ($\theta > 90$), and so when a three phase contact line forms, the oil recedes until it detaches from the surface. Roll-up requires overcoming the work of adhesion (Fig. 2.6d-f).

External forces that attempt to separate the oil from the fiber can be viscous, or buoyancy forces. Capillary forces, on the other hand, oppose the deformation of the oil film, hindering the separation of the oil (see Eq. 2.9). In reality, all forces exist at the same time and their magnitude are compared using dimensionless numbers. By comparing the dimensionless numbers, one can determine which force has greater contribution, and predict if the droplet will detach. The ratio of viscous forces to capillary forces is expressed as a capillary number (see Eq. 2.10), and the ratio of buoyancy forces to capillary forces is expressed as a Bond number :

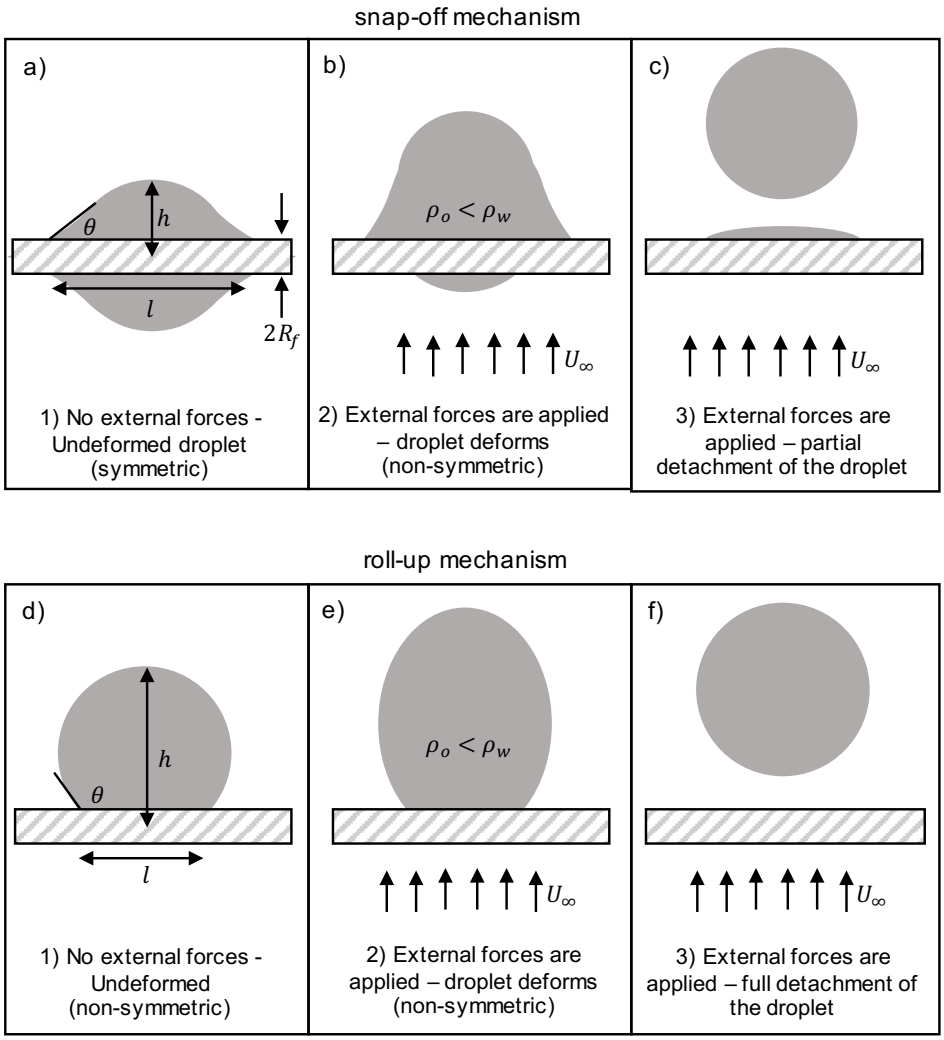

Figure 2.6. Illustration of oil detachment from a fiber by (a-c) snap-off and (d-f) roll-up mechanisms.

$$Bo = \frac{\Delta\rho g R_f^2}{\sigma_{o/w}} \tag{2.19}$$

For a given Ca and Bo there is a critical oil volume, beyond which the droplet can no longer hold on the fiber and will detach (Smith and van de Ven 1985b; Mehrabian et al. 2016).

To illustrate the effect of the Bond number on the detachment of oil from an oil-coated cylindrical surface we compared two systems with different oil-water interfacial tensions and oil densities. System 1 is olive oil that has a density of $\rho_o = 900\ kg/m^3$, and an oil-water interfacial tension of $\sigma_{o/w} = 17\ mN/m$ (Dopierala et al., 2011). System 2 is 1-decanol that has an density of $\rho_o = 850\ kg/m^3$, and oil-water interfacial tension of $\sigma_{o/w} = 1\ mN/m$ (MacLeod and Radke 1993). Fig. 2.7a shows the oil configuration of system 1 on a steel cylindrical

surface ($R_f = 250\,\mu m$). Each frame illustrates the oil droplet configuration with a known volume. At very low volumes the droplet forms a barrel shape, which then transforms to a clam shape at higher volumes. All the configurations reach a steady state shape and do not deform after some time. However, when the oil volume exceeds a critical value ($V/R_f^3 = 601$ for system 1 and $V/R_f^3 = 510$ for system 2) buoyancy forces overcome the capillary forces and lead to partial detachment (snap-off). The partial detachment process for system 1 is illustrated in Fig. 2.7b.

Figs. 2.7c and d compare the wetting length l/R_f and coating thickness $n = h/R_f$ of the two systems at oil volumes below their critical values. As the volume of the oil increases, l increases gradually until it reaches a plateau and no longer wets the surface. However, to compensate for the added volume the oil thickness (h) continuously increases until it can no longer form a stable shape, and then detaches. Substituting the parameters in Eq. 2.19, the Bond number for systems 1 and 2 become 3.6×10^{-3} and 9.2×10^{-2}, respectively. In summary, systems with a higher Bond number have a lower wetting length, and will detach more easily (at lower volumes).

A similar process takes place when the external forces are viscous. Viscous forces, of the order of $O(\frac{\mu_w U_w}{R_f})$, are due to the motion of the surrounding fluid and can be quantified using a capillary number when it is compared to capillary forces (see Eq. 2.10). At a low capillary number the oil droplet will remain on the fiber (i.e. it will be filtered), while above a critical value Ca_{crit}, the oil will deform and detach. The separation of an oil droplet from a sphere due to viscous forces has been extensively studied by Mehrabian et al. (2016, 2018a, 2014); Fan et al. (2010). Their results can be used to qualitatively understand the detachment process on a fiber configuration. For a given capillary number and oil-to-water viscosity ratio there is a critical oil volume, beyond which the oil will separate, and below which the oil will remain on the fiber. Maximum separation takes place when the oil-to-water viscosity ratio is close to 1 (Mehrabian et al. 2014, 2018a).

Based on Rubenstein and Koehl (1977) theory (Eqs. 2.15 to 2.18) the size of the emulsion R_o and flow velocity U_w are the two key parameters in the capturing process. These two parameters are also important in the detachment process based on the definition of the capillary number Ca and the Bond number Bo presented in Eqs. 2.10 and 2.19. A larger flow velocity increases the chances of a droplet being captured via inertial interaction (high

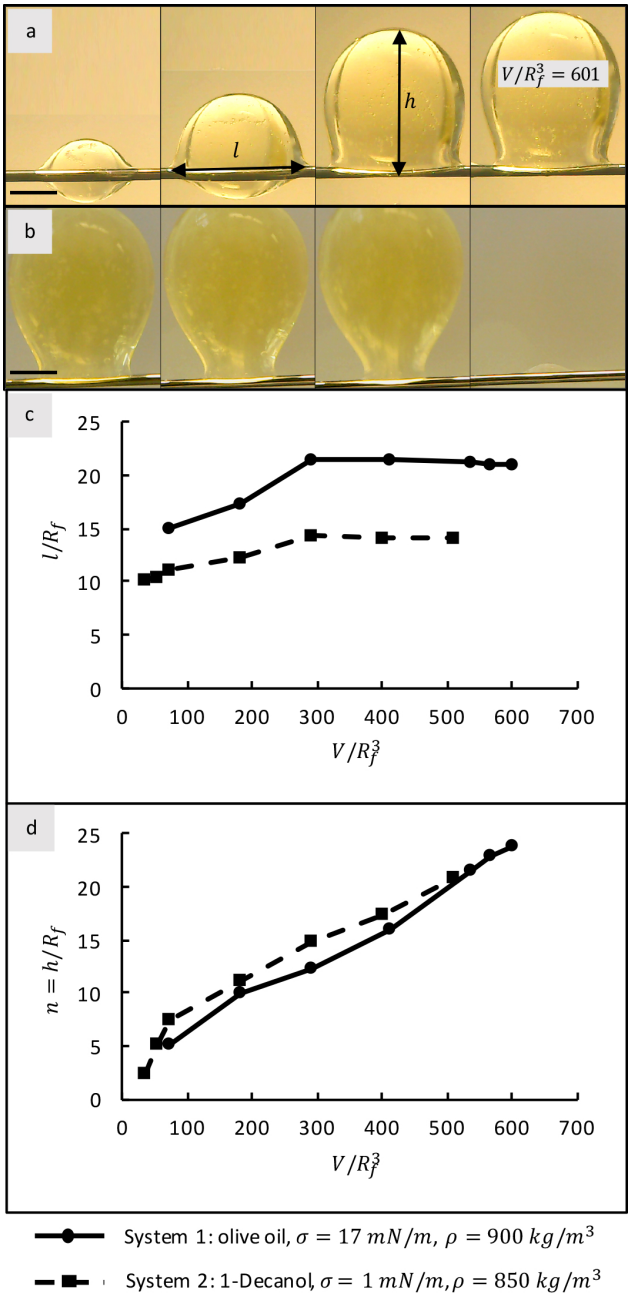

Figure 2.7. (a) Sequential illustration of system 1 of an oil droplet on a cylindrical surface at steady state for different oil volumes. Scale bar is 1000 μm (b) Partial detachment of oil for System 1 when the volume exceeds its critical value ($V/R_f^3 = 601$). Scale bar is 1000 μm (c) Wetting length versus oil volume. (d) oil coating thickness versus oil volume.

St_o based on Eq. 2.15), but if the velocity is too high, the captured oil will detach from the fiber (high Ca based on Eq. 2.10). This means that there is an intermediate range of velocity below which droplets will not be captured, and above which the captured droplet will separate. The relative velocity of water to the animal is typically low in the plankton, but

varies tremendously in benthic, sessile filter feeders including barnacles (Southward 1955; Marchinko and Palmer 2003) and porcelain crabs (Trager and Genin 1993; Achituv and Pedrotti 1999). The barnacle *Balanus glandula* resides in a velocity range of $O(10^{-3})$ to $O(1)$ m/s depending on the local habitat. Animals on wave exposed shores experience a much higher velocity than those from sheltered bays (Marchinko and Palmer 2003). This is significant because at any one velocity, there is a range of droplet size R_o where a particle will be captured (over a certain size) but will not detach (under a certain size). Large droplets tend to separate once captured as illustrated in Fig. 2.7.

Droplet size is an important factor in the capture and detachment of oil droplets by filter feeders (Burns 1968; Hebert and Poulet 1980; Gonçalves et al. 2014). Larger animals can ingest larger particles (Burns 1968). Documenting the relationship between oil droplet size and droplet capture/detachment is relevant to crude oil spill response because the use of chemical dispersants that create emulsions may increase the availability of oil to zooplankton. To capture an oil droplet a zooplankter must detect, select, and then attempt to capture the droplet. The choice to avoid sizes deemed too small to invest the energy in capturing, or too large (i.e. slicks and blobs) and potentially dangerous to approach, is in need of study. Here we address the potential for successful capture, once a capture is attempted. Droplets may be captured by inertial interaction, gravitational settling, direct interception, diffusion deposition, or sieving. Gravitational deposition of an oil droplet differs from a particle in that a particles typically sinks, whereas oil is typically buoyant, and so arrives at the bottom of the appendage by creaming.

2.4.3. Oil capture by sieving

The capture of an oil droplet between two cylindrical fibers is called sieving (Fig. 2.8). The presence of an oil droplets between the inter-fiber space reduces the permeability of the surrounding fluid through the inter-fiber space. As additional droplets from an unstable emulsion are sieved, the inter-fiber space is blocked by droplets that are formed by coalescence. Permeability reduction in the case of a stable emulsion is more pronounced when the droplet is larger than the inter-fiber distance, and the flow velocity is low (McAuliffe 1973; Hofman and Stein 1991) (Fig. 2.8a).

The motion of a droplet through an inter-fiber space has several parameters that determine its fate, including the geometry of the capillary pore (e.g. radius of the fiber and inter-fiber space), fluid properties (e.g. oil and water viscosities, and densities), and fluid-to-fluid relative flow velocity. Depending on these factors, a droplet can either flow through the space without breakup, breakup into daughter droplets, or become trapped at the narrow point or neck of the constriction. This phenomenon has been investigated by previous authors using constricted tube geometries (Olbricht 1996; Olbricht and Leal 1983; Martinez and Udell 1990a,b; Tsai and Miksis 1994; Soo and Radke 1984). Their results pertain to tube-shaped geometries, and so provide a useful guide for qualitatively interpret the effects of viscosity ratio p, droplet to inter-fiber distance (R_o/L), and capillary number Ca on the shape and velocity of the droplet.

A droplet will not pass through the space until the flow velocity is sufficient to provide a local dynamic pressure drop larger than the capillary pressure that resists the motion of the droplet (Soo and Radke 1984; Olbricht 1996; Martinez and Udell 1990b,a). When a droplet does move through an inter-fiber space or a pore throat it undergoes uniaxial extension in the narrow section (Fig. 2.8b). At low capillary numbers ($Ca < 0.5$ suggested by Martinez and Udell 1990b), the droplet recoils to a nearly spherical shape after passing through the narrow section, whereas at larger capillary numbers, the droplet deforms in the narrow section and does not recoil in the wide section. As Ca increases (by lowering the $\sigma_{o/w}$), the droplet deforms more easily and a thicker film is formed between the droplet and the solid boundary. Martinez and Udell (1990a) suggest that at even higher Ca, if the deformation timescale for the droplet is greater than the flow time-scale, the droplet will deform permanently into a thin filament that eventually breaks up into smaller droplets, and used the following criterion for this breakup process :

$$Ca > Ca_{crit} = \frac{2R_f}{R_o(1+p)}\frac{U_o}{U_w} \tag{2.20}$$

where V is the velocity of the droplet in the flow direction, and U_w is the free stream velocity. Unfortunately, values of U_p/U_w are unknown, but based on Martinez and Udell (1990a) who studied a wide range of viscosity ratios, capillary numbers, and droplet sizes values of U_p/U_w range from 0.95 to 1.46. Thus, it is apparent from Eq. 2.20 that larger capillary numbers

are needed to permanently deform and breakup small droplets. Also, a larger value of Ca is required to cause permanent deformation and breakup at lower viscosity ratios.

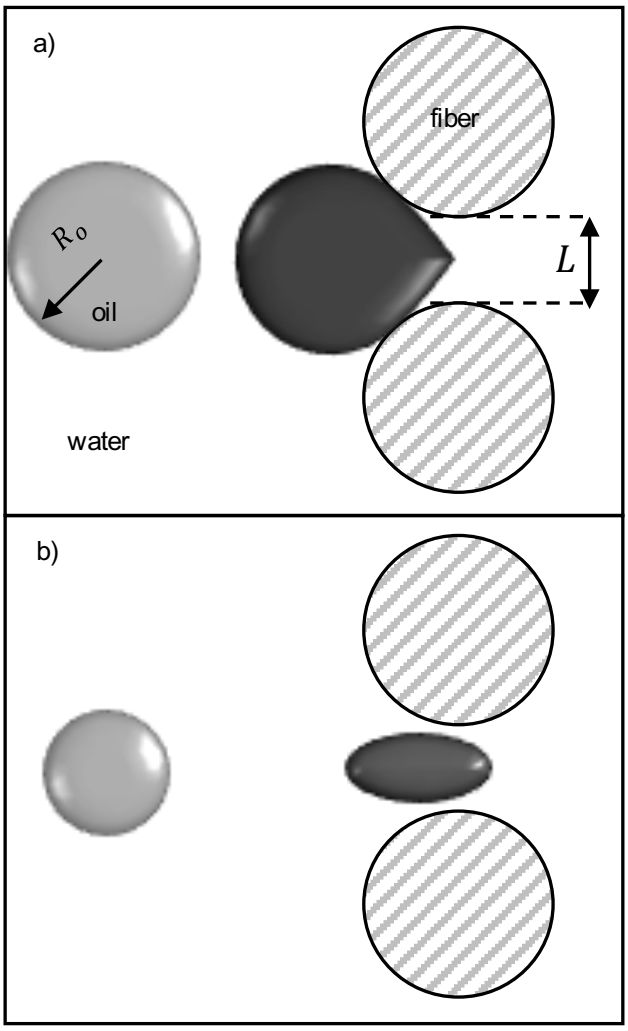

Figure 2.8. Illustration of a droplet being (a) captured by two fibers and (b) passing through two fibers.

2.5. Examples of oil droplets interacting with filter feeders

2.5.1. Daphnia

Species of the genus *Daphnia* use their modified thoracic legs (setae) to filter particles generally between the range of 1 to 25 μm depending on the species (Dodson, 2004). Their thoracic legs have short, spine-like extensions (setules) that filter. These filters will function

at the same intensity whether the food concentration is high or low. The filter combs help to create a unified current, and capture the food. The capturing of the food is either done by one of the setules (Eqs. 2.15 to 2.18), or through sieving. Once the food reaches the mouth, it can be rejected if the food is distasteful, too large, or the food concentration is high.

Video S1 demonstrates the ingestion and rejection of fish oil (Rite Aid) by *Daphnia magna*. To capture Video S1, a hair was attached to the dorsal side of a *Daphnia magna*, which was then put in an oil-in-water emulsion. The experiment was conducted in fresh water at 10^oC, with an oil-in-water emulsion concentration of 0.024 g/l. The oil droplets ranged from 2 to 11 μm, with an average of $R_o = 4.36\,\mu m$ (measured using ImageJ software). The oil viscosity and density are 46 cP (Cournarie et al., 2004) and 922 kg/m^3 (measured), respectively. The velocity of the oil droplets approaching the setae was $U \approx 1\ cm/s$ (measured using ImageJ software). The radius of the setae was 0.68 μm (Crittenden, 1981). Based on these values, the Reynolds number of the flow near the feeding appendages was of the order of $Re = \frac{\rho_w U(2R_f)}{\mu_w} = O(10^{-2})$. This small value indicates that viscous forces dominated the flow, and the boundary layer thickness was large, hence very little flow (with food) was leaked through the appendages. In other words, sieving is not the main mechanism of food capturing for this animal (Cheer and Koehl, 1987b).

Droplets with different size accumulated in the body in the form of flocculation. From here oil droplets were rejected, and injested. Large droplets were almost uniformly rejected, by moving the post-abdominal claw between the valves, and under the filter combs. The terminal end of the postabdominal claws have two setae that assisted with grasping and removing the droplets. Some of the smaller oil droplets were transporting towards the paired mandibles and ingested. The motion of the filter combs was coordinate with the movement of the mandibles. In general, only a small proportion of the captured droplets were ingested.

2.5.2. Barnacles

Barnacles are attached to a substrate, and use the thoracic legs, or cirri, to filter feed. Cirri are ramified with setae that assist in droplet capture. Video S2 demonstrates the feeding mechanism of an individual *Balanus glandula*. *B. glandula* filter food passively in high velocity flow, and actively in low velocity flow. When filtering passively, the cirri are held perpendicular to the flow to capture particles with minimal effort. The cirri may also

create a current by the feeding motion, which help guide the particles to the mouth. When actively capturing food, as shown in Video S2, the biramous cirri close, akin to the fingers of a fist, and direct the food towards the mouth, located inside of the shell. The numerous setae give the appendage a micro-scale rough surface, that inhibits droplet spreading (superlipophobic) (see Fig. 2.5b).

2.6. Other remarks

Filter feeders preferentially choose their food based on size, and chemical composition. Laboratory experiments with flavoured and untreated polystyrene spheres reveal major differences in taste discrimination among copepods, daphnias, cladocerans, and rotifers (Hartman and Hartman, 1977; Kerfoot and Kirk, 1991; DeMott and Watson, 1991; Friedman and Strickler, 1975). Different species of rotifers were found to ingest spheres non-selectively, preferentially, or were averse to spheres, demonstrating high interspecific variation among closely related taxa (DeMott 1986). In general, oils are highly nutritious. They are widely captured by zooplankton (Almeda et al., 2013, 2014a; Hansen et al., 2015; Conover, 1971), but nothing has been written on the preference of one oil, versus another, versus solid particles. The concentration of oil droplets is proportional to the encounter rate (Shimeta and Jumars, 1991), but little is known about how the composition and concentration of oils changes seasonally and regionally.

Animal and plant oils may contain surfactants, though more is known about the surfactants and related molecules in fossil hydrocarbons including bitumen. Bitumen contain asphaltenes and naphthenic amphiles, which are surface-active species that act like surfactants (Kiran et al. 2011). They have a hydrocarbon skeleton that is hydrophobic, and polar groups that are hydrophilic. They adsorb at the oil-water interface in such a way that the hydrophilic group is aligned in the water phase, while the hydrophobic tail is aligned in the oil phase. This lowers the oil-water interfacial tension and increases the dispersion of the oil in water. Hypothetically, these chemicals should increase the uptake of oil by zooplankton for two reasons ; i) they make available small droplet sizes, and ii) the molecular orientation makes the droplet surface active and lowers the interfacial tension (Papirer et al. 1982; Pfeiffer and Saal 1940). Copepods including *Calanus helgolandicus, and Pseudocalanus elongatus*, and *Temora longicornis* feed on oil droplets treated with or without surfactants (Spooner

and Corkett 1979). This reduces egg production, and hatching, and increases the number of fecal pellets (Hansen et al., 2015; Almeda et al., 2013, 2014a).

Water temperature, which may change seasonally, and regionally, can have a substantial effect on the rate of filter feeding. This reduction in feeding activity is due to changes in water viscosity, and physiology. At lower temperatures, the viscosity of water increases, the feeding appendages encounter higher resistance, and filter movement and speed is reduced as more effort is required (Loiterton et al. (2004)). With colder water, an individual's metabolism slows, which results in a slower feeding and filtering rate (Podolsky et al., 1994; Nishizaki and Carrington, 2015). Loiterton et al. (2004) found that viscosity alone is responsible for approximately 60% of this decrease for *Daphnia galeata*, and physiological factors and other unknown variables contributing to the remaining 40%. According to theory, an increase in water viscosity at lower temperatures will lower the Reynolds number, and promote the transition from a sieve to a paddle filtering mechanism (Koehl, 2001). Therefore, temperature impacts the rates of feeding, and the performance of the feeding mechanism.

We review the basic mechanisms by which a solid particle can be removed by any filter. We then review oil emulsion formation and stability, and enumerate oil droplet capture and detachment by a single fibre, and by a sieve. We use dimensionless numbers to indicate the role of oil droplet size, and water velocity on capture. Other key parameters to capture oil droplets with a filter are oil-to-water viscosity ratio, oil-water interfacial tension, oil and water density difference, and surface wettability, or texture, of the filter fibre. We hypothesize that there is an intermediate droplet size, and water velocity, where a droplet can be captured. We also hypothesize that animal filter surfaces will be lipophobic. Following capture, capillary force maintains the droplet at its location due to the oil-water interfacial tension. If the oil-coated fiber is subject to any external force such as viscous or gravitational forces, it may deform and separate from the fiber and re-enter the fluid stream. Awareness of these mechanisms and their interrelationships will provide a foundation for investigations into the efficiency of various modes of filter feeding.

2.7. Supporting information

Video S1. Filtering, rejecting and ingesting mechanisms of Daphnia, a fresh water crustacean, in an oil-in-water emulsion made with a mix of fish and krill oil (0.024 g/L). The water temperature was approximately 10 $^{\circ}C$.

Video S2. Active filtering mechanism of barnacles on fish oil droplets. Fish oil droplets were created using a thinned syringe needle. The water temperature was 15 $^{\circ}C$.

Chapitre 3 .

The interactions of oil droplets with filter feeders : A fluid mechanics approach

par

Francis Letendre[1], Sasan Mehrabian[1], Christopher B. Cameron[1] et Stéphane Etienne[2]

([1]) Département de sciences biologiques, Complexe des sciences, Université de Montréal, 1375 Avenue Thérèse-Lavoie-Roux, Montréal, Québec, H2V 0B3, Canada

([2]) Ecole Polytechnique de Montreal, C.P. 6079, succ. Centre-ville, Montreal, Quebec, H3C 3A7, Canada

Cet article a été publié dans :

Marine Environmental Research (2020), 161

DOI :/10.1016/j.marenvres.2020.105059

Cet article a été modifié pour les besoins de la thèse.

Rôle des auteurs

Francis Letendre : Conceptualisation du désign expérimental, création du matériel expérimental, conception de la méthodologie, revue de littérature, collecte des données, analyse des données, rédaction du manuscript, soumission et révision du manuscript

Sasan Mehrabian : Conceptualisation du désign expérimental, conception de la méthodologie, revue de littérature, collecte des données, analyse des données, rédaction du manuscript

Christopher Cameron : Conceptualisation du désign expérimental, validation des résultats, rédaction du manuscript, révision du manuscript, supervision et administration du projet, acquisition du financement

Stéphane Étienne : Révision du manuscript, acquisition du financement

Résumé.

Les organismes filtreurs capturent et perdent les gouttelettes d'huile en utilisant des cils ainsi que des appendices filtreurs ramifiés. Nous démontrons ici que les appendices de copépodes et de balanes sont en mesure de capturer des gouttelettes d'huile de poisson, de canola et de 1-decanol jusqu'à une taille de 11 μm en rayon, et cela sans sélectivité de taille, composition chimique, densité, viscosité et tension de surface. Après capture, les gouttelettes ont été ingérées ou perdues par détachement. Il n'y a pas de différence dans les mécanismes de capture entre un appendice de balane et un fil d'acier inoxydable de rayon $R_f = 50$ et 250 μm. Les paramètres clés régissant le détachement d'une gouttelette sont le ratio de taille entre la gouttelette et la fibre collectrice, ainsi que le nombre de Weber. Ainsi, un ratio de taille plus petit requiert un nombre de Weber du système plus élevé pour permettre le détachement de la gouttelette. Ces données permettent la création d'une courbe prédisant le comportement de la gouttelette, c'est-à-dire si celle-ci demeurera sur la fibre ou se détachera en retournera dans la colonne d'eau. Cette courbe incorpore les paramètres du milieu, de l'huile ainsi que la taille de la gouttelette et du collecteur. Suite à l'identification des espèces de zooplancton présentes dans une zone de déversement et à l'étude de la taille des gouttelettes présentes dans la colonne d'eau, la courbe présentée permet de déterminer quelles gouttelettes sont plus à risque d'être capturées par les appendices filtreurs.

Mots clés : alimentation par filtration, mécaniques des fluides, plancton, copépodes, balanes, gouttelettes d'huile, taille de particules, déversements de pétrole brut

Abstract.

Filter feeding animals capture and lose oil droplets using cilia or ramified appendages. Here we demonstrate that copepod and barnacle appendages capture fish, canola and 1-decanol oil droplets up to 11 μm without selectivity for size, chemistry, density, viscosity, or interfacial tension. Following capture, the droplets are ingested or lost via detachment. Capture and detachment did not differ between a barnacle appendage and stainless-steel wires of radii $R_f = 50$ and 250 μm. Key parameters to detachment include the ratio of oil droplet radius to fiber radius, and the Weber number. Smaller oil droplet size to fiber size ratio $r = R_o/R_f$, required a higher We for detachment. These data plot as a curve that predicts whether a droplet will remain captured or detach and re-enter the fluid stream, based on the fluid, the droplet radius to fiber radius ratio, and the oil droplet properties. After doing a quick identification of the zooplankton species in a spill zone and measuring the size distribution of the droplets, the curve can be used to predict oil retention by the filtering appendages.

Keywords: filter feeding, fluid mechanics, plankton, copepods, barnacles, oil droplets, particle size, oil spill

3.1. Introduction

Filter feeders use their filamentous appendages to capture food from water (Mehrabian et al., 2018b; Koehl, 1993; Jørgensen, 1983; LaBarbera, 1984). This food can be in the form of solid particles, or oil droplets. Solid particles ingested by filter feeders can be in the form of bacteria, protists, algae, debris from plants and animals or small planktonic live prey (Fenchel, 1984; Berk et al., 1977). Oil droplets ingested by filter feeders may come from decaying protists, plants, animals or as a result of an oil seep or spill (Almeda et al., 2014a; Shen and Yapa, 1988; Li and Garrett, 1998; Rasmussen, 1985). Ingested oil droplets serve zooplankton as a lipid reserve for overwintering, for gametogenesis and as an energy source for non-feeding larvae stages prior to settlement and metamorphosis (Sargent and Falk-Petersen, 1988; Visser and Jónasdóttir, 1999; Miller et al., 2000; Franco et al., 2016). Oil droplets can also help regulating the buoyancy of the organism during the dial vertical migration (Thorisson, 2006), the larvae's ontogenetic migration to reach a suitable habitat (Pennington and Emlet, 1986) and to limit vertical movement to reduce predation (Kattner et al., 2007). Oil from petroleum oil spills may be in the form of large surface slicks, sub-surface blobs, or micron-sized oil droplets. The droplets form by shear created by wind, waves, or natural and industrial surfactants (dispersant) (Rico-Martínez et al., 2013). These petroleum droplets may then have sublethal or lethal effects on the filter feeding animals. Individuals that ingest crude oil droplets show lower growth rates, lower egg production and hatching rates, higher faecal pellets counts, and higher mortality (Almeda et al., 2014c; Hansen et al., 2015). Recent studies even show that oil spills can promote harmful algal blooms by removing the grazers from the ecosystem (Almeda et al., 2018). The capture and detachment of solid particles by filter feeding animals has been investigated from theoretical, modeling, and experimental approaches. That of oil droplet capture has been investigated theoretically (Mehrabian et al., 2018b) and here we investigate capture and detachment, via detachment, experimentally. This work is significant to those interested in biological fluid mechanics, aquatic and marine ecology, biochemistry and toxicology, and biogeochemistry (eg., carbon nutrient cycles), and is central to mitigating the impact of oil spills in the marine and aquatic food webs. Spilled oil mainly enters the aquatic food webs via the ingestion of oil droplets by zooplankton. It is thus important to understand how these organisms filter and capture liquid particles from the water column.

The capture and detachment of oil droplets requires a basic understanding of the mechanisms by which filter feeding appendages operate from a fluid dynamic perspective including the topography of the feeding fibers, the physical properties of the oil droplets, and droplet surface chemistry. The bulk of filter feeding animals are crustacean arthropods. They use filtering appendages that consists of a main fiber that is ramified with setae, which are sometimes also ramified with smaller fibers called setules. The capturing of algae particles by copepods has been well documented and photographed (Koehl and Strickler, 1981; Koehl, 1993; Tiselius et al., 2013). The capture of solid particles has been investigated theoretically by Rubenstein and Koehl (1977), where they used aerosol theory to identify five mechanisms of particle capture by single fiber. These mechanisms are direct interception, inertial interaction, gravitational deposition, diffusion or motile deposition, and electrostatic attraction. They proposed non-dimensional numbers to estimate the encounter efficiency 'intensities' of filtration for different mechanisms. The proposed dimensionless numbers based on aerosol theory account for filter size, particle size, fluid viscosity and velocity and other parameters. Their results showed that the size of the particle and the flow velocity are the two most important parameters that determine the efficiency of particle capture. Particles can also be captured by two fibers in a process known as sieving. In sieving, all solid particles larger than gap size between two adjacent fibers (mesh size) are retained by being trapped on the fibers, while all particles smaller than the gap size pass through the fibers. To confirm that sieving is one of the mechanisms in play, a decrease in capture efficiency needs to be noted when the particles are smaller than the mesh size (LaBarbera, 1984). If the capture efficiency stays the same, then other mechanisms are in play. Mehrabian et al. (2018b) applied the same theory used by Rubenstein and Koehl (1977) for oil droplets captured and found that oil-to-water viscosity ratio also becomes important in the capturing mechanism. Oil viscosity is generally greater than water viscosity. Therefore, all parameters being equal, a less viscous oil droplet has a higher chance of being captured by a fiber compared to a higher viscosity oil droplet through inertial interaction and gravitation deposition (Mehrabian et al., 2018b). Copepods live at a scale where viscous forces are dominant and where momentum is minimal. At low Reynolds numbers, *i.e.* 10^{-2} to 10^{-1}, filter feeding copepods use these appendages as paddles (Koehl and Strickler, 1981). Indeed, instead of sieving particles through its setae, the organism will use its appendages to push parcels of water towards the mouth (Alcaraz and

Paffenhöfer, 1980). More specifically, the copepod will rapidly move its second maxillae outwards, which will result in a rush of water near the mouth. Then, while the second antennae and the first maxillae are pushing this parcel of water posteriorly, the second maxillae moves inward and forces the water through its appendages and then captures the food particles (Koehl and Strickler, 1981). The animal can also ingest particles that were captured by other appendages via the mechanisms listed above by combing them. For example, if a particle is captured by the first antennae via direct interception or inertial interaction, the animal will bend its antennae so that they are aligned ventrally with the rest of the body. They will then be scraped by the endites of the second maxillae, thus removing the captured particle (Price et al., 1983).

The traditional dimensionless number used to characterize flow over fibers and cylinders in general, in fluid dynamic is the Reynolds number, is defined as :

$$Re = \frac{\rho_w U_w (2R_f)}{\mu_w} \tag{3.1}$$

where ρ_w and μ_w are the density and viscosity of the surrounding water, respectively. U_w is the free stream velocity, and R_f is the fiber radius. The Reynolds number is a ratio that describes the relative importance of inertial and viscous forces for movement relative to a fluid. At the level of an individual element in the filtering structure (cirrus, setae, or setules), the Reynolds number for filter feeders can vary in orders of magnitude. Depending on the size of the filter structure and the flow velocity Re changes from 10^{-5} to 10^{2}. For example, flagellates and ciliates are in the low end of the spectrum (LaBarbera, 1984) and *glandula* barnacles in high wave exposures are in the high end of the spectrum (Vo et al., 2018). When a fluid flows over the appendage surface, the layer of fluid in contact with the surface does not slip with respect to the surface, hence, a velocity gradient develops between the surface and the flow. The lower the Re, the thicker the layer is. This layer, also known as the boundary layer thickness, is of the order of $O(R_f/\sqrt{Re})$, so the net flow is far from the filtering element, resulting in a very high pressure drop across the fiber (Sumer et al., 2006; LaBarbera, 1984).

The flow pattern around the fiber changes as Re increases. At $Re < 5$, the flow pattern around an isolated fiber is smooth and symmetrical around the cylinder with no discontinuities (no flow separation) and no turbulent wake (Fig. 3.1A). For the range of the Reynolds

number $5 < Re < 40$, a fixed pair of vortices forms behind the fiber. These vortices are stable and non turbulent (Fig. 3.1B). The length of the vortices increases with the Reynolds number. As the Reynolds number increases, the wake becomes unstable and the flow eventually creates vortex shedding, whereby vortices are shed alternately at either side of the cylinder at a certain frequency (Sumer et al., 2006; Vo et al., 2018). At $40 < Re < 200$, as depicted in Fig. 3.1C, which is the high end of the spectrum of Reynolds numbers for filter feeders, the vortex shedding is laminar and two-dimensional (Sumer et al., 2006).

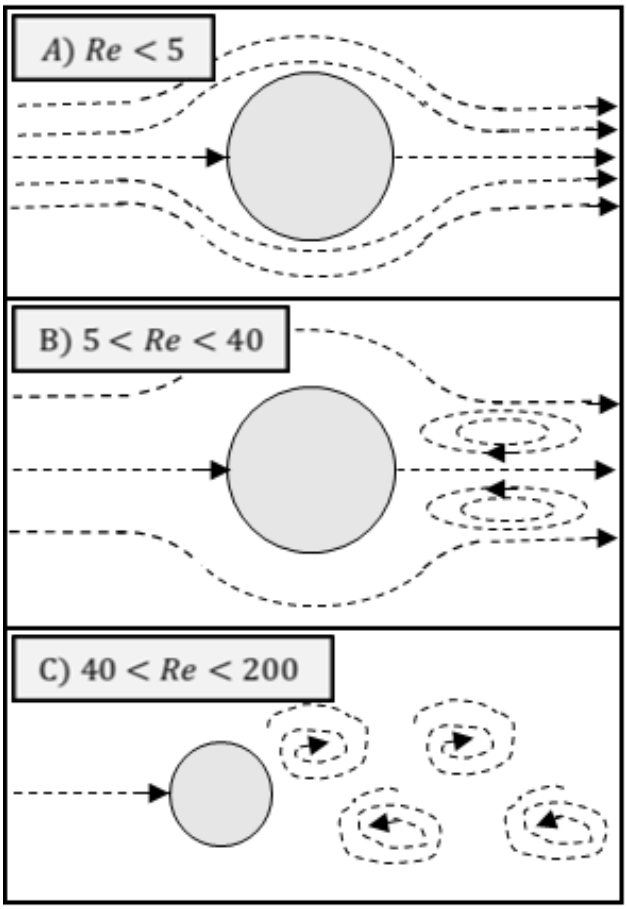

Figure 3.1. Flow pattern around an isolated fiber at (A) $Re < 5$, (B) $5 < Re < 40$, and (C) $40 < Re < 200$.

Once an oil droplet enters the boundary layer of a fiber and is captured, depending on the droplet size and the surface wettability of the fiber, the droplet may completely wet, partially wet, or remain spherical and not wet the fiber surface (refer to Mehrabian et al. (2018b)). The captured oil droplet may creep down toward the mouth, or deform and detach from the fiber and re-enter the fluid stream if the external forces are strong enough. Recent

observations even show that the oil droplet's diameter can be reduced via manipulation by copepod appendages (Marco et al., 2019). The external forces can be buoyant, viscous or inertial forces. All the forces mentioned above exist at the same time and their magnitudes are compared using dimensionless numbers.

Based on the definition of the Reynolds number in Eq. 3.1, if $Re < 1$, viscous forces are the dominating forces around the fiber. Therefore, the capillary number Ca is used to characterize the detachment of oil from fibers (Mehrabian et al., 2018b, 2016, 2018a). The capillary number expresses the ratio of viscous forces to capillary forces :

$$Ca = \frac{\mu_w U_w}{\sigma} \tag{3.2}$$

Viscous forces will shear and deform the oil that coats the fiber. Capillary forces, on the other hand, oppose the deformation of the oil film, hindering the detachment of the oil. If $Re > 1$, inertial forces are the dominating forces around the fiber, and are responsible for shearing and detaching the oil from the fiber. The ratio of inertial forces to capillary forces is expressed as the Weber number :

$$We = \frac{\rho_w U_w^2 (2R_f)}{\sigma} \tag{3.3}$$

Buoyancy forces become important in the detachment process if there is a density difference between the oil and water. The ratio of buoyancy forces to capillary forces is expressed as the Bond number :

$$Bo = \frac{\Delta\rho g R_f^2}{\sigma} \tag{3.4}$$

where σ is the oil-water interfacial tension, $\Delta\rho$ is the oil-water density difference, and g is the gravitational acceleration.

Here, we study the appendage-water-oil interaction at Reynolds numbers in the range of $10 < Re < 100$ where the inertial forces are greater than the viscous forces. For that reason, the Weber number is the accurate dimensionless number that characterizes oil droplet detachment in our system. We chose this range of Re because this is typically the range experienced by barnacles, the organism used for validation of our model, and because we wanted to use a single dimensionless number on all experiments *i.e.* the Weber number.

By choosing this range, the inertial forces are dominant and viscous and capillary forces are negligible. Our objectives were to experimentally observe and describe i) the range of droplet sizes that are captured and lost by a copepod and a benthic filter feeding barnacle, and ii) the capture and detachment mechanisms of oil droplets from a cylindrical feeding appendage in terms of the critical Weber number (ratio of inertial to capillary forces) as a function of oil droplet size in which the oil droplet detaches. We hypothesized that oil droplet capture and ingestion will be widespread in filter feeders, including copepods and a barnacle. We also hypothesized that bigger oil droplets will require a lower flow velocity in order to detach from the fiber/appendage. High viscosity oils will also detach at higher flow velocities due to higher capillary forces (*i.e.* higher oil/water interfacial tension).

3.2. Materials and Methods

3.2.1. Droplet size distribution

The first set of experiments was to quantify the range of droplet sizes captured by calanoid copepods (*Acartia tonsa, Calanus finmarchicus, Centropages typicus*), and to visualize this capture on dissected and stationary barnacle (*Balanus glandula*) legs, or cirri. Copepods were captured using a plankton net, and barnacles were collected from rocks, on site of the Darling Marine Centre, University of Maine, June 2018. The copepods were starved for 12 hours, then exposed to an oil-in-water emulsion for 12 hours, and then photographed, as illustrated in Fig. 3.2A. Starving was done to encourage individuals to feed and to facilitate observations of their guts, as the oils used were translucent and therefore easily masked by other gut contents. Oil droplet capture and detachment was observed on freshly dissected barnacle legs (cirri) in a flow tank. A fish oil-in-water emulsion was made by mixing it with a magnetic stirrer for 30 minutes, with a concentration of 300 mg/L at 12^oC. The droplet size distribution of the emulsion is illustrated in Fig. 3.3 with an average radius of $R_o = 4.49\ \mu m$. Because droplets smaller than 1 μm in radius were not visible and measurable inside the gut of copepods, there were not considered in the fish oil-in-water emulsion size distribution. When a droplet was observed inside the gut of an individual copepod or on one of its appendages, its diameter was measured using ImageJ 1.43 software (US National Institutes of Health) and recorded into one of three categories : droplets found in the gut of the individual, on its appendages,

or agglomerated in floccs close to the mouth and feeding appendages. The barnacle cirri were glued perpendicularly to a wire ($R_f = 50\mu m$) with the cirri positioned to face the flow. This position mimicked the way a live barnacle intercepts particles in passive filtering (Pechenik, 2014). The wire was pinned to modeling clay. This eliminated the movement of the legs, which allowed us to visualize the oil-appendage interaction, and control the velocity of the oil droplets relative to the appendages.

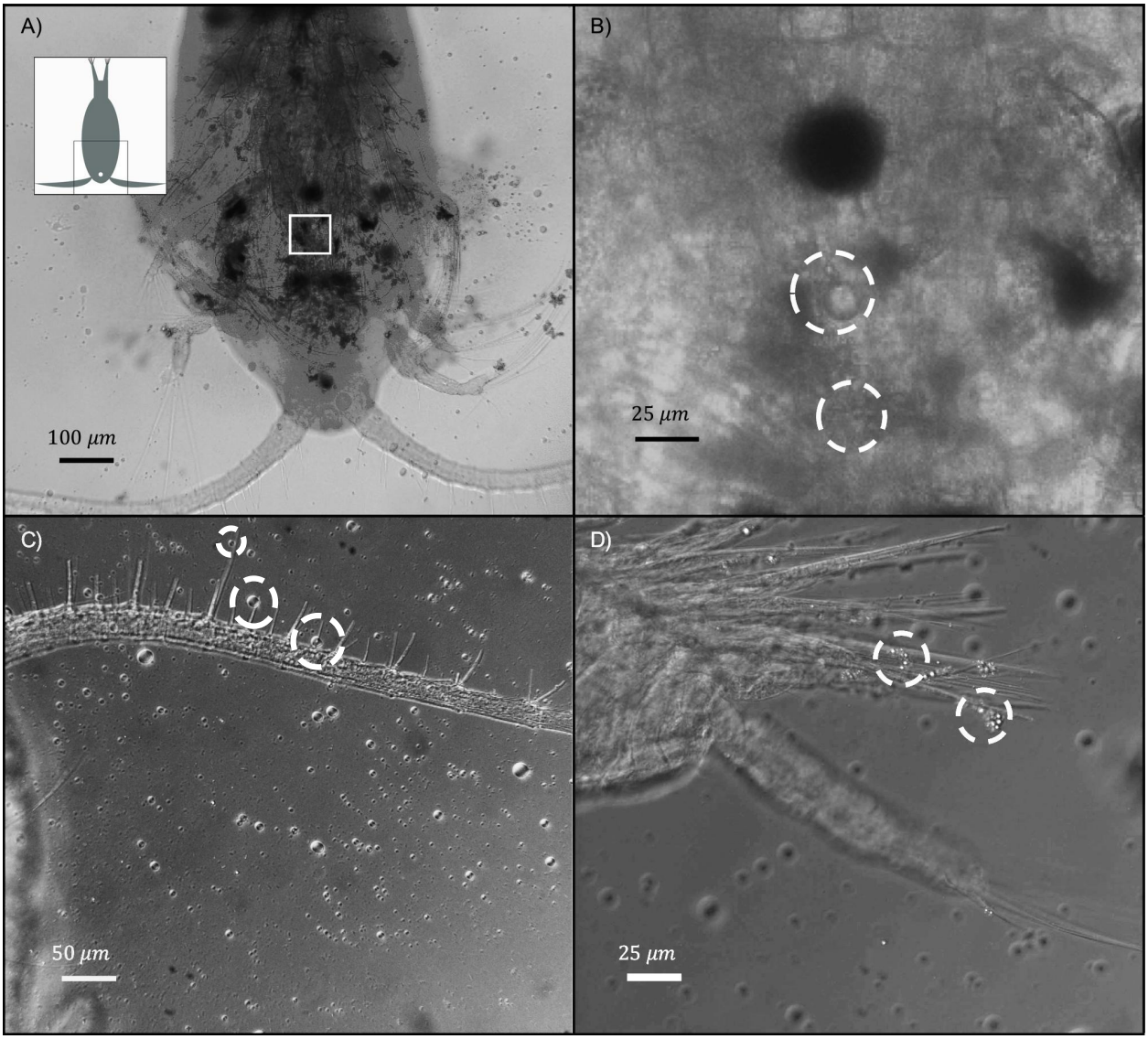

Figure 3.2. (A) A calanoid copepod photographed after being starved for 12 hours, followed by 12 hours of exposure to a fish oil emulsion. The cartoon in the upper left corner shows a simplification of a typical calanoid copepod. The black square highlights the portion of the copepod shown in the original photograph. (B) Magnified section of the square in (A) showing some oil droplets in the gut of the copepod. Dotted circles show ingested oil droplets. (C) Some oil droplets captured by the first antennae and its setae. (D) Oil droplets agglomerated in floccs and captured by the copepod's swimming legs. Dotted circles show flocculates.

3.2.2. Study of critical conditions for droplet detachment

The theoretical mechanisms by which droplets are captured are illustrated in Rubenstein and Koehl (1977) and Mehrabian et al. (2018b). The most important factors in the capturing process are the relative velocity of the oil to the filtering appendage, and the size of the

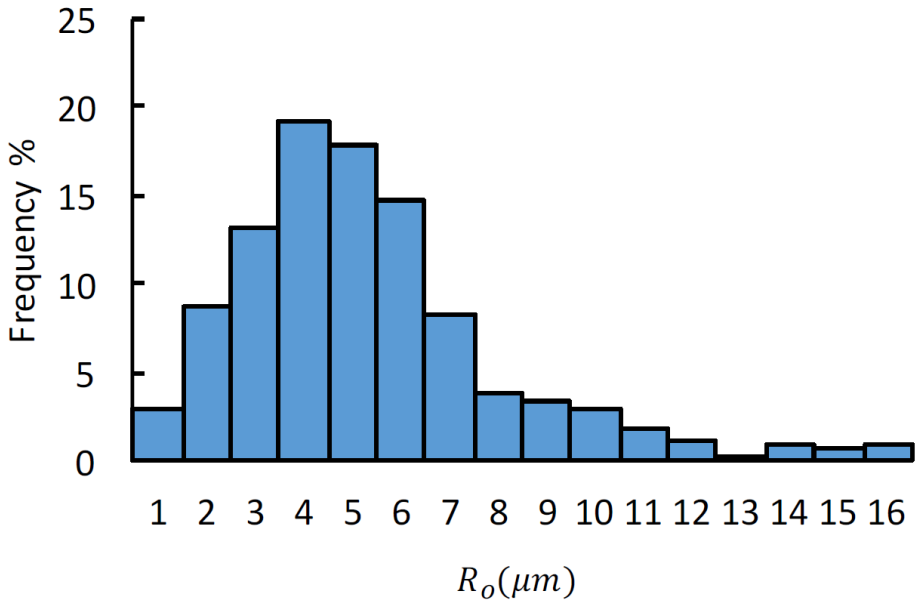

Figure 3.3. Droplet size distribution for fish oil-in-water emulsion. The emulsion concentration was 300 mg/L. (n=339)

droplet. Pelagic copepods swim in rapid bursts to capture food and then quickly slow down and sink before initiating another burst. Their swimming speed varies from 65 to 827 mm/s (Buskey and Hartline, 2003). This indicates that the Reynolds numbers around the setae are in the order of $Re = O(1)$ (Paffenhöfer and Loyd, 2000), or from 0.1 to 1. The increase in the inertial forces around a setae (or other filamentous appendage) when the individual initiates a burst should theoretically cause a captured droplet to detach and re-enter the fluid stream.

Similarly, a change in water velocity around a benthic filter feeder will impact the fate of a captured droplet. For example, barnacles in wave-swept environments are exposed to extreme flow variation, with water velocities ranging from 0.05 m/s to well over 10 m/s (Marchinko and Palmer, 2003). The Reynolds numbers for the most extreme case can be well above 100. Here we determined the low capture velocity and the high detachment velocity from stationary appendages. Inertial, gravitational, and viscous forces will shear and deform the oil that coats the appendage, whereas capillary forces will oppose the deformation of the oil, hindering the separation of the oil. In these experiments, only the capture and detachment events where the Reynolds number was between the orders of 10^1 to 10^2 were kept and analyzed. Therefore, inertial forces are the dominant forces separating the oil from the appendages.

Our second objective was to find the critical Weber number (ratio of inertial to capillary forces) as a function of oil droplet size in which the oil droplet detaches. To do this we needed to account for the different fibre radii of feeding appendages found among filter feeders. To determine the Weber number in a controlled experiment, we characterized the capture and detachment of oil droplets from stainless steel cylinders (R_f = 50 and 250 μm). This allowed us to determine the number without variations in appendage hydrophobic/-philicity or surface texture (wettability). Experiments were conducted inside a flume tank equipped with a motor-impeller that generated controlled flow velocities between 0.01 to 0.4 m/s. The dimensions of the flume tank were 110 × 20 × 20 cm. All trials were done in artificial sea water with density of 1024 kg/m^3 (Fig. 3.4), at 12^oC. Lights were positioned on top of the tank to provide adequate illumination for high speed video capture. Videos of oil droplets being captured and detached from the steel fibres were recorded using a MotionBLITZ Cube 4 high speed recording camera equipped with a Nikon 62mm macro lens.

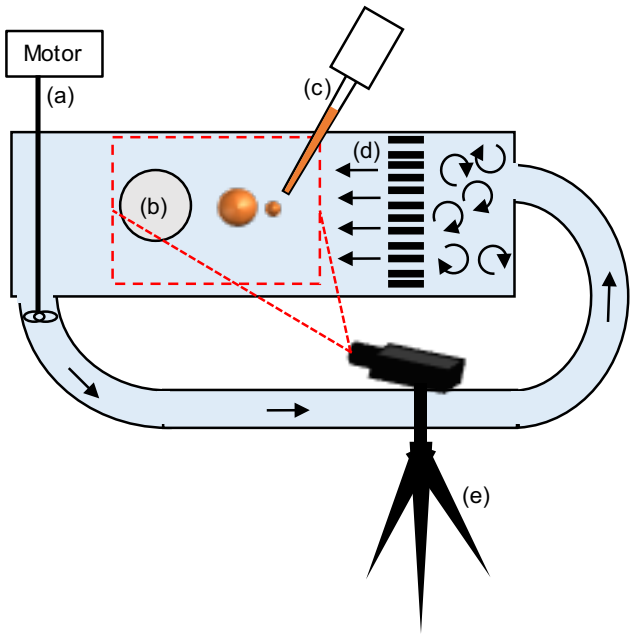

Figure 3.4. Schematic of the experimental setup. (a) Motor-impeller for creating a current in the flume tank. (b) Feeding appendage(s) or fiber. (c) Glass pipette for creating oil droplets. (d) Honeycomb structure to create a uniform flow. (e) High speed camera attached to a computer for video analysis. Black arrows in the diagram indicate flow direction.

Oil droplets were injected into the fluid stream through a glass pipette toward the fibre as depicted in Fig. 3.4. Droplet size was determined by the size of the pipette tip, which was made by pulling the tip over a flame. Droplets diameters ranged from 0.1 to 2.0 mm.

To study the effect of oil viscosity and oil-water interfacial tension three different oils were used : fish oil, canola oil, and 1-decanol (Sigma W236500). The fluid properties are presented in Table 3.1. An Anton Paar MCR 502 was used to measure the viscosity of the fluids, and a Dataphysics tensiometer was used to measure the interfacial tension between the oils and salt water using the pendant drop method. These three oils were chosen to sample a broad range of oil viscosities and interfacial tension that would still remain relevant to the marine environment. A broader range allows for a more comprehensive study of the effects these variables have on droplet behavior. Moreover, fish oil is naturally encountered by marine zooplankton and 1-decanol is carried by ships, therefore creating the possibility of a spill in aquatic ecosystems (Bengtsson and Tarkpea, 1983).

Table 3.1. The fluid properties of the three oils and saltwater used in this study.

Oil	Density ρ_o (kg/m^3)	Viscosity μ_o $(mPa \cdot s)$	O/W Interfacial Tension σ (mN/m)
Canola Oil	950	121	11.4
1-Decanol	815	22.3	9.6
Fish oil	902	40	10.1
Salt water	1020	1.42	—

3.3. Results

The first set of experiments showed that oil droplets of various sizes are captured by filtering appendages of live copepods, and dead, mounted barnacle (*Balanus glandula*) cirri. The copepods were starved and then exposed to an oil-in-water emulsion of either fish oil, canola oil, or 1-decanol for a period of 12 hours (as seen in Fig. 3.2). For copepods, the droplet radii were measured, and the positions sorted into three categories : droplets found in the gut of the individual (Fig. 3.2B), on its appendages (Fig. 3.2C), or agglomerated in floccs close to the mouth and feeding appendages (Fig. 3.2D). Those measurements were then compiled in Fig. 3.5, comprised of 105 droplets measured across all individuals and three copepods species (*Acartia tonsa, Calanus finmarchicus* and *Centropages typicus*. Since all three species showed no difference in their size selection, all the data was combined into

a single category. Droplets found attached to an appendage were as large as 11 μm with an average of $4.33 \pm 2.64\ \mu m$. Droplets found in the gut, did not show any significant maximum, as the encountered frequency was relatively constant across the distribution of the emulsions made with fish oil, canola oil and 1-decanol, as illustrated in Fig. 3.5, which varies from 1 to 16 μm in radius. Droplets that were found agglomerated in floccs were as large as 8 μm in radius. The average droplet radius for this category was $2.39 \pm 1.53\ \mu m$. Droplets captured by the appendages were either directed to the mouth or detached to re-enter the flow stream.

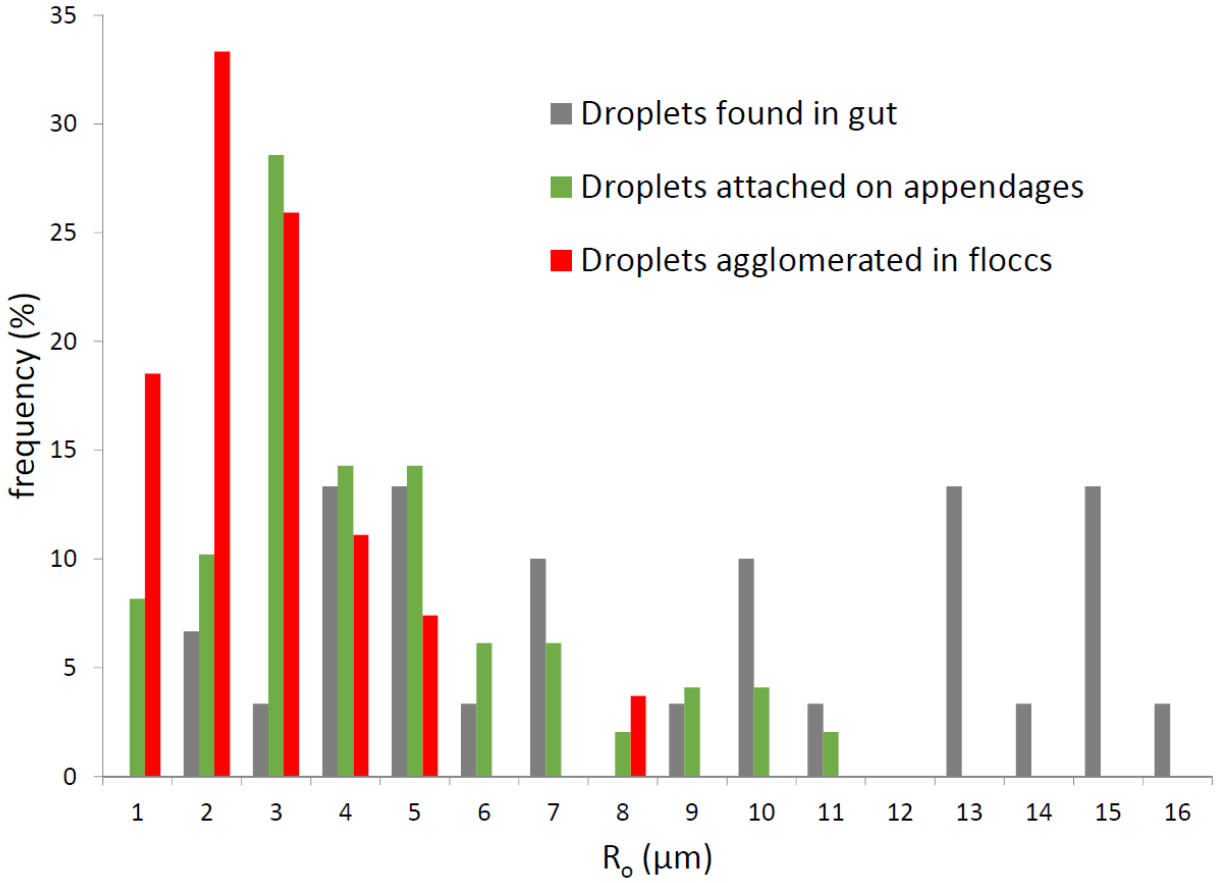

Figure 3.5. Distribution of fish oil, canola oil and 1-decanol droplets that were captured by *Acartia tonsa, Calanus finmarchicus* and *Centropages typicus*. Green bands show droplets captured by appendages, grey bands indicate droplets found in guts, and red bands indicate droplets agglomerated in floccs. (n=105)

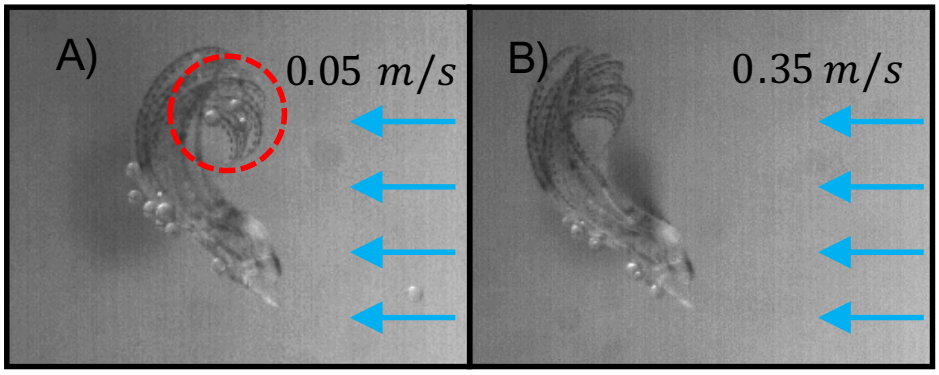

Figure 3.6. (A) Fish oil droplets being exposed to barnacle appendages and captured at $U = 0.05\,m/s$. (B) Droplets ranging from $100\,\mu m$ to $500\,\mu m$ in radius were then detached from the appendages at a higher velocity ($U = 0.35\,m/s$).

In a parallel experiment we exposed dissected and mounted barnacle cirri to fish oil droplets at seawater velocities from 0.01 to 0.35 m/s. Fish oil droplets ranging from 100 to $500\,\mu m$ in radius were captured passively at a low velocity ($0.05\,m/s$)(Fig. 3.6A), but detached at a higher velocity ($0.35\,m/s$)(Fig. 3.6B). A few droplets were seen attached behind the appendages, downstream to flow. Once a droplet is captured by the surface facing the flow, it will roll around the fiber if inertial forces are strong enough to overcome the capillary forces that otherwise maintain the droplet in place. Depending on the Reynolds number of the system and the size of the droplet, the droplet can either be sheltered from the flow passing around the fiber or oscillate due to vortices located behind the fiber (refer to Fig. 3.1A-B for both scenarios). At low Reynolds number, this could hinder the release of droplets but we highlight possible biological behaviors from barnacles that could prevent such accumulation of droplets in the discussion. We then isolated an individual cirrus to better photograph and illustrate capture and detachment. Figure 3.7 shows the interaction of a canola oil droplet ($R_o = 250\mu m$) with a barnacle cirrus. Frames A-D illustrate the capture event, where the free flow velocity was measured at $0.1\,m/s$. In frames A and B, the oil droplet approaches the tip of the cirrus. In frame C, the oil droplet is captured by the cirrus itself. In frame D, the droplet moves and continues to deform closer to the base of the cirrus due to inertial forces. This showcases a typical capture event of an oil droplet by a fiber. The detachment of the droplet is shown in frames E to H. For that droplet to detach from the cirrus, a critical Weber number of 0.36 was reached. In this case, this was achieved by gradually increasing the flow velocity using the variable speed motor of the flow tank. For this particular droplet,

the velocity that provided the conditions for detachment was $0.28\,m/s$. Frame E shows the captured droplet before any deformation can be seen. Frame F shows the moment where the system reaches the critical Weber number which results in further droplet deformation and detachment. Frames G and H show the oil droplet regaining its spherical shape after being detached from the cirrus. In frames E to H, the cirrus bends in direction of the flow. This is in fact an artifact of the isolation and dissection of said cirrus. When a live barnacle extends its cirri in the water column to feed, they are grouped relatively close together which limits the effects of the flow on a single fiber. Also, the animal can use the muscles in its appendages to counter the force exerted by the flow and have the majority of the cirrus' surface facing the flow. The left column of the figures show frames captured by the high speed camera with a time interval of $25\,ms/frame$. The right column shows a schematic version of the capture event where blue arrows indicate the flow's direction and the orange sphere the oil droplet.

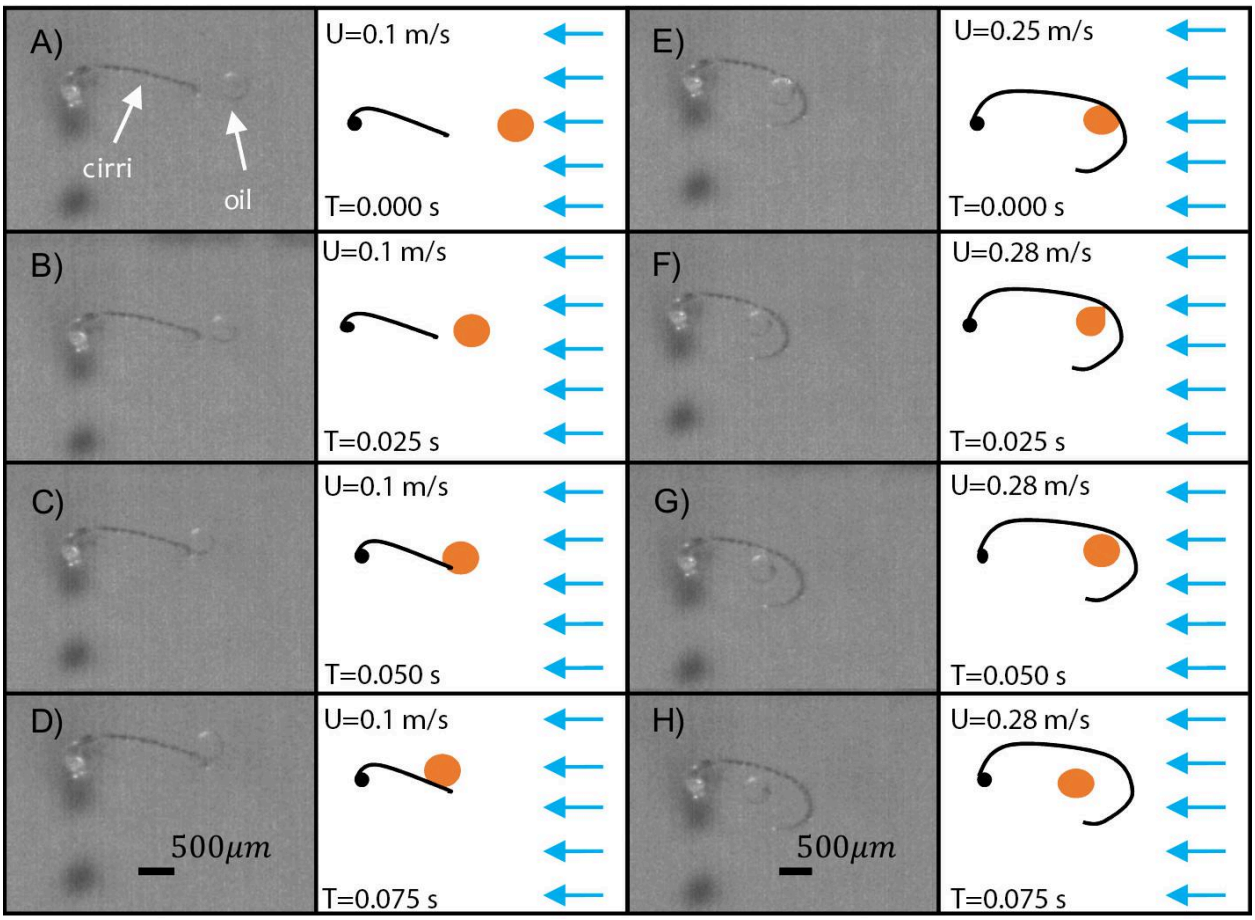

Figure 3.7. (A-D) Illustration of the capturing of a canola oil droplet ($R_o = 250\,\mu m$) by a barnacle cirrus ($R_f = 45\,\mu m$) at $U = 0.1\,m/s$ ($Re = 7.69$). E-H) Illustration of the same oil droplet detaching from the barnacle cirrus at $U = 0.28\,m/s$ ($Re = 21.56$). Time between each frame is $25\,ms$.

Our second objective consisted of finding the critical Weber number (ratio of inertial to capillary forces) as a function of oil droplet size in which oil droplets detached from stainless steel cylinders. Droplets of three oils (fish oil, canola oil, and 1-decanol) and of various sizes were filmed being captured by, and then detached from, steel cylindrical wires of two radii (50 and 250 μm). Our observations and the calculation of St, $\bar{R}$ and G for each droplet captured showed that inertial interaction and direct interception were the most common mechanisms for droplet capture. Indeed, St and $\bar{R}$ were of the same order of magnitude but were both higher than G, indicating that they are the main capture mechanisms (see Mehrabian et al. (2018b) for respective equations and for discussion on likelihood of capture by a particular mechanism based on droplet size and velocity). Therefore, larger droplet size with respect to the fiber size, and higher flow velocity increased the chances of a droplet

being captured. Also, oil droplets with a lower viscosity (*i.e.* 1-decanol) were more readily captured. These results are consistent with the theoretical findings of Rubenstein and Koehl (1977) and Mehrabian et al. (2018b).

Figure 3.8 illustrates the capture process of two fish oil droplets with different sizes ($r = R_o/R_f = 0.8$ & 1.2). Fig. 3.8 A-D show the motion of a droplet ($r = 0.8$) at $U = 0.08\,m/s$ moving towards a steel fiber with a window of $25\,ms$ in between each frame to showcase key moments of the capture. Frame A and B illustrates the oil droplet moments before capture. Frame C shows the capture event and frame D shows the droplet on the right side of the fiber without any further deformation. Values for inertial interaction, gravitational deposition, and direct interception were $St_o = 0.25$, $G_o = 0.09$, and $\bar{R} = 0.80$, respectively. See Mehrabian et al. (2018b) for details of St_o, G_o, and $\bar{R}$. Fig. 3.8 E-H shows a similar process but with a larger droplet ($r = 1.2$), and at a higher speed ($0.26\,m/s$). Because of the faster flow speed, frames E to H are separated by $12.5\,ms$. Frame E and F show the oil droplet before it is captured by the steel fiber. Frame G shows the oil droplet rolling towards the back of the fiber after the capture event. Frame H shows the oil droplet once it has stopped moving to the left, or downstream-side of the fiber. Values for inertial interaction, gravitational deposition, and direct interception were $St_o = 1.81$, $G_o = 0.06$, and $\bar{R} = 1.2$, respectively. In both experiments, values of intertial interaction St_o and direct interception $\bar{R}$ are the highest and have the same order of magnitude, indicating the main mechanisms responsible for capturing.

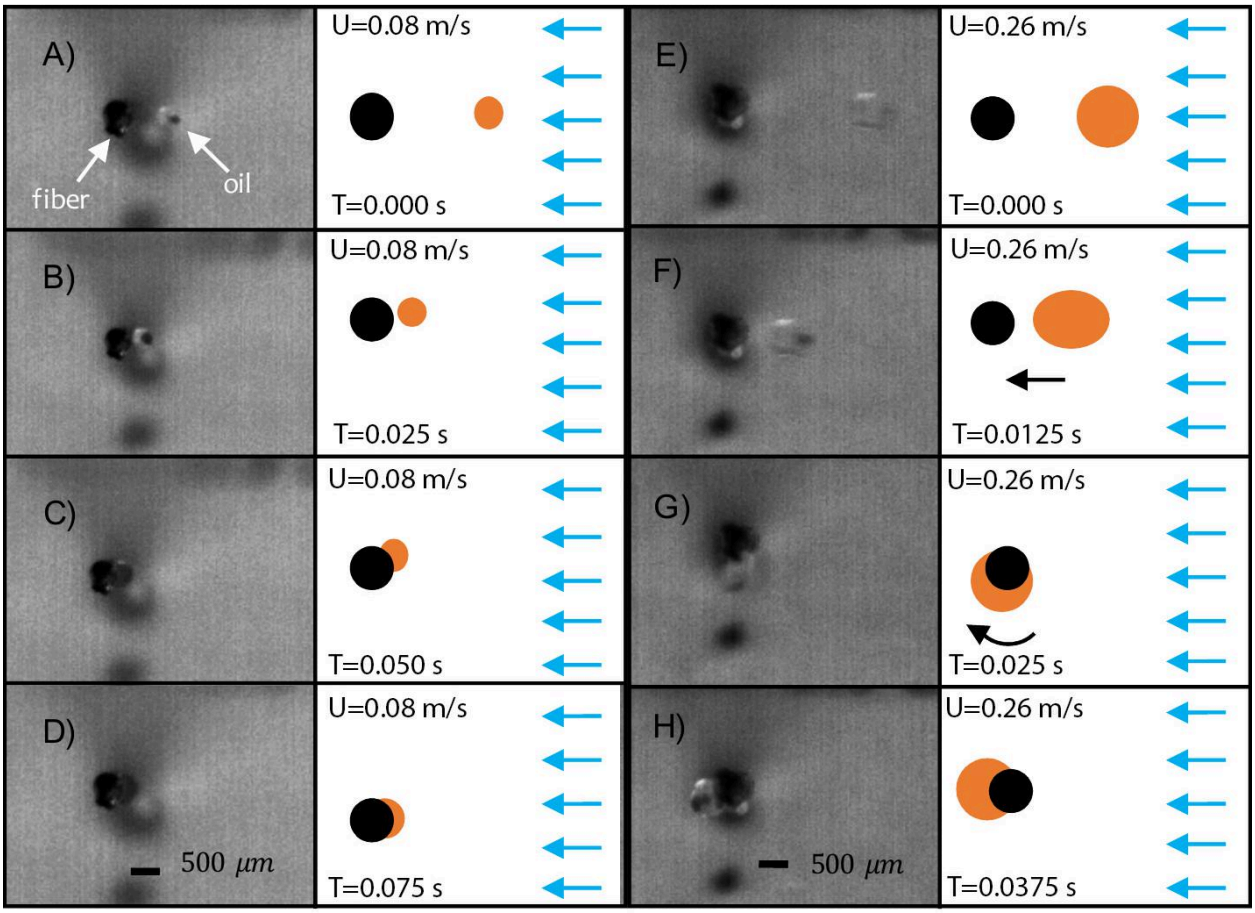

Figure 3.8. Two capture events of fish oil droplets. Frames A to D show an oil droplet of 200 μm being captured by a 250 μm cylindrical steel fiber at a velocity of 0.08 m/s. Each frame is separated by 25 ms. Frames E to H illustrates a similar process but with an oil droplet of 300 μm at a velocity of 0.26 m/s. Each frame is separated by 12.5 ms. Note that the oil droplet in frame E to H shifts towards the left side of the steel fiber due to a higher flow velocity.

The degree of oil movement from right to left after capture, which can be seen in frame H, but not in frame D of Fig. 3.8 is directly related to size of the droplet relative to the fiber, consistent with Mehrabian et al. (2016). The reason for this is that the flow at a given speed (U_w) will create a velocity at the oil-water interface. This interfacial velocity then creates a re-circulating internal flow within the oil film. The internal flow then deforms the oil and pushes it to the left, downstream-side of the fiber. In contrast, when the film thickness of the oil coating the fiber is too small (similar to frames A to D), the interfacial velocity will be too small because of the no-slip boundary condition ; hence less internal flow and less oil deformation from right to left.

Once a droplet was captured, the flow velocity in the flume tank was gradually increased until the droplet detached and re-entered the fluid stream. Fig. 3.9 shows a typical example of a 1-decanol droplet of 250 μm in radius detaching from a $R_f = 50\ \mu m$ steel fiber ($r = 5$). The velocity needed for the droplet to detach was measured at 0.21 m/s. Each frame is separated by 25 mm. Frames A and B show the droplet oscillating up and down due to the high Reynolds number of the system, which create vortexes behind the fiber (refer to Fig. 3.1B). After some time the droplet stretched due to external forces, and split into a larger droplet (daughter droplet), and a smaller droplet (satellite droplet) (Mehrabian et al., 2016). Frame C shows the initiation of the detachment mechanism where the daughter droplet started to form at the end of the elongated droplet. Frame D show the detachment where the daughter droplet fully detached and re-entered the fluid streams while regaining a spherical shape. A smaller satellite droplet is formed between the daughter droplet and the steel fiber and also re-entered the fluid streams. Finally, a small part of the initial droplet stayed on the fiber. A similar detachment process was observed with the stationary barnacle legs (data not shown).

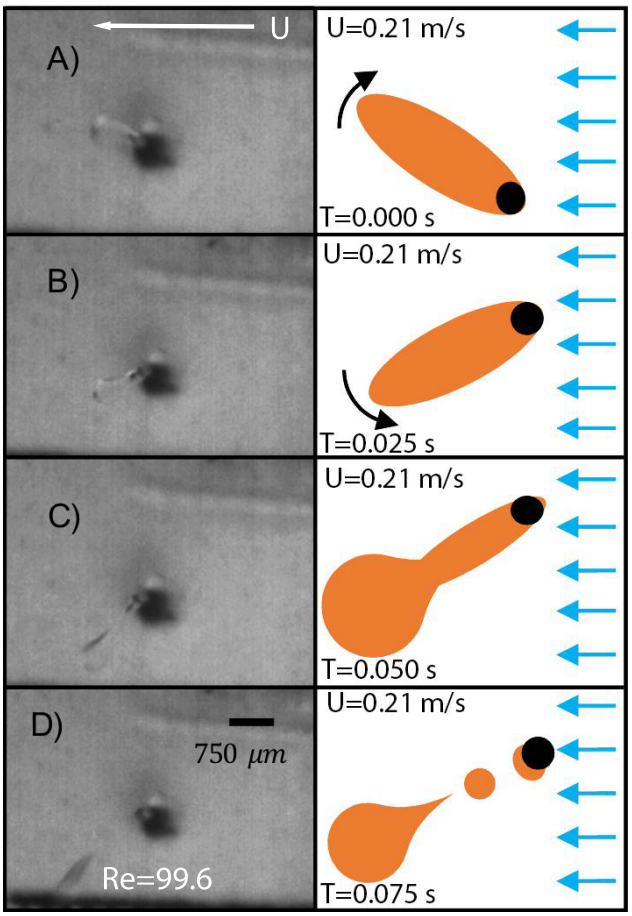

Figure 3.9. Detachment of a 1-Decanol droplet from a steel wire of radius 250 μm. Time between each frame is 25 ms and flow velocity is 0.21 m/s. The left column shows key moments of the detachment process, and the right column shows a schematic version of that process.

In order to be able to compare different oils, fiber and droplet sizes, dimensionless numbers were used. In these experiments, the Weber number We, oil-to-water viscosity ratio p, and $r = R_o/R_f$ were used to characterize the detachment process. The Weber number expresses the ratio of inertial and capillary forces. Fig. 3.10 shows a log/log graph of the droplet size to fiber ratio as a function of the Weber number. Each data point represents a critical Weber number at which the oil droplet detached from the fiber or filtering appendage experimentally. Only the data where the Reynolds number was in the range of the orders 10^1 to 10^2 were kept to ensure inertial forces were dominant over viscous and capillary. This means that when the critical Weber number was reached, the inertial forces overcame the capillary forces, which were responsible for maintaining the droplet's shape and preventing its detachment from the fiber. This graph is significant because conditions above those data points will force the oil

droplet to detach from the fiber and re-enter the fluid stream, and conditions below them will keep the droplets attached to the fiber. The results in Fig. 3.10 incorporate a series of experiments conducted on two fiber radii (50 and 250 μm) for all three oils (fish oil, canola oil, and 1-decanol). The range of We experienced was between the orders of 10^{-2} to 10, and the droplet size to fiber size ratio ranged from 0.4 to to 12. As Fig. 3.10 shows, the ratio of inertial to capillary forces needs to increase as the droplet to fiber size ratio becomes smaller for detachment to occur.

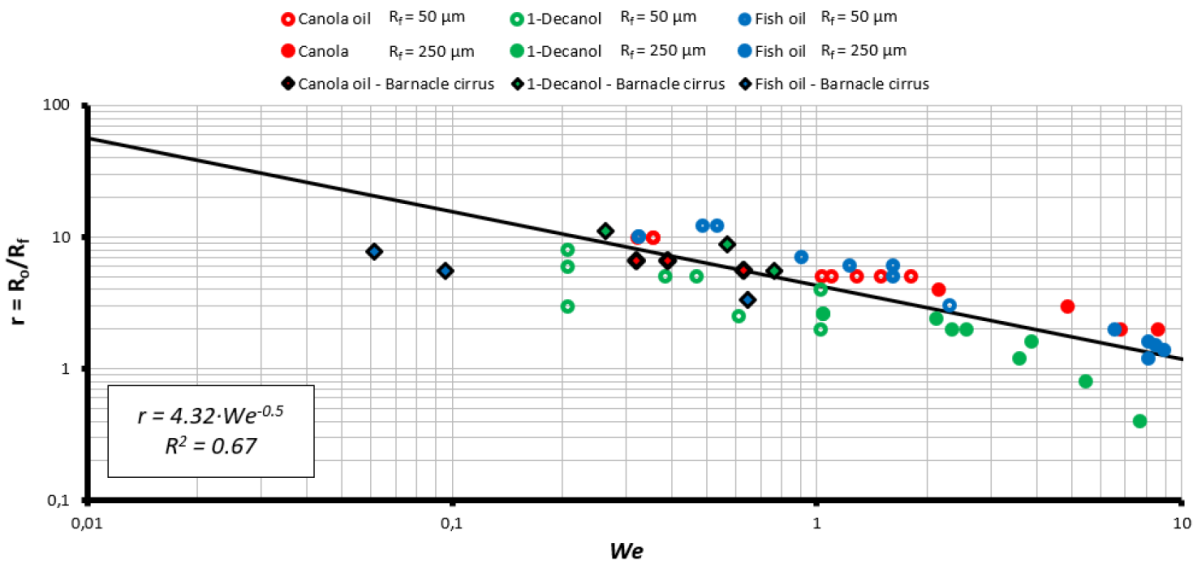

Figure 3.10. Log/log graph of the oil droplet size to fiber size ratio as a function of the Weber number. Each data point represents the critical Weber number at which the droplet will detach. Conditions below that critical point will keep the droplet attached, and conditions above it will force the oil droplet to detach and re-enter the fluid stream. Blue indicates fish oil droplets, red indicates canola oil droplets, and green indicates 1-decanol oil droplets. Hollow circles indicate that the fiber used has a radius of $R_f = 50\ \mu m$, full circles are for the fiber of $R_f = 250\ \mu m$, and diamonds correspond to when a barnacle cirrus was used as the fiber ($R_f = 45\ \mu m$). (n=52)

As already mentioned, the motion of the external flow will create a velocity gradient at the oil-water interface. This interfacial velocity will create a re-circulating internal flow within the oil film. The internal flow will then deform the oil and try to overcome the capillary forces and detach from the fiber. However, more viscous oils will have harder time to detach because the internal flow will be slower. Fig. 3.11 illustrates the changes in the Weber number as a function of oil-to-water viscosity ratio p for different oil droplet sizes $r = R_o/R_f$ intervals *i. e.* 0 to 4, 4 to 8 and 8 to 12. We found that a more viscous oil required a higher Weber

number in order to detach from the fiber. For a given droplet to fiber size ratio, a less viscous oil detached from the appendage at a lower Weber number. However, for all droplet to fiber ratio intervals, there seems to be very little difference in the critical Weber number for canola and fish oil. Our hypothesis is that beyond a certain viscosity ratio, the viscosity does not play a role in the detachment process of the droplet. This would explain why canola and fish oil, which have two distinct viscosities, still have relatively similar Weber number for droplet detachment.

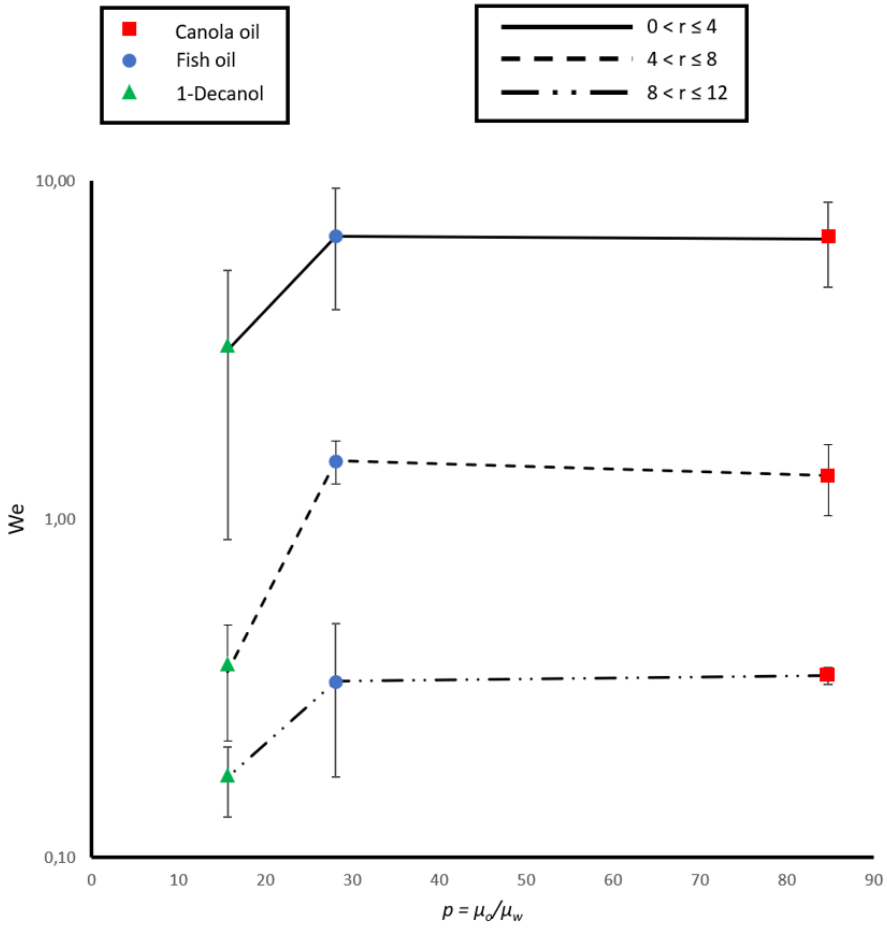

Figure 3.11. Changes in the critical Weber number for droplet detachment as a function of oil-to-water viscosity ratio p for different oil droplet sizes $r = R_o/R_f$ intervals. (n=48)

3.4. Discussion

Oil is a natural product of life, released into water from decaying animals, plants, protists or as petroleum. In general, oils are highly nutritious, and are widely captured by zooplankton

(Almeda et al., 2013, 2014a; Hansen et al., 2015; Conover, 1971). Here we show that fish oil, canola oil, and 1-decanol droplets were captured and consumed by calenoid copepods. Droplet of all sizes were captured and consumed, suggesting no size preference in the 1 to 16 μm range (Fig. 3.5). It remains to be tested if oil is generally consumed by filter feeding animals, or if some species reject oil droplet by size, or chemistry. Laboratory experiments with flavoured and untreated polystyrene spheres reveal major differences in taste discrimination among copepods, daphnias, cladocerans, and rotifers (Hartman and Hartman, 1977; Kerfoot and Kirk, 1991; DeMott and Watson, 1991; Friedman and Strickler, 1975).

We found that mounted, stationary barnacle legs captured fish oil droplets of up to 500 μm in radius at 0.05 m/s. We then slowly increased the seawater velocity to 0.35 m/s where the droplets detached and re-entered the flow stream. *Balanus glandula* in wave-swept environments are exposed to water velocities ranging from 0.05 m/s to well over 10 m/s (Marchinko and Palmer, 2003), where the potential for detachment of oil is significant. At low flow speeds, barnacles actively feed by closing the biramous cirrus and numerous setae around particles and droplets, and contract into the shell for ingestion. Still, some droplets detached, and this is governed by the ratio of oil droplet to fibre size radius, oil-to-water viscosity ratio, and the Weber number. The Weber number accounts for flow velocity, water density, fiber size and the interfacial tension between water and oil.

Figure 3.10 characterizes the role of Weber number on the detachment of oil droplets from steel fibres and a barnacle leg. The black curve is the fitted line obtained from data points of three types of oil (fish oil, canola oil, and 1-decanol) using the steel wires. The Reynolds number for all data points vary from 10 to 161.7. The diamond data points were obtained using the same oil droplets but with a barnacle cirrus, which validates the curve obtained from the steel wires for biological purposes. The fiber radius R_f used to calculate the Weber number was taken at the middle of the cirrus for consistency. This average radius was $R_f = 45\ \mu m$. Although the barnacle cirrus may be rougher due to the setae, the critical Weber number for a droplet to detach was similar to a smooth steel surface, indicating that surface roughness was less important at these Reynolds numbers.

The exponential regression provide in Figure 3.10 allowed us to validate the results obtained in Figure 3.5. Figure 3.5 shows that the distributions of oil droplet sizes captured by copepods was the same as the normal distribution provided to them (see Fig. 3.3). The

biggest droplets in the emulsion were of 16 μm in radius. This size, however, was not observed on any of the appendages reported in Fig. 3.5. Indeed, the biggest droplet that was attached to an appendage had a radius of 11 μm. A copepod setae can vary in diameter from the base to the tip from 4 to 0.5 μm, where the middle section has a 1 μm diameter (Paffenhöfer and Loyd, 2000). When using the *Acartia tonsa*'s average bursting speed of 600 mm/s (Buskey and Hartline, 2003), the approximate Weber number for a fish oil droplet is $We = 3.63 \times 10^{-2}$. With this Weber number and the regression curve of Fig. 3.10 $r = 4.32We^{-0.5}$, an oil droplet to fiber size ratio of $r = 22.66$ is obtained. Knowing that $r = R_o/R_f$ and that the radius of the fiber is in average 0.5 μm, it is then possible to estimate the maximum oil droplet radius that can remain captured by the appendage to approximately 11.33 μm. Therefore, bigger droplets will detach from the fiber and re-enter the fluid stream, which is very similar to the biggest droplet measured on an appendage of 11 μm in radius. These conclusions do have to be validated using high speed videography, since they are taken out of the data range provided by our experiments. In other words, the bursting behavior of the copepod will increase the Weber number of the system above the critical value, resulting in the detachment of droplets larger than the calculated threshold. This could prove an effective way for planktonic filter feeders like copepods to prevent or limit major fouling in the event of an oil spill.

However, since zooplankton can showcase an enormous diversity of body plan and appendage morphology, it is to be expected that the setae size, surface structure and wettability may vary across taxa and species. This could prove true even throughout the life of a single organism. Indeed, during the first larval stages of the calanoid *Pseudodiaptomus hessei*, the number of setae and their size are considerably smaller than at the adult stage, thus increasing the oil droplet to fiber size ratio (Jerling and Wooldridge, 1989). This could prove beneficial to the larvae as it would require a smaller Weber number for droplet detachment compared to that same droplet captured by an adult appendage. Filter feeding copepods can generally capture and ingest particles ranging from $2 - 200\,\mu m$ in diameter. They can also discriminate particles based on size, taste and toxicity (Almeda et al., 2016). However, each species has a minimal size threshhold, *i.e.* $5 - 10\,\mu m$ in diameter, at which it cannot detect and reject a particle (Gonçalves et al., 2014). These smaller particles could then be ingested even if the organism does not wish to. This is especially important with crude oil

since it can cause sublethal effects to zooplanktonic species and increase mortality. Moreover, the surface chemistry and texture can also affect the potential capture of oil droplets. The chemicals produced by the organisms may create a lipophilic surface, making it harder for the droplet to detach ; or a lipophobic surface, enabling conditions for detachment of the droplet. This has been studied theoretically using steel fibers in Mehrabian et al. (2018b), but further studies are needed to determine the hydrophobicity or hydrophilicity of biological structures. The surface texture of these structures may also contribute to the capture and detachment process. The results in Fig. 3.10 using the barnacle cirrus indicate that its ramifications and texture do not impact droplet detachment since the data is very similar to when using steel fibers.

We observed large droplets inside the guts of copepods, even when those sizes should not remain on an appendage long enough to allow for handling and ingestion. Droplets of 11 μm in radius and higher were few in the emulsion distribution (Fig. 3.3), yet the observed frequency of these large droplets was comparatively high in the guts (Fig. 3.5). Since droplets over 11 μm in radius are likely to detach from the appendages, the fact that these big droplets are found in the gut hints to coalescence or that they were consumed almost instantly before they could detach from the appendage. Coalescence is a mechanism by which two small droplets come together and the water film between them reaches a critical thickness (Mehrabian et al., 2018b). When this critical thickness is reached, the oil-water interface breaks and the two oil films fuse, to create one droplet of greater volume. The crowding of droplets is likely to happen inside the guts of animals, and further coalescence events can create droplets with the radii observed in Fig. 3.5. Then, Figure 3.10 is generally useful to know the conditions required for detachment of oil droplets from fibers.

The detachment of oil droplets from a filtering appendage is an important mechanism as it can potentially decrease the amount of oil that is ingested during an oil spill. In high flow velocity environments such as coastal ecosystems, benthic or sessile filter feeders could have their potential oil intake drastically reduced. For example, a barnacle exposing its cirri to the flow could be able to get rid of unwanted captured particles. In Fig. 3.6, most oil droplets detached from the specimen when the flow velocity reached 0.35 m/s. According to Geierman and Emlet (2009); Marchinko (2003); Marchinko and Palmer (2003), this velocity is well within the range at which these barnacles may feed, supporting the hypothesis that

only smaller droplets may stay attached to the appendages of benthic filter feeders. Indeed, as bigger droplets require a lower Weber number to detach, the organism would be left only with the smaller oil droplets. Furthermore, barnacles or other filter feeders using ramified fibers could increase the number of detachment events by augmenting the spacing between fibers. This would increase leakiness of the appendage and allow more fluid to pass through gaps (Koehl, 1993). The Weber number would increase locally and enable detachment of a droplet for which its Weber number was previously below the critical value. When thinking about oil spill clean-up methods, it could be possible to select a surfactant whereby the oil droplets in the oil-in-water emulsion are above the corresponding critical r in Fig. 3.10. By doing so, the effects of an oil spill on benthic filter feeding communities would be limited to a mimimum as almost no oil would remain captured and ingested by these organisms.

Figure 3.11 shows the critical Weber number for oil droplet detachment as a function of oil/water viscosity ratio. This was done for all three oils and for three different oil droplet/fiber size ratio intervals r. For lower viscosity ratios, the critical Weber number for droplet detachment is lower than at higher viscosity ratios. Then, a less viscous oil is more likely to detach in environments with low flow. When looking at a single oil but at different r, a bigger droplet will require a lower flow velocity to detach from the fiber than a droplet that is closer to the fiber in size. This could be explained by the fact that a droplet matching the size of the fiber has a higher proportion of its volume that is inside the boundary layer of the fiber. There is therefore less internal flow inside the droplet and deformation is less important. When water flows over the droplet, a movement at the oil/water interface is created. The movement at this interface then creates a flow inside the oil droplet. A more viscous oil will have a slower internal flow making it harder for these droplets to deform and overcome the capillary forces that are keeping it attached to the fiber. To obtain the same level of internal flow of a less viscous oil, a higher external flow velocity is needed, which translates in a higher Weber number. It can also be observed that for a given r interval, the Weber numbers for canola and fish oil are very similar. This could be due to the viscosity playing no role beyond a specific oil to water viscosity ratio. If the viscosity does not affect detachment, then two oils with different viscosities, but with the same droplet size would detach in the same flow conditions.

Figure 3.10 is a powerful tool for predicting the detachment of oil droplets from a filter feeding appendages following an oil spill. If one can measure a few key parameters of the system including flow velocity, oil droplet size distribution, and the filtering appendage sizes of the dominant zooplankton (from a plankton tow), then the oil droplet to fiber size ratio and Weber number can be approximated. Once these parameters are know, the oil droplet to fiber size ratio and the Weber number can be compared to the curve and the behaviour of the droplets predicted. If the data point is higher than the fitted curve, the oil droplets will detach from the appendages and re-enter the fluid stream. If the data point is lower, then the droplets will remain captured. This tool is especially useful when coupled with a range of surfactants, that create different emulsion distributions. Knowing these distributions, the surfactant that increase the probability of oil droplet detachment from filter feeder appendages can be applied. Current oil spills protocols mainly focus on preventing the oil from reaching the shores and the coastal ecosystems (Tewari and Sirvaiya, 2015). This study adds another tool for assessing the risk specific droplets sizes can have on planktonic species at the site of the spill.

The role of surfactants in the event of an oil spill are complicated. A surfactant will increase the size range of petroleum and beneficial oils in the environment. These modified oils will more readily detach from the feeding appendages of zooplankton, limiting their entrance to the marine food web. Limiting access to naturally occurring oils could negatively impact growth, reproduction and metamorphosis of zooplankton. The cyprid larval stage of barnacles, for example, is a non-feeding larva that depends solely on its lipids reserve to find a suitable habitat for settlement, and metamorphosis into a sessile, feeding adult (Franco et al., 2016). If the larval stages prior to the cyprid cannot feed on nutritious oils, then settlement and metamorphosis would be diminished. Complicating things further is the finding that larger droplets are retained on the appendage for a brief moment before detachment. Indeed, observations from Figure 3.7, 3.8 and 3.9 show that even when the conditions reach the critical point for detachment, the droplet does not detach instantly. In some cases, this allows time for the droplet to be manipulated by the filtering appendages. Copepods can use this opportunity to effectively reduce the size distribution of an oil-in-water emulsion (Marco et al., 2019). Although the surfactant prevents the majority of droplets from captured, copepods could sever these big droplets in smaller daughter droplets that could

then remain captured and ingested. Moreover, the detachment of a big droplet can create a satellite droplet that is significantly smaller than the original droplet (Fig. 3.9D).

The choice to use surfactants is further complicated because copepods and other zooplankton can contribute positively to the fate of an oil spill by pelletizing the oil droplets (Conover, 1971; Lee et al., 2012; Sleeter and Butler, 1982; Almeda et al., 2016). Since oils usually have a density that is lower than water, they will tend to rise to the surface or, with the use of surfactants, they will stay in the water column for extended periods of time (Mehrabian et al., 2018b). When compacted into a feacal pellet, however, the overall density of the pellet is greater than water and it will sink *i.e.* 100-300 m/day, towards the seabed (Sleeter and Butler, 1982). Nepstad et al. (2015) estimated that copepods populations may filter up to 40% of the spilled oil, which would then be pelletized, defecated and degraded by the microbial benthic fauna. This could also prove an effective way to clean the water column, but it would also mean that the oil would be available to the higher trophic levels via the predation of the copepods. However, Fernandez et al. (2022) found that the main surfactants used in oil spills reduce the size of droplets well below the optimal size for dmicrobial degradation. Then, chemically-dispersed oil can stay longer in the water since it is degraded at a lower rate. Considering that the main entry point for crude oil in the marine ecosystems is via zooplankton communities, the following question arises. Should we consider using a surfactant, thus hindering the ingestion of both detrimental and beneficial oils, or should we let the zooplankton ingest and pelletize the oil droplets ? In situ community based studies that integrate ecology, ecotoxicology and fluid dynamics are needed to assess the implications and consequences of each approach. This study focuses on the conditions needed for detachment of oil from filtering appendages. By understanding how a droplet is likely to detach, it is then possible to facilitate these conditions and in turn reduce the amount of oil introduced into aquatic systems.

Chapitre 4 .

The capture of crude oil droplets by filter feeders at high and low Reynolds number

par

Francis Letendre[1] et Christopher B. Cameron[1]

([1]) Département de sciences biologiques, Complexe des sciences, Université de Montréal, 1375 Avenue Thérèse-Lavoie-Roux, Montréal, Québec, H2V 0B3, Canada

Cet article a été publié dans :

Journal of Experimental Biology (2022), 225 : no 8.

DOI : /org/10.1242/jeb.243819

Cet article a été modifié pour les besoins de la thèse.

Rôle des auteurs

Francis Letendre : Conceptualisation du désign expérimental, création du matériel expérimental, conception de la méthodologie, revue de littérature, collecte des données, analyse des données, rédaction du manuscript, soumission et révision du manuscript

Christopher Cameron : Conceptualisation du désign expérimental, validation des résultats, révision du manuscript, supervision et administration du projet, acquisition du financement

Résumé.

Les crustacés filtreurs capturent les gouttelettes d'huile par le biais de leurs appendices ramifiés. Ces appendices agissent comme des palmes ou des tamis, dépendamment du nombre de Reynolds du système. Ici, nous utilisons l'imagerie à haute vitesse, la microscopie électronique à balayage et la mécanique des fluides afin d'étudier les mécanismes de capture de gouttelettes de pétrole brut ainsi que la mouillabilité de deux espèces de balanes (*Balanus glandula* et *Balanus crenatus*) et du cladocère *Daphnia magna*. Nos résultats démontrent que les appendices de balanes vont se comporter en tant que palmes et capturer des gouttelettes dans leur couche limite à bas nombre de Reynolds. À haut nombre de Reynolds, les gouttelettes sont majoritairement capturées par interception directe. Il existe un intervalle intermédiaire de nombre de Reynolds où les gouttelettes sont capturés par les deux mécanismes simultanément. *Daphnia magna* capture les gouttelettes dans les couches limites de la troisième et quatrième paires de pattes thoraciques lors du mouvement métachronal de ses appendices. Toutes les surfaces étudiées se sont révélées hautement lipophobiques, montrant des gouttelettes capturées avec de très grands angles de contact. Nous discutons aussi des implications de ces types de capture et de la mouillabilité sur l'ingestion potentielle de pétrole brut par les organismes filtreurs. Ces résultats contribuent à augmenter nos connaissances sur la capture du pétrole brut par les organismes filtreurs, et sur le principal point d'entrée de celui-ci dans les réseaux trophiques marins.

Mots clés : alimentation par filtration, mécaniques des fluides, mouillabilité, nombre de Reynolds, pétrole brut, zooplancton

Abstract.

Crustacean filter feeders capture oil droplets with the use of their ramified appendages. These appendages behave as paddles or sieves, based on the system's Reynolds number. Here we used high-speed videography, scanning electron microscopy and fluid mechanics to study the capture mechanisms of crude oil droplets and the filtering appendage's wettability by two species of barnacles (*Balanus glandula* and *Balanus crenatus*) and of the freshwater cladoceran *Daphnia magna*. Our results show that barnacles appendages will behave as paddles and capture droplets in their boundary layers at low Reynolds number. At high Reynolds number, droplets are most likely to be captured via direct interception. There is an intermediate range of Reynolds number where droplets can be captured by both mechanisms at the same time. *Daphnia magna* captures droplets in the boundary layers of the third and fourth pair of thoracic legs with a metachronal motion of the appendages. All studied surfaces were revealed to be highly lipophobic, demonstrating captured oil droplets with high contact angles. We also discuss implications of such capture mechanisms and wettability on potential ingestion of crude oil by filter feeders. These results further our understanding of the capture of crude oil by filter feeders, shedding light onto the main entry point of oil in the marine food webs.

Keywords: filter feeding, fluid mechanics, wettability, Reynolds number, crude oil, zooplankton

4.1. Introduction

Filter feeding is widespread across phyla, body sizes and ecosystems (Jørgensen, 1955). It consists of capturing particles of various sizes and origins that are dispersed in the water column using a filtering apparatus. Depending on the species, filter feeders select particles from the water column based on size, shape, taste, chemical cues and even texture (Gerritsen and Porter, 1982; Gonçalves et al., 2014; Hartmann and Kunkel, 1991; Tiselius et al., 2013). These particles may be debris, bacteria, algae, protists or plankton. Less appreciated is that filter feeders also feed on suspended oil droplets (Conover, 1971; Nordtug et al., 2015). These droplets may be lipids of decaying plants and animals or petroleum droplets from a spill, pipe seepage or other anthropogenic activities. The naturally occurring oils serve many beneficial functions for zooplankton, including regulating buoyancy during vertical migrations or as a lipid reserve for gametogenesis and overwintering (Thorisson, 2006; Visser and Jónasdóttir, 1999). The cyprid larva of a barnacle depends on lipid droplet provisions to locate a suitable settlement site (Franco et al., 2016). The ingestion of crude oil droplets may have detrimental and sublethal effects, including lower egg counts and hatching rates, an increase in faecal pellet production and a general decrease in feeding and swimming activity (Almeda et al., 2014a; Cohen et al., 2014; Nordtug et al., 2015).

The capture of solid particles by filter feeders has been studied extensively from a theoretical (Rubenstein and Koehl, 1977) and biological perspective (Kiørboe, 2011). We do not have an experimental understanding of oil droplet capture by a feeding appendage or appendages. This subject is significant because droplet capture is how oil enters the food web. Petroleum oil ecotoxicology is widely studied at the species and community levels (Daly et al., 2021; Lemcke et al., 2019; Yilmaz and İşinibilir, 2018). To prevent these toxic effects, we must begin with an understanding of droplet capture mechanics. We have provided a theoretical foundation to understand these mechanics (Mehrabian et al., 2018b). In theory, oil droplet capture is largely determined by the same factors that regulate solid particle capture, but there are additional variables to consider.

Like solid particles, the variables important to droplet capture include the droplet size, density, and Reynolds number (Rubenstein and Koehl, 1977). A Reynolds number is a dimensionless number that is used to study the flow and capture mechanisms of particles by a

single cylindrical appendage. It is obtained by the following equation :

$$Re = \frac{\rho_w U_w (2R_f)}{\mu_w} \tag{4.1}$$

where ρ_w is the water density, U_w is the stream velocity, R_f is the radius of the fiber and μ_w is the viscosity of the water. The majority of filter feeders feed in an environment where the Reynolds number is in the order of 10^{-5} to 10^{2} (Koehl, 1993). A copepod appendage operates at the lower end because of the diminutive size of the setae and setules, whereas a barnacle from a high flow velocity location operates at the upper end of the spectrum.

The amount of fluid that will pass between two cylindrical appendages, or leakiness, is also determined by the system's Reynolds number. An appendage that is fully leaky will have as much fluid pass between two fibers as it would in that same area at free-stream velocity. In other words, the presence of fibers will not alter the volume of fluid able to pass through (Cheer and Koehl, 1987b). As a general rule, Koehl (1993) established that if the Reynolds number is equal or lower than the order of magnitude 10^{-2} the appendage will behave as a paddle. Little to no fluid will pass between the appendages and particles are mainly trapped in the boundary layer. However, the leakiness of an appendage is also dependant on the gap-to-diameter ratio of the fibers. Increasing the spacing of the fibers at this Reynolds number will increase the appendage's leakiness and allow for more fluid to pass between fibers. The order of magnitude of the boundary layer around a single cylindrical appendage can be approximated using the following equation (Boudina et al., 2020; LaBarbera, 1984) :

$$\delta = D/\sqrt{Re} \tag{4.2}$$

When the system's Reynolds number is in between the orders of 10^{-2} to 1, appendages tend to behave as leaky paddles, where some fluid may pass between appendages. At this scale, a subtle change in flow velocity or cylinder spacing can shift the capture mechanism to sieving. At this range of Reynolds number, increasing the gap-to-diameter ratio, either by using smaller fibers or spreading them further apart, will also increase the leakiness of the appendage (Cheer and Koehl, 1987b). Thus, the appendage's leakiness is highly variable at this regime and a small morphological or behavioral change can alter the flow profiles around and in between fibers. If the Reynolds number is over 1, the boundary layer around the appendages will be narrower than in a viscosity-driven system. This permits fluid to fully

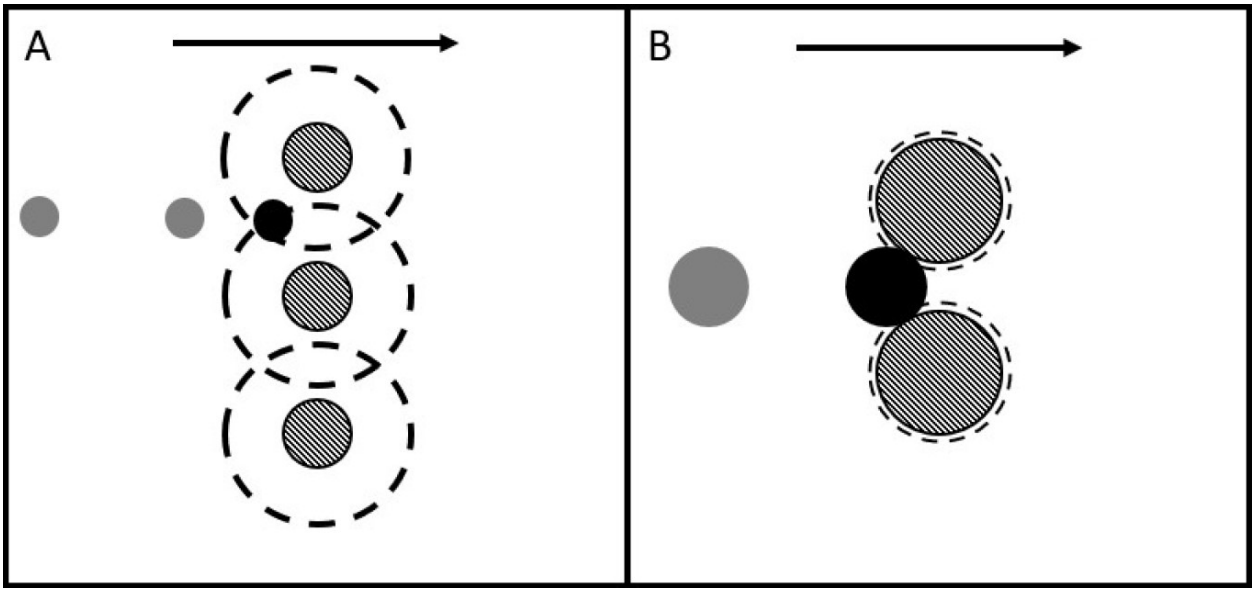

Figure 4.1. Schematic representation of (A) an appendage behaving as a paddle and (B) as a sieve. Black arrows indicate the direction of flow, black circles represent captured oil droplets, grey circles represent past positions of oil droplets, dotted circles illustrate the boundary layers and hatched circles are fibers. Note that the boundary layer thickness should vary around the fiber. However, for clarity, they are displayed as perfect circles.

pass in between appendages and free-stream velocities to occur closer to the cylinders. Since particles can pass between the appendages, sieving can occur. Solid particles that are larger than the mesh size are captured by two adjacent fibers. Examples of an appendage capturing a particle while behaving as a paddle and a sieve are visible in Fig.4.1. Oil droplets, on the other hand, may squeeze through if external forces are sufficient and if the collecting surface has a low wettability (Letendre et al., 2020; Mehrabian et al., 2018b).

In addition to droplet size, density, and Reynolds number, the wettability of a fiber impacts the capture of an oil droplet (Mehrabian et al., 2018b) (Conova, 1999; Gerritsen and Porter, 1982). Wettability consists of the affinity a fluid has for a solid surface and the degree that it will spread on it. The wetting of a surface is governed by its texture, surface chemistry and hydrophobicity. Models suggest that particle capture is enhanced when the collection surface has low wettability (Conova, 1997). The exoskeleton of *Daphnia sp.* has low

wettability and displays hydrophobic characteristics (Dodson, 2004; Gerritsen and Porter, 1982).

Oil droplet capture mechanics are largely the same as those for particles. They are direct interception, inertial interaction and gravitational deposition (Rubenstein and Koehl, 1977; Mehrabian et al., 2018b). Direct interception is in play when a particle reaches a minimum distance of its radius from the fiber and contacts it. Recent work by Boudina et al. (2020) estimated that, in inertia-governed systems, particle size must not be more than 70% of the fiber's boundary layer for direct interception to be considered. Otherwise, inertial interaction is likely the main capture mechanism. Inertial interaction occurs when forces on the particle are strong enough to deviate it from its streamline and cause it to touch the fiber. Gravitational deposition takes place when a difference of density between the particle and fluid exists. This will cause it to move upward or downward depending upon whether the particle is more or less buoyant that the fluid. The particle can then contact the fiber and be captured.

With respect to oil droplets, the intensity of each of these mechanisms can be expressed by a dimensionless number. Then, the dimensionless number *i.e.*, $\bar{R}$ for direct interception, St for inertial interaction or G for gravitational deposition, with the highest order of magnitude would determine the more probable capturing mechanisms. The intensity of direct interception can be obtained using the following equation :

$$\bar{R} = \frac{R_p}{R_f} \tag{4.3}$$

where R_p and R_f are the radius of the particle and the fiber respectively. The importance of inertial interaction is measured using the Stokes number, which can be expressed as followed :

$$St = \frac{(2R_p)^2(\rho_p - \rho_w)U_w}{18\mu_w R_f} \tag{4.4}$$

Where ρ_p and ρ_w are the densities of the particle, or the oil, and of the water respectively. Finally, the dimensionless number used for measuring the intensity of gravitational deposition is calculated in a similar way. However, the main force acting on the particle is now the gravitational pull and not the stream velocity. The equation for this particular capture mechanism's intensity is :

$$G = \frac{(2R_p)^2(\rho_p - \rho_w)g}{18\mu_w U_w} \tag{4.5}$$

where g is the gravitational acceleration.

Thus, flow velocity, particle radius and density play an important role in particle capture. Increasing the droplet size or stream velocity will result in a higher probability of capture by direct interception or inertial interaction. As with particles, all capture mechanisms can occur simultaneously, usually one or two will predominate (Rubenstein and Koehl, 1977). Again, the dimensionless number with the highest index will determine the capturing mechanism that is the most likely to take place. Once a droplet (or particle) is captured by a fiber, it can remain in contact with the fiber, be manipulated by appendages for ingestion or detach from the fiber if external forces permit. Letendre et al. (2020) describes conditions for such detachment of oil droplets to occur. For a droplet to detach the fiber and re-enter the water column, the critical ratio of inertial to capillary forces must be achieved, which can be increased by a higher flow velocity or a lower oil/water interfacial tension.

The goals of this paper are to identify the capture mechanisms of crude oil droplets using the cladoceran *Daphnia magna* and two species of barnacles (*Balanus glandula* and *Balanus crenatus*) (see Fig. 4.2 for pictures of studied species). We also describe the wettability of the filtering appendages of these species and discuss its role in the capture and retention of oil droplets.

4.2. Materials and Methods

4.2.1. Specimen preparation for SEM

To ensure good visibility of the appendages and to minimize fixation artefacts, specimens were first relaxed in a solution of magnesium chloride. $MgCl_2$ was introduced drop by drop until *Daphnia* had minimal appendage movement and barnacles stopped feeding. At this point barnacles were removed from their calcareous plates and the cirri were removed. Individuals were then fixed in a 2.5% gluteraldehyde buffered in a 0.2M phosphate buffer (7.6 pH) for 3 hours. The carapace of *Daphnia* was removed for better observations of the filtering thoracic legs. Specimens were transferred in a 2% OsO_4 buffered solution for 2 hours. Samples were then rinsed three times for a period of 5 minutes in the phosphate

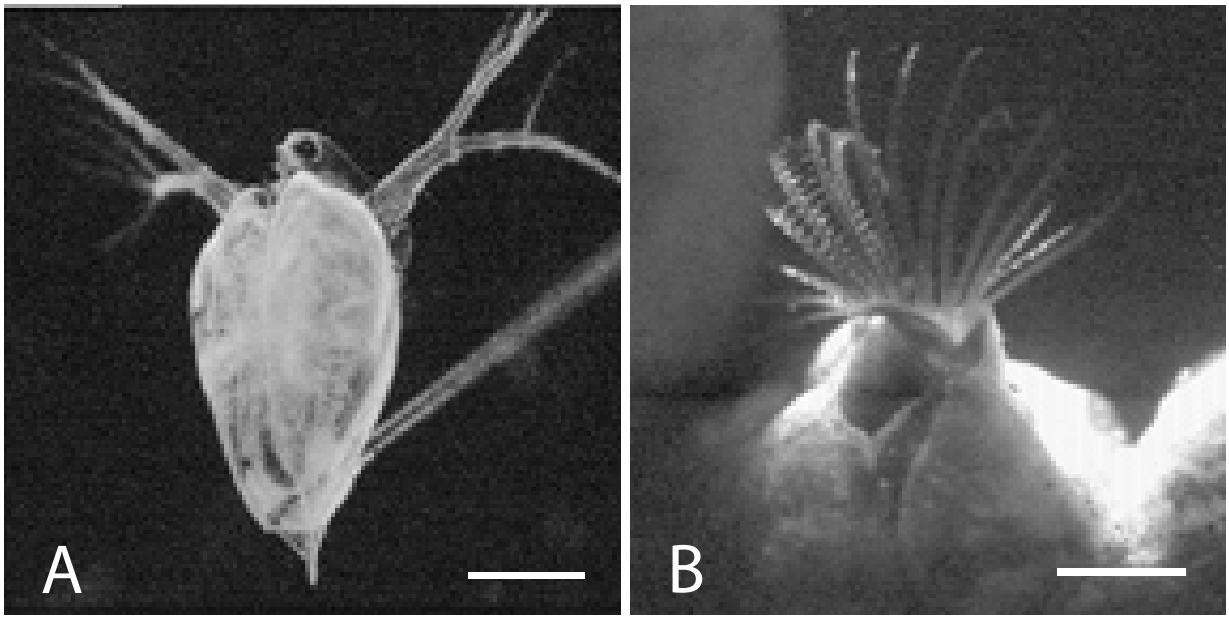

Figure 4.2. Pictures of the two filter feeders studied : (A) The freshwater cladoceran *Daphnia magna* (scale bar is 1 mm) and (B) an acorn barnacle with its rami extended in the water column (scale bar is 2 mm).

buffer. At this point the samples went through a graded ethanol series from 30 to 90% with 10% increment, then 95% and 100% three times. Each step was 15 minutes. The samples were mounted on aluminum stubs and placed in an air dried desiccator overnight, then a 15 μm of layer of gold was applied to the stubs, before SEM observations. The samples of *Daphnia* were observed at the École Polytechnique de Montréal using a JEOL JSM-7699F SEM. Barnacle were observed at the same location but with an environmental SEM. SEM samples were used to accurately measure appendage morphology and to study the surface texture of the various filtering appendages.

4.2.2. Observation of feeding and particle capture

4.2.2.1. Barnacles. Two species of barnacles were used to quantify oil droplet capture - the relatively large *Balanus glandula* and the small *Balanus crenatus*. Specimens were acquired by Westwind Sealabs from the south coast of Vancouver Island, Canada. Specimens were gently scraped off their substrate and placed in a 80 gallon saltwater tank at 10 °C. These species were chosen to observe capture events at different flow velocities and Reynolds numbers, since they have different cirrus length, width and spacing. Observations were made in a 3x4x18 inch rectangular flow tank equipped with a variable speed motor. The camera was positioned

to the side of the flow tank so that an animal was filmed from a side view. The animals were individually put on modeling clay and stuck to the bottom of the flume tank. A sufficient amount of clay was used to elevate the animal where it would experience the free-stream velocity of the flume and not be affected by flume's boundary layer. A $532\,nm$ Aries green laser was placed above the flume and a crystal split the beam in a thin sheet parallel to the water flow. That sheet was then positioned above the barnacle. To create the crude oil-in-water emulsion, $75\,\mu L$ of crude oil was pipetted in $1\,L$ of conditioned tap water. The crude oil used has a density of $855\,kg/m^3$, a viscosity of $98\,mPa \cdot s$ and an interfacial tension of $27.1\,mN/m$. The emulsion was mixed at 900 rpm for 20 minutes on a stirring plate using a magnetic stirrer. This guarantied a normal distribution of oil droplet size. The emulsion was then poured into the flume. When feeding occurred, whether passive or active, four seconds of video were captured at 1057 frames per second. A schematic of the experimental setup can be consulted in Fig. 4.3.

When studying the interactions of oil droplets with filtering appendages in water, the key parameters are flow velocity, appendage radius, and droplet radius (Letendre et al., 2020). The velocities used for the Reynolds number and capture mechanisms intensity calculations were the free-stream velocity of the flume tank, which was constant when the animal was placed at its center. For these velocity measurements, a $15\,cm$ ruler was placed at the center of the flume and parallel to the flow. The laser sheet was positioned on the same plane as the ruler. When particles were in focus with the gradation of the ruler, they were filmed with a Chronos 1.4 v.0.3.1 high speed camera. This footage was then analyzed with the image processing software ImageJ using the TrackMate plugin to determine the free-stream velocity (Tinevez et al., 2017). Only trajectories that contained at least 50 frames were used and 1000 particles trajectories were considered for the mean velocities of each increment on the variable speed motor. Flow-stream velocities varied from $1.40\,cm/s$ to $24\,cm/s$. This range of velocities was chosen for Reynolds numbers that allowed for observations of passive and active filtering of the two species and because they are in the range of previous fluid mechanics (Vo et al., 2018) and feeding studies (Eckman and Duggins, 1993; Geierman and Emlet, 2009; Nishizaki and Carrington, 2014) of *Balanus glandula* and *Balanus crenatus*.

SEM image analysis was also made using ImageJ. Rami and setae diameter were measured at the middle of the fiber and at its tip for both species of barnacles. Only the sixth pair of

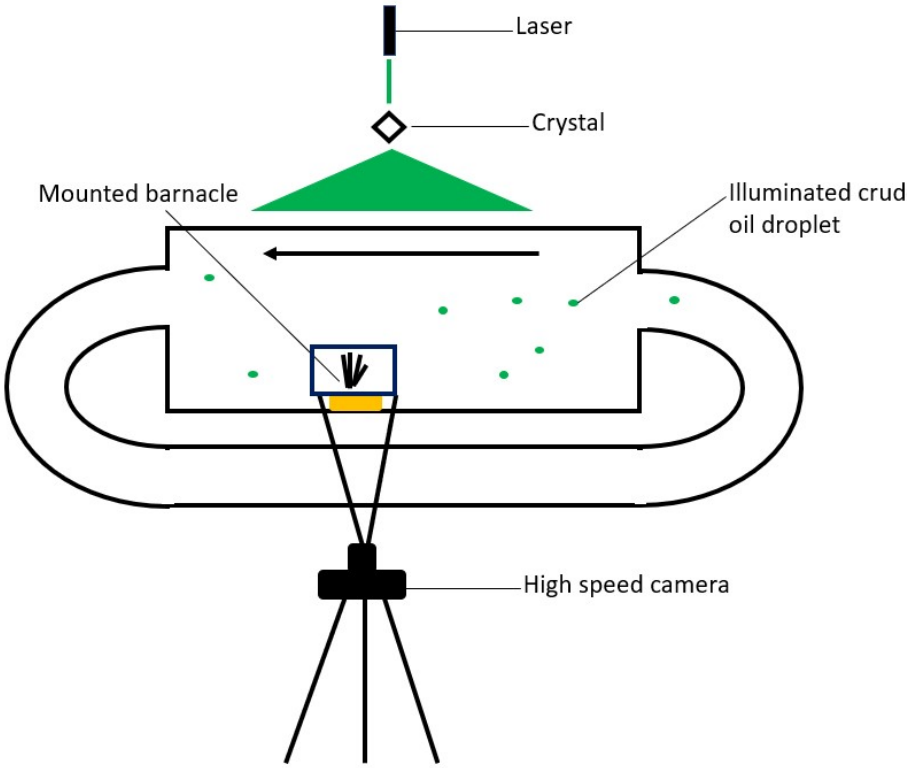

Figure 4.3. Schematic of the flume and the setup used for the observations of the capture of crude oil droplets by filtering barnacles. A crystal placed over the flume was used to split a laser beam into a thin sheet, illuminating the crude oil droplet in the water. These droplets were then filmed while they were being captured by the barnacle. The black arrow indicates the direction of flow.

setae from each segment was measured as it is the longest and widest fiber. Setae spacing was measured as the distance between the center of two setae at half-length (*i.e.,* where the diameter was also measured). The spacing of the rami was measured from the high-speed videos of the barnacles feeding. The measurement was made when two rami were in focus, facing the lens and passively feeding in the flume.

4.2.2.2. Daphnia magna. The specimens were purchased from Boreal Science and kept in an incubator at 21 °C. They were fed every three days with *Spirulina* powder. The crude oil-in-water emulsion was mixed as previously described. During the mixing, a *Daphnia* was selected and its carapace was dried using a paper wipe, assuring a dry surface. A drop of non-toxic super glue was applied to the dorsal posterior end of the animal to secure it to a $100\,\mu m$ insect pin. The animal was then pinned on a silicone pad inside a petri dish. This way, the animal could move all its appendages freely while resulting in minimal movement, permitting ideal filming conditions. The ventral side of the animal was then positioned upwards for microscope observations. The laser sheet was projected horizontally, but positioned slightly above the ventral surface of the animal in order to see the oil droplets that were displaced by its feeding current. This setup was placed under an Olympus S2X16 dissection scope equipped with the same high speed camera. Observations were filmed at 200 frames per second for 20 seconds periods and at 1057 frames per second for 4 second periods. We recorded when there was metachronal movement of the thoracic legs but minimal movement of the second pair of antenna. Indeed, since the second pair of antenna are mainly for swimming, their movement results in a distortion of the flow around the animal.

Setae and setule diameter of the four pair of thoracic legs and the second pair of antenna were measured using SEM microscopy. The measurements were made at the middle point of each fiber. The intersetular distance was measured for each appendage as the center to center distance of two adjacent setules. Only the intersetae distance of the third and fourth pair of thoracic legs were measured. SEM also permitted observations of the surface texture to comment on the wettability of the appendages. Data for appendage and droplet velocities were obtained by analyzing the high speed videos in ImageJ. All four pairs of thoracic legs were tracked manually for several full cycles of filtering.

To validate that oil droplets were being ingested, a feeding experiment similar to the one on calanoid copepods in Letendre et al. (2020) was done. For each treatment, $20 - 30$ individuals of *Daphnia magna* were introduced in an crude oil-in-water emulsion. The concentrations of the emulsions were $10, 50$ and $300\,\mu L/L$. Prior to this, the individuals were starved overnight to allow for an empty gut and better observations of ingested droplets. Animals were left in the emulsion for 48 hours and were observed immediately afterward. Since crude oil auto-fluoresces, observations under a fluorescence microscope were made. Observations

of the antennae, gut and thoracic legs were done. To comment on the lipophobicity and surface texture of the filtering appendages, the contact angles of captured crude oil droplets by live specimens were measured with ImageJ. Only the contact angles of droplets that were captured by the antennaes or filtering appendages and not agglomerated in floccs were considered.

To determine the droplet size distribution in the flume, a few drops of the crude oil-in-water emulsion were photographed under a fluorescence microscope using a TRITC filter. The oil droplet diameters in the emulsion were measured using the analyze particle tool of ImageJ. A Shapiro-Wilk test was done to verify normality at a significance of $p \leq 0.05$ using the open source software R 4.0.5.

4.3. Results

4.3.1. Capture mechanisms by *B. crenatus* and *B. glandula*

Measurements of appendage morphology of *Balanus glandula, Balanus crenatus* and *Daphnia magna* were done using SEM imagery. Key morphology measurements of the barnacles are consolidated in Table 4.1 and examples of barnacles morphology are shown in Figure 4.4. For *B. glandula*, the diameter of the rami and of the setae are respectively $91.4 \pm 5.2\,\mu m$ and $5.5 \pm 0.6\,\mu m$ and are evenly spaced at an average of $14.1 \pm 1.2\,\mu m$. The mean gap-to-diameter ratio of the setae is 2.6 ± 0.3. The average distance between the middle point of each rami is $476\,\mu m$. The setae of this species are serrulate ; the setules are sharp and needle-like (Chan et al., 2008). The insertion site of the setules alternates from side to side. The setules are almost parallel to the setae, meaning that they do not extend outward.

Table 4.1. Diameter and interfiber distance of the rami, setae and setules of *Balanus glandula*, *Balanus crenatus* and the thoracic legs (Tl) of *Daphnia magna*

Species and appendage	Parameters					
	Rami diameter (μm)	Setae diameter (μm)	Intersetae distance (μm)	Setule diameter (μm)	Intersetular distance (μm)	Setule G/D
B. glandula	91.4 ± 5.2	5.5 ± 0.6	14.1 ± 1.2	N/A	N/A	2.6 ± 0.3
B. crenatus	51.8 ± 1.4	4.6 ± 0.5	10.9 ± 1.4	N/A	N/A	2.4 ± 0.2
D. magna 2nd antennaes	N/A	11.5 ± 1.0	N/A	2.2 ± 0.3	7.5 ± 0.6	3.4 ± 0.5
D. magna 1st Tl	N/A	N/A	1.3 ± 0.1	N/A	0.7 ± 0.2	0.60 ± 0.14
D. magna 2nd Tl (comb-like)	N/A	7.8 ± 0.5	N/A	1.2 ± 0.1	3.0 ± 0.8	2.5 ± 0.7
D. magna 2nd Tl (feather-like)	N/A	9.8 ± 0.5	N/A	0.6 ± 0.1	3.9 ± 0.4	6.9 ± 1.7
D. magna 3rd and 4th Tl	N/A	2.5 ± 0.3	5.4 ± 0.9	0.20 ± 0.02	0.29 ± 0.05	1.4 ± 0.2

For *B. crenatus*, the diameter of the rami is $51.8 \pm 1.4\ \mu m$ and $4.6 \pm 0.5\ \mu m$ for the setae. The setae spacing for this species is $10.9 \pm 1.4\ \mu m$ and the rami spacing is $282\ \mu m$. The gap-to-diameter ratio of the filtering fibers is 2.4 ± 0.2. Since the flow velocities measured in our experiments vary roughly from $1.40\ cm/s$ to $24\ cm/s$, a wide range of Reynolds number and boundary layer thickness were witnessed. The setule morphology of *B. crenatus* is similar to that of *B. glandula*. The setae are also serrulate, and the setules remain close to the setae.

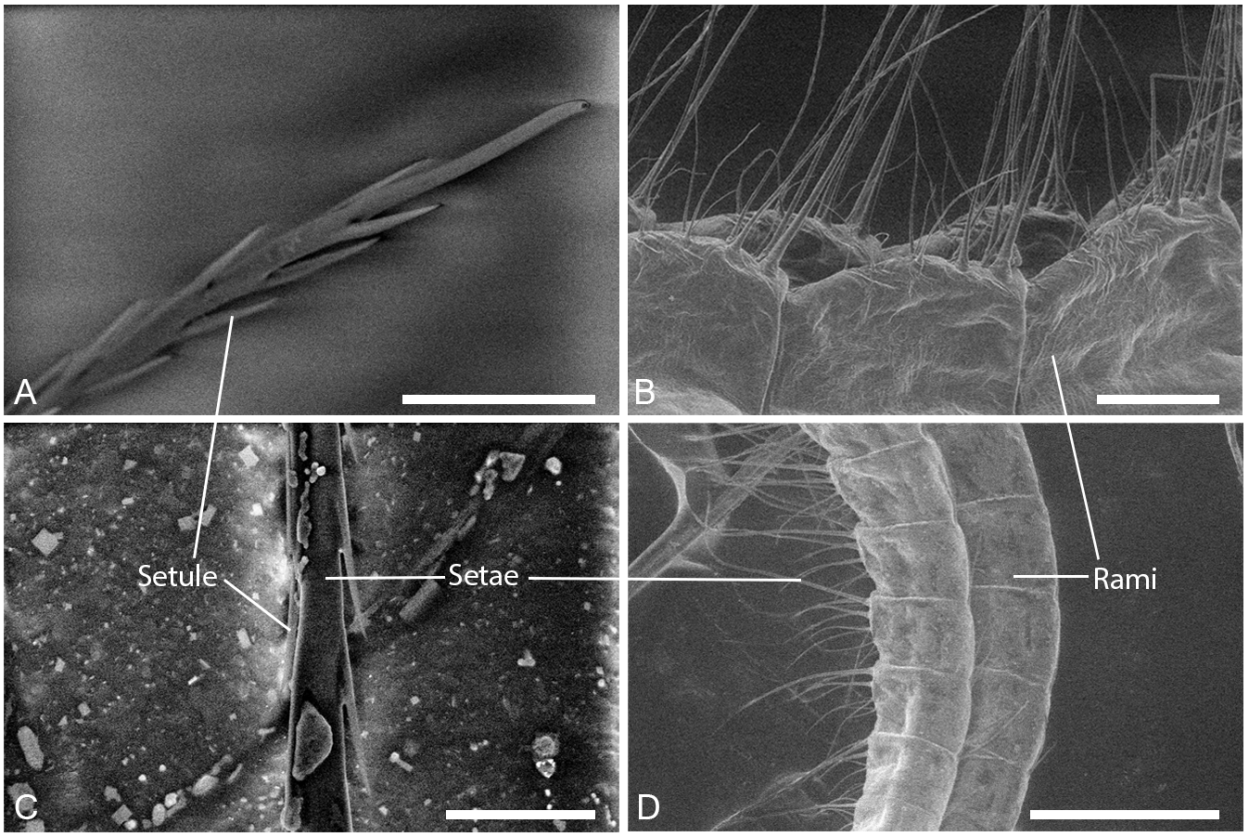

Figure 4.4. SEM observations of the rami and setae of *Balanus glandula* (A-B) and *Balanus crenatus* (C-D). (A) The tip of the serrulate setae of *B. glandula*. Scale bar is $10\ \mu m$. (B) Three segments of a rami from *B. glandula*. Scale bar is $100\ \mu m$. (C) The serrulate tip of the setae from *B. crenatus*. Scale bar is $10\ \mu m$. (D) Parts of two rami from *B. crenatus*. Scale bar is $300\ \mu m$.

The Reynolds number, thickness of boundary layers and different capture intensities for both species of barnacles are compiled in Table 4.2. For *B. glandula*, the Reynolds number experienced at the scale of the rami ranged from 1.24 to 20.78. Using Eq. 4.2, the boundary layer thickness is estimated at $82.0\ \mu m$ at lower Reynolds number and $20.1\ \mu m$ at higher Reynolds number. Around the setae, the Reynolds number ranged from 7.09×10^{-2} to 1.25.

The boundary layers around the setae were estimated at 20.1 μm and 4.91 μm respectively. Considering that the spacing of the setae for this species is measured at 14.1 $\pm$ 1.2 μm, the boundary layer is 1.3 times larger than the spacing at lower Reynolds number. Thus, boundary layers of adjacent setae overlap and appendage leakiness is very low, or null. At the higher Reynolds number observed, the boundary layer thickness to setae spacing ratio is estimated to be 0.3, meaning that boundary layers do not overlap, allowing a portion of the fluid to pass through the fibers at free-stream velocity.

The Reynolds number around the rami of the smaller *B. crenatus* was 0.704 and 11.70 at the lowest and highest velocities. At those speeds, the thickness of the boundary layer surrounding the rami changed from 61.8 μm to 15.1 μm. *B. crenatus* setae's Reynolds number varied from 6.21×10^{-2} to 1.05 and the boundary layer varied from 18.4 μm to 4.51 μm. Thus, at low Reynolds number, the thickness of the boundary layer is 1.7 times greater than the distance between two adjacent fibers. The leakiness of an appendage at this regime is then negligible. At the higher end of our measured Reynolds number, this ratio is 0.4, which would permit some fluid to pass in between fibers. However, this amount would be less than with *Balanus glandula*, since the boundary layers of two adjacent fibers would account for 80% of the area between them.

Table 4.2. Flow velocity, rami and setae Reynolds number, rami and setae boundary layer thickness and capture intensities of direct interception ($\bar{R}$), inertial interaction (St) and gravitational deposition (G) for the setae of *Balanus glandula* and *Balanus crenatus*.

Species	Flow velocity (m/s)	Reynolds - rami	Reynolds - setae	Boundary layer - rami (μm)	Boundary layer - setae (μm)	$\bar{R}$	St	G
B. glandula	0.0140	1.24	7.09×10^{-2}	82.0	20.1	0.443	1.35×10^{-4}	3.56×10^{-5}
	0.0450	3.94	0.240	46.1	11.3	0.443	4.27×10^{-4}	1.12×10^{-5}
	0.100	8.69	0.522	31.0	7.64	0.443	9.42×10^{-4}	5.09×10^{-6}
	0.201	17.5	1.06	21.9	5.43	0.443	1.90×10^{-3}	2.53×10^{-6}
	0.239	20.8	1.25	20.1	4.91	0.443	2.25×10^{-3}	2.13×10^{-6}
B. crenatus	0.0140	0.704	6.21×10^{-2}	61.8	18.4	0.529	1.61×10^{-4}	3.56×10^{-5}
	0.0450	2.23	0.201	34.7	10.4	0.529	5.10×10^{-4}	1.12×10^{-5}
	0.100	4.93	0.44	23.4	7.04	0.529	1.13×10^{-3}	5.09×10^{-6}
	0.201	9.92	0.883	16.5	4.93	0.529	2.27×10^{-3}	2.53×10^{-6}
	0.239	11.8	1.05	15.1	4.51	0.529	2.69×10^{-3}	2.13×10^{-6}

$\bar{R}$, St and G, which are the dimensionless number for direct interception, inertial interaction and gravitational deposition, were measured for both species at all five tested velocities. Since all three equations require the diameter of the droplet, the average diameter of the droplets found in the emulsion was calculated. To ensure that the droplet sizes followed a normal distribution, a kurtosis and skewdness tests were done. The respective tests established a value of 1.699 and 0.919, both being in the acceptable range for a normal distribution. A Shapiro-Wilk test was also done (p= 0.19), meaning that we cannot reject the null hypothesis of normality. The average droplet diameter, which is $2.4 \pm 1.3\,\mu m$, is relatively close to the median *i.e.* $2.3\,\mu m$. Thus, we felt that the use of the average droplet diameter would be appropriate and relevant for the calculations of various capture intensities.

Values of $\bar{R}$ for *Balanus glandula* and *Balanus crenatus* are respectively 0.443 and 0.529 (Table 4.2). At lower velocities, values of St and G for *B. glandula* are 1.35×10^{-4} and 3.56×10^{-5}. At the highest measured velocities, the intensities of inertial interaction and gravitational deposition are 2.25×10^{-3} and 2.13×10^{-6}. On *B. crenatus*, capture intensities at lower free-stream velocities are $St = 1.61 \times 10^{-4}$ and $G = 3.56 \times 10^{-4}$. At our highest measured velocities, the capture intensities are $St = 2.69 \times 10^{-3}$ and $G = 2.13 \times 10^{-6}$. Since the setae diameter used was measured at the middle of the setae, these intensities are relevant for capture around the middle of the fiber.

At low velocities, *i.e.* lower range of Reynolds number, barnacle cirri behaved as paddles and capture crude oil droplets in their thick overlapping boundary layers. Figure 4.5 depicts *Balanus crenatus* actively feeding in an oil-in-water emulsion inside a flume at $1.40\,cm/s$ (see *Supplementary Video 1* for an example of active feeding at that velocity). At low velocities, the barnacles would actively feed by repeatedly extending the cirri into the water column and then retracting them into the mantle cavity. This allowed the animal to trap parcels of water in the area created by the curved rami and then transport it near to the mouth. The cycle began with the opening of the operculum and the extension of the cirri into the water column (Fig. 4.5A). Then, it would spread its cirri, allowing water to rush into the space created by this movement (Fig. 4.5B). The curving of the rami thus creates a sheltered space which we refer to as the "cage". Once the cage was filled, the animal would begin to retract the cirri into the mantle cavity which would reduce the distances between individual rami

(Fig. 4.5C). Then, it fully retracted into the mantle cavity, with the oil droplets that were trapped in the appendage's boundary layer inside of its calcareous shell (Fig. 4.5D).

At 1.40 cm/s, the Reynolds number around the rami of *B. crenatus* is 0.704 (Table 4.2). For this particular experiment, the boundary layer around a setule was 18.42 μm. Since the setule spacing of *B. crenatus* is $10.9 \pm 1.4\ \mu m$ (Table. 4.1), the boundary layers overlap and little to no fluid may pass through the setules. Considering the serrulate tip of the setules, it is unlikely that true sieving happens even at high flow for this particular level of ramification (Fig. 4.4A and C). With such a thick boundary layer, particles will not contact the rami and will be entrapped in its boundary layer.

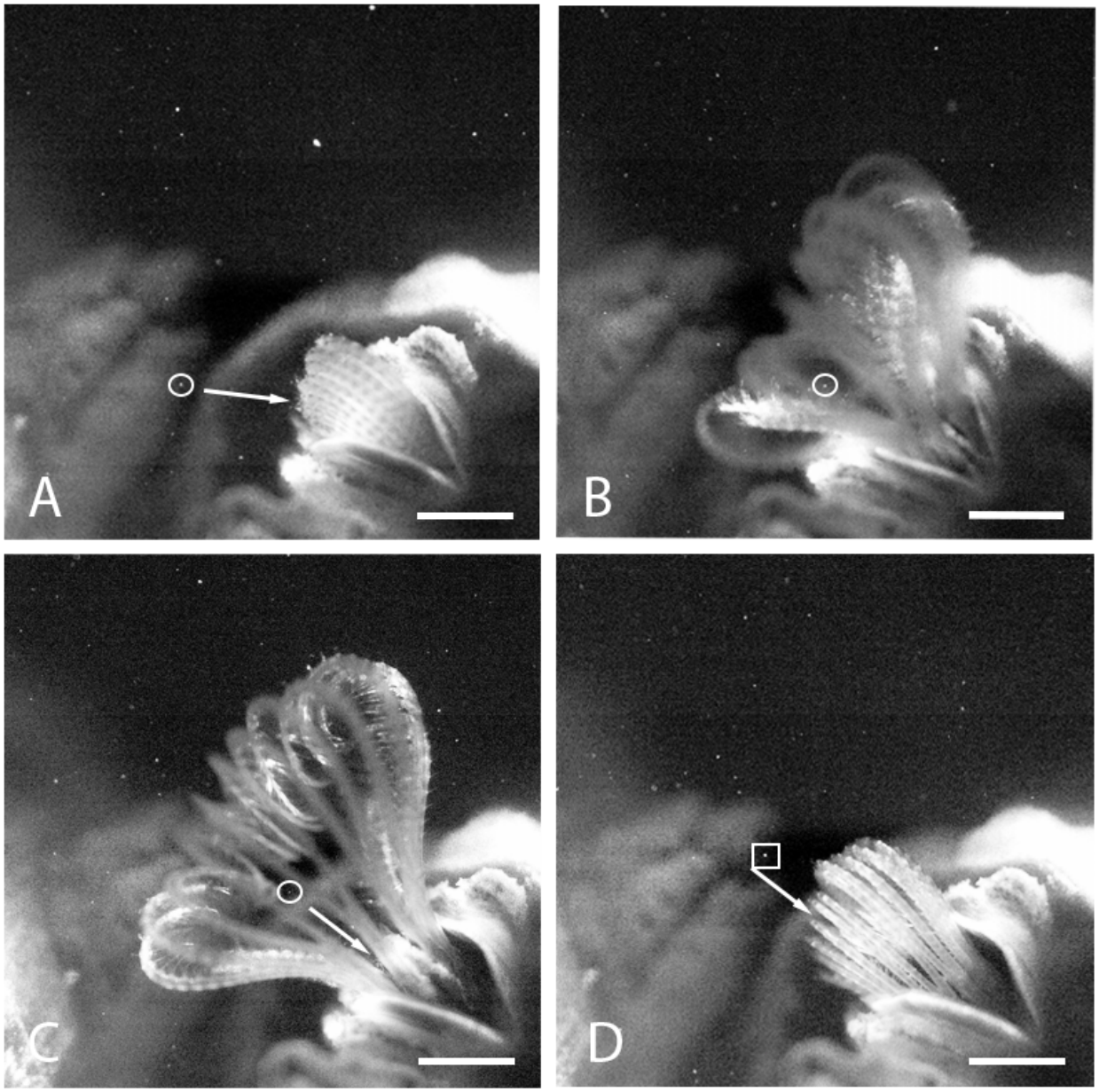

Figure 4.5. The active filtering of *Balanus crenatus*. The circled droplet in A-C is the same droplet that is being captured and the white square in D shows a droplet trapped in the appendage's boundary layer. The droplet eventually moved inside the mantle cavity as the animal fully retracted. The white arrows represent the direction of flow during the different steps of active filtering. All scale bars correspond to 2000 μm and free-stream velocity is 1.4 cm/s.

There was a range of intermediate velocities where some droplets were captured by both mechanisms *i.e.*, the leaky-sieve transition zone (Koehl, 2001). Figure 4.6 shows *Balanus crenatus* passively feeding in the flume's oil-in-water emulsion at 10 cm/s. In this particular system, the Reynolds number of the setae and the rami are respectively 10^{-1} and 10^{1} in orders

of magnitude. Considering the gap-to-diameter ratio of this filter feeding species (Table 4.1), these Reynolds numbers represent the transition zone, where a change in spacing or behavior can greatly influence the leakiness of an appendage (Koehl, 1993). This is in fact what we observe in this figure. The circled droplet approached the appendage close to the rami's insertion and slowed (Fig. 4.6A), but did not pass between the fibers. Instead, it moved across all rami from left to right (Fig. 4.6B-C), around the animal, and re-entered the fluid stream (Fig. 4.6D). This is an example of an appendage behaving as a paddle, where little to no fluid passes between fibers. On the other hand, the droplet identified by the white square approached the appendage with the same original velocity, but met the rami at a much higher point on the appendage. Near the tip, the gap-to-diameter ratio is higher than at the insertion point. This caused a local increase in the appendage's leakiness, and allowed the oil droplet to pass between the rami (Fig. 4.6C). Should the droplet be big enough, it could have been captured through sieving. In accordance with Koehl (1993), these flow regimes are where a change in this spacing causes the most increase in appendage leakiness. Droplets that are captured by a single fiber are likely to be captured via direct interception as it is the mechanism with the highest index (Table. 4.2).

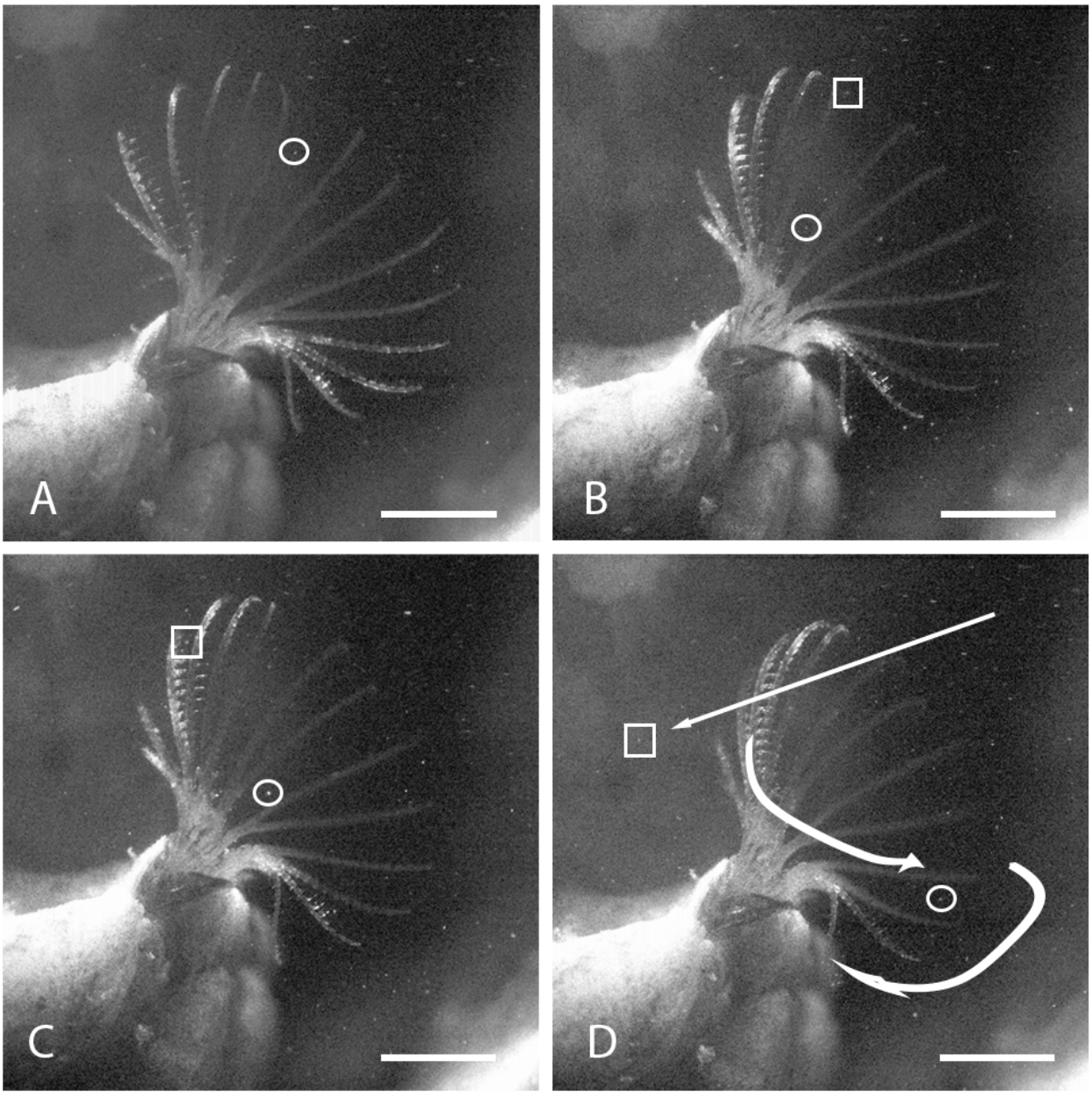

Figure 4.6. An example of *Balanus crenatus* passively feeding where the appendage behaves as a leaky sieve. The free-stream velocity in the flume was 10 cm/s. The white circle identifies a crude oil droplet that showcases the paddle behavior of the appendage. (D) The top arrow represent the direction of flow near the tip of the cirri whereas the bottom arrows represent the flow near their insertion. All scale bars correspond to 2000 μm.

At higher velocities, fluid passed between the cirri and oil droplets and was captured mainly by direct interception (see *Supplementary Video 2* for an example of a barnacle passively feeding). In true sieving, particles that are larger than the fiber spacing will be captured (Rubenstein and Koehl, 1977). However, since fluid passes much closer to the

fibers, droplets smaller than the fiber spacing can contact the fibers and be captured via direct interception. Figure 4.7 displays such a capture by *Balanus glandula*. Indeed, the circled droplet approached the rami at a $10\,cm/s$ free-stream velocity (Fig. 4.7A-B), and adhered to the rami. Figure 4.7D, shows that the droplet was captured by the rami and not by a setae. At this velocity, the values for direct interception, inertial interaction and gravitational deposition were respectively $\bar{R} = 0.443$, $St = 9.42 \times 10^{-4}$ and $G = 5.09 \times 10^{-6}$ (Table 4.2), making direct interception the most likely mechanism. Once a droplet has been captured, the organism can decide to retract its cirri into its shell and scrape off collected particle using its mouthparts *e.g.*, maxillae and maxillipeds.

However, all the setae of *Balanus glandula* do not have the same length and width. Indeed, the sixth pair of setae is significantly shorter and narrower than the first pair, the first pair being the one inserted at the segment's end closer to the tip of the appendage (Vo et al., 2018). This can have a major impact in the capturing potential of a setae. For example, the length of the sixth pair of setae was measured at $62 \pm 12\,\mu m$ in Vo et al. (2018). Considering that the rami's boundary layer is $82.0\,\mu m$ at our lowest measured velocity (Table 4.2), the tip of the setae is still well within the boundary layer. In these conditions, this setae serves little purpose as it is encapsulated in the boundary layer of the bigger fiber.

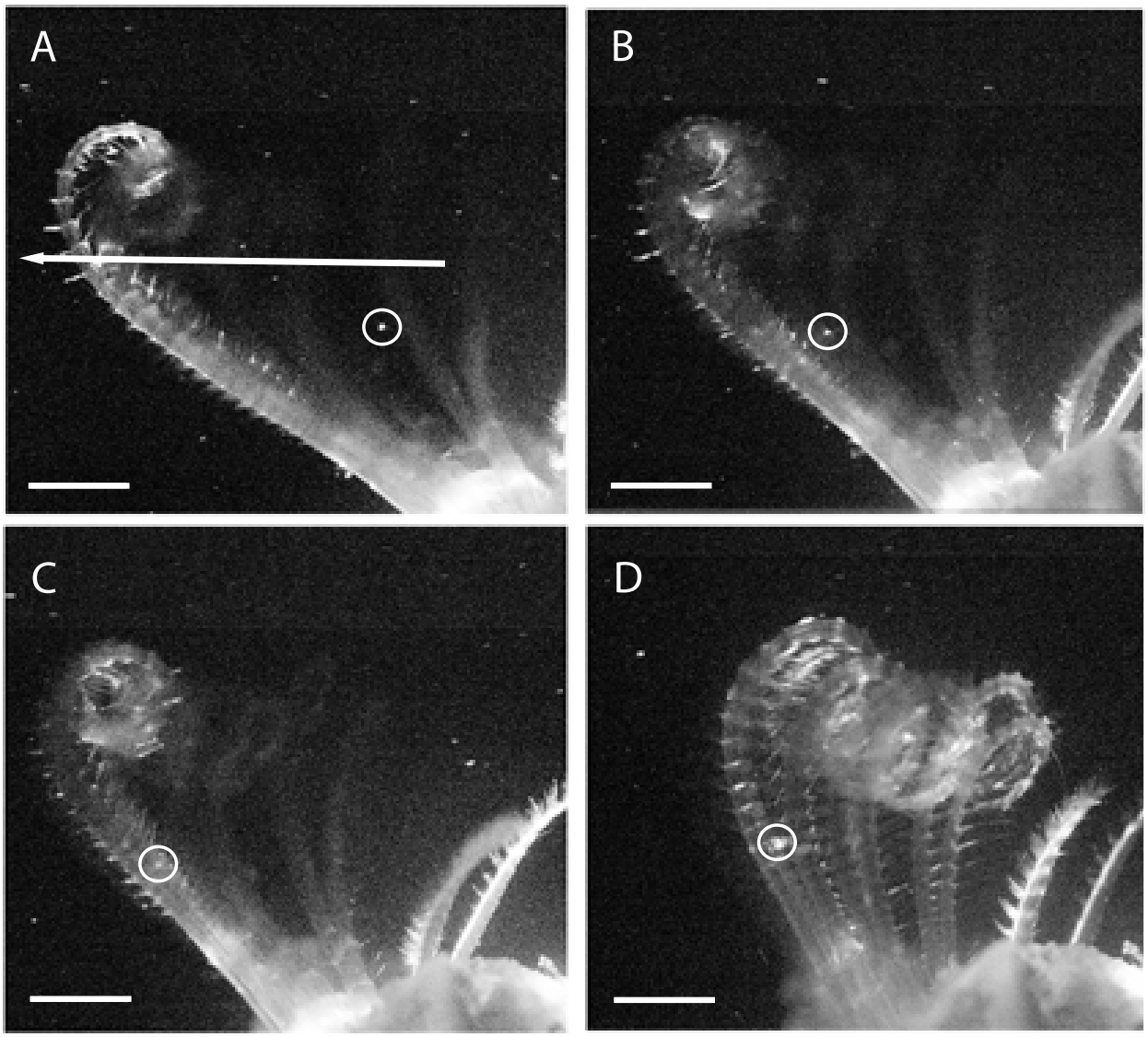

Figure 4.7. *Balanus glandula* filtering passively. The white arrow in (A) illustrates the direction of flow going between the cirri of the barnacle. The free-stream velocity was 10 cm/s. The white circle indicates a crude oil droplet that was likely captured by the rami by direct interception. All scale bars are 2000 μm.

4.3.2. Capture mechanisms by *Daphnia magna*

On *Daphnia magna*, the diameter of the second pair of antennas' setae was $11.5 \pm 1.0\ \mu m$ and $2.2 \pm 0.3\ \mu m$ for the setule (Fig. 4.8B). The distance between setules was on average $7.5 \pm 0.6\ \mu m$ (Table 4.1). The setule diameter of the first pair of thoracic legs was $1.3 \pm 0.3\ \mu m$ and were evenly spaced by $0.7 \pm 0.2\ \mu m$. The setules of this appendage were rigid and tooth-like, with little space between individual setules. Two different setae were observed on the

second pair of thoracic legs (Fig. 4.8C-D). Consistent with the observations of Watts and Petri (1981), the second pair bear a setae with peg-like setules, giving it the appearance of a comb. The diameter of this setae was $7.8 \pm 0.5\ \mu m$. The setules of this setae were $1.2 \pm 0.1\ \mu m$ in width and the center-to-center distance was $3.0 \pm 0.8\ \mu m$. These rigid setules were wide at their insertion but decreased in width, ending in a sharp tip. The second type of setae found on the second pair of thoracic legs bears setules that are more feather-like. The setae width was $9.8 \pm 0.3\ \mu m$ and the setule width was $0.6 \pm 0.1\ \mu m$. The intersetular distance was $3.9 \pm 0.4\ \mu m$. The third and fourth thoracic legs are an extensive network of setae ramified with perpendicularly positioned setules (Fig. 4.8F). The spacing of each setae was regular and consequently these were the only setae spacing that could be measured, *i.e.* $5.4 \pm 0.9\ \mu m$. Opposing setules of adjacent setae touched near the tips, creating a regular grid of fibers. The diameter of these setae was $2.5 \pm 0.3\ \mu m$. The setules of these two pairs of legs were $0.20 \pm 0.02\ \mu m$ in diameter and were $0.29 \pm 0.05\ \mu m$ apart.

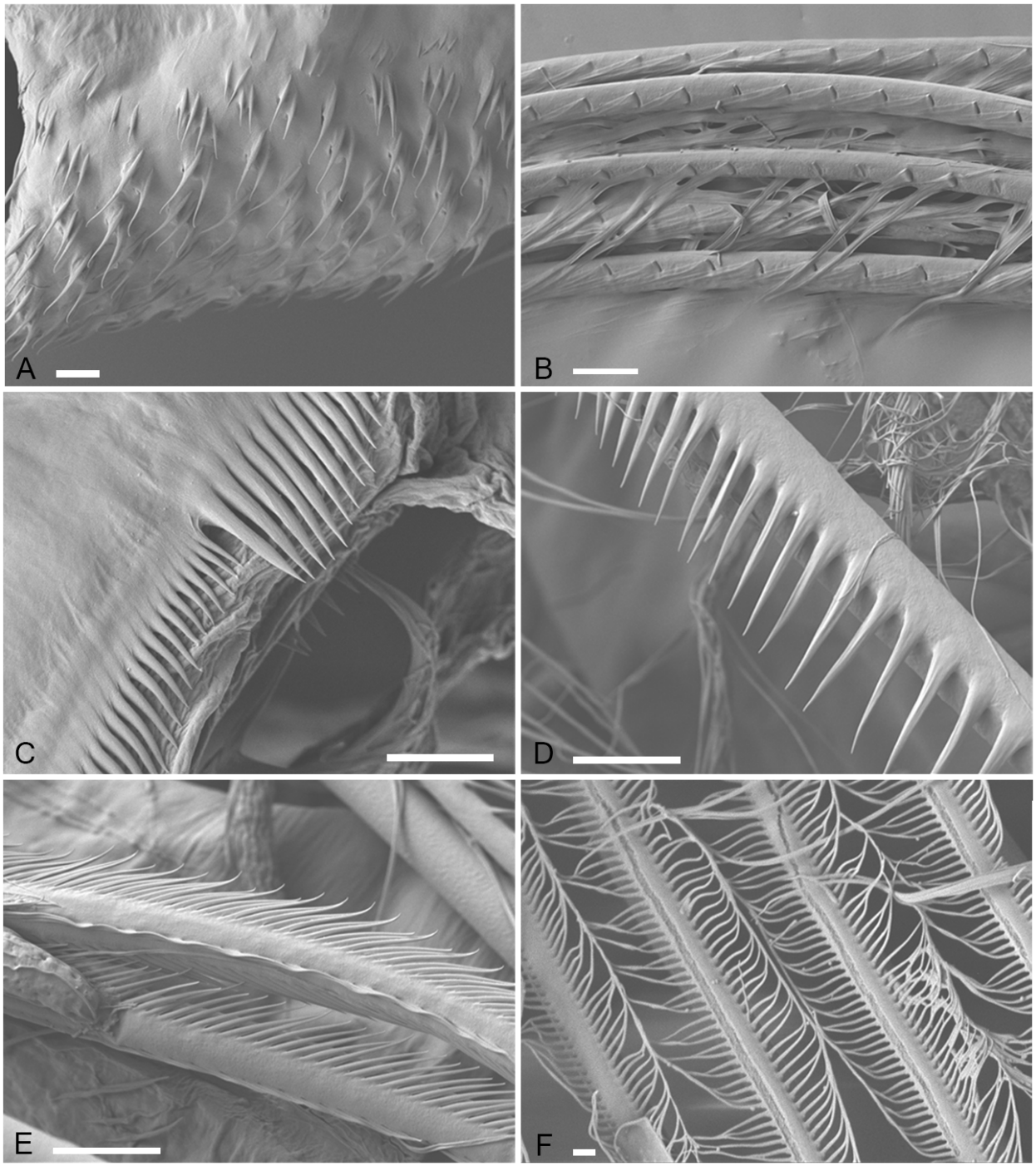

Figure 4.8. Morphology of the post-abdominal claw and various appendages of *Daphnia magna*. (A) The post-abdominal claw with double hooked protuberances. (B) Various setae of the second pair of antennaes. (C) The setae and setules of the first thoracic leg. (D) The comb-like setae of the second TL. (E) The feather-like setae of the second TL. (F) The filtering setae and setules of the third and fourth TL. (A-E) Scale bars are 10 μm. (F) Scale bar is 1 μm.

Table 4.3. Flow velocity, setae and setule Reynolds number, setae and setule boundary layer thickness and capture intensities of direct interception ($\bar{R}$), inertial interaction (St) and gravitational deposition (G) for the setules of the second pair of antenna and the first four pairs of thoracic legs of *Daphnia magna*.

Appendage ID	Capture mechanisms							
	Flow velocity (m/s)	Reynolds - setae	Reynolds - setule	Boundary layer - setae (μm)	Boundary layer - setule (μm)	$\bar{R}$	St	G
2nd antennaes	4.24×10^{-2}	4.83×10^{-1}	9.33×10^{-2}	16.5	7.41	1.10	9.06×10^{-4}	1.09×10^{-5}
1st Tl	6.71×10^{-3}	N/A	8.56×10^{-3}	N/A	13.8	1.92	1.44×10^{-4}	6.91×10^{-5}
2nd Tl (comb-like)	5.52×10^{-3}	4.29×10^{-2}	6.43×10^{-3}	37.7	14.6	2.09	1.18×10^{-4}	8.40×10^{-5}
2nd Tl (feather-like)	5.52×10^{-3}	5.37×10^{-2}	3.08×10^{-3}	42.1	10.1	4.36	1.18×10^{-4}	8.40×10^{-5}
3rd and 4th Tl	5.78×10^{-3}	1.45×10^{-2}	1.19×10^{-3}	20.9	6.04	11.8	1.24×10^{-4}	8.02×10^{-5}

The order of magnitude of the second antennae's Reynolds number was 10^{-1} for the setae and 10^{-2} for the setule. Since it was not possible to measure the diameter of the first thoracic leg setae, its Reynolds number and its boundary layer thickness were not calculated. For the first four pairs of thoracic legs, the Reynolds number was at the order of magnitude of 10^{-2} for the setae and 10^{-3} for the setule. The second antennae had the highest velocity at approximately $4.24\,cm/s$. Table 4.3 summarises the calculations for the boundary layer thicknesses and capture intensities for the different appendages.

Daphnia magna captured crude oil droplets by a metachronal paddle motion of the third and fourth thoracic legs by entrapment in the appendage boundary layers (see *Supplementary Video 3* for an example of this metachronal motion). If left undisturbed, *D. magna* would filter feed with a constant beat of the appendages (Fig. 4.9). A full cycle for the thoracic appendages is roughly half of a second. The four pairs of thoracic legs moved in a synchronous fashion creating a metachronal wave that started with the fourth pair of legs in a sequence similar to the Antarctic krill's pleopods (Murphy et al., 2013). Fig. 4.9A shows all four thoracic legs at the start of the cycle. Then, the fourth thoracic legs initiate the cycle and begin to move posteriorly (Fig. 4.9B). With a 0.05 to 0.08 s lag, the next pair of thoracic legs would initiate its movement along the anterior to posterior axis (Fig. 4.9C-E). When the appendages finished their downward movement, they would move toward the center of the animal where the food groove is located. However, the first pair of thoracic legs would move more latero-ventrally than the other appendages. Also, in agreement with Gerritsen et al. (1988), we observed that the first pair of thoracic legs did not always follow the metachronal wave. Indeed, the first pair can move independently to clean other appendages. The velocities of each appendages are compiled in Table 4.3.

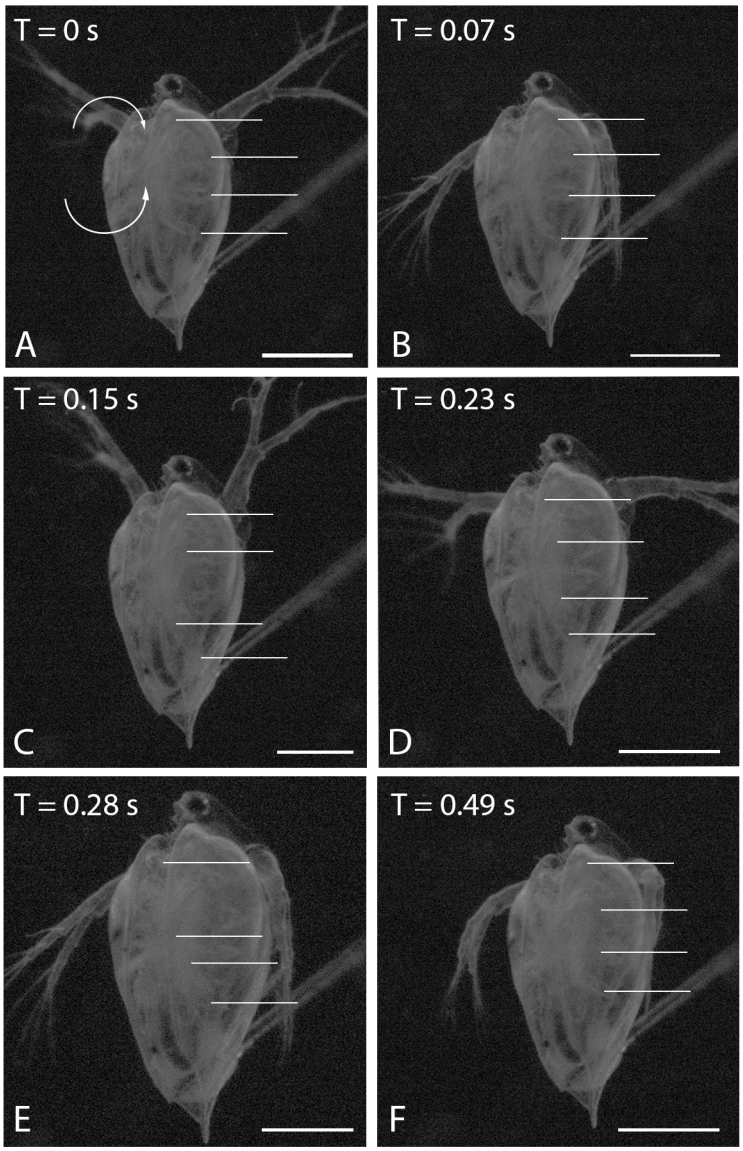

Figure 4.9. A complete cycle of the filtering behavior of *Daphnia magna*. The flume's free-stream velocity was 1.40 cm/s. The arrows in frame A show the direction of flow resulting of the metachronal beating of the thoracic legs. Frame A and F show the resting positions of all thoracic legs (TL) between cycles. The left edge of the four lines each pinpoint the terminus of one of the four left TL, the top-most line showing the first and the bottom-most showing the fourth. Time stamps indicate the amount of time that has passed since frame A. Scale bars indicate 1000 μm.

Given its size and morphology, *Daphnia magna* feeds at Reynolds number well below 1, where viscosity rules over inertia (Table 4.3). This means that a particle close to the animal will move or stop almost immediately in concert with the appendages. In the absence of external movement we found that the particles would gradually approach the food groove

with each metachronal wave. The velocity of oil droplets approaching the food groove was $0.19\,cm/s$, until it arrived in the area above the food groove, where it accelerated rapidly to $1 - 1.67\,cm/s$, consistent with the findings of Gerritsen et al. (1988).

At these velocities and scale of the thoracic legs, the setules' boundary layer were 20 times thicker than the intersetular spacing, and the fluid had difficulty passing through the appendage during the beating motion (Table 4.3). Instead, water flowed with the appendage and was pushed toward the food groove, along with oil droplets. This finding is in agreement with several other work on *Daphnia sp.*, where sieving is said to be improbable and/or not the main filtering mechanism (Ganf and Shiel, 1985; Gerritsen et al., 1988; Porter et al., 1983). We found that in most cases, crude oil droplets were transported to the mouth of *Daphnia magna* without touching an appendage.

Daphnids use their second pair of antenna to swim in the water column. Even though the Reynolds number of the antennae is one order of magnitude higher than the other appendages (Table. 4.3), viscosity still dominates over inertial forces and boundary layers are thick. Our results show that the boundary layer around a setae almost matches the intersetular distance, meaning that the antennae likely function as a paddle. This is good for propulsion but means that droplet capture by single fibers is unlikely. Indeed, using the antennae beating velocity (Table 4.3) and our average droplet diameter revealed a stopping distance of the order of $1 \times 10^{-3}\,\mu m$. In other words, the droplet loses all momentum almost instantly after entering the setae's boundary layer. In some cases we found that droplets aggregated with organic debris to create a flocculate, increasing the size of the particle and allowing it to move through the boundary layer and contact the fiber (Fig. 4.10C). This finding suggests that antennae of daphnids may be a site for droplet capture and oil fouling via flocculation. If droplets were captured by a single fiber, then direct interception is the likely mechanism (Table 4.3). However, for droplets or flocculations larger than $100\,\mu m$ in diameter, inertial interaction starts to become another possible capture mechanism. We provide no further data on flocculations here.

Following the 48 hour feeding period in the crude oil-in-water emulsion, individuals were photographed under a fluorescence microscope to observe autofluorescent oil droplets in the gut (Fig. 4.10A-B). Animals were starved prior to the feeding trials so that we could be sure that illuminated particles in frame B were captured crude oil droplets. Every individual

observed from all three crude oil concentrations had oil droplets in their gut. Frame C and D display oil droplets that were captured by setules of the second pair of antenna. Furthermore, these droplets aggregated to created flocculates, which is a phenomenon of oil-in-water emulsions (Mehrabian et al., 2018b). Frame E and F show oil droplets that were captured by the setae and setules of the third or fourth pair of thoracic legs. In this animal feeding trial, a single droplet was larger than the setal gap and was captured via sieving (Fig. 4.10F).

4.3.3. Wettability

On wettability, we found that the filtering appendages of the three species studied exhibited lipophobic characteristics. When observed under a dissection microscope and measured in ImageJ, contact angles of captured crude oil droplets by live individuals in water were higher than 90°, replicating detachment conditions observed in Letendre et al. (2020). Observations of captured droplets revealed that the second antennae and filtering appendage setae of *D. magna* has a very low wettability for the crude oil used. Indeed, contact angle of all captured droplets were well above 90° and displayed a clam shape configuration when captured (Fig. 4.10C-F) (Mehrabian et al., 2018b). A clam shape configuration implies that the area of the droplet in contact with the fiber was minimal and oil did not fully coat the setae. Instead, the droplet rested on top of the fiber without surrounding it. Wettability is based on the shape, surface chemistry and texture of the fiber. Our SEM observations show that the appendages, setae and setules of *D. magna* and both species of barnacles had smooth surfaces (Figs. 4.4 and 4.8). Moreover, all filtering appendages of *D. magna*, *B. crenatus* and *B. glandula* were lipophobic ; the oil droplets touching the appendages in the flume had a spherical shape. Both barnacle taxa had similar appendage morphology, fiber arrangement and smooth filtering surfaces.

4.4. Discussion

Naturally occurring and crude oils are omnipresent in the diet of aquatic filter feeders (Conover, 1971; Kattner et al., 2007; Nepstad et al., 2015). Here we use experiments to understand how and under what conditions oil droplets are captured, and the variables that determine the capture mechanics. Our results indicate that oil droplets will be captured at

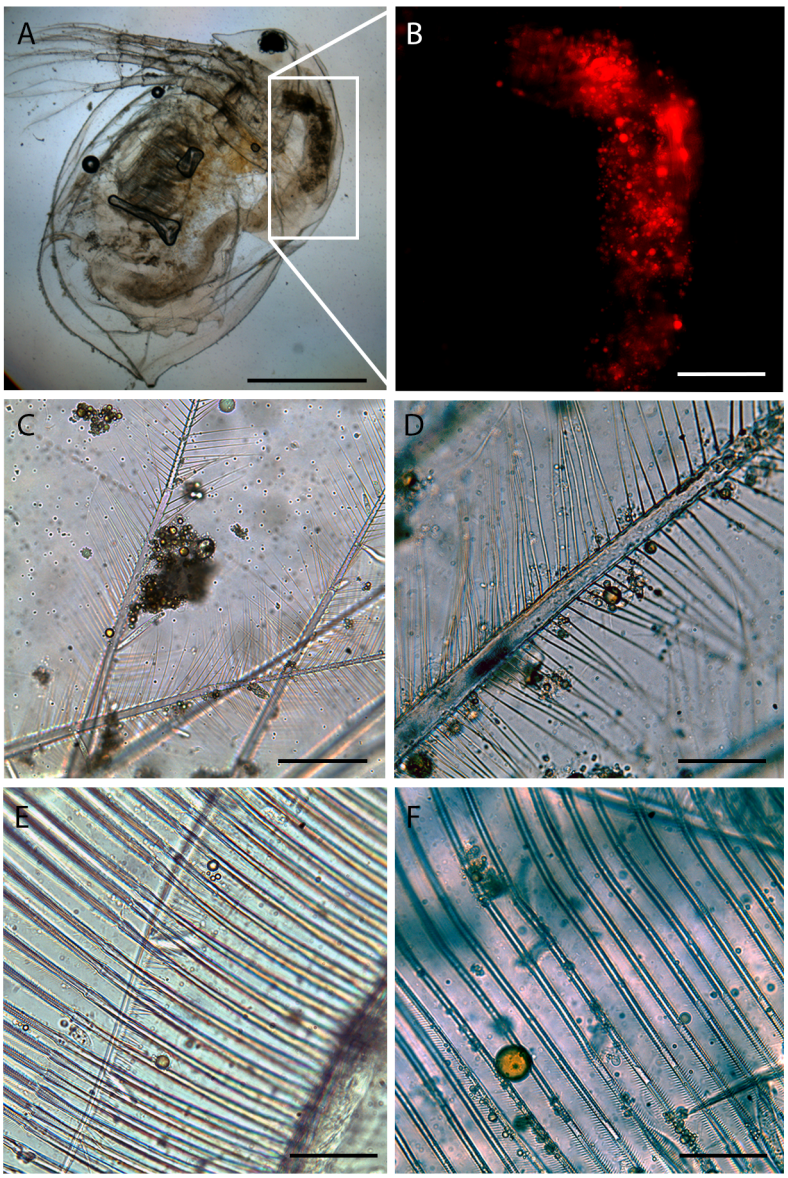

Figure 4.10. Captured and ingested crude oil droplets by *Daphnia magna* following the feeding in an oil-in-water emulsion experiment. (A) Complete individual after the feeding period. The anterior gut is identified. Scale bar is 1000 μm. (B) Anterior gut viewed with TRITC fluorescence filter highlighting the oil droplets. Scale bar is 200 μm. (C) Example of droplet flocculation and capture by the second pair of antenna. Scale bar is 100 μm. (D) Oil droplets captured by the second antennae's setae displaying very high contact angles and clam shape configuration. (E-F) Captured oil droplets on the setae and setules of the third or fourth pair of TL displaying low wettability. Scale bar for D-F are 50 μm.

both high and low Re numbers. At low Reynolds numbers, the boundary layers of setae overlap and little to no fluid will pass between. Oil droplets were captured by the boundary layer and did not contact the setae. At high Re numbers, direct interception is the predominant capture mechanisms. Between these two extremes, there was a transition zone at

which barnacles displayed paddle and sieve characteristics where droplets were captured in the setae boundary layers and by direct interception, simultaneously.

When actively feeding, barnacles make full use of the thick boundary layer around their rami. Although fluid will pass through the appendage when it is fully extended, bringing the rami closer and reducing the G/D ratio will decrease the leakiness of an appendage, depending on its Reynolds number. (Koehl, 2001) established that for $Re = 0.5$, the maximum decrease in leakiness happens when the G/D ratio goes below 5, which is the ratio of *B. crenatus* when it fully extends. Indeed, the animal needs to move its rami by half of the initial spacing for the rami's boundary layer to overlap and shift toward a paddle behavior. This exact process is shown in Figure 4.5. Thus, capture by a single fiber is unlikely at low Reynolds numbers for its small filter morphology.

In all barnacle experiments, direct interception was the mechanism with the highest index. Indeed, inertial interaction and gravitational deposition are several orders of magnitude lower (Table 4.1). There are several possible reasons for such a gap in intensities, the main one being the small size of the oil droplets used in the experiments. Since larger particle have higher inertia, they would deviate from their flow stream easier than small droplets. For example, using a theoretical droplet diameter of 100 μm, which is well within their feeding range (Nishizaki and Carrington, 2014), the intensities for direct interception, inertial interaction and gravitational deposition at our intermediate velocities are respectively 18.15, 1621.75 and 8.77. In this case, since it has the highest calculated index, inertial interaction is the most likely capture mechanism, and gravitational deposition the least. Increasing the particle size will then increase the indexes of direct interception, inertial interaction and gravitational deposition, but will have a higher impact on inertial interaction (Mehrabian et al., 2018b). Also, the indexes St and G incorporate the density difference between the particle and water. In this sense, lighter oils are more likely to be captured by such mechanisms (LaBarbera, 1984). The capture intensity when increasing the flow velocity will have no impact on direct interception, but will increase the index for inertial interaction and decrease it for gravitational deposition. Considering this, a flow velocity edging toward zero would make gravitational deposition the main capture mechanism. However, when there is no flow, barnacles will either not feed or feed actively, essentially creating their own flow and capturing particles with other mechanisms. Gravitational deposition also highly depends on

the orientation of the collecting fibers. Since it requires for particles to sink along the vertical axis, an appendage parallel to that plane, *e.g.* barnacle legs, are not optimal for such capture. Animals such as zoanthids and ophiuroids are better adapted for deposition feeding (Rubenstein and Koehl, 1977). In sum, direct interception is the main capture mechanism when the boundary layer is thin enough to allow fluid close to the rami. Inertial interaction would be a potential mechanism when studying big droplets and high flow. Gravitational deposition is not a probable mechanism for barnacles under any conditions.

Barnacles are a good example of an organism that will alter its movement and setae spacing with changes in the flow environment. This adaptation permits them to live in low flow bays, rocky tide pools, wave-swept shores, and boat hulls. In these cases, the barnacles operate at a scale for which a small change in morphology can greatly affect the appendage's behavior. Thus, the appendage can shift between the paddle and sieve feeding behavior. This change in behavior and alter in turn alter the main capturing mechanism by a setae (Koehl, 1993, 2001).

The main oil droplet capture mechanism for *Daphnia magna* is entrapment in the overlapping boundary layers of the third and fourth pair of thoracic legs. Our results agree with (Watts and Petri, 1981) that the feeding current is created by the beating of the same legs. These capture observations, made with a high speed camera, were supported by visualizing and measuring ingested crude oil droplets in the gut using fluorescence microscopy. After calculations of appendages velocities and measurements of setae and setules via SEM, we determined that sieving is not the main capture mechanism for this organism. However, our calculations of the boundary layers around fibers of all three species studied here are approximations. Indeed, these data were obtained assuming that the flow around the fiber is steady and does not vary in time. This is often not the case since the appendages often begin their filtering motion from a resting position *i.e.*, no moving velocity, thus creating an acceleration which influences the thickness of the boundary layers. Also, the filtering surfaces were assumed to be smooth to facilitate the calculations and their interpretation. Even though the filtering surfaces observed in this study are relatively smooth (Fig. 4.4, 4.8), other species could have rougher setae. These changes in surface texture could alter the flow profiles around the fibers and their boundary layers, which could in turn change the behavior of the appendage.

There is a certain range of particle size and flow velocity for which wettability plays a role in particle capture, *e.g.* up to 4 cm/s Conova (1999). Our flow velocities of the third and fourth appendages of *D. magna*, *i.e.* $1 - 1.67\ cm/s$, are within that range. Their results also show that particles of 0.50 to 10 μm in diameter are less likely to be capture when they have high wettability. Since this range of particle size is observed in captured droplets by *Daphnia magna*, wettability might play a role in capture efficiency for this organism. Even though our results show that the surface of *D. magna* is lipophobic, its exoskeleton is also hydrophobic (Gerritsen et al., 1988). Considering that both the appendage and droplet surfaces are hydrophobic, the capture efficiency of oil droplets by single fiber, when possible, might be enhanced. Indeed, when both the collector and the particle have low wettability, capture efficiency is increased (Conova, 1999). This is because water is easily displaced between two hydrophobic surfaces. Therefore, for small droplets, the low surface wettability of the studied species may facilitate the capture of oil.

The low wettability and smooth texture of crustacean filter feeding appendages increase oil droplet capture and permits the manipulation and transfer of droplets between appendages. The filtering appendages of the two barnacles and the *Daphnia* were highly lipophobic and smooth in texture. The oil droplets adhered to the appendages with a high contact angle and minimal contact area. Several other fresh and saltwater filter feeding crustacean taxa also possess these qualities, highlighting a general phenomenon in nature. These taxa include calanoid copepods (Romano et al., 1999), shrimps (Felgenhauer and Abele, 1983), *Triops* (Møller et al., 2003) and rotifers (Silva-Briano et al., 2015). Since droplet capture is greater when the appendage and the droplet have low wettability, the widespread lipophobicity and smoothness of appendages may be adaptations to feed on lipid droplets(Gerritsen and Porter, 1982). Decaying organisms will release lipid droplets that are rich in nutrients. An appendage with low wettability thus increases the probability of droplet capture, creating a feeding opportunity for these filter feeders. Also, oil fouling increases the energy needed for appendage movement by augmenting drag, and it clogs filtering surfaces. A captured droplet with a high contact angle requires less energy to allow detachment, lowering the risk of fouling (Becker et al., 2000).

This study is the first to characterize the capture of oil droplets by individual barnacles and a zooplankton. It is an experimental, lab based study, where oil droplet size was less than

10 μm in diameter. We chose this size range because small droplets tend to remain in the water column longer. Small droplets are also appropriate to study because pelagic copepods will lower the size distribution of crude oil droplets via manipulation by the appendages and defecation (Uttieri et al., 2019), making these droplets sizes persist in the environment. Nevertheless, work is needed to characterize the capture of large droplets. Larger droplets emerge from decaying organic materials and emulsified oil droplets from a tanker or oil rig spill range from 0.5 μm to several millimeters in diameter Jordan and Payne (1980). Even less is known about how aggregations of animals effect oil droplet capture. Pullen and LaBarbera (1991) shows that hill-shaped barnacle colonies will capture more particles than flat ones. This would indicate that at a certain flow, certain aggregations have more success at capturing oil than others.

Whereas the harmful effects of oil, dispersed oil and its water-soluble fraction on zooplankton are well known (Almeda et al., 2013, 2014a; Lee, 2013; Seuront, 2010). Here we begin to understand the variables that govern the capture and ingestion of an oil droplet, and therefore how oil enters marine and aquatic food webs. These variables include appendage morphology, wettability, and flow velocity. Future studies need to quantify droplet capture in a more realistic and complex mesocosm study, because population and community factors can alter capture (Almeda et al., 2013; Uttieri et al., 2019). Future efforts should also include PIV or other flow visualization tools to further understand the flows around these complex filtering structures. Analogous experiments with oil and surfactants are also needed to inform the debate about their efficacy.

4.5. Supplementary material

Supplementary Video 1. *Balanus crenatus* actively feeding inside a flume on crude oil droplets filmed at 1057 frames per second. Flow velocity inside the flume was 1.4 cm/s. At this scale, cirri spacing and flow velocity, the appendage behaves as a paddle.

Supplementary Video 2. *Balanus crenatus* passively feeding inside a flume on crude oil droplets filmed at 1057 frames per second. Flow velocity was measured at 20 cm/s. Here, fluid and particles flow between the cirri of the individual.

Supplementary Video 3. The metachronal filtering motion of the thoracic legs of *Daphnia magna* is filmed at 1057 frames per second under a dissection scope. The animal is in an crude oil-in-water emulsion.

Chapitre 5 .

The loss of crude oil droplets by filter feeders and the role of surfactants

par

Francis Letendre[1], Paloma Arena Serrano Ramos[1] et Christopher B. Cameron[1]

([1]) Département de sciences biologiques, Complexe des sciences, Université de Montréal, 1375 Avenue Thérèse-Lavoie-Roux, Montréal, Québec, H2V 0B3, Canada

Cet article a été publié dans :

Proceedings of the 44th Arctic and Marine Oil Pollution Technical Seminar on Environmental Contamination and Response

Conférence virtuelle du 7 au 9 juin 2022

Cet article a été modifié pour les besoins de la thèse.

Rôle des auteurs

Francis Letendre : Conceptualisation du désign expérimental, création du matériel expérimental, conception de la méthodologie, revue de littérature, collecte des données, analyse des données, rédaction du manuscript, soumission et révision du manuscript

Paloma Arena Serrano Ramos : Revue de littérature, collecte des données, analyse des données

Christopher Cameron : Conceptualisation du désign expérimental, validation des résultats, rédaction du manuscript, révision du manuscript, supervision et administration du projet, acquisition du financement

Résumé.

Il existe plusieurs méthodes de remédiation de déversements pétroliers, *e.g.*, l'utilisation de bouées flottantes, le brûlage contrôlé et le déversement de surfactants. Ces surfactants agissent en tant qu'agent dispersant en facilitant la formation de gouttelettes de quelques microns de diamètre. Ici, nous étudions l'impact de ces surfactants sur la distribution de taille de gouttelettes dans la colonne d'eau et dans le tube digestif du filtreur *Daphnia magna*. Nous étudions aussi l'effet qu'un surfactant peut avoir sur les conditions critiques de détachement de gouttelettes mécaniquement et chimiquement dispersées en mesurant le nombre de Weber et le ratio de taille entre la gouttelette et la fibre. Nos résultats montrent qu'inclure du sulfosuccinate de dioctyle et de sodium solubilisé lors de la fabrication de l'émulsion produit des gouttelettes de plus petites tailles et diminue l'étendue de la distribution dans la colonne d'eau. Dans le tube digestif, la taille des gouttelettes mécaniquement et chimiquement dispersée ne change pas, ce qui pourrait être dû à un processus de sélection ou en raison de l'action mécanique des appendices filtreurs. De plus, les gouttelettes chimiquement dispersées vont se détacher de la fibre à une vélocité moindre en raison d'une plus faible tension d'interface. Le taux auquel les conditions critiques de détachement augmentent est aussi plus faible en présence d'un surfactant. Cette étude permet de mieux comprendre l'impact qu'un surfactant peut avoir sur la manipulation et l'ingestion de gouttelettes de pétrole brut par les organismes filtreurs en comparant les conditions critiques de détachement du pétrole dispersé mécaniquement et chimiquement.

Mots clés : pétrole brut, zooplancton, gouttelette, détachment, nombre de Weber

Abstract.

Various methods of oil spill remediation exist, *e.g.*, floating booms, controlled burning and the release of chemical surfactants. These surfactants act as a dispersing agent by facilitating the breakup of the slick into micron-sized droplets. Here, we studied the impact such surfactants have on the size distribution of oil droplets in the water column and in the gut of the filter feeder *Daphnia magna*. We also studied the effect of surfactants on detachment conditions of oil droplets from capture fibers by measuring the critical Weber number and the droplet to fiber size ratio of mechanically and chemically dispersed crude oil. Our results show that including solubilized dioctyl sulfosuccinate sodium salt in the mixing of the emulsion produces smaller droplets and a narrower size distribution in the water. In the gut, the size of ingested droplets does not change whether the oil is mixed mechanically or chemically, which could be due to a size selection by the organism or by breakup of the droplets by the appendages. Also, droplets that are coated with surfactants detach at a lower velocity than mechanically dispersed droplet because of their lower oil/water interfacial tension. The rate at which the critical detachment conditions increase is also slower when a surfactant is present. This study allows for a better understanding of the impact a surfactant has on the handling and ingestion of oil droplets by filter feeders by comparing the critical conditions needed for appendage detachment of both mechanically and chemically dispersed crude oil.

Keywords: crude oil, zooplankton, surfactant, oil droplet, detachment, Weber number

5.1. Introduction

Oil spills can occur as a pulse from an offshore rig or an oil tanker or as a continuous spill. The volume of crude oil spills into pelagic and coastal environments range from a few to hundreds of millions of liters (Li et al., 2011). The 2010 *Deepwater Horizon* spill in the Gulf of Mexico and the 1989 wreck of the *Exxon Valdez* in Prince William Sound are two examples of spills. These ecological disasters have enormous consequences on the marine environment that still persist to this day. Indeed, Nixon and Michel (2018) estimated that approximately 227 tons of crude oil are still present in the sediments near the shorelines of Prince Williams Sound.

Oil spill cleanup methods include the use of floating booms and skimmers, controlled burning and the use of chemical dispersants, *i.e.*, surfactants (Lehr et al., 2010a). After the *Deepwater Horizon* spill, close to 7 millions liters of surfactants were released at the surface of the water and at the location of the leak 1600 m underwater (Almeda et al., 2014c; John et al., 2016). The main chemical surfactant used was Corexit9500a. Chemical dispersants are composed of amphiphilic molecules, for these molecules possess an hydrophilic head and an hydrophobic tail. These characteristics orient the surfactant around oil droplets and lower the water-oil interfacial tension (IFT). With a lower IFT, the breakup of these oil droplets by waves, wind and other external forces is made easier. Thus, the use of a surfactant will produce an oil-in-water emulsion with a smaller size distribution. The idea behind the release of a surfactant is to make the droplets small, *i.e.*, 70 μm in diameter, so that they will not rise to the surface (Van Hamme and Ward, 1999; Xu et al., 2018). This increases their residency time in the water column for optimal microbial degradation.

However, the use of a chemical dispersant as a remediation method has several negative consequences. Almeda et al. (2013) concluded that crude oil dispersed using a chemical dispersant is 2.3 to 2.4 times more toxic to the mesozooplankton than mechanically dispersed oil. For three species of copepods, *Acartia tonsa, Temora turbinata* and *Parvocalanus crassirostris* and their larval stages, the chemically dispersed oil was more toxic than the mechanically dispersed (Almeda et al., 2014a). The presence of the chemically dispersed oil resulted in lower fecal pellets counts and lower egg production and hatching rates. Similar results have been observed with microzooplankton (Almeda et al., 2014c). Barnacle nauplii and tornaria larvae have lower growth rates when in contact with chemically dispersed oil

(Almeda et al., 2014b). Chemically dispersed oil is 50 times more toxic to rotifers than their separate components (Rico-Martínez et al., 2013). The vastly commercialized nordic shrimp *Pandalus borealis* is also more sensitive to chemically dispersed oil (Arnberg et al., 2019). Considering that the surfactant contributes to a smaller emulsion size distribution and better emulsion stability, these smaller droplet could be more readily ingested by planktonic filter feeders since they feed on particles of similar sizes (Conover, 1971). It is clear that the use of a chemical surfactant is a highly debated issue with consequences on both the fate of the oil and the various filter feeders that inhabit the water column and benthos.

While the subject of solid particle capture by planktonic zooplankton and other filter feeders is one that has been extensively studied (Cheer and Koehl, 1987b; Rubenstein and Koehl, 1977; Jørgensen, 1955), the capture and loss of liquid particles are less understood. Since filter feeding zooplankton are considered an entry point of crude oil into the marine trophic systems, either via predation or oil-filled fecal pellets (Almeda et al., 2016; Conover, 1971; Turner and Ferrante, 1979), it is imperative to understand the mechanics involved in oil capture and potential loss. Rubenstein and Koehl (1977) established the basis for particle capture by describing the five main mechanisms by which a fiber can collect a particle form the water column. These mechanisms are direct interception, inertial interaction, gravitational deposition, diffusion and electrostatic attraction. Our previous works (Letendre et al., 2020; Mehrabian et al., 2018b) built upon these mechanisms and adapted them for liquid particle capture. We established the theoretical basis of oil droplet filtering and studied the droplet detachment conditions experimentally. We also observed and quantified the capture of oil droplets at both high and low Reynolds number (Letendre and Cameron, 2022).

The Reynolds number is usually calculated to rapidly describe the flow. This dimensionless number comparing the inertial to viscous forces can be obtained using the following equation :

$$Re = \frac{\rho_w U_w (2R_f)}{\mu_w} \tag{5.1}$$

Here ρ_w is the density of the water, U_w is the flow's velocity, R_f is the radius of the fiber and μ_w is the dynamic viscosity of the water. If $Re > 1$, then inertial forces overcome the viscous forces and govern the system. The Reynolds number can be used to predict the

behavior of filtering appendages, *e.g.*, if a particle will be captured by contacting a fiber or by entering its boundary layer (Koehl, 1993).

When studying the detachment of an oil droplet from a fiber, the system's Reynolds number needs to be known in order to use the correct dimensionless index. When $Re < 1$, viscous forces dominate and the capillary number Ca is used. This number represents the viscous to capillary forces ratio. Viscous forces will deform the droplet that is attached to the fiber, whereas the capillary forces will keep the droplet on the fiber. This number can be obtained using this equation :

$$Ca = \frac{\mu_w U_w}{\sigma} \tag{5.2}$$

where σ corresponds to the oil/water interfacial tension. However, when the Reynolds number is greater than 1, inertial forces overcome the viscous forces and the Weber number needs to be used instead. This number is the ratio of the inertial to capillary forces and can be obtained like so :

$$We = \frac{\rho_w U_w^2 (2R_f)}{\sigma} \tag{5.3}$$

In our detachment experiments, the Reynolds number is in the orders of 1 to 10^2, which is why the Weber number is used to compare detachment conditions. This means that whenever a particular system will reach its critical Weber number, the inertial forces will overpower the capillary forces and thus allow for droplet detachment. This range of Reynolds number is one that is typically experienced be several sessile filter feeders such as barnacles (Letendre and Cameron, 2022).

The goal of this paper is to identify the role a surfactant on the critical conditions for droplet detachment from a fiber. We also compared chemically and mechanically dispersed oil droplets sizes in the water column and in the gut of the freshwater zooplankton *Daphnia magna*. This work is relevant to anyone in fluid mechanics, ecotoxicology, marine ecology and biogeochemistry since it provides insight on how crude oil is filtered and captured by zooplankton.

5.2. Materials and Methods

To study and compare coated and uncoated oil droplets ingested by the cladoceran *Daphnia magna*, two types of crude oil emulsions were prepared. The uncoated emulsion was mixed using a light crude oil ($API = 34$) and dechlorinated tap water. Then, 75 μL of crude oil was pipeted into 1 L of water. The emulsion with coated oil droplets was prepared the same way, except that a surfactant was added to the oil before mixing. The surfactant was dioctyl sulfosuccinate sodium salt (DOSS, Sigma 323586) solubilized in propylene glycol at 0.3 g/L. DOSS and propylene glycol are both components of Corexit 9500a, a surfactant used in oil spills remediation. The solubilized surfactant was added to the emulsion at a 1 : 20 surfactant to oil ratio (DOR), based on previous studies and governmental guidelines (Almeda et al., 2013, 2014b; Lehr et al., 2010b). Both solutions were then mixed for 10 minutes using a magnetic stirrer at 900 RPM.

5.2.1. Feeding experiment

For both mechanically and chemically dispersed emulsions, oil droplets were observed under fluorescence microscopy immediately after the 10 minutes of stirring, then photographed and measured. Then, 20 to 30 mature individuals of *Daphnia magna* were put into a 1 L beaker with either mechanically or chemically dispersed oil prepared as mentioned above. Each beaker was stored in an incubator at 20^oC and periodically stirred for 24h. Prior to the incubation period, individuals were starved for one day to ensure a clear digestive tract and to facilitate oil observations. After the feeding period, individuals were put onto slides and photographed under fluorescence microscopy using a TRITC filter. Since crude oil autofluoresces, ingested droplets found in the gut were measured and analyzed using the software ImageJ. We then created droplet diameter distributions of mechanically and chemically dispersed oil in the water column and in the gut of *Daphnia magna*. Only droplets with a least 90% circularity were considered to ensure that the measurements of diameters were accurate and 2000 droplets were considered for each distributions. Since the distributions did not meet the condition of normality, a non-parametric Kruskal-Wallis test was made to compare all four distributions at a statistical significance of $P < 0.05$. A post-hoc analysis was done to identify further difference between samples using the Dunn test with a statistical significance of $P < 0.05$.

5.2.2. Droplet detachment experiment

The experimental protocol of this experiment is based on prior experiments from Letendre et al. (2020). Crude oil droplets were attached to steel wires of 50 μm and 250 μm in radius. These wires were then mounted on a microscope slide using modelling clay. The slide was placed in a flume to allow the wire to be perpendicular to the flume's flow. Droplet were created using a thinned glass pipette. The droplet was photographed next to a ruler for scale and measurement of droplet radius. Once a droplet was attached to the steel wire, the flume speed was gradually increased until the crude oil droplet detached from the fiber. These experiments were done in artificial sea water with a density of 1024 kg/m^3 and at a temperature of 20^oC. A high speed camera was used to capture the detachment event at 200 frames per second. The flume's free-stream velocity was obtained by measuring the velocity of free-streaming particles in the tank with ImageJ. This experiment was repeated several times for different droplet and fiber size ratios.

We also filmed and measured the detachment events of oil droplets coated with solubilized DOSS in order to study the effect of surfactants on detachment conditions. To study the detachment of oil droplets, we used the ratio of inertial to capillary forces, also known as the Weber number. In order to test the effect of a surfactant on the detachment of droplets, the data was transformed in log-data and linear regressions were made on both coated and uncoated droplet data in R. Then, an ANCOVA analysis was made with both these regressions to test if the type of droplet had an impact on their detachment (statistical significance of $P < 0.05$). Uncoated and coated droplet data were separated in the graph to compare and visualize the surfactant's effect. This experiment was then repeated, but the steel wires were replaced with a dissected barnacle cirrus ($R_f = 50\,\mu m$). With the cirrus facing the direction of flow, the forces acting on the droplet were equivalent to those acting on a droplet captured on a passively feeding barnacle. This was done to study the roles of surface texture and wettability on detachment. To measure the viscosity of the oil and of the surfactant, we used an Anton Paar MCR 501 and we used the pendant drop method to measure oil/water interfacial tension. These properties are compiled in Table 5.1.

Table 5.1. The fluid properties of the crude oil, chemically dispersed crude oil and saltwater used in this study.

Oil	Density ρ_o (kg/m^3)	Viscosity μ_o $(mPa \cdot s)$	O/W Interfacial Tension σ (mN/m)
Crude oil	855	98	27.1
Crude + DOSS	1035	51	6.02
Salt water	1024	1.33	—

5.3. Results

5.3.1. Feeding experiment

To understand the role a surfactant has on the droplet size distribution and potential ingestion of crude oil, we conducted a feeding experiment using the freshwater cladoceran *Daphnia magna*. Figure 5.1 displays all four distributions of oil droplets using box plots. The average mechanically dispersed droplet diameter was 2.07 $\pm$ 1.45 μm but varied from 0.11 to 6.28 μm (Fig. 5.2A). Droplets that were chemically dispersed however, were 0.40 $\pm$ 0.39 μm in diameter and were up to 1.46 μm (Fig. 5.2B). Droplets found in the gut of *Daphnia magna* were distributed similarly. For mechanically dispersed droplets that were ingested, the diameters were 0.49 $\pm$ 0.85 μm (Fig. 5.2C). Finally, for chemically dispersed droplets in the gut, the diameters were 0.39 $\pm$ 0.55 μm (Fig. 5.2D).

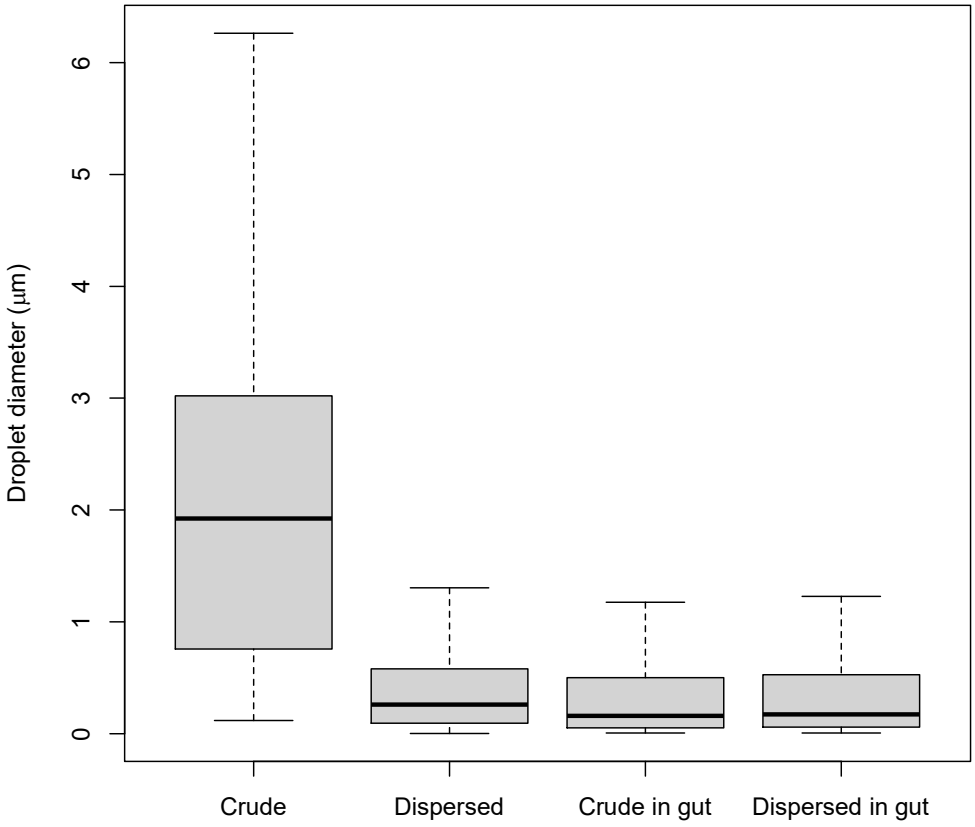

Figure 5.1. Boxplot of all four size distribution of oil droplets diameters measured in the feeding experiment. From left to right, the distribution shown are : mechanically dispersed crude oil in the water column, chemically dispersed crude oil in the water column, mechanically dispersed crude oil in the gut of *Daphnia magna* and chemically dispersed crude oil in the gut of *Daphnia magna*.

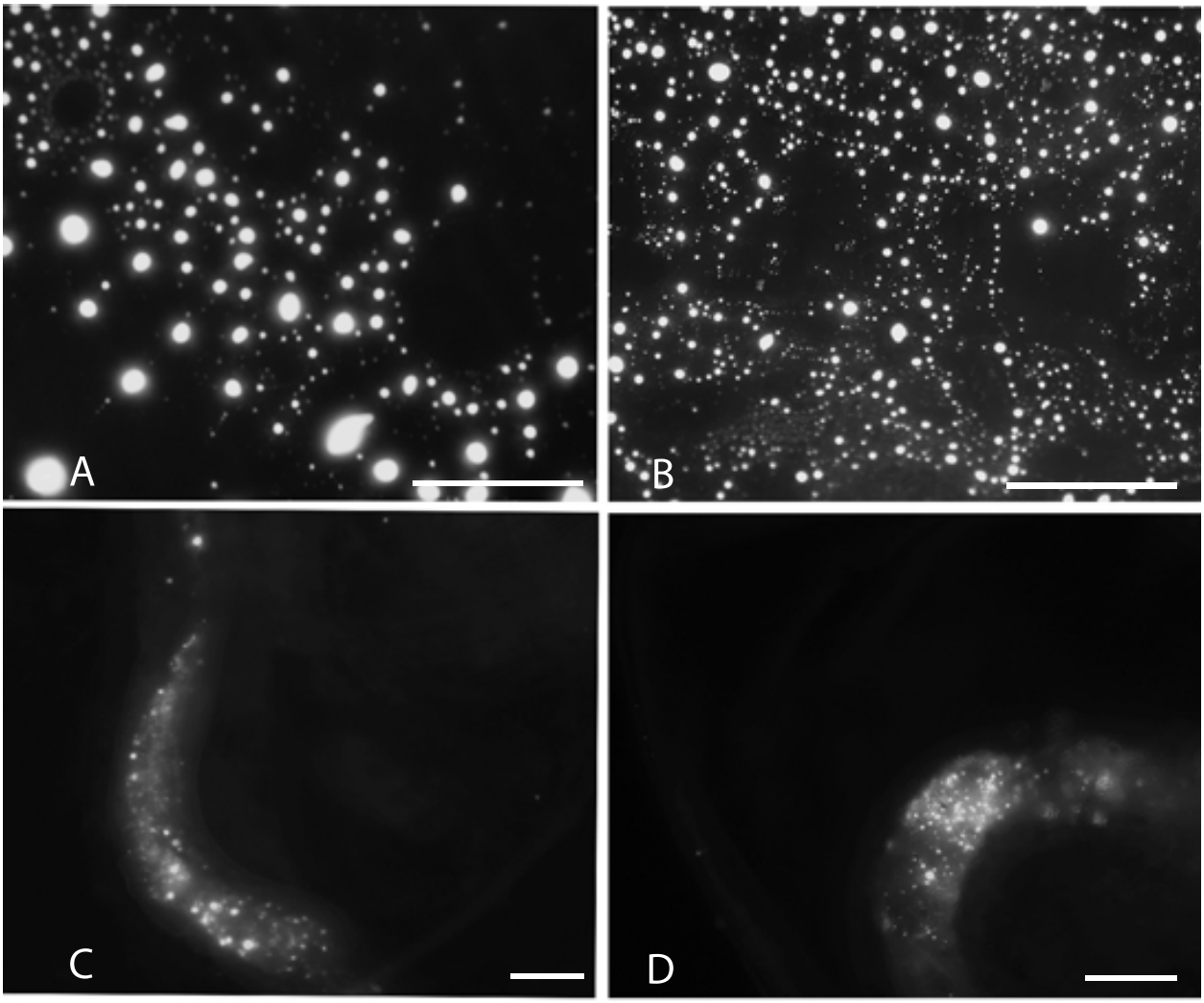

Figure 5.2. Samples of all four measured distributions. (A) Mechanically dispersed crude oil-in-water emulsion. (B) Chemically dispersed crude oil-in-water emulsion using solubilized DOSS. (C) Mechanically dispersed oil droplets in the digestive tract of *Daphnia magna*. (D) Chemically dispersed oil droplets in the digestive tract of *Daphnia magna*. Scale bars are 20 μm in frames A and B and 100 μm in frames C and D.

Following the Kruskal-Wallis rank sum test in R, these p-values were obtained :(Table 5.2) :

Table 5.2. Adujsted P-values obtained following the Dunn test using the Bonferroni correction on the size distributions of oil droplets from the feeding experiment.

Sample	Crude	Dispersed	Crude in gut
Dispersed	3.5×10^{-240}	—	—
Crude in gut	1.3×10^{-210}	9.1×10^{-5}	—
Dispersed in gut	7.6×10^{-138}	3.1×10^{-2}	0.61

Most importantly, the difference in the distributions of mechanically and chemically dispersed oil in the water column is statistically significant ($P = 3.5 \times 10^{-240}$), but not in the gut ($P = 0.61$).

5.3.2. Droplet detachment experiment

The impact of a surfactant on the detachment of a droplet from a cylindrical fiber was also studied. For this, droplets were filmed in a flume while the flow velocity was gradually increased. The velocity at which a particular droplet detached and its droplet to fiber size ratio were measured. The detaching velocities across all experiments varied from $2\,cm/s$ to $46\,cm/s$.

The experiment was repeated with surfactant-coated droplets and regular droplets, both on a stainless steel fiber and on barnacle cirri. These four data groups were transformed into log-data and compiled in Fig. 5.3. Linear regressions were added to the graph in the effort of proving that adding a surfactant to the crude oil emulsion affected the detachment process. The regression's equation for uncoated droplets is $log(R) = -0.3632 \cdot log(We) + 0.5289$ and has a coefficient of determination of 0.88. On the surfactant-coated data, the regression's equation is $log(R) = -0.4132 \cdot log(We) + 0.7969$ and the R^2 is 0.90. Then, to confirm if the treatment of oil droplets with a surfactant interacted with the detachment mechanics, an ANCOVA analysis was done using both regressions. Both individual linear regressions proved to be adequately representing the data ($P = 2 \times 10^{-16}$). The interaction between the treatment, *i.e.* with and without a surfactant, and our explanatory variable the critical Weber number was also statistically significant ($P = 4.69 \times 10^{-5}$). In other words, the two

linear regressions are not parallel, meaning that the treatment affected the relation of our two variables.

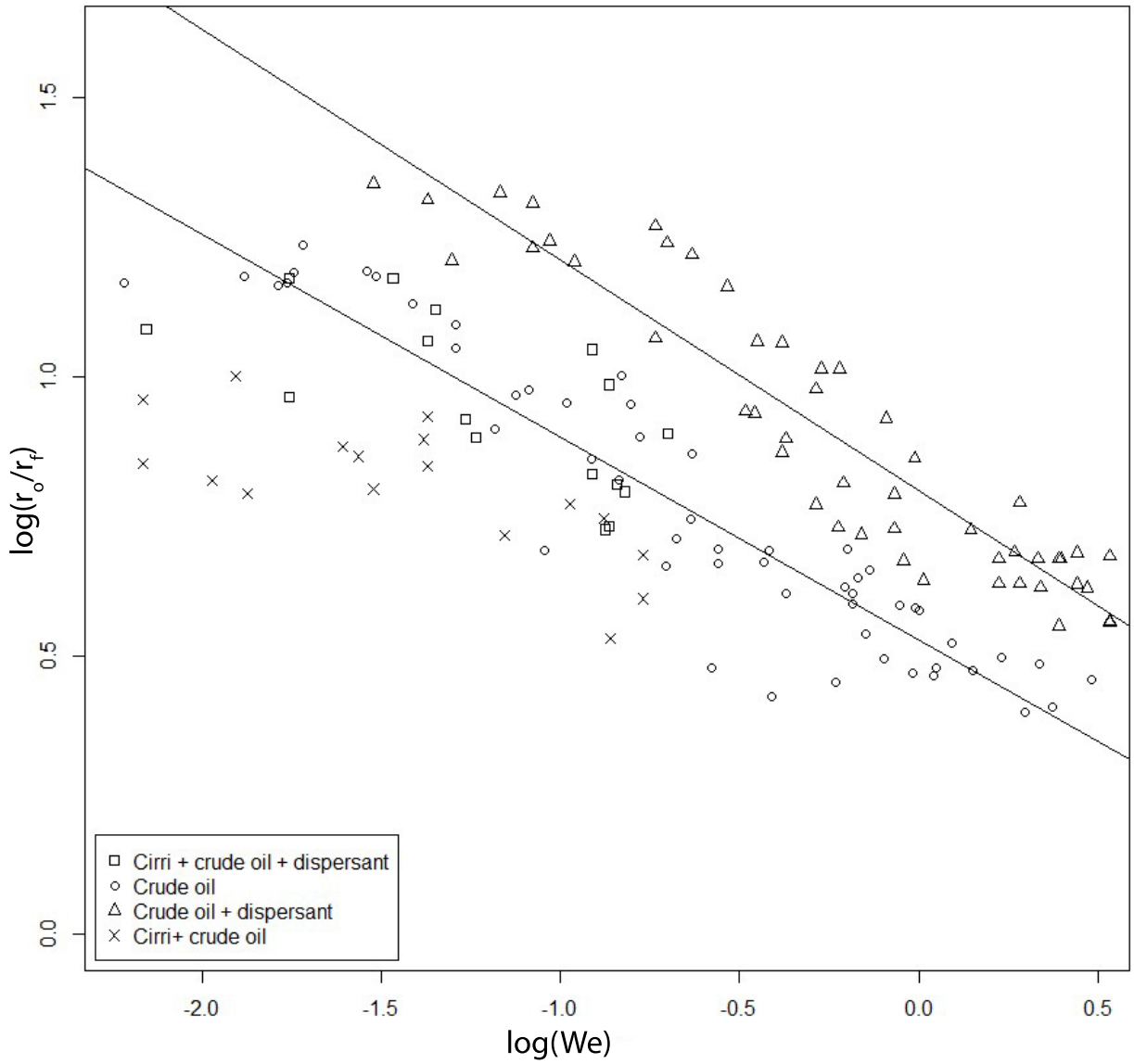

Figure 5.3. Graph of the droplet to fiber size ratio in function of the Weber number. All data was log-transformed. Each data point represents the critical conditions needed for a particular droplet to detach from the fiber. The equation of the crude oil linear regression is $log(R) = -0.3632 \cdot log(We) + 0.5289$ and has a R^2 of 0.88. The equation of the linear regression for the chemically dispersed crude oil is $log(R) = -0.4132 \cdot log(We) + 0.7969$ and the R^2 is 0.90. Circles correspond to mechanically dispersed droplets. Triangles are chemically dispersed droplets. Crosses and squares are respectively mechanically and chemically dispersed droplets detached from a barnacle cirri.

Figure 5.4 shows the detachment process of a mechanically dispersed oil droplet and a droplet dispersed using the solubilized dioctyl sulfosuccinate sodium salt. Both droplets have the same droplet to fiber size ratio, meaning that the only variable changing in both treatment is the presence or absence of the surfactant. When an uncoated droplet would attach to a stainless steel fiber, it would acquire a clam shape, meaning that the contact angle was at least $\theta = 60°$ (Carroll, 1976). When the flume's flow velocity increased, the droplet gradually elongated following the stream lines. If the droplet size was sufficient, its furthest part would start rapidly oscillating up and down due to vortex shedding (Vogel, 2020). Upon reaching the critical Weber number (from the increasing flow velocity), the attached droplet would breakup into a daughter droplet and a satellite droplet (Fig. 5.4C). These satellite droplets were very small in size. In this figure, the uncoated droplet detaching velocity and critical Weber number were respectively $18\,cm/s$ and 0.63. When using mechanically dispersed droplets, some residuals of crude oil often stayed on the fiber after detachment, *i.e.* partial detachment.

Figures 5.4 D-F show the detachment process of a chemically dispersed oil droplet. When solubilized DOSS was added into the crude oil-in-water emulsion, the droplet still acquired a clam shape when attached to the fiber, but spread less on the surface and showed less affinity for the fiber. The contact angle were also higher when using chemically dispersed oil (Fig. 5.4D). Also, when detachment of the droplet occurred, no satellite droplets were created (Fig. 5.4F). The detachment velocity for this particular droplet was $14\,cm/s$ and its critical Weber number was 2.46. Even though anecdotal, we observed that droplets coated with a surfactant were less prone to elongate when subjected to external forces. They would remain somewhat spherical on the fiber.

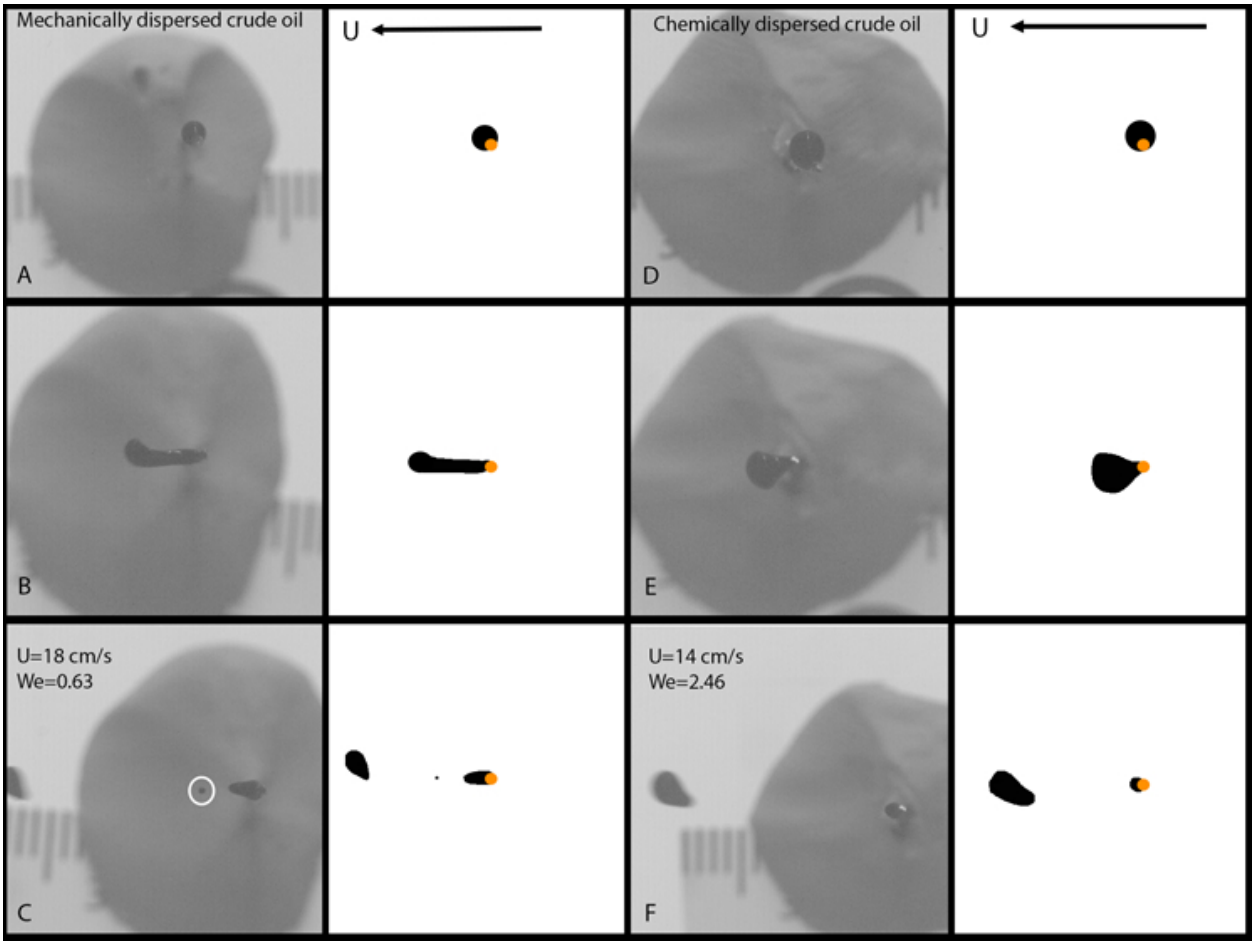

Figure 5.4. Detachment process of a mechanically and chemically dispersed oil droplet. Both droplet have the same droplet to fiber size ratio. The left panel shows the photo of the detachment process, while the right panel displays a simplified schematic. The orange sphere represents the fiber and the black shape is the crude oil droplet. A to C shows the detachment process of a mechanically dispersed crude oil droplet. (A) Attached droplet with no flow in the flume. (B) As the velocity increased, the droplet elongated and oscillated in the flow. (C) Detachment of the droplet at 18 cm/s into a daughter and satellite droplet (white circle). D to F show the detachment of chemically dispersed crude oil droplet. (D) Attached droplet with no flow. (E) The droplet slightly elongates as the flow in the flume increased. (F) Detachment of the droplet without any satellite droplet. Detachment velocity was 14 cm/s.

Oil droplets, whether mechanically or chemically dispersed, showed very high contact angles when attached to barnacle cirri. This is in agreement with our previous observations in (Letendre and Cameron, 2022). Droplets were almost perfectly spherical and had little surface in contact with the fiber. When the flow was increased, the droplet would creep along the cirri toward the apical end. This is because, unlike the stainless steel fiber, the cirri is flexible. The flow bent the cirri backward and pushed the droplet to its tip. Then, it would

stop sliding and remain there until the critical detachment conditions were met. Figure 5.5 shows two detachment events for two same-sized droplets of both types of crude oil. For the mechanically dispersed oil, the velocity at detachment was 18 cm/s and the system's Weber number was 0.12. For the droplet coated with a surfactant, the detachment velocity was lowered to 10 cm/s and the Weber number was 0.17. The coated droplet was able to detach at a much lower velocity because of its lower interfacial tension. This caused a higher inertial to capillary forces. Then, the intensity of the inertial forces, via an increase of velocity, does not need to be as high to overcome the capillary forces maintaining the droplet in place. For coated droplets, our high speed camera observations showed that they tended to remain spherical even under high flow.

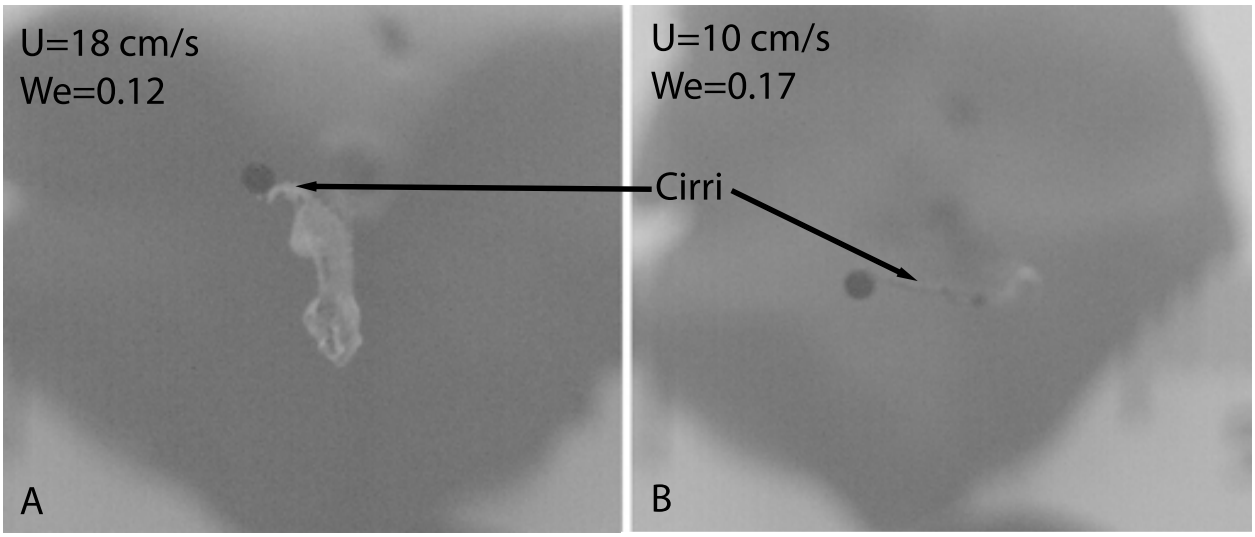

Figure 5.5. Comparison of the detachment conditions for a mechanically (A) and chemically (B) dispersed oil droplet from a barnacle cirri.

5.4. Discussion

The purpose of this study was to discover the potential role a surfactant could have on droplet size outside and inside a filter feeder's gut and on the detachment process from filtering appendages. We compared the diameters of mechanically and chemically dispersed crude oil to see if the surfactant would lower the size distribution. We also hypothesized that the presence of a surfactant would allow for easier droplet detachment, *i.e.* that they would detach at a lower velocity.

The results of our feeding experiment with the freshwater zooplankton *Daphnia magna* show that they fed on both mechanically and chemically dispersed oil. Indeed, Figure 5.2 C,D portray the gut of individuals and the fluorescence of the crude oil makes it clear that the ingestion of these hydrocarbons is not a trivial observation. Every individual observed had ingested crude oil to some extent. This validates that crude oil is ingested by *Daphnia magna*, for which the filtering mechanics were described in (Letendre and Cameron, 2022). However, this present effort builds upon these results by proving that they will also feed on surfactant coated crude oil droplets. To our knowledge, this is the first instance where ingestion of coated crude oil by a freshwater zooplankton is reported. This is a significant finding, considering that such a chemical is used as a remediation method by governments and oil companies and that freshwater bodies are not immune from oil spills (Bertrand and Hare, 2017; Vandermeulen and Ross, 1995). Indeed, this study describes how chemically dispersed oil is captured by zooplankton, essentially entering the aquatic food webs. Several studies have shown that surfactants in aquatic systems are very toxic for the plankton communities, both in marine (Almeda et al., 2014b,c) and freshwater systems (Bobra et al., 1989; Toyota et al., 2017). In some cases, the presence of both the surfactant and the crude oil was more toxic than any chemical alone for the cladoceran *Daphnia pulex* (Bhattacharyya et al., 2003). Toyota et al. (2017) even reported that when in the presence of the surfactant Corexit9500, no male daphnids offspring were produced. Though scientists have made progress on assessing the toxicity of chemically dispersed oils, more work is needed to identify remediation methods where oil is less likely to be ingested.

The use of a surfactant also affects the droplet size distribution in the water column by lowering the average diameter and by narrowing the distribution. Indeed, the difference in size between chemically and mechanically dispersed was statistically significant at $P < 0.05$ (Table 5.2). When adding a surfactant during the mixing process, the average droplet diameter lowered from $2.07 \pm 1.45\,\mu m$ to $0.40 \pm 0.39\,\mu m$. The range of diameters was also narrower, meaning that droplet size had less variation when mixed with a surfactant. The mechanism of a surfactant on oil is well-known (Nasr-El-Din and Taylor, 1992; Rudin and Wasan, 1992). The surfactant being an amphiphilic molecule, the hydrophobic tail will orient itself toward the crude oil droplet and completely surround it. The hydrophilic head will face outward in the water column. This coating of surfactant will reduce the interfacial

tension between the crude oil and the surrounding water, as our measurements confirmed, *i.e.*, the interfacial tension lowered from 27.1 mN/m to 6.02 mN/m when solubilized DOSS was present (Table 5.1). A lower interfacial tension means that the crude oil droplets will require less energy to breakup, thus creating smaller droplets. However, other variables are worth considering. Indeed, Steffy et al. (2011) observed that the efficacy of solubilized DOSS decreases as ambient water gets colder. This would mean that in colder waters, *e.g.*, in deeper waters or at higher latitudes, the difference in size distribution for mechanically and chemically dispersed oils could be of lesser significance.

Smaller droplet size has consequences on the capture and detachment mechanics. Since the droplet size is used in the calculation of the direct interception, inertial interaction and gravitational deposition, it is expected that adding a surfactant will modify the relative intensities of each of these capturing mechanisms (Letendre et al., 2020; Rubenstein and Koehl, 1977). If all other parameters do not vary, lowering the average size of a crude oil droplet will reduce the index for all three mechanisms, but will have a bigger impact on inertial interaction and gravitational deposition (Mehrabian et al., 2018b). Also, dispersing a given volume of oil into smaller droplets creates a larger number of those droplets. A higher number of droplets allows for more encounters with filter feeders. Lowering the size distribution of the droplets also opens up the possibility of smaller zooplankton or even protists to capture and ingest these hydrocarbons. It was not possible for us to effectively compare the ingested volume of mechanically and chemically dispersed oils in this study, though it is a relevant and worthwhile path of research. One might suspect that since chemically dispersed oils are broken up into more droplets, the ingested volume might be higher than with chemically dispersed oils. However, it is also possible that the added toxicity of the surfactant prevents feeding or kills the animals before they can ingest a significant volume.

Based on our results from Table 5.2, it is possible to state that regardless of the treatment for the mixing of the emulsion, the ingested droplet sizes are the same, and always in line with what *Daphnia* ingests. Indeed, the difference between the mechanically and chemically dispersed ingested droplet is the only one that is not significant. This means that adding a surfactant does not change the size of the droplets that are being ingested by *Daphnia magna*. Although the difference between the dispersed distribution in the water column and in the gut is statistically significant, they are both similar in range, *i.e.* approximately up to 1.5 μm

in diameter. What is much more significant is that the wide distribution of mechanically dispersed droplet is greatly reduced when they are measured in the gut of the filter feeder to match the distribution of chemically dispersed ingested droplets. There are two possible explanations for this particular result. The more obvious one is that *Daphnia magna* selects food particles based on their size, which would be in this case lower than 1.5 μm in diameter. Several studies have in fact identified this to be the case, as some species of *Daphnia* will favor particles smaller than 1 μm (Gophen and Geller, 1984; Hessen, 1985). However, these same studies observed that the individuals would also ingest far larger particles up to 35 μm in diameter. In our experiments, we did not measure any particle greater than 1.5 μm in the guts, considering that droplets of up to 6.28 μm were available (Fig. 5.1). Another possible explanation is that the movement of the organism's appendages could contribute to droplet breakup. Indeed, (Uttieri et al., 2019) observed that the beating motion of the copepod's filtering appendages lowered the size distribution of crude oil in the water column by a factor of 2-3. Given the fact that *Daphnia magna* is a large planktonic filter feeder, it is possible that the fast beating of second antennae and the metachronal motion of the thoracic legs could also break larger droplets into daughter droplets. This could contribute to altering the size distribution of mechanically dispersed crude oil. All in all, with and without a surfactant in the emulsion, *Daphnia magna* ends up with the same size distribution of crude oil droplets in its gut. In sum, using a surfactant will not prevent ingestion and will not change the size of the droplets that are ingested.

The use of a surfactant facilitates droplet detachment by lowering the interfacial tension and greatly increasing the Weber number of the system. Figure 5.3 illustrates the effect that a surfactant had on the conditions needed for a droplet to detach from a capture fiber. The lower curve compiles data from mechanically dispersed droplet and the curve above it is from chemically dispersed oil droplets. The ANCOVA analysis confirmed that the difference between the two slopes is significant, meaning that adding a surfactant affects the detachment process. The slope for the mechanically and chemically dispersed droplet were respectively -0.3632 and -0.4132. The slope being negative means that the smaller the droplet to fiber size ratio, the higher the Weber number needs to be to allow for detachment. Increasing the Weber number can be done by increasing the velocity of the water, or by reducing the oil/water interfacial tension. In Figure 5.3, both regressions show critical conditions

for detachment. Above a certain curve, the droplets will not stay on the fiber and will return to the water column. The main mechanism behind an easier detachment with a surfactant is that the interfacial tension is reduced (Powell and Chauhan, 2016). With a lower IFT, the Weber number is drastically increased compared to a mechanically dispersed droplet of the same size ratio. This places the chemically dispersed droplet above critical detachment conditions established by the mechanically dispersed linear regression. In our study, the IFT was lowered from 27.1 mN/m to 6.02 mN/m. However, using the dispersant Corexit9500, Brandvik et al. (2019) measured more than a ten-fold reduction of the IFT, further facilitating the detachment conditions. Thus, at the same droplet to fiber size ratio, the critical Weber number for a chemically dispersed droplet is obtained at a much lower velocity, facilitating detachment (Fig. 5.4 and 5.5). Filter feeders who captured chemically dispersed droplets will then have to use less energy to reach the threshold velocity and clean their appendages. Also, sessile individuals like barnacles could be less subject to fouling when the oil is chemically dispersed since droplets would detach at a slower current.

While linear regressions were not done on the data using a barnacle cirri as the collecting fiber, a similar pattern was observed (Fig. 5.3). The data with coated droplets were all slightly to the right of the data obtained with uncoated droplets. Thus, for same sized droplets, the Weber number of chemically dispersed droplets was higher and detachment would occur at lower velocities. Also, all data obtained with barnacle cirri are located in the same general cluster obtained with stainless steel fibers. This would build upon our initial finding in Letendre et al. (2020), in which we observed that the detachment behavior of droplets from barnacle cirri did not differ from smooth cylindrical fibers. The organic and ramified surface of a barnacle does not seem to alter the detachment process. We found that a surfactant will facilitate droplet detachment from a fiber and that the surfactant will lower the size distribution of the droplets. Since a smaller droplet to fiber size ratio requires a higher Weber number to detach (Fig. 5.3, Letendre et al. (2020)), one might wonder which effect overcomes the other. Considering that droplets are smaller, but that the interfacial tension is reduced, will this result in a higher or a lower crude oil intake when compared to mechanically dispersed crude oil ? Further studies comparing the intake of both types of oil are needed to fully assess the risks and benefits of using a surfactant as an oil spill remediation method. The total volume of oil ingested should be compared in the presence

and absence of surfactants, to determine if one treatment integrates more hydrocarbons into the food webs than the other, and if so, what is the main factor behind this difference *e.g.*, droplet size, interfacial tension, higher number of encounters.

Chapitre 6.

Conclusion

Cette section présente les résultats principaux et les contributions de cette thèse à la communauté scientifique. Par la suite, les implications de ces résultats dans un contexte écosystémique ainsi que des pistes et des opportunités de recherche à considérer sont discutées.

Les déversements de pétrole brut représentent une véritable menace sur nos écosystèmes marins. Considérant que les organismes filtreurs représentent un point d'entrée important de ce pétrole dans les réseaux trophiques marins (Almeda et al., 2016; Graham et al., 2010), il est important d'étudier sa capture par ces organismes. Le but principal de cette thèse était donc de comprendre les mécanismes de capture et de détachement de ces gouttelettes d'huile par les organismes filtreurs. Pour cela, quatre objectifs ont été établis, qui seront réitérés ici :

(1) Déterminer si les organismes filtreurs ingèrent les gouttelettes d'huile en émulsion dans la colonne d'eau et établir la distribution de taille des gouttelettes capturées et ingérées. (**Chapitre 2, 3, 4** et **5**)

(2) Observer et décrire la capture et le détachement de gouttelettes d'huile et déterminer les paramètres qui contrôlent ces différents mécanismes. (**Chapitre 3** et **4**)

(3) Déterminer les caractéristiques lipophobes/hydrophobes et la mouillabilité des appendices des organismes filtreurs. (**Chapitre 4**)

(4) Déterminer l'effet que les surfactants ont sur le détachement des gouttelettes d'huile et sur les distributions de taille des gouttelettes ingérées. (**Chapitre 5**)

Durant ma thèse, je me suis d'abord penché sur les aspects théoriques de l'alimentation par filtration. Les cinq mécanismes de capture (interception directe, interaction inertielle, dépôt gravitationnel, dépôt par diffusion et attraction électrostatique) ont été étudiés et adaptés à la capture de particules liquides (**Chapitre 2**). Les bases de la mécanique des fluides à deux phases liquides ainsi que les concepts d'émulsion et de mouillabilité ont été

explorés. Le rôle de la tension d'interface et de la densité sur le volume critique de détachement a été étudié. En effet, plus celles-ci sont basses, plus le volume critique de détachement de la gouttelette sera bas. En d'autres mots, les huiles ayant une faible densité ou une faible tension d'interface se détacheront plus facilement d'un collecteur.

Dans le **Chapitre 3**, il est question des paramètres régissant le détachement de gouttelettes d'huile lorsque soumises à un courant. En effet, dans la plupart des cas, les organismes filtreurs utilisent le courant existant dans la colonne d'eau ou créent eux-mêmes leur courant en bougeant leurs appendices filtreurs. Nous nous sommes donc penchés sur les variables qui pourraient influencer le détachement d'huiles des collecteurs, limitant ainsi l'ingestion potentielle de pétrole brut. Nos résultats nous ont permis de conclure que le ratio de taille entre la gouttelette et le collecteur, la vitesse d'écoulement et la tension d'interface entre l'huile et l'eau sont tous des paramètres importants lors du processus de détachement. Plus le ratio de taille est haut, moins le nombre de Weber (un nombre sans dimension utilisant la vitesse d'écoulement et la tension d'interface) doit être élévé pour permettre un détachement de la gouttelette. Cette découverte nous a alors permis d'établir une courbe prédictive du comportement des gouttelettes en fonction des conditions environnementales et des propriétés de l'huile et du collecteur. Nous avons aussi observé que le détachement de gouttelettes des appendices filtreurs de balanes concordait à notre courbe, ce qui semblerait indiquer que la texture et le relief de ceux-ci n'influencent pas les mécanismes de détachement.

Le **Chapitre 4** est davantage concentré sur la capture des gouttelettes par les organismes filtreurs. Ainsi, les balanes *Balanus glandula* et *Balanus crenatus* et le cladocère *Daphnia magna* ont été observés à l'aide d'une caméra haute vitesse afin de décrire les mécanismes de capture du pétrole brut. Chez les balanes, les gouttelettes sont capturées dans la couche limite des appendices lorsque le nombre de Reynolds du système est bas et elles sont principalement capturées par interception directe lorsque le nombre de Reynolds est élevé. Il existe une zone de vélocité intermédiaire ou les gouttelettes sont capturées par la couche limite près de l'insertion des cirri et par interception directe vers la portion apicale de ceux-ci. *Daphnia magna* capturent les gouttelettes par les couches limites de ses troisième et quatrième paires de pattes thoraciques. Le mouvement métachronal de celles-ci apporte les gouttelettes vers le sillon ventral où elles peuvent être ingérées. Nos observations des gouttelettes capturées et des appendices filtreurs à la microscopie électronique à balayage ont démontré que les

surfaces collectrices sont hautement lipophobes. Les gouttelettes capturées montraient des angles de contact bien au-delà de 90°.

Le but du **Chapitre 5** était de déterminer l'effet des surfactants sur le processus de détachement d'une gouttelette d'huile et sur la distribution de la taille des gouttelettes dans la colonne d'eau et dans le tube digestif de *Daphnia magna*. Nos résultats indiquent que les émulsions de gouttelettes avec et sans surfactants ont des distributions significativement différentes. Nous avons aussi confirmé que *Daphnia magna* capturait et ingérait les gouttelettes dispersées à l'aide d'un surfactant. De plus, peu importe le traitement, la taille des gouttelettes retrouvées dans le tube digestif de *Daphnia magna* était la même, ce qui impliquerait possiblement un processus de sélection ou de modification de la taille des gouttelettes par les appendices filtreurs. Finalement, une analyse des régressions nous a permis d'affirmer que la présence d'un surfactant affecte significativement le processus de détachement de gouttelettes, rendant celui-ci plus facile.

Donc, concernant l'objectif (1), toutes les espèces testées (*Calanus finmarchicus, Acartia tonsa, Centropages typicus, Balanus glandula, Balanus crenatus* et *Daphnia magna*) ont été observées avec des gouttelettes de pétrole dans leur tube digestif. La taille maximale des gouttelettes capturées par les copépodes calanoïdes était d'environ 11 μm de diamètre. Au **Chapitre 5**, il a été démontré que l'utilisation d'un surfactant a baissé la distribution de tailles des gouttelettes d'un maximum de 6 μm à près de 1.5 μm de diamètre. Les tailles des gouttelettes ingérées par *Daphnia magna* étaient aussi d'un maximum de 1.5 μm en diamètre.

En ce qui a trait à l'objectif (2), les gouttelettes sont capturées à un large intervalle de nombre de Reynolds. À faible nombre de Reynolds, les gouttelettes individuelles seront capturées dans la couche limite des appendices alors qu'à haut nombre de Reynolds, elles sont principalement capturées par interception directe. Pour ce qui est du détachement, le ratio de taille entre la gouttelette et le collecteur, ainsi que le nombre de Weber du système permettent de déterminer si la gouttelette restera ou non sur l'appendice.

Concernant l'objectif (3), les appendices filtreurs des espèces étudiées montrent des surfaces lisses avec un minimum de relief, et possèdent des caractéristiques extrêmement lipophobes. Les angles de contact entre la gouttelette et le collecteur sont largement au-dessus de 90°.

Finalement, il a été démontré que l'utilisation d'un surfactant facilite le détachement des gouttelettes de pétrole d'une fibre cylindrique (objectif 4). Le surfactant contribue aussi à diminuer significativement la distribution de tailles des gouttelettes dans la colonne d'eau, mais pas celle des gouttelettes retrouvées dans le tube digestif de *Daphnia magna*.

Bien que ces recherches doctorales répondent à plusieurs questions concernant la capture et le détachement des huiles par les organismes filtreurs, la réalité est qu'il en reste énormément à découvrir et plusieurs autres facteurs à considérer. La section suivante décrit certains de ces facteurs et propose des avenues de recherches futures.

6.1. Les processus d'altération du pétrole brut

Les recherches subséquentes sur la capture et le détachement de gouttelettes de pétrole devraient aussi tenter d'incorporer les processus biologiques, chimiques et physiques que l'on peut retrouver à l'interface eau-air et dans la colonne d'eau lors d'un déversement de pétrole. En effet, un déversement pétrolier est tout sauf un événement statique. La composition du pétrole brut, ses propriétés chimiques et physiques, ainsi que son emplacement sont tous des éléments constamment en changement. Un déversement peut se produire à la surface de l'eau ou dans la colonne d'eau, créant ainsi une couche d'épaisseur variable au-dessus de l'eau ou des poches sous-marines d'hydrocarbures. Les vents, les vagues et l'utilisation de surfactants vont contribuer à fractionner ces grandes surfaces en minuscules gouttelettes de quelques microns de diamètre, augmentant ainsi leur temps de résidence dans la colonne d'eau. Au fil du temps, la densité, la composition relative des différents hydrocarbures et la viscosité sont toutes des éléments qui seront modifiés par les processus naturels d'altération observables après un déversement (Jordan and Payne, 1980; Wheeler, 1978; Wolfe et al., 1994). Bien entendu, ces processus vont varier en importance en fonction de la localisation du déversement et de la chronologie de l'événement. Puisque ces processus altèrent les propriétés du pétrole brut, il est escompté que ceux-ci vont modifier les mécanismes de capture et de détachement d'un organisme filtreur.

L'évaporation est un des processus d'altération principaux, pouvant causer une réduction du volume du déversement allant jusqu'à 50% du volume initial. En effet, après une période de 24 heures, les chaînes d'hydrocarbures de moins de C_{12} vont entièrement s'évaporer, laissant seulement les molécules plus lourdes dans la colonne d'eau. Cela aura comme conséquence

d'augmenter la masse volumique générale du pétrole brut et de permettre aux gouttelettes de couler plus facilement. Par exemple, un échantillon de pétrole brut du Koweït passe d'une masse volumique de 0.870 g/mL à 1.023 g/mL après les processus d'altération, ce qui est très près de la masse volumique de l'eau salée (Jordan and Payne, 1980). Une gouttelette ayant une masse volumique plus élevée implique aussi que son volume de détachement critique, lorsqu'elle est seulement sujette aux forces de portance, sera lui aussi plus élevé (Mehrabian et al., 2018b). Bien évidemment, l'intensité de l'évaporation de ces hydrocarbures dépend de plusieurs facteurs. Par exemple, une température de l'air plus élevée favorisera l'évaporation. De plus, la turbulence à la surface de l'océan aura un effet sur l'évaporation. Une mer avec peu de vagues limitera l'introduction du pétrole sous la surface de l'eau et accélérera le processus d'évaporation. La présence de vents permettra aussi à la couche de pétrole à la surface de l'eau de s'étendre plus facilement, ce qui va augmenter la surface en contact avec l'air ambiant et favoriser l'évaporation (Jordan and Payne, 1980). Bien que de moins grande importance (environ 1% du volume évaporé (Harrison et al., 1975)), le processus de dissolution des alcanes à faible poids moléculaire contribue aussi à augmenter la densité générale du déversement dans les premières heures de celui-ci (Blumer et al., 1973). Tous ces facteurs sont des éléments à considérer, car ils vont altérer le comportement de la gouttelette d'huile.

Ce changement dans la composition chimique du pétrole brut, couplé avec le processus de floculation avec la matière en suspension, *e.g.*, neige marine, phytoplancton et exuvies, peut altérer l'intensité relative des différents mécanismes de capture des gouttelettes. En effet, la floculation avec la matière organique dans la colonne d'eau et l'augmentation de la densité de l'huile vont augmenter la densité et la taille générale du floculant matière organique/pétrole brut. Ces changements auront pour conséquence de graduellement augmenter les index de l'interaction inertielle et de l'interception directe. Les résultats obtenus au **Chapitre 4** démontraient que le mécanisme principal de capture à haut nombre de Reynolds est l'interception directe. Cependant, cela était pour des gouttelettes individuelles. Du moment où la floculation entre en jeu, la taille des floculants est drastiquement augmentée et l'intensité de l'interaction inertielle monte en flèche. La floculation de gouttelettes d'huile avec des particules d'argile est effectivement une méthode de remédiation qui a déjà été utilisée et s'est montrée relativement efficace (Bragg and Yang, 1995; Lee et al., 1997). Elle a même été

récemment testée afin de contrôler la prolifération d'algues nocives (HABs) (Alshahri et al., 2021). Les effets que la floculation du pétrole et de la matière organique en suspension ont sur la capture par les organismes filtreurs demeurent un sujet qui n'a pas été étudié, mais le comportement des floculants et leur rôle lors de l'altération d'un déversement sont bien connus (Bragg and Yang, 1995; Muschenheim and Lee, 2002). L'hydrophobicité intrinsèque des gouttelettes de pétrole implique que celles-ci auront tendance à floculer ensemble dans la colonne d'eau. Un brassage plus important, *e.g.*, vents, vagues ou courants sous-marins, implique plus d'événements de collisions entre ces gouttelettes, ce qui contribuera aussi à augmenter la taille générale des gouttelettes et leur chance de capture (Kranck, 1984). Les travaux de Gordon Jr et al. (1973) estiment qu'entre 87% et 98% du pétrole déversé se retrouvera éventuellement sous forme de floculant pétrole-pétrole ou pétrole-matière en suspension. Blumer et al. (1973) affirme qu'un floculant contenant de la matière organique et inorganique coule significativement plus rapidement qu'un floculant uniquement composé de gouttelettes. Par contre, l'utilisation d'un surfactant pourrait permettre d'augmenter la mouillabilité des gouttelettes et de limiter l'agglomération (Gerritsen and Porter, 1982). Cependant, le processus de floculation est moins important en milieux lacustres qu'en milieux marins. En effet, l'eau salée perturbe les charges ioniques de la matière en suspension et permet un plus haut taux de floculation, ce qui n'est pas le cas en eau douce (Nelson-Smith, 1972). Considérant la grande proportion de pétrole brut se retrouvant sous la forme de floculants, il en convient d'étudier les paramètres régissant leur capture et ceux favorisant leur détachement.

L'émulsification est le processus par lequel la couche de pétrole brut à la surface de l'eau se retrouve en petites gouttelettes dans la colonne d'eau. C'est ce processus qui est le plus étudié dans cette thèse (**Chapitre 2**, **3**, **4** et **5**), car c'est sous cette forme que le pétrole brut est principalement ingéré par le zooplancton filtreur (Almeda et al., 2014a; Conova, 1997). L'intensité de ce processus dépend du niveau d'énergie du système. En effet, des grands vents ou une grande quantité de vagues vont favoriser l'introduction périodique de petits volumes de pétrole dans la colonne d'eau sous forme de gouttelettes généralement entre 0.5 à 1000 μm de diamètre (Jordan and Payne, 1980). À la surface du déversement, la turbulence va aussi introduire des petits volumes d'eau dans le volume de pétrole brut, ce qui peut parfois créer une mousse, qui est en fait une émulsion d'eau dans l'huile. L'utilisation d'un

surfactant tente de favoriser l'émulsification du pétrole brut où il pourra alors floculer et potentiellement couler ou être dégradé par les communautés microbiennes. Ce surfactant agit en diminuant la tension d'interface entre le pétrole et l'eau, ce qui facilite la formation de gouttelettes (**Chapitre 5**).

Malgré les conséquences importantes que l'ingestion de pétrole implique, les organismes filtreurs comme les copépodes pélagiques et les tuniciers pourraient accélérer le processus de nettoyage de la colonne d'eau en l'ingérant et en l'évacuant sous forme de pelettes fécales (Conover, 1971; Lee et al., 2012). La densité d'une pelette fécale étant supérieure à celle de l'eau salée, celles-ci vont couler vers le benthos où elles pourront alors être dégradées par les communautés bactériennes. Les modèles de Nepstad et al. (2015) montrent que le copépode calanoïde *Calanus finmarchicus* pourrait filtrer et incorporer dans ses pelettes fécales entre 1 et 40% du pétrole déversé, tout dépendant des facteurs environnementaux. De façon similaire, la méduse *Aurelia aurita* va produire de grandes quantités de mucus qui auront l'effet de concentrer les gouttelettes de pétrole (Gemmell et al., 2016). Ce mélange de pétrole et de mucus est alors dégradé significativement plus rapidement que des gouttelettes individuelles dans la colonne d'eau. Ces exemples nous confirment que l'on ne peut pas se fier uniquement aux processus chimiques et physiques d'altération du pétrole déversé. Les organismes biologiques agissent aussi de plusieurs façons sur ce volume de pétrole, pouvant même accélérer le processus de remédiation. C'est pourquoi il est essentiel de poursuivre ces recherches à plus grande échelle.

6.2. La localisation du déversement

La section précédente portait sur les principaux mécanismes d'altération du pétrole brut lors d'un déversement, soient l'évaporation, la dissolution, la floculation et l'émulsification. Or, les intensités relatives de ces mécanismes vont fortement varier selon plusieurs facteurs, comme la composition chimique initiale du pétrole brut déversé, les conditions environnementales, le lieu du déversement et les types d'écosystèmes touchés par celui-ci. Puisque la grande partie du volume des océans est en zone pélagique dans la colonne d'eau, cette thèse s'est davantage orientée vers un tel scénario lors de la conception des expérimentations. Par contre, il demeure pertinent de se pencher sur la capture et le détachement de gouttelettes dans d'autres milieux. Nous discuterons ici des implications d'un déversement de pétrole sur

les organismes filtreurs vivant à la surface de l'océan et dans la colonne d'eau, près des plages et des berges, et en profondeur près du fond marin.

6.2.1. À la surface et dans la colonne d'eau

En haute mer, l'évaporation est un mécanisme très important contribuant à augmenter la densité et la viscosité du pétrole brut (Jordan and Payne, 1980). La floculation est aussi un mécanisme extrêmement important pouvant avoir lieu dans la colonne d'eau. Ainsi, la grande majorité du pétrole dispersé se retrouvera sous forme de floculant après le processus d'évaporation (Gordon Jr et al., 1973). Ces deux processus vont non seulement modifier la composition du pétrole, mais ils vont aussi modifier les mécanismes de capture et de détachement des organismes filtreurs dans la colonne d'eau. En effet, puisque les floculants sont de plus grandes tailles, les index de l'interception directe et de l'interaction inertielle augmenteront aussi. Le pétrole étant plus dense et sous forme de floculants, il coulera plus rapidement et les index d'interaction inertielle et de dépôt gravitationnel augmenteront à leur tour. Ainsi, dans la colonne d'eau, les mécanismes de capture dominants vont changer au fil de temps. De plus, les travaux du **Chapitre 3** ont démontré que le ratio de viscosité entre l'huile et l'eau est un facteur important lorsque l'on étudie le détachement de gouttelettes. En effet, lorsque les ratios de tailles entre la gouttelette et le collecteur sont de 2 ou 3, un ratio de viscosité plus élevé implique un nombre de Weber critique plus élevé au moment du détachement (Fig. 3.11). Donc, il est probable que les petites gouttelettes nécessiteront plus de forces externes pour permettre le détachement, considérant que les processus d'altération contribuent à augmenter la viscosité du pétrole. Les processus de capture et de détachement ne sont donc pas statiques, mais constamment en changement en raison de l'altération du pétrole dans la colonne d'eau.

6.2.2. En zones côtières

Les vagues et les courants peuvent éventuellement apporter des volumes de pétrole déversé vers les berges et les plages. De plus, un déversement provenant d'une usine côtière ou d'un bateau à port déverserait directement le pétrole brut dans ces écosystèmes. La turbulence est le processus le plus important lorsqu'il est question de floculation entre la matière en suspension et les gouttelettes de pétrole (Delvigne et al., 1987). En effet, la turbulence

permet plus d'événements de contact et favorise ainsi la formation de floculants. Puisque les zones côtières sont fortement sujettes à la turbulence, *e.g.*, fortes vagues, marées, activités humaines, les sédiments sont constamment remis en suspension. Cela fait en sorte que c'est dans ces écosystèmes que le ratio de pétrole et de matière en suspension est idéal pour une floculation maximale (Gong et al., 2014). Donc, compte tenu du grand diamètre des floculants et de la turbulence, *i.e.* vitesse d'écoulement, les organismes filtreurs vont principalement capturer le pétrole brut via interception directe ou interaction inertielle. Par contre, Gong et al. (2014) estime que le pétrole brut plus visqueux (plus de $9500\,mPa/s$) ne formera pas de floculant. L'utilisation d'un surfactant, peu importe la localisation initiale du déversement, aura aussi des conséquences sur les écosystèmes côtiers. En effet, l'utilisation d'un surfactant crée une distribution de taille plus petite, ce qui permet au pétrole de couler plus profondément dans les sédiments côtiers (jusqu'à plus de $50\,cm$) et devient ainsi accessible aux organismes méiofauniques (Jordan and Payne, 1980).

Un élément à considérer est aussi celui de la souillure des appendices filtreurs par le pétrole brut. En effet, bien que les surfaces filtrantes semblent être lipophobes (**Chapitre 4**), il est possible que celles-ci s'encrassent si le volume de pétrole déversé est assez important. Si la quantité de pétrole souillant l'appendice filtreur est suffisante, il est fort probable que le mécanisme de filtration soit altéré. Par exemple, si l'appendice filtre la colonne d'eau en tant que tamis, il est possible que le pétrole brut souillant l'appendice vienne empêcher le fluide de passer entre les fibres collectrices. Si cela est le cas, alors l'appendice fonctionnerait plutôt comme une palme. Puisque le fluide ne peut plus passer entre les fibres, mais que la vitesse d'écoulement devrait le permettre, la force de traînée exercée sur l'appendice sera beaucoup plus forte qu'à l'origine. Cela peut causer le délogement de l'individu s'il est mobile, ou le bris des appendices s'il est sessile (Koehl, 1999). Le comportement filtrant d'un organisme lors d'un déversement n'a pas encore été étudié, mais il serait pertinent de déterminer si ou à quel point la souillure des appendices peut changer la mécanique de filtration. Il serait aussi intéressant d'étudier un invertébré filtreur ayant une forte plasticité telle que *Balanus glandula* et de tester sa réponse phénotypique en situation de souillure et en fonction de la turbulence de son milieu. Suchanek (1993) a observé que les balanes sont extrêmement tolérantes au pétrole brut et sont seulement affectées lorsqu'elles sont complètement recouvertes, ce qui fait d'elles de bonnes candidates pour une telle recherche. Puisque les balanes vivant

dans un milieu à faible turbulence ont généralement des cirres plus longs (Li and Garrett, 1998; Vo et al., 2018), il est possible qu'en situation de souillure ou d'exposition chronique au pétrole brut la taille moyenne des cirres de la population raccourcisse afin de limiter les dégâts dus aux forces de traînées augmentées.

6.2.3. En profondeur

Le pétrole brut peut se rendre dans les fonds marins de plusieurs façons. Le pétrole peut provenir d'une poche naturelle, d'un bris d'équipement d'une station d'extraction en profondeur, *e.g.*, *Deepwater Horizon*, ou via son incorporation dans des pelettes fécales. En effet, comme mentionné précédemment, la pelletisation du pétrole brut par le zooplancton est un mécanisme permettant à ces hydrocarbures d'atteindre les profondeurs des océans (Almeda et al., 2014a; Conover, 1971). Karinen (1980) estime qu'une pelette prend en moyenne 40 à 100 jours pour se rendre à une profondeur de 5400 m, laissant amplement de temps aux processus d'altération de modifier les propriétés initiales du pétrole brut. Les régions océaniques où la surface est moins agitée sont aussi plus propices à acheminer du pétrole en profondeur. Les températures plus froides et les pressions parfois extrêmes que l'on retrouve en profondeur vont aussi affecter les mécanismes de capture et de détachement des gouttelettes. En effet, les eaux froides augmentent la viscosité du pétrole (Mehrotra, 1990), ce qui fait en sorte que les gouttelettes capturées auront encore plus de difficulté à se détacher de l'appendice filtreur. De plus, une augmentation de la pression environnante a comme effet d'augmenter la tension d'interface entre l'eau et le pétrole (Okasha, 2018). L'augmentation de la tension d'interface augmente les forces capillaires retenant les gouttelettes sur les appendices filtreurs. Il sera alors plus difficile pour les forces externes, *e.g.*, courant, mouvement de l'organisme, de déformer les gouttelettes et de permettre le détachement. Cela fait en sorte que la probabilité d'un détachement partiel est aussi plus élevée.

La température a aussi un effet important sur la façon dont les organismes vont filtrer leur environnement. En effet, lorsque la température descend, la viscosité du fluide augmente. Cela est expliqué par le fait qu'il y a moins d'énergie cinétique dans le fluide et donc les forces d'attraction entre les molécules sont plus fortes, résultant en une viscosité plus élevée. Ce changement en température et en viscosité cause une baisse dans la vitesse de mouvement et de filtration des organismes en raison de facteurs physiologiques et physiques (Podolsky

et al., 1994). Avec de l'eau plus froide, le métabolisme de l'individu ralentit ce qui résulte en une filtration et un mouvement plus lent. Avec une viscosité plus élevée, les appendices filtreurs rencontrent une plus grande résistance ce qui contribue aussi au ralentissement de la filtration et du mouvement. Selon Loiterton et al. (2004), la viscosité à elle seule est responsable d'approximativement 60% de ce ralentissement chez *Daphnia galeata*, où les facteurs physiologiques et d'autres variables inconnues contribuent aux 40% restant. Aussi, le crustacé *Balanus glandula* filtre à plus basse fréquence en eaux froides (5°C) qu'en eaux plus chaudes (25°C) (Nishizaki and Carrington, 2014). De plus, en raison de cette augmentation en viscosité, de la diminution de la vitesse des appendices filtreurs et de la petite taille de certains organismes, il est possible que le nombre de Reynolds diminue, ce qui affecte les mécanismes de filtration. Ceci va favoriser la transition du mécanisme «tamis» vers le mécanisme «palme» (Koehl, 2001). Ainsi, la température n'affecte pas seulement les vitesses de filtration et de mouvement, mais aussi sur les mécanismes en jeu. Puisqu'il existe un gradient latitudinal de température dans les océans, il est fort probable qu'une même espèce ayant une très grande distribution utilise différents mécanismes en fonction d'où elle se situe. Par exemple, une espèce filtrant la colonne d'eau selon le mécanisme tamis dans la région des tropiques pourrait filtrer selon le mécanisme palme près du cercle arctique si la différence en température cause un changement de viscosité suffisant.

6.3. Perspectives futures

Les avenues de recherches futures que ces résultats apportent sont nombreuses. Tout d'abord, il est évident qu'un déversement est un événement qui change en composition et en localisation dans le temps. Comme mentionné plus haut, l'évaporation, la dissolution, la floculation et l'émulsification sont tous des mécanismes contribuant à modifier les mécanismes de capture et de détachement. Il en convient aussi que l'endroit du déversement peut avoir une influence drastique sur la filtration des gouttelettes dans la colonne d'eau. Par contre, ces changements aux mécanismes proposés plus haut n'ont pas encore été testés. Il est donc important de tester l'influence de ceux-ci sur la capture et le détachement des appendices filtreurs. Par exemple, est-ce que le processus de floculation augmente la quantité de pétrole capturé en milieux côtiers ? Le pétrole altéré se rendant en profondeur est-il réellement plus difficile à détacher des appendices ? À quel point la température de l'eau (et donc

sa viscosité) influence la quantité de fluide passant entre deux setae d'une balane ou d'un copépode ? Toutes ces questions méritent d'être étudiées afin de mieux comprendre l'impact d'un déversement en fonction de sa localisation.

Les résultats de cette thèse ont été obtenus en étudiant un seul individu à la fois. Or, dans des conditions naturelles, les organismes filtreurs sont retrouvés en grande densité dans la colonne d'eau ou sur le substrat. Ainsi, il est probable que la présence d'autres individus filtrant la colonne d'eau affecte la filtration d'un individu. Par exemple, lorsque les balanes se fixent au substrat, elles s'enferment dans une carapace de calcium. Ces structures peuvent devenir impressionnantes, advenant un bon développement de la population. Donc, le courant passant au-dessus de cette colonie ne sera pas tout à fait uniforme pour tous les organismes. Les organismes filtreurs vivant dans de forts courants auront tendance à être plus aplaties afin de réduire la force de traînée (Koehl, 1999). De plus, lorsque la croissance est suffisante, il est possible que la colonie croisse en hauteur et s'éloigne du substrat d'origine, donc subira moins les effets de la couche limite du substrat. Sebens (1984) démontre que les colonies sont généralement plus grosses lorsque le courant est plus important. Par contre, est-ce que les organismes à l'arrière de la colonie, donc ceux recevant les parcelles d'eau en dernier, sont moins à risque de capturer le pétrole brut ? La forme de la colonie peut aussi changer en fonction de la force du courant. Lorsque le courant est fort, les colonies de balanes ont la forme d'une montagne, avec un flot laminaire au sommet et turbulent à la base (Pullen and LaBarbera, 1991). Donc au sein même d'une colonie, les individus ne vont pas capturer les particules par les mêmes mécanismes. L'effet de la forme des colonies sur la capture et le détachement du pétrole brut demeure un sujet qui n'a pas encore été approché, mais dont la communauté scientifique bénéficierait grandement. De telles recherches permettraient de plus facilement identifier les espèces et les conditions pour lesquelles les probabilités de capture de gouttelettes de pétrole brut sont élevées.

De plus, dans le cadre de nos expériences, le courant était unidirectionnel. Par contre, cela n'est pas toujours le cas dans les milieux naturels. Les courants peuvent provenir de plusieurs directions simultanément, et un organisme filtreur fixé au substrat doit être en mesure de s'adapter. Il serait intéressant d'étudier la capture du pétrole brut dans un milieu ou ce type de courant est recréé, afin de déterminer si d'autres facteurs entrent en jeu dans la capture et le détachement.

Finalement, il a été démontré qu'en présence d'une émulsion de pétrole dans l'eau, le copépode *Paracartia grani* va modifier la distribution de la taille des gouttelettes via le mouvement de ses appendices filtreurs et la pelletisation (Uttieri et al., 2019). Donc, en plus d'étudier les processus d'altération physiques et chimiques du pétrole brut, nous devons aussi nous pencher sur les changements que les communautés planctoniques filtrantes peuvent apporter à l'émulsion de pétrole dans l'eau. C'est pourquoi je propose l'étude d'un déversement de pétrole brut en microcosme, puis en mésocosme. Ainsi, il nous sera possible d'observer les interactions entre les nombreuses espèces filtrantes et le pétrole, et cela en considérant l'altération du pétrole. Il s'agit d'un gros saut des recherches faites ici sur l'individu lui-même, mais elles en demeurent pas moins essentielles pour la bonne compréhension des enjeux qu'apporte un déversement et pour une prise de décisions éclairée lors du choix des méthodes de remédiation.

6.4. Conclusion

Les travaux de cette thèse mettent en évidence les principaux facteurs régissant la capture et le détachement des gouttelettes d'huile par les organismes filtreurs. Les paramètres contrôlant les principaux mécanismes de capture sont étudiés et la filtration d'organismes clés est observée. Les conditions critiques de détachement des gouttelettes sont aussi étudiées et discutées. La mouillabilité des appendices filtreurs est étudiée et les implications d'une surface lipophobe sont abordées. Finalement, le rôle d'un surfactant sur les conditions critiques de détachement ainsi que sur la distribution de taille des gouttelettes est étudié. Cette thèse propose les bases de la filtration des particules liquides par les organismes filtreurs aquatiques. Il s'agit d'un sujet qui, comme cette section le démontre, requiert davantage de recherches, tant sur l'individu que sur les communautés filtrantes et sur les différents écosystèmes aquatiques.

Bibliographie

Achituv, Y., Pedrotti, M.L., 1999. Costs and gains of porcelain crab suspension feeding in different flow conditions. Marine Ecology Progress Series 184, 161–169.

Alcaraz, M., Paffenhöfer, G.A., 1980. Catching the algae : A first account of visual observations on filter-feeding calanoids. Evolution and ecology of zooplankton communities 3, 241.

Almeda, R., Baca, S., Hyatt, C., Buskey, E.J., 2014a. Ingestion and sublethal effects of physically and chemically dispersed crude oil on marine planktonic copepods. Ecotoxicology 23, 988–1003.

Almeda, R., Bona, S., Foster, C.R., Buskey, E.J., 2014b. Dispersant corexit 9500a and chemically dispersed crude oil decreases the growth rates of meroplanktonic barnacle nauplii (*Amphibalanus improvisus*) and tornaria larvae (*Schizocardium sp.*). Marine Environmental Research 99, 212–217.

Almeda, R., Connelly, T.L., Buskey, E.J., 2016. How much crude oil can zooplankton ingest ? Estimating the quantity of dispersed crude oil defecated by planktonic copepods. Environmental Pollution 208, 645–654.

Almeda, R., Cosgrove, S., Buskey, E.J., 2018. Oil spills and dispersants can cause the initiation of potentially harmful dinoflagellate blooms ("red tides"). Environmental Science & Technology .

Almeda, R., Hyatt, C., Buskey, E.J., 2014c. Toxicity of dispersant Corexit 9500a and crude oil to marine microzooplankton. Ecotoxicology and Environmental Safety 106, 76–85.

Almeda, R., Wambaugh, Z., Wang, Z., Hyatt, C., Liu, Z., Buskey, E.J., 2013. Interactions between zooplankton and crude oil : toxic effects and bioaccumulation of polycyclic aromatic hydrocarbons. PLoS ONE 8, e67212.

Alshahri, A.H., Fortunato, L., Ghaffour, N., Leiknes, T., 2021. Controlling harmful algal blooms (HABs) by coagulation-flocculation-sedimentation using liquid ferrate and clay. Chemosphere 274, 129676.

Arnberg, M., Keitel-Gröner, F., Westerlund, S., Ramanand, S., Bechmann, R.K., Baussant, T., 2019. Exposure to chemically-dispersed oil is more harmful to early developmental stages of the northern shrimp *Pandalus borealis* than mechanically-dispersed oil. Marine

pollution bulletin 145, 409–417.

Arsenault, D.J., Marchinko, K.B., Palmer, A.R., 2001. Precise tuning of barnacle leg length to coastal wave action. Proceedings of the Royal Society of London. Series B : Biological Sciences 268, 2149–2154.

Aveyard, R., Binks, B.P., Clint, J.H., 2003. Emulsions stabilised solely by colloidal particles. Advances in Colloid and Interface Science 100, 503–546.

Ayaz, F., Pedley, T.J., 1999. Flow through and particle interception by an infinite array of closely-spaced circular cylinders. European Journal of Mechanics-B/Fluids 18, 173–196.

Becker, K., Hormchong, T., Wahl, M., 2000. Relevance of crustacean carapace wettability for fouling, in : Life at Interfaces and Under Extreme Conditions. Springer, pp. 193–201.

Bengtsson, B.E., Tarkpea, M., 1983. The acute aquatic toxicity of some substances carried by ships. Marine Pollution Bulletin 14, 213–214.

Bentley, B.J., Leal, L.G., 1986a. A computer-controlled four-roll mill for investigations of particle and drop dynamics in two-dimensional linear shear flows. Journal of Fluid Mechanics 167, 219–240.

Bentley, B.J., Leal, L.G., 1986b. An experimental investigation of drop deformation and breakup in steady, two-dimensional linear flows. Journal of Fluid Mechanics 167, 241–283.

Berk, S., Brownlee, D., Heinle, D., Kling, H., Colwell, R., 1977. Ciliates as a food source for marine planktonic copepods. Microbial Ecology 4, 27–40.

Bertrand, K., Hare, L., 2017. Evaluating benthic recovery decades after a major oil spill in the Laurentian Great Lakes. Environmental science & technology 51, 9561–9568.

Bhattacharyya, S., Klerks, P., Nyman, J., 2003. Toxicity to freshwater organisms from oils and oil spill chemical treatments in laboratory microcosms. Environmental Pollution 122, 205–215.

Bhushan, B., 2009. Biomimetics : lessons from nature–an overview. Philosophical Transactions of the Royal Society of London A : Mathematical, Physical and Engineering Sciences 367, 1445–1486.

Bhushan, B., Jung, Y.C., 2011. Natural and biomimetic artificial surfaces for superhydrophobicity, self-cleaning, low adhesion, and drag reduction. Progress in Materials Science 56, 1–108.

Bidegain, G., Powell, E.N., Klinck, J.M., Ben-Horin, T., Hofmann, E.E., 2016. Marine infectious disease dynamics and outbreak thresholds : contact transmission, pandemic infection, and the potential role of filter feeders. Ecosphere 7, e01286.

Binks, B.P., 2002. Particles as surfactants similarities and differences. Current Opinion in Colloid & Interface Science 7, 21–41.

Blumer, M., Ehrhardt, M., Jones, J., 1973. The environmental fate of stranded crude oil, in : Deep Sea Research and Oceanographic Abstracts, Elsevier. pp. 239–259.

Bobra, A.M., Shiu, W.Y., Mackay, D., Goodman, R.H., 1989. Acute toxicity of dispersed fresh and weathered crude oil and dispersants to *Daphnia magna*. Chemosphere 19, 1199–1222.

Boudina, M., Gosselin, F.P., Étienne, S., 2020. Direct interception or inertial impaction ? A theoretical derivation of the efficiency power law for a simple and practical definition of capture modes. Physics of Fluids 32, 123603.

Bragg, J.R., Yang, S.H., 1995. Clay-oil flocculation and its role in natural cleansing in Prince William Sound following the Exxon Valdez oil spill, in : Exxon Valdez Oil Spill : fate and effects in Alaskan waters. ASTM International, pp. 178–214.

Brandvik, P.J., Daling, P.S., Leirvik, F., Krause, D.F., 2019. Interfacial tension between oil and seawater as a function of dispersant dosage. Marine pollution bulletin 143, 109–114.

Brusca, R.C., Brusca, G.J., et al., 2003. Invertebrates. QL 362. B78 2003, Basingstoke.

Burns, C.W., 1968. The relationship between body size of filter-feeding Cladocera and the maximum size of particle ingested. Limnol. Oceanogr 13, 675–678.

Buskey, E.J., Hartline, D.K., 2003. High-speed video analysis of the escape responses of the copepod *Arcatia tonsa* to shadows. The Biological Bulletin 204, 28–37.

Cai, F., Yu, C., 1988. Inertial and interceptional deposition of spherical particles and fibers in a bifurcating airway. Journal of Aerosol Science 19, 679–688.

Carroll, B.J., 1976. The accurate measurement of contact angle, phase contact areas, drop volume, and laplace excess pressure in drop-on-fiber systems. Journal of Colloid and Interface Science 57, 488–495.

Carroll, B.J., 1981. The kinetics of solubilization of nonpolar oils by nonionic surfactant solutions. Journal of Colloid and Interface Science 79, 126–135.

Carroll, B.J., 1984. The equilibrium of liquid drops on smooth and rough circular cylinders. Journal of Colloid and Interface Science 97, 195–200.

Carroll, B.J., 1986. Equilibrium conformations of liquid drops on thin cylinders under forces of capillarity. A theory for the roll-up process. Langmuir 2, 248–250.

Carroll, B.J., 1989. Droplet formation and contact angles of liquids on mammalian hair fibres. Journal of the Chemical Society, Faraday Transactions 1 : Physical Chemistry in Condensed Phases 85, 3853–3860.

Cavan, E.L., Henson, S.A., Belcher, A., Sanders, R., 2017. Role of zooplankton in determining the efficiency of the biological carbon pump. Biogeosciences 14, 177–186.

Chan, B., Garm, A., Høeg, J., 2008. Setal morphology and cirral setation of thoracican barnacle cirri : adaptations and implications for thoracican evolution. Journal of Zoology 275, 294–306.

Cheer, A.Y.L., Koehl, M.A.R., 1987a. Fluid flow through filtering appendages of insects. Mathematical Medicine and Biology 4, 185–199.

Cheer, A.Y.L., Koehl, M.A.R., 1987b. Paddles and rakes : fluid flow through bristled appendages of small organisms. Journal of Theoretical Biology 129, 17–39.

Chen, C.Y., 1955. Filtration of aerosols by fibrous media. Chemical Reviews 55, 595–623.

Cohen, J.H., McCormick, L.R., Burkhardt, S.M., 2014. Effects of dispersant and oil on survival and swimming activity in a marine copepod. Bulletin of environmental contamination and toxicology 92, 381–387.

Conova, S., 1999. Role of particle wettability in capture by a suspension-feeding crab (*Emerita talpoida*). Marine biology 133, 419–428.

Conova, S.S., 1997. Adhesion of particles to solid surfaces : The role of wettability in suspension-feeding. Duke University.

Conover, R.J., 1971. Some relations between zooplankton and bunker C oil in Chedabucto Bay following the wreck of the tanker Arrow. Journal of the Fisheries Board of Canada 28, 1327–1330.

Cournarie, F., Savelli, M.P., Rosilio, V., Bretez, F., Vauthier, C., Grossiord, J.L., Seiller, M., 2004. Insulin-loaded W/O/W multiple emulsions : comparison of the performances of systems prepared with medium-chain-triglycerides and fish oil. European Journal of Pharmaceutics and Biopharmaceutics 58, 477–482.

Cremaldi, J.C., Khosla, T., Jin, K., Cutting, D., Wollman, K., Pesika, N., 2015. Interaction of oil drops with surfaces of different interfacial energy and topography. Langmuir 31, 3385–3390.

Crittenden, R.N., 1981. Morphological characteristics and dimensions of the filter structures from three species of *Daphnia* (Cladocera). Crustaceana 41, 233–248.

Daly, K.L., Remsen, A., Outram, D.M., Broadbent, H., Kramer, K., Dubickas, K., 2021. Resilience of the zooplankton community in the northeast Gulf of Mexico during and after the Deepwater Horizon oil spill. Marine Pollution Bulletin 163, 111882.

Delvigne, G., Van der Stel, J., Sweeney, C., 1987. Measurement of vertical turbulent dispersion and diffusion of oil droplets and oiled particles. Engineering Hydraulics.

Demott, W., Dörthe, M.N., 1997. The importance of highly unsaturated fatty acids in zooplankton nutrition : evidence from experiments with *Daphnia*, a cyanobacterium and lipid emulsions. Freshwater Biology 38, 649–664.

DeMott, W.R., 1986. The role of taste in food selection by freshwater zooplankton. Oecologia 69, 334–340.

DeMott, W.R., Watson, M.D., 1991. Remote detection of algae by copepods : responses to algal size, odors and motility. Journal of Plankton Research 13, 1203–1222.

Dodson, S.I., 2004. Introduction to limnology. BioOne.

Dopierala, K., Javadi, A., Krägel, J., Schano, K.H., Kalogianni, E.P., Leser, M.E., Miller, R., 2011. Dynamic interfacial tensions of dietary oils. Colloids and Surfaces A : Physicochemical and Engineering Aspects 382, 261–265.

Eckman, J.E., Duggins, D.O., 1993. Effects of flow speed on growth of benthic suspension feeders. The Biological Bulletin 185, 28–41.

Eggers, J., Villermaux, E., 2008. Physics of liquid jets. Rep. Prog. Phys. 71, 036601.

Esteban, B., Riba, J.R., Baquero, G., Rius, A., Puig, R., 2012. Temperature dependence of density and viscosity of vegetable oils. Biomass and bioenergy 42, 164–171.

Fan, E.S.C., Bussmann, M., Acosta, E., 2010. Equilibrium configuration of drops attached to spheres immersed in a uniform laminar flow. Canadian Journal of Chemical Engineering 89, 707–716.

Fanslow, D.L., Nalepa, T.F., Lang, G.A., 1995. Filtration rates of the zebra mussel (*Dreissena polymorpha*) on natural seston from Saginaw Bay, Lake Huron. Journal of Great Lakes Research 21, 489–500.

Felgenhauer, B.E., Abele, L.G., 1983. Ultrastructure and functional morphology of feeding and associated appendages in the tropical fresh-water shrimp *Atya innocous* (Herbst) with notes on its ecology. Journal of Crustacean Biology 3, 336–363.

Fenchel, T., 1980. Relation between particle size selection and clearance in suspension-feeding ciliates. Limnology and Oceanography 25, 733–738.

Fenchel, T., 1984. Suspended marine bacteria as a food source. Flows of Energy and Materials in Marine Ecosystems , 301–315.

Fernandez, V.I., Stocker, R., Juarez, G., 2022. A tradeoff between physical encounters and consumption determines an optimal droplet size for microbial degradation of dispersed oil. Scientific reports 12, 1–10.

Franco, S.C., Aldred, N., Cruz, T., Clare, A.S., 2016. Modulation of gregarious settlement of the stalked barnacle, *Pollicipes pollicipes* : a laboratory study. Scientia Marina 80, 217–228.

Friedman, M.M., Strickler, J.R., 1975. Chemoreceptors and feeding in calanoid copepods (arthropoda : Crustacea). Proceedings of the National Academy of Sciences 72, 4185–4188.

Gafonova, O.V., Yarranton, H.W., 2001. The stabilization of water-in-hydrocarbon emulsions by asphaltenes and resins. Journal of Colloid and Interface Science 241, 469–478.

Ganf, G., Shiel, R., 1985. Particle capture by *Daphnia carinata*. Marine and Freshwater Research 36, 371–381.

Geierman, C., Emlet, R., 2009. Feeding behavior, cirral fan anatomy, reynolds numbers, and leakiness of *Balanus glandula*, from post-metamorphic juvenile to the adult. Journal of Experimental Marine Biology and Ecology 379, 68–76.

Geller, W., Müller, H., 1981. The filtration apparatus of Cladocera : filter mesh-sizes and their implications on food selectivity. Oecologia 49, 316–321.

Gemmell, B.J., Bacosa, H.P., Liu, Z., Buskey, E.J., 2016. Can gelatinous zooplankton influence the fate of crude oil in marine environments ? Marine pollution bulletin 113, 483–487.

Gerritsen, J., Porter, K.G., 1982. The role of surface chemistry in filter feeding by zooplankton. Science 216, 1225–1227.

Gerritsen, J., Porter, K.G., Strickler, J.R., 1988. Not by sieving alone : observations of suspension feeding in *Daphnia*. Bulletin of Marine Science 43, 366–376.

Gonçalves, R.J., van Someren Gréve, H., Couespel, D., Kiørboe, T., 2014. Mechanisms of prey size selection in a suspension-feeding copepod, *Temora Longicornis*. Marine Ecology Progress Series 517, 61–74.

Gong, Y., Zhao, X., Cai, Z., O'reilly, S., Hao, X., Zhao, D., 2014. A review of oil, dispersed oil and sediment interactions in the aquatic environment : influence on the fate, transport and remediation of oil spills. Marine pollution bulletin 79, 16–33.

Gophen, M., Geller, W., 1984. Filter mesh size and food particle uptake by *Daphnia*. Oecologia 64, 408–412.

Gordon Jr, D.C., Keizer, P.D., Prouse, N.J., 1973. Laboratory studies of the accommodation of some crude and residual fuel oils in sea water. Journal of the Fisheries Board of Canada 30, 1611–1618.

Grace, H.P., 1982. Dispersion phenomena in high viscosity immiscible fluid systems and application of static mixers as dispersion devices in such systems. Chemical Engineering Communications 14, 225–277.

Graham, W.M., Condon, R.H., Carmichael, R.H., D'Ambra, I., Patterson, H.K., Linn, L.J., Hernandez Jr, F.J., 2010. Oil carbon entered the coastal planktonic food web during the Deepwater Horizon oil spill. Environmental Research Letters 5, 045301.

Hadamard, J., 1911. Mouvement permanent lent d'une sphère liquide et visqueuse dans un liquide visqueux. Comptes Rendus De L'Academie Des Sciences (French) 152, 1735–1738.

Hansen, B.H., Salaberria, I., Olsen, A.J., Read, K.E., Øverjordet, I.B., Hammer, K.M., Altin, D., Nordtug, T., 2015. Reproduction dynamics in copepods following exposure to chemically and mechanically dispersed crude oil. Environmental Science & Technology 49, 3822–3829.

Harrison, W., Winnik, M.A., Kwong, P.T., Mackay, D., 1975. Crude oil spills. disappearance of aromatic and aliphatic components from small sea-surface slicks. Environmental Science & Technology 9, 231–234.

Harrop, J.A., Stenhouse, J.I.T., 1969. The theoretical prediction of inertial impaction efficiencies in fibrous filters. Chemical Engineering Science 24, 1475–1481.

Hart, M.W., 1991. Particle captures and the method of suspension feeding by echinoderm larvae. The Biological Bulletin 180, 12–27.

Hartman, H.B., Hartman, M.S., 1977. The stimulation of filter feeding in the porcelain crab *Petrolisthes cinctipes* randall by amino acids and sugars. Comparative Biochemistry and Physiology Part A : Physiology 56, 19–22.

Hartmann, H.J., Kunkel, D.D., 1991. Mechanisms of food selection in *Daphnia*, in : Biology of Cladocera. Springer, pp. 129–154.

Hebert, R., Poulet, S.A., 1980. Effect of modification of particle size of emulsions of Venezuelan crude oil on feeding, survival and growth of marine zooplankton. Marine Environmental Research 4, 121–134.

Hessen, D.O., 1985. Filtering structures and particle size selection in coexisting Cladocera. Oecologia 66, 368–372.

Hinze, J., 1955. Fundamentals of the hydrodynamic mechanism of splitting in dispersion processes. AIChE Journal 1, 289–295.

Hofman, J.A.M.H., Stein, H.N., 1991. Permeability reduction of porous media on transport of emulsions through them. Colloids and Surfaces 61, 317–329.

Janssen, J.M.H., Meijer, H., 1995. Dynamics of liquid-liquid mixing : A 2-zone model. Polymer Engineering & Science 35, 1766–1780.

Jerling, H., Wooldridge, T., 1989. The developmental stages of *Pseudodiaptomus hessei* (Copepoda : Calanoida). African Zoology 24, 139–145.

John, V., Arnosti, C., Field, J., Kujawinski, E., McCormick, A., 2016. The role of dispersants in oil spill remediation : fundamental concepts, rationale for use, fate, and transport issues. Oceanography 29, 108–117.

Jónasdóttir, S.H., 1999. Lipid content of *Calanus finmarchicus* during overwintering in the faroe–shetland channel. Fisheries Oceanography 8, 61–72.

Jónasdóttir, S.H., Visser, A.W., Richardson, K., Heath, M.R., 2015. Seasonal copepod lipid pump promotes carbon sequestration in the deep North Atlantic. Proceedings of the National Academy of Sciences 112, 12122–12126.

Jordan, R.E., Payne, J.R., 1980. Fate and weathering of petroleum spills in the marine environment : a literature review and synopsis. Ann Arbor Science Publishers, Inc., Ann Arbor, MI.

Jørgensen, C.B., 1955. Quantitative aspects of filter feeding in invertebrates. Biological Reviews 30, 391–453.

Jørgensen, C.B., 1983. Fluid mechanical aspects of suspension feeding. Marine Ecology Progress Series , 89–103.

Jørgensen, C.B., 1996. Bivalve filter feeding revisited. Marine Ecology Progress Series 142, 287–302.

Jørgensen, C.B., Famme, P., Kristensen, H.S., Larsen, P.S., Møhlenberg, F., Riisgård, H., 1986. The bivalve pump. Marine Ecology Progress Series , 69–77.

Karinen, J.F., 1980. Petroleum in the deep sea environment : potential for damage to biota. Environment International 3, 135–144.

Kattner, G., Hagen, W., Lee, R.F., Campbell, R., Deibel, D., Falk-Petersen, S., Graeve, M., Hansen, B.W., Hirche, H.J., Jonasdottir, S.H., et al., 2007. Perspectives on marine zooplankton lipids. Canadian Journal of Fisheries and Aquatic Sciences 64, 1628–1639.

Kerfoot, W.C., Kirk, K.L., 1991. Degree of taste discrimination among suspension-feeding cladocerans and copepods : Implications for detritivory and herbivory. Limnology and Oceanography 36, 1107–1123.

Kiørboe, T., 2011. How zooplankton feed : mechanisms, traits and trade-offs. Biological reviews 86, 311–339.

Kiran, S.K., Ng, S., Acosta, E., 2011. Impact of asphaltenes and naphthenic amphiphiles on the phase behavior of solvent-bitumen-water systems. Energy & Fuels 25, 2223–2231.

Knothe, G., Steidley, K.R., 2007. Kinematic viscosity of biodiesel components (fatty acid alkyl esters) and related compounds at low temperatures. Fuel 86, 2560–2567.

Koehl, M., 1999. Ecological biomechanics of benthic organisms : life history, mechanical design and temporal patterns of mechanical stress. Journal of Experimental biology 202, 3469–3476.

Koehl, M.A.R., 1993. Hairy little legs : Feeding, smelling, and swimming at low Reynolds numbers. Contemporary Mathematics 141, 33–64.

Koehl, M.A.R., 2001. Transitions in function at low reynolds number : hair-bearing animal appendages. Mathematical methods in the applied sciences 24, 1523–1532.

Koehl, M.A.R., 2003. Physical modelling in biomechanics. Philosophical Transaction of Royal Society B : Biological Sciences 358, 1589–1596.

Koehl, M.A.R., 2004. Biomechanics of microscopic appendages : functional shifts caused by changes in speed. Journal of Biomechanics 37, 789–795.

Koehl, M.A.R., Strickler, J.R., 1981. Copepod feeding currents : food capture at low Reynolds number. Limnology and Oceanography 26, 1062–1073.

Kolmogorov, A., 1949. On the breakage of drops in a turbulent flow. Doklady Akademii Nauk SSSR 66, 825–828.

Koo, J.K., James, D.F., 1973. Fluid flow around and through a screen. Journal of Fluid Mechanics 60, 513–538.

Kranck, K., 1984. The role of flocculation in the filtering of particulate matter in estuaries, in : The estuary as a filter. Elsevier, pp. 159–175.

Labarbera, M., 1978. Particle capture by a pacific brittle star : experimental test of the aerosol suspension feeding model. Science 201, 1147–1149.

LaBarbera, M., 1984. Feeding currents and particle capture mechanisms in suspension feeding animals. American Zoologist 24, 71–84.

Lampert, W., Brendelberger, H., 1996. Strategies of phenotypic low-food adaptation in *Daphnia* : Filter screens, mesh sizes, and appendage beat rates. Limnology and Oceanography 41, 216–223.

Ledda, F.D., Pronzato, R., Manconi, R., 2014. Mariculture for bacterial and organic waste removal : a field study of sponge filtering activity in experimental farming. Aquaculture Research 45, 1389–1401.

Lee, K., Lunel, T., Wood, P., Swannell, R., Stoffyn-Egli, P., 1997. Shoreline cleanup by acceleration of clay-oil flocculation processes, in : International oil spill conference, American Petroleum Institute. pp. 235–240.

Lee, K.W., Liu, B.Y.H., 1982. Theoretical study of aerosol filtration by fibrous filters. Aerosol Science and Technology 1, 147–161.

Lee, R., 2013. Ingestion and effects of dispersed oil on marine zooplankton. Anchorage, Alaska., Prepared for : Prince William Sound Regional Citizens' Advisory Council (PWSRCAC) .

Lee, R.F., Köster, M., Paffenhöfer, G.A., 2012. Ingestion and defecation of dispersed oil droplets by pelagic tunicates. Journal of Plankton Research 34, 1058–1063.

Lehr, B., Bristol, S., Possolo, A., 2010a. Oil budget calculator deepwater horizon. Washington, DC 217.

Lehr, W., Bristol, S., Possolo, A., 2010b. Federal interagency solutions group, oil budget calculator science and engineering team. Oil budget calculator .

Lemcke, S., Holding, J., Møller, E.F., Thyrring, J., Gustavson, K., Juul-Pedersen, T., Sejr, M.K., 2019. Acute oil exposure reduces physiological process rates in Arctic phyto- and zooplankton. Ecotoxicology 28, 26–36.

Letendre, F., Cameron, C.B., 2022. The capture of crude oil droplets by filter feeders at high and low reynolds numbers. Journal of Experimental Biology 225, jeb243819.

Letendre, F., Mehrabian, S., Etienne, S., Cameron, C.B., 2020. The interactions of oil droplets with filter feeders : A fluid mechanics approach. Marine Environmental Research 161, 105059.

Li, M., Garrett, C., 1998. The relationship between oil droplet size and upper ocean turbulence. Marine Pollution Bulletin 36, 961–970.

Li, N.K., Denny, M.W., 2004. Limits to phenotypic plasticity : flow effects on barnacle feeding appendages. The Biological Bulletin 206, 121–124.

Li, Z., Lee, K., Kepkey, P.E., Mikkelsen, O., Pottsmith, C., 2011. Monitoring dispersed oil droplet size distribution at the gulf of mexico deepwater horizon spill site, in : International Oil Spill Conference Proceedings, International Oil Spill Conference Washington, DC. p. abs377.

Loiterton, B., Sundbom, M., Vrede, T., 2004. Separating physical and physiological effects of temperature on zooplankton feeding rate. Aquatic Sciences-Research Across Boundaries 66, 123–129.

Longhurst, A., Williams, R., 1992. Carbon flux by seasonal vertical migrant copepods is a small number. Journal of Plankton Research 14, 1495–1509.

MacLeod, C., Radke, C., 1993. A growing drop technique for measuring dynamic interfacial tension. Journal of Colloid and Interface Science 160, 435–448.

Maghami, G.G., Roberts, G.A., 1988. Evaluation of the viscometric constants for chitosan. Macromolecular chemistry and physics 189, 195–200.

Manca, M., Martin, P., Penalva-Arana, D.C., Benzie, J.A.H., 2006. Re-description of *Daphnia* (*Ctenodaphnia*) from lakes in the Khumbu Region, Nepalese Himalayas, with the erection of a new species, *Daphnia himalaya*, and a note on an intersex individual. Journal of Limnology 65, 132–140.

Marchinko, K.B., 2003. Dramatic phenotypic plasticity in barnacle legs (*Balanus glandula* Darwin) : magnitude, age dependence, and speed of response. Evolution 57, 1281–1290.

Marchinko, K.B., Palmer, A.R., 2003. Feeding in flow extremes : dependence of cirrus form on wave-exposure in four barnacle species. Zoology 106, 127–141.

Marco, U., Ai, N., Hinow, P., Jeffrey, M., Houshuo, J., Miquel, A., Rudi, S.J., 2019. Copepod manipulation of oil droplet size distribution. Scientific Reports 9.

Martinez, M.J., Udell, K.S., 1990a. Axisymmetric creeping motion of drops through a periodically constricted tube, in : AIP Conference Proceedings CONF-8809192, pp. 222–234.

Martinez, M.J., Udell, K.S., 1990b. Axisymmetric creeping motion of drops through circular tubes. Journal of Fluid Mechanics 210, 565–591.

Maruzzo, D., Minelli, A., Fusco, G., 2009. Segmental mismatch in crustacean appendages : The naupliar antennal exopod of *Artemia* (Crustacea, Branchiopoda, Anostraca). Arthropod Structure & Development 38, 163–172.

McAuliffe, C.D., 1973. Oil-in-water emulsions and their flow properties in porous media. Journal of Petroleum Technology 25, 727–733.

McMahon, J., Rigler, F., 1963. Mechanisms regulating the feeding rate of *Daphnia magna* Straus. Canadian Journal of Zoology 41, 321–332.

Mehrabian, S., Abbaspour, N., Bussmann, M., Acosta, E., 2014. The effect of viscosity ratio on the hydrodynamics of separation from an oil-coated particle, in : ASME 2014 4th Joint US-European Fluids Engineering Division Summer Meeting collocated with the ASME 2014 12th International Conference on Nanochannels, Microchannels, and Minichannels, American Society of Mechanical Engineers. pp. V01AT05A005–V01AT05A005.

Mehrabian, S., Acosta, E., Bussmann, M., 2016. Oil-particle separation in a falling sphere configuration : Effect of oil film thickness. Energy & Fuels 30, 8776–8786.

Mehrabian, S., Acosta, E., Bussmann, M., 2018a. Oil-particle separation in a falling sphere configuration : Effect of viscosity ratio & interfacial tension. International Journal of Multiphase Flow 98, 120–127.

Mehrabian, S., Bussmann, M., Acosta, E., 2015. Breakup of high solid volume fraction oil–particle cluster in simple shear flow. Colloids and Surfaces A : Physicochemical and Engineering Aspects 483, 25–35.

Mehrabian, S., Letendre, F., Cameron, C.B., 2018b. The mechanisms of filter feeding on oil droplets : Theoretical considerations. Marine Environmental Research 135, 29–42.

Mehrotra, A.K., 1990. Modeling the effects of temperature, pressure, and composition on the viscosity of crude oil mixtures. Industrial & engineering chemistry research 29, 1574–1578.

Meyer, D., 1979. Length and spacing of the tube feet in crinoids (Echinodermata) and their role in suspension-feeding. Marine Biology 51, 361–369.

Miller, C.A., Raney, K.H., 1993. Solubilization - emulsification mechanisms of detergency. Colloids and Surfaces A : Physicochemical and Engineering Aspects 74, 169–215.

Miller, C.B., Crain, J.A., Morgan, C.A., 2000. Oil storage variability in *Calanus finmarchicus*. ICES Journal of Marine Science : Journal du Conseil 57, 1786–1799.

Milliken, W.J., Stone, H.A., Leal, L.G., 1993. The effect of surfactant on the transient motion of Newtonian drops. Physics of Fluids A : Fluid Dynamics 5, 69–79.

Møller, O.S., Olesen, J., Høeg, J.T., 2003. SEM studies on the early larval development of *Triops cancriformis* (bosc)(Crustacea : Branchiopoda, Notostraca). Acta Zoologica 84, 267–284.

Morton, B., 1990. The Bivalvia : proceedings of a Memorial Symposium in Honour of Sir Charles Maurice Yonge, Edinburgh, 1986. Hong Kong University Press.

Murphy, D.W., Webster, D.R., Yen, J., 2013. The hydrodynamics of hovering in Antarctic krill. Limnology and Oceanography : Fluids and Environments 3, 240–255.

Muschenheim, D., Lee, K., 2002. Removal of oil from the sea surface through particulate interactions : review and prospectus. Spill Science & Technology Bulletin 8, 9–18.

Nakamura, Y., Kerciku, F., 2000. Effects of filter-feeding bivalves on the distribution of water quality and nutrient cycling in a eutrophic coastal lagoon. Journal of Marine Systems 26, 209–221.

Nasr-El-Din, H.A., Taylor, K.C., 1992. Dynamic interfacial tension of crude oil/alkali/surfactant systems. Colloids and surfaces 66, 23–37.

Nelson-Smith, A., 1972. Oil pollution and marine ecology. Elek Science.

Nepstad, R., Størdal, I.F., Brönner, U., Nordtug, T., Hansen, B.H., 2015. Modeling filtration of dispersed crude oil droplets by the copepod *Calanus finmarchicus*. Marine Environmental Research 105, 1–7.

Nishida, S., Ohtsuka, S., 1981. infrastructure of the mouthpart sensory setae in mesopelagic copepods of the family Scolecitrichidae. Plankton Biology and Ecology 44, 1997.

Nishizaki, M.T., Carrington, E., 2014. Temperature and water flow influence feeding behavior and success in the barnacle *Balanus glandula*. Marine Ecology Progress Series 507, 207–218.

Nishizaki, M.T., Carrington, E., 2015. The effect of water temperature and velocity on barnacle growth : Quantifying the impact of multiple environmental stressors. Journal of thermal biology 54, 37–46.

Nixon, Z., Michel, J., 2018. A review of distribution and quantity of lingering subsurface oil from the Exxon Valdez Oil Spill. Deep Sea Research Part II : Topical Studies in Oceanography 147, 20–26.

Nordtug, T., Olsen, A.J., Salaberria, I., Øverjordet, I.B., Altin, D., Størdal, I.F., Hansen, B.H., 2015. Oil droplet ingestion and oil fouling in the copepod *Calanus finmarchicus*

exposed to mechanically and chemically dispersed crude oil. Environmental toxicology and chemistry 34, 1899–1906.

Okasha, T., 2018. Investigation of the effect of temperature and pressure on interfacial tension and wettability, in : international symposium of the society of core analysts, Trondheim, Norway.

Olbricht, W.L., 1996. Pore-scale prototypes of multiphase flow in porous media. Annual Review of Fluid Mechanics 28, 187–213.

Olbricht, W.L., Leal, L.G., 1983. The creeping motion of immiscible drops through a converging/diverging tube. Journal of Fluid Mechanics 134, 329–355.

Paffenhöfer, G.A., Loyd, P., 2000. Ultrastructure of cephalic appendage setae of marine planktonic copepods. Marine Ecology Progress Series 203, 171–180.

Papirer, E., Bourgeois, C., Siffert, B., Balard, H., 1982. Chemical nature and water/oil emulsifying properties of asphaltenes. Fuel 61, 732–734.

Pechenik, J., 2014. Biology of the Invertebrates. McGraw-Hill Education.

Pennington, J.T., Emlet, R.B., 1986. Ontogenetic and diel vertical migration of a planktonic echinoid larva, *Dendraster excentricus* (Eschcholtz) : occurrence, causes, and probable consequences. Journal of Experimental Marine Biology and Ecology 104, 69–95.

Pentcheff, N., 1991. Resistance to crushing from wave-borne debris in the barnacle *Balanus glandula*. Marine Biology 110, 399–408.

Peterson, B.J., Chester, C.M., Jochem, F.J., Fourqurean, J.W., 2006. Potential role of sponge communities in controlling phytoplankton blooms in Florida Bay. Marine Ecology Progress Series 328, 93–103.

Pfeiffer, J.P., Saal, R.N.J., 1940. Asphaltic bitumen as colloid system. The Journal of Physical Chemistry 44, 139–149.

Pichot, R., Spyropoulos, F., Norton, I., 2010. O/W emulsions stabilised by both low molecular weight surfactants and colloidal particles : The effect of surfactant type and concentration. Journal of Colloid and Interface Science 352, 128–135.

Podolsky, R.D., et al., 1994. Temperature and water viscosity : physiological versus mechanical effects on suspension feeding. Science 265, 100–103.

Porter, K.G., Feig, Y.S., Vetter, E.F., 1983. Morphology, flow regimes, and filtering rates of *Daphnia*, *Ceriodaphnia*, and *Bosmina* fed natural bacteria. Oecologia 58, 156–163.

Powell, K.C., Chauhan, A., 2016. Dynamic interfacial tension and dilational rheology of dispersant Corexit 9500. Colloids and Surfaces A : Physicochemical and Engineering Aspects 497, 352–361.

Price, H.J., Paffenhöfer, G.A., Strickler, J.R., 1983. Modes of cell capture in calanoid copepods 1. Limnology and Oceanography 28, 116–123.

Pullen, J., LaBarbera, M., 1991. Modes of feeding in aggregations of barnacles and the shape of aggregations. The Biological Bulletin 181, 442–452.

Quéré, D., 2008. Wetting and roughness. Annual Review of Materials Research 38, 71–99.

Rasmussen, D., 1985. Oil spill modeling-a tool for cleanup operations. International Oil Spill Conference 1985, 243–249.

Reiswig, H.M., 1971. Particle feeding in natural populations of three marine demosponges. The Biological Bulletin 141, 568–591.

Reiswig, H.M., 1974. Water transport, respiration and energetics of three tropical marine sponges. Journal of experimental marine Biology and Ecology 14, 231–249.

Rico-Martínez, R., Snell, T.W., Shearer, T.L., 2013. Synergistic toxicity of Macondo crude oil and dispersant Corexit 9500a® to the *Brachionus plicatilis* species complex (Rotifera). Environmental Pollution 173, 5–10.

Riisgård, H.U., Larsen, P.S., 2000. Comparative ecophysiology of active zoobenthic filter feeding, essence of current knowledge. Journal of Sea Research 44, 169–193.

Riisgård, H.U., Larsen, P.S., 2010. Particle capture mechanisms in suspension-feeding invertebrates. Marine Ecology Progress Series 418, 255–293.

Romano, P., Feletti, M., Mariottini, G., Carli, A., 1999. Ecological and nutritional implications of the mandibular structure in the Antarctic calanoid copepod *Metridia gerlachei* Giesbrecht, 1902 : an ultrastructural study. Polar Biology 22, 7–12.

Rubenstein, D.I., Koehl, M.A.R., 1977. The mechanisms of filter feeding : some theoretical considerations. American Naturalist 111, 981–994.

Rudin, J., Wasan, D.T., 1992. Mechanisms for lowering of interfacial tension in alkali/acidic oil systems 1. experimental studies. Colloids and surfaces 68, 67–79.

Rybczynski, W., 1911. On the translatory motion of a fluid sphere in a viscous medium. Bulletin International de l'Academie des Sciences de Cracovie Series A (German) , 40–46.

Saffman, P., Delbrück, M., 1975. Brownian motion in biological membranes. Proceedings of the National Academy of Sciences 72, 3111–3113.

Sandberg, P.A., 1970. Scanning electron microscopy of freeze-dried Ostracoda (Crustacea). Transactions of the American Microscopical Society 89, 113–124.

Santos, R.G., Loh, W., Bannwart, A.C., Trevisan, O.V., 2014. An overview of heavy oil properties and its recovery and transportation methods. Brazilian Journal of Chemical Engineering 31, 571–590.

Sargent, J.R., Falk-Petersen, S., 1988. The lipid biochemistry of calanoid copepods, in : Biology of Copepods. Springer, pp. 101–114.

Satpute, S.K., Banat, I.M., Dhakephalkar, P.K., Banpurkar, A.G., Chopade, B.A., 2010. Biosurfactants, bioemulsifiers and exopolysaccharides from marine microorganisms. Biotechnology Advances 28, 436–450.

Schlichting, H., Gersten, K., 2016. Boundary-layer theory. Springer.

Schramm, L.L., 2006. Emulsions, foams, and suspensions : fundamentals and applications. John Wiley & Sons,.

Sebens, K., 1984. Water flow and coral colony size : interhabitat comparisons of the octocoral *Alcyonium siderium*. Proceedings of the National Academy of Sciences 81, 5473–5477.

Seuront, L., 2010. Zooplankton avoidance behaviour as a response to point sources of hydrocarbon-contaminated water. Marine and Freshwater Research 61, 263–270.

Shen, H.T., Yapa, P.D., 1988. Oil slick transport in rivers. Journal of Hydraulic Engineering 114, 529–543.

Shimeta, J., Jumars, P.A., 1991. Physical mechanisms and rates of particle capture by suspension-feeders. Oceanography and Marine Biology - An Annual Review 29, l–257.

Shumway, S.E., Cucci, T.L., Newell, R.C., Yentsch, C.M., 1985. Particle selection, ingestion, and absorption in filter-feeding bivalves. Journal of experimental marine biology and ecology 91, 77–92.

Siegel, D.A., Buesseler, K.O., Doney, S.C., Sailley, S.F., Behrenfeld, M.J., Boyd, P.W., 2014. Global assessment of ocean carbon export by combining satellite observations and food-web models. Global Biogeochemical Cycles 28, 181–196.

Silva-Briano, M., Adabache-Ortiz, A., Guerrero-Jiménez, G., Rico-Martínez, R., Zavala-Padilla, G., 2015. Ultrastructural and morphological description of the three major groups of freshwater zooplankton (Rotifera, Cladocera, and Copepoda) from the State of Aguascalientes, Mexico. INTECH open science/open minds , 307–325.

Sleeter, T.D., Butler, J.N., 1982. Petroleum hydrocarbons in zooplankton faecal pellets from the Sargasso Sea. Marine Pollution Bulletin 13, 54–56.

Smith, P.G., van de Ven, T.G.M., 1985a. Interactions between drops and particles in simple shear. Colloids and Surfaces 15, 211–231.

Smith, P.G., van de Ven, T.G.M., 1985b. The separation of a liquid drop from a stationary solid sphere in a gravitational field. Journal of Colloid and Interface Science 105, 7–20.

Smith, P.G., van de Ven, T.G.M., 1985c. Shear-induced deformation and rupture of suspended solid/liquid clusters. Colloids and Surfaces 15, 191–210.

Soo, H., Radke, C.J., 1984. Velocity effects in emulsion flow through porous media. Journal of Colloid and Interface Science 102, 462–476.

Southward, A., 1955. On the behaviour of barnacles ii. the influence of habitat and tide-level on cirral activity. Journal of the Marine Biological Association of the United Kingdom 34, 423–433.

Spielman, L., Goren, S.L., 1968. Model for predicting pressure drop and filtration efficiency in fibrous media. Environmental Science & Technology 2, 279–287.

Spooner, M.F., Corkett, C.J., 1979. Effects of Kuwait oils on feeding rates of copepods. Marine Pollution Bulletin 10, 197–202.

Stabili, L., Licciano, M., Giangrande, A., Longo, C., Mercurio, M., Marzano, C.N., Corriero, G., 2006. Filtering activity of *Spongia officinalis var. adriatica* (Schmidt)(Porifera, Demospongiae) on bacterioplankton : implications for bioremediation of polluted seawater. Water research 40, 3083–3090.

Steffy, D.A., Nichols, A.C., Kiplagat, G., 2011. Investigating the effectiveness of the surfactant dioctyl sodium sulfosuccinate to disperse oil in a changing marine environment. Ocean Science Journal 46, 299–305.

Steinberg, D.K., Landry, M.R., 2017. Zooplankton and the ocean carbon cycle. Annual review of marine science 9, 413–444.

Stone, H.A., Bentley, B.J., Leal, L.G., 1986. An experimental study of transient effects in the breakup of viscous drops. Journal of Fluid Mechanics 173, 131–158.

Stone, H.A., Leal, L.G., 1990. The effects of surfactants on drop deformation and breakup. Journal of Fluid Mechanics 220, 161–186.

Strathmann, R.R., 1971. The feeding behavior of planktotrophic echinoderm larvae : mechanisms, regulation, and rates of suspension-feeding. Journal of Experimental Marine Biology and Ecology 6, 109–160.

Strathmann, R.R., 1978. The evolution and loss of feeding larval stages of marine invertebrates. Evolution , 894–906.

Strathmann, R.R., 1982. Cinefilms of particle capture by an induced local change of beat of lateral cilia of a bryozoan. Journal of experimental marine biology and ecology 62, 225–236.

Strathmann, R.R., Jahn, T.L., Fonseca, J.R., 1972. Suspension feeding by marine invertebrate larvae : clearance of particles by ciliated bands of a rotifer, pluteus, and trochophore. The Biological Bulletin 142, 505–519.

Subramanyam, S.V., 1969. A note on the damping and oscillations of a fluid drop moving in another fluid. Journal of Fluid Mechanics 37, 715–725.

Suchanek, T.H., 1993. Oil impacts on marine invertebrate populations and communities. American Zoologist 33, 510–523.

Sumer, B.M., et al., 2006. Hydrodynamics around cylindrical structures. volume 26. World scientific.

Taylor, G.I., 1932. The viscosity of a fluid containing small drops of another fluid. Proceedings of the Royal Society of London, Series A 138, 41–48.

Taylor, G.I., 1934. The formation of emulsions in definable fields of flow. Proceedings of the Royal Society of London. Series A 146, 501–523.

Taylor, T.D., Acrivos, A., 1964. On the deformation and drag of a falling viscous drop at low Reynolds number. Journal of Fluid Mechanics 18, 466–476.

Tewari, S., Sirvaiya, A., 2015. Oil spill remediation and its regulation. International Journal of Engineering Research and General Science 1, 1–7.

Thompson, L., 1994. The role of oil detachment mechanisms in determining optimum detergency conditions. Journal of Colloid Interface Science 163, 61–73.

Thorisson, K., 2006. How are the vertical migrations of copepods controlled ? Journal of Experimental Marine Biology and Ecology 329, 86–100.

Tinevez, J.Y., Perry, N., Schindelin, J., Hoopes, G.M., Reynolds, G.D., Laplantine, E., Bednarek, S.Y., Shorte, S.L., Eliceiri, K.W., 2017. Trackmate : An open and extensible platform for single-particle tracking. Methods 115, 80–90.

Tiselius, P., Saiz, E., Kiørboe, T., 2013. Sensory capabilities and food capture of two small copepods, *Paracalanus parvus* and *Pseudocalanus sp.* Limnology and Oceanography 58, 1657–1666.

Toyota, K., McNabb, N.A., Spyropoulos, D.D., Iguchi, T., Kohno, S., 2017. Toxic effects of chemical dispersant Corexit 9500 on water flea *Daphnia magna.* Journal of Applied Toxicology 37, 201–206.

Trager, G., Genin, A., 1993. Flow velocity induces a switch from active to passive suspension feeding in the porcelain crab *Petrolisthes leptocheles* (Heller). Biological Bulletin 185, 20–27.

Tsai, T.M., Miksis, M.J., 1994. Dynamics of a drop in a constricted capillary tube. Journal of Fluid Mechanics 274, 197–217.

Turner, J.T., Ferrante, J.G., 1979. Zooplankton fecal pellets in aquatic ecosystems. BioScience 29, 670–677.

Uttieri, M., Nihongi, A., Hinow, P., Motschman, J., Jiang, H., Alcaraz, M., Strickler, J.R., 2019. Copepod manipulation of oil droplet size distribution. Scientific reports 9, 1–8.

Van Hamme, J., Ward, O., 1999. Influence of chemical surfactants on the biodegradation of crude oil by a mixed bacterial culture. Canadian Journal of Microbiology 45, 130–137.

Vandermeulen, J.H., Ross, C.W., 1995. Oil spill response in freshwater : assessment of the impact of cleanup as a management tool. Journal of environmental management 44, 297–308.

Visser, A.W., Jónasdóttir, S.H., 1999. Lipids, buoyancy and the seasonal vertical migration of *Calanus finmarchicus*. Fisheries Oceanography 8, 100–106.

Vo, M., Mehrabian, S., Villalpando, F., Etienne, S., Pelletier, D., Cameron, C.B., 2018. The fluid dynamics of *Balanus glandula* barnacles : Adaptations to sheltered and exposed habitats. Journal of Biomechanics 71, 225–235.

Vogel, S., 1994. Life in moving fluids : the physical biology of flow. Princeton University Press, Princton, New Jersey.

Vogel, S., 2020. Life in Moving Fluids : The Physical Biology of Flow-Revised and Expanded Second Edition. Princeton University Press.

Wagner, M.G., Slattery, J.C., 1971. Slow flow of a non-newtonian fluid past a droplet. AIChE Journal 17, 1198–1207.

Wallace, J.B., Webster, J.R., Woodall, W.R., 1977. The role of filter feeders in flowing waters. Arch. Hydrobiol 79, 506–S32.

Walstra, P., 1993. Principles of emulsion formation. Chemical Engineering Science 48, 333–349.

Watts, E., Petri, M., 1981. A scanning electron microscope study of the thoracic appendages of *Daphnia magna* Straus. Journal of Natural history 15, 463–473.

Wellek, R.M., Agrawal, A.K., Skelland, A.H.P., 1966. Shape of liquid drops moving in liquid media. AIChE Journal 12, 854–862.

Wheeler, R., 1978. The fate of petroleum in the marine environment. Exxon Production Research Company.

White, F.M., Corfield, I., 2006. Viscous fluid flow. volume 3. McGraw-Hill, New York.

Wilkinson, S.B., Zheng, W., Allen, J.R., Fielding, N.J., Wanstall, V.C., Russell, G., Hawkins, S.J., 1996. Water quality improvements in liverpool docks : the role of filter feeders in algal and nutrient dynamics. Marine Ecology 17, 197–211.

Wolfe, D., Michel, J., Hameedi, M., Payne, J., Galt, J., Watabayashi, G., Braddock, J., Short, J., O'Claire, C., Rice, S., 1994. The fate of the oil spilled from the Exxon Valdez. Environmental Science & Technology 28, 560A–568A.

Xu, R., Zhang, Z., Wang, L., Yin, N., Zhan, X., 2018. Surfactant-enhanced biodegradation of crude oil by mixed bacterial consortium in contaminated soil. Environmental Science

and Pollution Research 25, 14437–14446.

Yan, Z., Elliott, J.A.W., Masliyah, J.H., 1999. Roles of various bitumen components in the stability of water-in-diluted-bitumen emulsions. Journal of Colloid and Interface Science 220, 329–337.

Yang, H., Park, C.C., Hu, Y.T., Leal, L.G., 2001. The coalescence of two equal-sized drops in a two-dimensional linear flow. Physics of Fluids 13, 1087–1106.

Yeh, H.C., Liu, B.Y.H., 1974. Aerosol filtration by fibrous filters - I. Theoretical. Journal of Aerosol Science 5, 191–204.

Yilmaz, İ.N., İşinibilir, M., 2018. Interactions between zooplankton and oil spills : Lessons learned from global accidents and a proposal for zooplankton monitoring. Oil Spill along the Turkish Straits , 238.

Zhao, X., 2007. Drop breakup in dilute newtonian emulsions in simple shear flow : New drop breakup mechanisms. Journal of Rheology 51, 367–392.